THE UNIVERSITY OF QUEENSLAND

AUSTRALIA

Anti-herpesvirus CD4$^+$ T cell function

Joseph Yunis

Bachelor of Science (Hons)

A thesis submitted for the degree of Doctor of Philosophy at

The University of Queensland in 2018

School of Chemistry and Molecular Biosciences

Abstract

Gamma-herpesviruses can cancers. For example, Epstein-Barr virus (EBV) causes B cell Burkitt's lymphoma and nasopharyngeal carcinoma. EBV infection is endemic world-wide with a sero-prevalence of 75-95%. Our understanding of how EBV infects *in vivo* and how it might be controlled is limited. For example, how EBV enters the host is still a contested debate. This has made vaccination a distant challenge. Vaccine trials to date have reduced the symptoms of primary infection (infectious mononucleosis) but not the long-term viral loads that likely lead to cancers. The species specificity of EBV has made new vaccines difficult to develop.

Murid-herpesvirus 4 (strain MHV-68), readily infects inbred laboratory mice, and has provided an accessible way to understand gamma-herpesvirus infection and control. Like EBV, it persists in memory B cells. Live-attenuated MHV-68 that lacks the ORF73 open reading frame, and so is deficient in latency and persistence, protects mice against long-term wild type infection. Dissecting natural and vaccine-induced infection control has identified distinct roles for $CD4^+$ T cells, $CD8^+$ T cells and antibody. $CD4^+$ T cells play a particular role in controlling chronic lytic infection. As yet, the immune effectors responsible for controlling latency remain ill-defined. $CD8^+$ T cells specific for latent viral antigens play some role, but vaccination to prime these cells has not reduced long-term viral loads.

Recently, cytomegaloviruses have gained prominence as vaccine vectors. To test protection by $CD4^+$ T cell priming, a recombinant murine cytomegalovirus that expresses membrane bound ovalbumin from the viral genome was used to vaccinate against a recombinant MHV-68 that expresses the same membrane bound ovalbumin from a lytic promoter. Vaccinated mice controlled lytic infection but failed to reduce long-term infection. Nor was a combination of $CD4^+$ and $CD8^+$ T cell priming fully effective. In trying to improve recombinant cytomegalovirus-based priming, MHC class II down-regulation was noted in infected cells, along with relatively weak $CD4^+$ T cell priming. This down-regulation was found to depend on the viral M78 gene. M78-deficient MCMV was characterised *in vitro* and *in vivo*. More than one defect was identified, but a significant component was found to be $CD4^+$ T cell-dependent. This represents a possible future basis for better cytomegalovirus-mediated $CD4^+$ T cell priming, and so better protection against long-term gamma-herpesvirus infection.

Declaration by author

This thesis is composed of my original work, and contains no material previously published or written by another person except where due reference has been made in the text. I have clearly stated the contribution by others to jointly-authored works that I have included in my thesis.

I have clearly stated the contribution of others to my thesis as a whole, including statistical assistance, survey design, data analysis, significant technical procedures, professional editorial advice, financial support and any other original research work used or reported in my thesis. The content of my thesis is the result of work I have carried out since the commencement of my higher degree by research candidature and does not include a substantial part of work that has been submitted to qualify for the award of any other degree or diploma in any university or other tertiary institution. I have clearly stated which parts of my thesis, if any, have been submitted to qualify for another award.

I acknowledge that an electronic copy of my thesis must be lodged with the University Library and, subject to the policy and procedures of The University of Queensland, the thesis be made available for research and study in accordance with the Copyright Act 1968 unless a period of embargo has been approved by the Dean of the Graduate School.

I acknowledge that copyright of all material contained in my thesis resides with the copyright holder(s) of that material. Where appropriate I have obtained copyright permission from the copyright holder to reproduce material in this thesis and have sought permission from co-authors for any jointly authored works included in the thesis.

Publications during candidature

Peer-reviewed papers

Yunis J, Farrell HE, Bruce K, Lawler C, Sidenius S, Wyer O, Davis-Poynter N, Stevenson PG. Murine cytomegalovirus degrades MHC class II to colonize the salivary glands. PLoS Pathog. 2018 Feb 15;14(2):e1006905. doi: 10.1371/journal.ppat.1006905.

Farrell H, Oliveira M, Macdonald K, **Yunis J**, Mach M, Bruce K, Stevenson P, Cardin R, Davis-Poynter N. Luciferase-tagged wild-type and tropism-deficient mouse cytomegaloviruses reveal early dynamics of host colonization following peripheral challenge. J Gen Virol. 2016 Dec;97(12):3379-3391. doi: 10.1099/jgv.0.000642. Epub 2016 Oct 26.

Davis-Poynter N, **Yunis J**, Farrell HE. The Cytoplasmic C-Tail of the Mouse Cytomegalovirus 7 Transmembrane Receptor Homologue, M78, Regulates Endocytosis of the Receptor and Modulates Virus Replication in Different Cell Types. PLoS One. 2016 Oct 19;11(10):e0165066. doi: 10.1371/journal.pone.0165066. eCollection 2016.

Conference abstracts

Yunis J, Farrell H, Bruce K, Lawler C, Sidenius S, Wyer O, Davis-Poynter N, Stevenson P. 2017. Murine cytomegalovirus degrades MHC class II to colonize the salivary glands. 42nd Annual International Herpesvirus Workshop, Ghent, Belgium. (Poster presentation)

Yunis J, & Stevenson P. 2016. A murine Cytomegalovirus Vaccine Vector Protects Against Murine Gammaherpesvirus 68. 16th International Congress of Immunology Conference, Melbourne, Australia. (Poster presentation)

Oral presentations

Yunis J, & Stevenson P. 2016. Murine Cytomegalovirus M78, a seven-transmembrane receptor homologue is implicated in CD4^{+} T cell evasion and colonialization of the salivary gland. 12th Annual School of Chemistry and Molecular Bioscience Research Student Conference Symposium, University of Queensland.

Yunis J, & Stevenson P. 2016. How murine cytomegalovirus evades $CD4^+$ T cells and colonises the host. Infection and Immunity Symposium, Australian Infectious Disease Research Centre, University of Queensland.

Publications included in this thesis

Yunis J, Farrell HE, Bruce K, Lawler C, Sidenius S, Wyer O, Davis-Poynter N, Stevenson PG. Murine cytomegalovirus degrades MHC class II to colonize the salivary glands. PLoS Pathog. 2018 Feb 15;14(2):e1006905. doi: 10.1371/journal.ppat.1006905.

Publication citation –incorporated as Chapter 4.

Contributor	Statement of contribution
Joseph Yunis	Conception and design (50%) Analysis and interpretation (30%) Drafting and production (30%)
Helen Farrell	Conception and design (10%) Analysis and interpretation (5%) Drafting and production (10%)
Kimberley Bruce	Conception and design (0%) Analysis and interpretation (5%) Drafting and production (0%)
Clara Lawler	Conception and design (0%) Analysis and interpretation (5%) Drafting and production (0%)
Stine Sidenius	Conception and design (0%) Analysis and interpretation (5%) Drafting and production (0%)
Orry Wyer	Conception and design (0%) Analysis and interpretation (5%) Drafting and production (0%)
Nicholas Davis-Poynter	Conception and design (5%) Analysis and interpretation (5%)

	Drafting and production (0%)
Philip G. Stevenson	Conception and design (35%) Analysis and interpretation (40%) Drafting and production (60%)

Contributions by others to the thesis

Philip Stevenson contributed to the conception and design of the project and interpretation of research data. Clara Lawler, Dr Helen Farrell and Dr Nicholas Davis-Poynter contributed to editing the thesis.

Statement of parts of the thesis submitted to qualify for the award of another degree

None

Research Involving Human or Animal Subjects

All procedures and experiments were approved by the University of Queensland Animal Ethics Committee in accordance with the Australian National Health and Medical Research Council guidelines. Ethics approval numbers since commencement of candidature are listed below;

1. SASVRC/301/13/ARC/NHMRC/BELGIUM
2. SCMB/341/16
3. SCMB/479/15/NHMRC

Copies of the ethics approval letters are included in the appendix of this thesis.

Acknowledgements

I would like to thank God for his protection and guidance, strength and wisdom. I would also like to thank my family particularly my mother Sharfa Alamini Tebe who has been my rock. She has sacrificed much and endured great suffering to give me an opportunity to an education that I am grateful.

I would also like to thank my twin brother John Yunis, who always offered to pick me up late from the laboratory. To Stephen Kamal, Hawaya Yunis and Emanuel Yunis, I thank them for their moral support. To Clara Lawler, thank you for editing this thesis and contribution to the publication on M78. You have been a wonderful friend and colleague. I'm grateful for your invaluable support. Always patient and welling to listen to my mumbles and crazy ideas and thoughts on several topics.

I would also like to thank past and present members of the Stevenson and Davis-Poynter lab for the conducive atmosphere I experienced during my candidature. A special thank you to Martha Oliveira, for the wonderful times we spent during those early days of my candidature; Dr Cindy Tan, for her supervision and motivation; Kimberley Bruce and Orry Wyer for helping with processing and tittering of tissue homogenates; Stine, for her work on the M78 publication particularly on M78 and MHC II internalisation and introducing me to rock climbing.

To my mentor and supervisor Dr Philip Stevenson, I thank you for the opportunity to learn under your stewardship. I could not have done it without your invaluable support and direction. Thank you. To Dr Nicholas Davis-Poynter and Dr Helen Farrell, I'm indebted for the chance to have studied under your supervision during honours and also during my PhD. A special thank you to Dr Alec Redwood for the MCMV OVA^{+} viruses.

To the School of Chemistry and Molecular Biosciences, thank you for the travel grants that took me to countries I could not have otherwise visited.

Finally, I would like to dedicate this thesis to my late father Yunis Abusodur Manzoul whom I have not seen or know much about. Thinking of you dad, gave me strength to carry on when all hope was lost. I hope you are proud of how far I have come dad.

Financial support

This research was supported by an Australian Government Research Training Program Scholarship

Keywords

Vaccination, degradation, downregulation, intranasal, MHV-68, MCMV, latency, lytic, rescue, attenuated.

Australian and New Zealand Standard Research Classifications (ANZSRC)

ANZSRC code: 060506, Virology, 50%
ANZSRC code: 110799, Immunology not elsewhere classified, 50%

Fields of Research (FoR) Classification

FoR code: 0605, Microbiology, 50%
FoR code: 1107, Immunology, 50%

Table of Contents

CHAPTER 1: INTRODUCTION 22
1.1 Significance 23
1.2 Aims 24
1.2.1 Specific aims 24
1.3 Literature Review 25
1.3.1 Clinical background 25
1.3.2 EBV pathogenesis 25
1.3.3 Transmission 28
1.3.4 Epidemiology of EBV 28
1.3.5 EBV replication 28
1.3.6 Immune responses 29
1.4 Animal model systems for EBV vaccination studies. 31
1.4.1 Rhesus Lymphocryptovirus 31
1.4.2 Live attenuated vaccines 31
1.4.3 Murine gamma-herpesvirus 68 32
CHAPTER 2: MATERIALS AND METHODS 38
2.1 Reagents and consumables 39
2.2 Media and solutions 39
2.3 Bacteria 40
2.3.1 Bacterial strain 40
2.3.2 Growth and storage 40
2.4 Making recombinant BAC$^+$ Δ73 mutant using BAC technology 41
2.4.1 Construction and analysis of shuttle vector and BAC plasmid DNA 41
2.4.2 Preparation of competent DH10B *E.coli* containing BAC$^+$ Δ73 41
2.4.3 Recombination MHV-68 BAC$^+$ Δ73 sOVA 41
2.4.4 Reconstitution MHV-68 BAC$^+$ Δ73 sOVA 42
2.4.5 Removal of BAC cassette 42
2.5 Mice 43
2.5.1 Facility 43
2.5.2 Infections 43
2.5.3 *In vivo* depletions and anti-IFN-γ administration 43
2.6 Mammalian cell culture 43
2.6.1 Cell lines 43

2.6.2 Cell culture 45
2.7 Viruses 45
2.8 Preparation of virus stocks 48
2.9 MHV-68 48
2.10 MCMV 48
2.10.1 Working stocks 48
2.10.2 Concentrated clean stocks 48
2.10.3 Virion detection stocks 48
2.11 In vitro growth kinetics 49
2.12 Multi-step growth kinetics- low multiplicity of infection 49
2.12.1 MHV-68 49
2.12.2 MCMV 49
2.13 Multi-step growth kinetics- high multiplicity of infection 49
2.13.1 MCMV 49
2.14 Single-step growth kinetics 50
2.14.1 MCMV 50
2.15 Viral infectivity assays 50
2.16 Plaque assay- measure of lytic virus 50
2.16.1 MHV-68 50
2.16.2 MCMV 50
2.17 Infectious centre assay- measure of latently infected reactivating cells 51
2.18 Determining virus titer in infected cells and tissues 51
2.19 DNA extraction protocols 51
2.19.1 Plasmid DNA extraction- miniprep 51
2.19.2 BAC DNA extraction- Alkaline/SDS lysis 52
2.19.3 Viral DNA extraction from cell free virion stocks 52
2.19.4 Genomic DNA extraction from tissues 53
2.19.5 Genomic DNA extraction from blood 53
2.20 RNA extraction protocol 54
2.20.1 DNase 1 treatment 54
2.20.2 Single strand cDNA synthesis using reverse transcriptase 55
2.21 Spectrophotometry of nucleic acid 55
2.22 Transcription analysis using PCR 55
2.23 Polymerase Chain Reaction (PCR) 56
2.24 Quantitative real-time PCR (QPCR) 57

2.25 Gel electrophoresis....58
2.26 Western blot....58
2.27 Generation of RAW-C2TA and BALB/c-3T3-C2TA expressing cell lines....59
2.27.1 PCR purification....59
2.27.2 Restriction digest....59
2.27.3 Transformation....60
2.27.4 To confirm ligation and transformation....60
2.27.5 Transfection....60
2.27.6 Transduction of BALB/c-3T3-C2TA and RAW-C2TA....61
2.28 Generation of clones by limiting dilution....61
2.29 NO_2 test....62
2.30 Antigen presentation assay....62
2.30.1 BALB/c-3T3-C2TA....62
2.30.2 RAW-C2TA....63
2.31 Enzyme-linked immunosorbent assay (ELISA)....63
2.31.1 IL-2....63
2.31.2 Preparation of sera from mouse blood....63
2.31.3 IgM and IgG....64
2.32 The Enzyme-Linked Immunospot assay (ELISPOT)....65
2.32.1 Coating plates....65
2.32.2 Ficoll plaque gradient lymphocyte isolation....65
2.32.3 $CD4^+$ T cell enrichment using Mouse Depletion Dynabeads....65
2.33 Immunohistochemistry....67
2.34 Immunofluorescence....68
2.35 Microscopy....73
2.35.1 Epi-fluorescence....73
2.35.2 Confocal laser....73
2.36 Image analysis....73
2.37 Flow cytometry....73
2.37.1 Genotyping....73
2.37.2 Primary cells....74
2.37.3 Immortalised cells....74
2.38 Statistical analysis....78
CHAPTER 3: MCMV AS A LIVE-ATTENUATED PERSISTENT VACCINE VECTOR. 79
3.1 Results....80

3.1.1 Characterisation of recombinant OVA$^+$ MCMV viruses 80
3.1.2 *In vitro* characterisation of MCMV recombinant OVA viruses 80
3.1.3 *In vivo* replication kinetics of recombinant MCMV OVA virus 83
3.2 MCMV sOVA as a model live attenuated vaccine vector to secreted ovalbumin .. 85
3.2.1 Does MCMV sOVA protect against MHV-68 M3 sOVA lytic infection? 85
3.2.2 Antibody response to MCMV and ovalbumin 85
3.2.3 Response to MHV-68 M3 sOVA in MCMV sOVA and mOVA vaccinated mice 87
3.2.4 Does adoptive transfer of $OVA_{323-339}$ transgenic CD4$^+$ T cells protect BALB/c mice against MHV-68 infection? 89
3.3 MCMV mOVA, a model live attenuated vaccine vector to induce CD4$^+$ T cell immunity. 96
3.3.1 BALB/c vaccination restricts lytic mucosal infection but not lymphoproliferative disease 96
3.3.2 How do CD4$^+$ T cells restrict MHV-68 mOVA lytic infection in BALB/c? 98
3.3.3 DO11.10 transgenic mice are heterogeneous 102
3.3.4 C57BL/6 vaccination confers protection against mucosal infection and short-term lymphoproliferative disease 104
3.3.5 To understand T cell mediated immune control of MHV-68 mOVA using F1 mice 106
3.3.6 F1 mice fail to control latent infection 109
3.3.7 Primed lytic CD4$^+$ T cells restrict splenomegaly in MHV-68 IiOVA infected mice 112
3.4 Can pre-existing antibody restrict mucosal infection? 114
3.4.1 gH/gL antibody in BALB/c mice controls MHV-68 infection 114
3.4.2 gH/gL antibody in C57BL/6 mice fails to control MHV-68 infection 116
3.5 Discussion 119
CHAPTER 4: MURINE CYTOMEGALOVIRUS DEGRADES MHC CLASS II TO COLONIZE THE SALIVARY GLANDS 122
4.1 Unpublished supporting research data. 155
4.1.1 Characterising BALB/c-3T3-C2TA and RAW-C2TA cells 155
4.1.2 Generation of uniform MHC II expressing clones 157
4.1.3 MCMV restricted CD4$^+$ T cell stimulation *in vitro* 159
4.1.4 Confirmation of M78 expression in WT and absence in M78$^-$ virus 162
4.1.5 Kinetics of MHC II downregulation and degradation 164

4.1.6 Bafilomycin prevents MHC II endocytosis. 164
4.1.7 Characterising thioglycollate stimulated peritoneal macrophage cells 166
4.1.8 M78 c-terminal domain is dispensable for MHC II degradation 167
4.1.9 Generating M78 expressing BALB/c-3T3-C2TA and RAW-C2TA cells 169
4.1.10 Can complementing M78$^-$ virus downregulate MHC II? 173
4.1.11 Other candidate genes involved in MHC II downregulation 174
4.2 In vivo 176
4.2.1 M78 infects primary lung cells as WT and retains MHC II expression 176
4.2.2 M78 targets MHC II expression in CD11c$^+$ cells 178
4.2.3 Inhibiting IFN-γ partially rescues M78$^-$ salivary gland defect 179
4.2.4 M78$^-$ virus dissemination is restricted by CD4$^+$ T cells after i.p infection 180
4.2.5 M78 C-terminus is critical for virus dissemination 180
4.3 Discussion 182
CHAPTER 5: USING ORF73-DEFICIENT, OVALBUMIN+ MHV-68, TO TRACK ANTIGEN-SPECIFIC CD4$^+$ T CELLS IN AN ESTABLISHED PROTECTION MODEL ..183
5.1 Introduction 184
5.2 Results 187
5.2.1 Diagnosing the presence of ovalbumin in the psk pA sOVA M3 shuttle vector 187
5.2.2 Transformation of BAC$^+$ Δ73 mutant DH10B *E.coli* 187
5.2.3 Confirmation of BAC$^+$ Δ73 sOVA by restriction digest 187
5.2.4 Reconstitution of BHK-21 cells 189
5.2.5 Expression of ovalbumin in MHV-68 Δ73 sOVA constructs. 190
5.2.6 Characterising OVA expression and presentation using a defined CD4+ T cell assay. 193
5.2.7 Δ73 sOVA is dispensable for replication *in vitro* 195
5.2.8 Δ73 sOVA is severely attenuated in lymphoid organs 196
5.2.9 Δ73 sOVA virus stimulates B and CD4$^+$ T cells in BALB/c mice 198
5.3 Discussion 200
CHAPTER 6: GENERAL DISCUSSION AND FUTURE DIRECTIONS 203
6.1 MHV-68 vaccination restricts lytic infection 204
CHAPTER 7: REFERENCES 206
APPENDIX 228
6.2 Ethics approval certificates 228

List of Figures

Fig. 3. 1. *In vitro* characterisation of recombinant MCMV ovalbumin viruses. 81
Fig. 3. 2. MCMV OVA viruses induce IL-2 secretion. 82
Fig. 3. 3. MCMV OVA viruses are defective in SG colonisation. 84
Fig. 3. 4. MCMV and OVA-specific primary antibody response following i.p infection. 86
Fig. 3. 5. Immune response to MHV-68 sOVA following intranasal infection. 88
Fig. 3. 6. Presence of adoptively transferred DO11.10 $CD4^+$ T cells in treated BALB/c mice. 90
Fig. 3. 7. Absence of adoptively transferred DO11.10 $CD4^+$ T cells in treated BALB/c. 93
Fig. 3. 8. MCMV sOVA priming does not stimulate OVA-specific DO11.10 $CD4^+$ T cells. 95
Fig. 3. 9. MHC I and MHC II epitopes in MCMV mOVA and sOVA. 95
Fig. 3. 10. MCMV mOVA vaccination primes OVA-specific $CD4^+$ T cells. 98
Fig. 3. 11. Frequency of IFN-γ producing T lymphocytes 99
Fig. 3. 12. OVA primed $CD4^+$ and $CD8^+$ T cells control lytic infection. 102
Fig. 3. 13. $OVA_{323-339}$-specific DO11.10 transgenic mice are heterogeneous. 103
Fig. 3. 14. MCMV mOVA primes OVA-specific $CD8^+$ T cells. 106
Fig. 3. 15. Lytically primed OVA-specific $CD4^+$ T cells restrict lytic infection. 109
Fig. 3. 16. Lytically primed OVA-specific $CD4^+$ T cells restrict acute but not long-term infection 110
Fig. 3. 17. F1 mice retain elevated levels of OVA-specific antibody IgG. 111
Fig. 3. 18. Lytically primed OVA-specific $CD4^+$ T cells restrict splenomegaly. 113
Fig. 3. 19. Pre-existing gH/gL controls acute lytic infection and B cell lymphoproliferation. 116
Fig. 3. 20. Pre-existing gH/gL fails to control lytic infection and B cell lymphoproliferation. 118

Fig. 4. 1. BALB/c-3T3-C2TA and RAW-C2TA constitutively express MHC II. 157
Fig. 4. 2. RAW-C2TA clones uniformly express MHC II and stimulate $CD4^+$ T cells. 158
Fig. 4. 3. MCMV restricts CD4+ T cell stimulation in RAW-C2TA cells. 160
Fig. 4. 4. BALB/c-3T3-C2TA retain MHC II expression. 162
Fig. 4. 5. M78 deficient virus does not express M78. 163
Fig. 4. 6. MHC II downregulation is dose dependent and occurs as early as 6 hours p.i. 165
Fig. 4. 7. Characterising thioglycollate stimulated peritoneal macrophages. 167
Fig. 4. 8. M78 C-terminus is dispensable for downregulation of MHC II. 168

Fig. 4. 9. Amplification of M78 from K181 viral DNA and HAM78 plasmid. 170
Fig. 4. 10. M78 localises with MHC II in the cytoplasm of BALB/c-3T3-C2TA. 172
Fig. 4. 11. M78 expressing RAW-C2TA fail to complement $M78^-$ virus. 174
Fig. 4. 12. MCMV glycoprotein mutants downregulate MHC II. 175
Fig. 4. 13. $M78^-$ and WT infect similar cell types in BALB/c lung. 177
Fig. 4. 14. MCMV targets CD11c+ cells in the lung. 178
Fig. 4. 15. Anti-IFN-γ treatment partially rescues $M78^-$ salivary gland defect. 179
Fig. 4. 16. M78 C-terminus is critical for virus dissemination. 181

Fig. 5. 1. Analysis of shuttle vector and diagnosis of BAC^+ Δ73 sOVA plasmid DNA. 188
Fig. 5. 2. Confirmation of BAC cassette cleavage by Cre recombinase. 190
Fig. 5. 3. Detection of ovalbumin in Δ73 sOVA. 193
Fig. 5. 4. MHV-68 OVA viruses induce IL-2 secretion. 194
Fig. 5. 5. *In vitro* characterization of BAC^- Δ73 sOVA. 195
Fig. 5. 6. *In vivo* characterisation of Δ73 sOVA. 198
Fig. 5. 7. Δ73 sOVA induces antibody and IFN-γ in BALB/c mice. 199

List of Tables

Table 1: Reagents 39
Table 2: Cell and cell lines 44
Table 3: Viruses used in the thesis 46
Table 4. RNA primer list 56
Table 5. PCR primer list 56
Table 6. QPCR primer list 57
Table 7. IL-2 ELISA detection antibodies 64
Table 8. IFN-γ detection peptides and antibodies 67
Table 9. Primary antibody list 69
Table 10. Secondary antibody list 71
Table 11. Flow cytometry antibodies 76

List of Abbreviations used in this thesis

BM	Bone marrow
B-LCL	B lymphoblastoid cell lines
BAC	Bacterial artificial chromosome
EBV	Epstein-Barr virus also known Human herpesvirus 4 (HHV4)
EBNA1, 3A, 3B, 3C	EBV nuclear antigen 1, 3A, 3B, 3C
EF1a	Elongation factor 1-alpha
ELISA	Enzyme linked immunosorbent assay
ELISpot	Enzyme linked Immunospot assay
cDNA	complementary DNA
CMV	Cytomegalovirus
CPE	Cytopathic effect
Cre	Cre-recombinase
CREB	cyclic AMP response element-binding protein
C2TA	Class II, major histocompatibility complex transactivator
DC	Dendritic cell
DNA	Deoxyribonucleic acid
dNTP	deoxynucleotide triphosphate
FACS	Flow cytometry cell sorting
FBS	Foetal bovine serum
FCS	Foetal calf serum
GFP	Green fluorescent protein
gH, gL, gO,gp	Glycoprotein H, L, O, 150
GPCR	G-protein coupled receptor
HA	Hemagglutinin
HCMV	Human cytomegalovirus
HIV	Human immunodeficiency virus
MHC II, I, E	Major histocompatibility complex class II, I E
HLA	Human leukocyte antigen

HSV	Herpes simplex virus
IE1	Immediate early 1
IF	Immunofluorescence
IFN-γ	Interferon gamma
IL-10	Interleukin-10
IKK	IκB kinase complex
i.n	Intranasal
i.p	Intraperitoneal
IR	Internal repeats
IRF-4	Interferon regulatory factor-4
i.v	Intravenous
LCMV	Lymphocytic choriomeningitis virus
LMP2	Latent membrane protein 2
MOI	multiplicity of infection
MHV-68	Murine Herpesvirus-68
mRNA	Messenger ribonucleic acid
MS	Multiple sclerosis
NF-Y	Nuclear factor Y
pp65	Phosphoprotein 65 (MCMV)
QPCR	Quantitative (real-time) polymerase chain reaction
RFX	Regulatory factor X
RPM	Rotation per minute
RNA	Ribonucleic acid
Rta	Replication and transcription factor
RT-PCR	Reverse transcription polymerase chain reaction
RT	Room temperature
ORF	Open reading frame
oriP	Origin of replication
OVA	Ovalbumin
SP	Spleen
SCLN	Superficial cervical lymph node
MLN	Mediastinal lymph node

PMBC	Peripheral blood mononuclear cell
PCR	Polymerase chain reaction
PEL	Primary effusion lymphoma
TCR	T cell receptor
TNFα	Tumour necrosis factor alpha
JAK	Janus kinase
K181	MCMV Perth laboratory strain
Kb	Kilobase
KDa	Kilo Daltons
NK	Natural Killer cells
p.i	Post infection
PFU	Plaque forming units
SEM	Standard error of mean
SG	Salivary glands
IM	Infectious mononucleosis
Vac	Vaccinia virus
Cont	Control
PTLD	Post-transplant lymphoproliferative
APC	Allophycocyanin
FITC	Fluorescein isothiocyanate
PE	Phycoerythrin
Per CP Cy5.5	Peridinin chlorophyll protein complex Cyanine 5.5
BV421	Brilliant Violet 421

CHAPTER 1: INTRODUCTION

1.1 Significance

Epstein-Barr virus (EBV) is an oncogenic virus that infects more than 95% of adults world-wide (1) with no licenced preventative or therapeutic vaccine. It is associated with African Burkitt's lymphoma and nasopharyngeal carcinoma in which nearly all tumour cells contain EBV genomes (2). Burkitt's lymphoma is the most common childhood cancer of sub-Saharan Africa while nasopharyngeal carcinoma is prevalent in Southern China (2, 3). The median age of developing Burkitt's lymphoma in Africa is 8 years (4). The virus infects approximately 50% of children by the age of 1 and is generally asymptomatic (4). In developed countries, primary EBV infection is delayed in young adults and is the main cause of infectious mononucleosis (IM) (5).

1.2 Aims

The overall aim of this thesis is to test whether a recombinant murine cytomegalovirus can vaccinate against MHV-68, using ovalbumin as a shared model antigen.

1.2.1 Specific aims

a) Characterise T cell mediated immune control against MHV-68 in;

    i. BALB/c mice, that make a strong $CD4^+$ T cell response to ovalbumin
    ii. C57BL/6 mice, which make a strong $CD8^+$ T cell response to ovalbumin and a weak $CD4^+$ T cell response.
    iii. F1 mice (BALB/c x C57BL/6), that make comparable $CD4^+$ and $CD8^+$ T cell responses to ovalbumin.

b) Determine whether a recombinant vaccinia virus expressing the MHV-68 gH/gL can protect.
c) Understand how MCMV limits antigen presentation to $CD4^+$ T cells, and how this contributes to host colonisation.
d) Using ORF73-deficient, ovalbumin$^+$ MHV-68, to track antigen-specific $CD4^+$ T cells in an established protection model.

1.3 Literature Review

This review will cover vaccine initiatives against EBV and the use of animal models to understand virus-host interactions that are important for protection against infection. There are many elegant reviews that detail the physical structure, genetic and replicative properties of EBV (2, 6-13) and these are not detailed in this thesis.

1.3.1 Clinical background

EBV pathology is associated with primary infection or reactivating virus in immunocompromised hosts and is the major cause of post-transplant lymphoproliferative disorder (PTLD). PTLD is a complication of solid organ transplants and haematopoietic cell transplants (14-16). PTLDs from solid organ transplants originate from recipient lymphoid cells while in bone-marrow or stem cell transplant, PTLDs are usually of donor origin (15). Most PTLDs studied are of B cell origin, particularly germinal centre B cells and may develop at different times after organ transplant (15, 17, 18). Early onset of PTLDs are usually EBV driven after an episode of primary infection or virus reactivation where EBV oncogenes drive polyclonal B cell proliferation. Late onset of PTLDs which are not always associated with EBV infection are predominately monoclonal lymphoid malignancies (19-21). In EBV driven lymphoproliferation, infected cells are immune targets (22). In these patients, immune function can be restored by administrating Rituximab (anti-CD20) which eliminates B cells that harbour virus, thus reducing virus load (23). Chemotherapy can also be used when Rituximab fails or if tumours are EBV negative (23).

1.3.2 EBV pathogenesis

1.3.2.1 Infectious mononucleosis

Primary EBV infection in children is asymptomatic but in adults manifests as IM, a benign lymphoproliferative disorder characterised by expansion of EBV infected B-lymphoid blasts (24) and proliferation of activated T cells (25). IM symptoms range from; fever, skin lesions, pneumonitis, hepatitis, encephalitis, hemolysis, leukopenia, and thrombocytopenia (13, 26).

1.3.2.2 Burkitt's lymphoma

B cell Burkitt's lymphoma was first characterised by Dr Denis Burkitt while working as a surgeon in Uganda (27, 28). Burkitt's lymphoma is an aggressive form of non-Hodgkin B cell lymphoma derived from germinal center B cells (29). It is characterised by uncontrolled proliferation of malignant cells due to translocation of the c-MYC gene (30). BL is sub-divided into three clinical classification; endemic, sporadic, and immunodeficiency-associated variants distinguishable only by their clinical and geographical presentations (31). Endemic Burkitt's lymphoma occurs predominately in children aged 5 to 8 years along the equatorial part of Africa and Papua New Guinea and accounts for 74% of childhood non-Hodgkin's lymphoma (32). In adults, the sporadic form occurs in Western Europe and in the United States and accounts for 1-2% of all adult lymphomas (33). HIV associated Burkitt's lymphoma accounts for 30-50% of all EBV positive lymphomas worldwide (34). This increase has been attributed to the HIV epidemic (35). Onset of Burkitt's lymphoma leads to the development of high titer IgG antibodies to Burkitt's lymphoma cell line Jiyoye when used as source of antigen (36) and the EBV viral capsid antigen (37).

1.3.2.3 Nasopharyngeal carcinoma

This is a carcinoma associated with the presence of monoclonal EBV episomes in epithelial cells of the nasopharynx (38, 39) and is a major health problem in Southern and Eastern Asia (40). In Southern China and Southeast Asia, the incidence of NPC is relatively high, about 25% compared to the rest of the world, where the incidence is below 1/100,000 per year, in Caucasians from North America and Western Europe (38). NPC peaks at 50-60 years of age but can also be observed in childhood (41). It is more prevalent in men that in women and is independent of race or ethnicity (42). EBV induced NPC is classified in three forms, keratinising squamous cell carcinoma (SCC) type I, a non-keratinising differentiated type II and non-keratinising undifferentiated type III according to the World Health Organisation (WHO) classification of NPCs based on tumour cell morphology by light microscopy (3, 43). Type II (23%) and III (60%) account for most NPC cases worldwide with type 1 accounting for less than 20% of all NPC cancers (38). In NPC, EBV exists in its latent form (3). Patients with type II and type III NPC but not type I also develop high titer IgG and IgA to viral capsid antigens, and EBV early antigen (44). Currently, the standard treatment for NPC is radiotherapy but patients can also undergo chemotherapy or combined chemoradiation therapy in cases of advanced

disease (45, 46). The response to radiation or chemotherapy varies with NPC type (39). In Southeast Asia, particularly in Indonesia, patients diagnosed with type III but not type I NPC at the time of radiotherapy had an overall survival of 70%-80% and 3 years of event free NPC (40).

1.3.2.4 EBV associated gastric carcinoma

The association between EBV and gastric carcinoma (EBVaGC) was first proposed in the early 1990s when DNA from paraffin-embedded block of an undifferentiated lymphoepithelial gastric carcinoma was positive for EBV genome by PCR and was histologically distinct from other carcinomas of the stomach (47, 48). EBVaGC represents 10% of all gastric carcinomas worldwide and is predominately found in males (49, 50). EBV exists as episomes in infected gastric carcinoma cells without active replication (51). How EBV causes gastric carcinogenesis is still not well understood. Nonetheless, there is growing evidence that like *Helicobacter Pylori* (*H.pylori*), EBV is a co-factor in gastric carcinomas (51-53). EBV is also thought to be associated with a number of other malignancies for example acquired immune deficiency syndrome associated B-cell lymphomas, NK/T cell lymphoma, Hodgkin lymphoma. These are critically reviewed elsewhere (9, 11, 34) and not included in this thesis.

1.3.2.5 Multiple sclerosis

The link between EBV and multiple sclerosis (MS) was first proposed in the early 1980s when patients with a history of infectious mononucleosis (IM) developed MS (54). In the early 1990s, relapsing chronic or acute demyelinating disease following IM in five patients was attributed to EBV infection (55). MS risk factors are thought to be high levels of EBV-specific antibodies and onset of IM (56, 57). This was found to be age dependent, with higher titers to EBNA-1 by 25 or later in life predictive of MS (58, 59). Despite these etiological studies, no direct brain infection has been demonstrated raising interesting questions; for example why is MS not prevalent despite EBV infections being common in the population and what causes MS in EBV seronegative patients? (60). Genetic predisposition and age at primary infection or infection with other microbes are possible factors (57). Thus, a cause and effect and a better understanding of the mechanism of how EBV drives or leads to MS is critical particularly in EBV seronegative patients (57, 60).

1.3.3 Transmission

How EBV enters the host is still a matter of debate. Why is this important? Virus entry is the first essential process for the virus to begin replication. Blocking entry into the first target cell subsequently suppresses virus load and provides an attractive vaccination strategy. This was the reasoning behind the glycoprotein 350 (gp350) vaccine to target complement receptor type 2 required for B cell entry (61) as a prophylactic vaccine. This vaccine failed to prevent transmission and persistence associated with EBV pathogenesis. This showed epithelial cell infection precedes B cell infection. And the high prevalence of EBV suggests transmission efficiency between individuals is high. Oral transmission is thought to be the main route of entry because of the presence of virus in the saliva (13, 18, 62). In the mid-1980s to early 1990s when EBV DNA was detected in cervical secretions of women and in urethral discharge of men, sexual transmission was proposed as an alternative route of transmission (63, 64). Thus, identifying a consensus route of entry can inform vaccine design and strategies to block entry and prevent transmission.

1.3.4 Epidemiology of EBV

Identifying risk groups provide key vaccine targets. Epidemiological studies into the risks of acquiring EBV showed an association between sexual intercourse and EBV sero-positivity that correlated with sexual partners in a study of university and college students (13, 65, 66). No study has yet demonstrated a direct link between the presence of EBV in sexually active individuals to either sexual intercourse, kissing or oral-genital contact suggesting that, kissing or sexual intercourse play a role in EBV transmission

1.3.5 EBV replication

EBV is thought to infect and initiate lytic replication in epithelial cells of the oral mucosa that drives viral DNA replication and lytic antigen expression (1). Naïve infiltrating B cells or lymphocytes around the lymphoid tissue that surrounds the oropharynx (67) are then infected and induced to proliferate. This expands the latent pool of infected cells that either differentiate into memory or plasma cells (67). In memory B cells, EBV is transcriptionally silent, and is invisible to the immune system particularly cytotoxic T cell lymphocytes (68). The virus can sporadically reactivate from latency when memory B cells differentiate into plasma cells. What triggers this reactivation is currently unknown? Plasma cells (20) then re-enter the circulation and circulate to peripheral sites to establish latency in epithelial or

B cell sites (1, 69). Latent form of EBV is maintained as a stable viral genome (22) with no detection of lytic replication (2). Immunosuppressed individuals tend to have expansive latently infected memory B cells in the blood than in healthy carriers (68) suggesting frequent reactivation.

1.3.6 Immune responses

T cells are essential to control EBV (67). Innate and adaptive immunity play complementary roles in EBV control. In this thesis, the focus is on cell mediated immunity particularly $CD4^+$ and $CD8^+$ T cells and the vaccine strategies that have been tried.

1.3.6.1 $CD8^+$ T cell responses

In immunocompetent hosts, symptomatic infection that manifests as IM elicits a strong $CD8^+$ T cell response that is effective at limiting virus load. Cytotoxic $CD8^+$ T cells target EBV immediate-early or early lytic proteins (BZLF1, BRLF1 and BMLF1) and to some extent latent proteins (EBNA3A, 3B, 3C and LMP2). These protein targets were identified using *in vitro* assays involving rechallenging polyclonal $CD8^+$ T cell lymphocytes isolated from peripheral blood or by direct detection using peptide-specific MHC I tetramers (22, 70-73). How $CD8^+$ T cells restrict virus replication in immunosuppressed individuals, is not clear. During latency as virus load decreases, $CD8^+$ T cells become less effective, in part due to immune evasion. EBV encodes several genes that interfere with HLA-1 processing and antigen presentation; BNLF2a inhibits peptide and ATP binding of TAP (74), BGLF5 shuts off host protein synthesis (75) and BILF1 downregulates HLA-1 (76). These processes interfere with HLA-I antigen presentation and modulate the $CD8^+$ T cell immune responses to EBV. However, whether these genes directly influence the $CD8^+$ T cell response *in vivo* remains to be determined.

1.3.6.2 $CD4^+$ T cell responses

$CD4^+$ T cell responses to EBV are not well characterised but are predominately directed to enhancing B cell maturation and differentiation necessary for high affinity antibody production (22) and in generating and maintaining memory $CD8^+$ T cells (77). Cytotoxic $CD4^+$ T cells have been reported to EBV lytic (78) and latent epitopes LMP1 and LMP2 (79). These have been characterised *in vitro* using vaccinia viruses expressing lytic or latent EBV proteins on B lymphoblastoid cell lines (B-LCL) or dendritic cells (DCs) or EBV-transformed LCL established by infecting peripheral blood lymphocytes (78). Attempts to

determine the $CD4^+$ T cell cytotoxic response to EBNA1 found no cytotoxic activity when B-LCL cells were infected with vaccinia virus expressing EBNA1. $CD4^+$ CTLs were unable to lyse EBV-infected B cells suggesting that EBNA1 may not be endogenously processed and presented to the host $CD4^+$ CTL (80). Whether these cytotoxic $CD4^+$ T cells are even readily detectable *in vivo* remains to be determined. $CD4^+$ T cells from patients with IM showed a burst in frequency of effector $CD4^+$ T cells that declined with a small proportion persisting during chronic infection (81). Expansion and inflation of EBV-specific $CD4^+$ T cells was found to correlate with peripheral blood EBV load suggesting $CD4^+$ T cell responses to EBV are antigen driven (82).

1.3.6.3 Vaccination

Glycoprotein 350 (gp350) as a prophylactic vaccine failed to prevent transmission and persistence associated with EBV pathogenesis (23). In China, a single dose of gp350 expressed by a vaccinia virus conferred no protection to EBV seronegative vaccinated children (83). A single-phase two trial of a recombinant subunit gp350 vaccine reduced the rate of IM in healthy EBV seronegative young adults but could not prevent asymptomatic infection (84, 85). Similarly, vaccination of children with chronic kidney disease awaiting organ transplant was found to be ineffective (86).

The failure of EBV glycoprotein gp350 to confer protection has led to alternative approaches to improve efficacy or use peptides directed against other EBV proteins to elicit cellular mediated immune responses. Thus, a $CD8^+$ T cell epitope based vaccine against a latency associated protein EBNA3 was well tolerated with no side effects (87). Four out of eight EBV seronegative vaccinees seroconverted and had no symptoms of IM (87). *Ex vivo* IFN-γ ELISPOT confirmed vaccine induced response in three of the vaccinees. However, due to the small sample size, it is difficult to correlate protection to immune response induced by the vaccine.

Other EBV glycoproteins such as gp42 that binds to HLA class II molecules as a receptor (88) and gH/gL that is thought to interact with integrin receptors (89) have also been shown to be targets for neutralisation. Monoclonal antibodies directed against gp42 inhibited B cell infection while gH/gL inhibited epithelial cell infection (90). Recently a tripartite nano-particle based vaccine targeted against gH/gL/ gp42 showed promising results *in vitro* and generated high titer antibodies in mice (91). No human trials have been performed to date.

1.4 Animal model systems for EBV vaccination studies.

To understand how new vaccine combinations work, and which vaccine platforms to use, animal models are critical as proof of concept and to reveal mechanisms of control since host specificity has hindered vaccine design.

1.4.1 Rhesus Lymphocryptovirus

EBV, unlike all gamma-1-herpesviruses (lymphocryptovirus) is not present in all primates (92, 93). Gamma-2-herpesviruses (rhadinoviruses), which includes KSHV and MHV-68, occur in all mammals (94). Rhesus lymphocryptovirus is the main primate model for EBV and reproduces key aspects of human EBV infection; atypical lymphocytosis, lymphadenopathy, latent infection in peripheral blood, and virus persistence in oropharyngeal secretion (95). Vaccination of rhesus monkeys with soluble gp350 to mimic gp350 vaccinations in humans, reduced the level of LCV DNA loads in blood months after LCV infection (96). In contrast, rhesus monkeys that received virus like replicon particles to latent antigens EBNA-3A and EBNA-3AB to model $CD4^+$ and $CD8^+$ T cell induced protection, were ineffective in reducing virus loads (96). The results showed that although gp350-specific responses targeted lytic infection they had no effect on persistent infection. Priming $CD4^+$ and $CD8^+$ T lymphocytes against latent epitopes had no anti-viral effect. These findings are consistent with human EBV vaccine trials and demonstrates the low antigenicity and limited efficacy of epitope and soluble vaccines.

1.4.2 Live attenuated vaccines

Live attenuated vaccines have now been shown to be effective and have had major impact on human health against acute virus infections, particularly influenza, rotavirus, measles, mumps, yellow fever and polio (97). Developing vaccines against persistent viruses have posed significant challenges throughout history because of safety concerns. The only successful herpesvirus vaccine against a persistent virus is the live attenuated vaccine against varicella zoster virus, a herpesvirus related to herpes simplex 1 and 2. The vaccine was slow to develop because of technical difficulties, identifying markers for virus attenuation, evaluating the risk of vaccine morbidity and mortality in healthy individuals and the duration of immunity following vaccination (98). The anti-viral treatment of choice, acyclovir, provides minimal benefits, reinforcing the need for prevention-based therapy using a vaccine that was safe and effective. In 1974, the first clinical trial of a live

attenuated varicella zoster Oka strain in 70 healthy individuals was tested in Japan (99). Subsequently, the vaccine was licenced for general use in 1988 and showed promise in immunocompromised individuals (99, 100). It was then licenced in the US in 1995 for persons 12 months of age and older (101). The mechanism of action is still not well understood. Protection is thought to be mediated by antibody directed against structural glycoproteins, nucleocapsid and tegument proteins based on *in vitro* neutralising assays (98). Nevertheless, more than 90% of vaccine responders maintain antibody for at least 6 years (99) and it is well tolerated and safe (101).

A live attenuated EBV vaccine has not yet been tried. Since EBV is an oncogenic virus, a live attenuated vaccine poses potential risk. Thus, a replication deficient recombinant vaccine vector targeting lytic and latent epitopes of EBV seems essential. This is difficult to do in humans. The poor characterisation of EBV infection processes and host specificity further hinders vaccine design and testing. Thus, to develop strategies, animal models are critical to elucidate the biology of vaccine targets, vaccine vectors, mechanism of action and demonstrate safety.

1.4.3 Murine gamma-herpesvirus 68

Murine gamma-herpesvirus 68 (MHV-68) also known as (Murid Herpesvirus-4) was first isolated from bank voles in Slovakia and found to cause cytopathic effects (CPE) in epithelial and fibroblast cell lines (102). MHV-68 infects B cells and becomes latent with sporadic reactivation. This was demonstrated in NSO, a mouse myeloma cell line, and A20, a B cell hybridoma cell line derived from lymphoma *in vitro* (103). Similar to EBV, MHV-68 causes IM like syndrome, splenomegaly (enlargement of the spleen due to B cell expansion), lymphoproliferative disease (proliferation of B cells in the lymph nodes), persists in memory B cells and causes $CD8^+$ T cell peripheral lymphocytosis (103-105). It is a naturally occurring herpesvirus of wild rodents and readily infects laboratory mice, the least expensive, easy to handle and ethically less challenging animal model to work with to develop a basic understanding of what could work against EBV (105). MHV-68 is also genetically related to Epstein-Barr virus (105). About 80% of their genes are close homologs (106). However, due to host adaptation, these viruses have evolved divergent functions specific to their respective hosts. Thus, MHV-68 as an EBV model is limited to understanding mechanisms of host colonisation and protection but not efficacy or safety of vaccines.

1.4.3.1 Normal infection

How MHV-68 colonises the host has been characterised. The virus infects via the upper respiratory track causing epithelial nose infection, specifically the olfactory neuroepithelium (107-109). The neuroepithelium is a poorly characterised site, but is targeted by HSV-1(110) and MCMV (111) suggesting, it is an important site for herpesvirus entry. The virus can also infect alveolar epithelial cells in the lungs after lower respiratory tract intranasal inoculation under anaesthesia (105, 107, 112). MHV-68 causes no infection when given orally (107). Sexual transmission has recently been demonstrated in naïve males caged with latently infected females (113).This raises interesting questions on whether sexual transmission is a normal route of transmission for all gamma-herpesviruses as postulated for EBV. However, this is unlikely to be the most common natural route of infection.

To model natural EBV infection in humans, MHV-68 is given via the i.n route without anaesthesia, delivery is inefficient, most of the virus gets swallowed and infection is slow to develop while in anesthetised mice, virus delivery to the lungs is more controlled as delivery is effective (107, 109). In this thesis, both upper and lower respiratory tract inoculations are used, with lower respiratory tract infection serving as a positive control because of its convenience and reproducibility to better understand immune responses.

Acute primary lytic infection in the nose or lung, seeds the virus to the superficial cervical lymph nodes that drain the nose or the mediastinal lymph nodes (SCLN or MLN) that drains the lungs. In these lymph nodes, B cell proliferation is induced by cells that traffic virus from the nose or lung (107, 114, 115). Infection then progresses to the spleen where there is extensive B cell proliferation (103). The timing is dependent on dose and route of infection (107, 109). After lung inoculation, spleen infection peaks 13 to 14 days post infection and reaches steady state by day 30 (109, 116) . After nose infection however, peak spleen infection occurs after 20 days (109). MHV-68 persists in memory B cells (117). Most of this infection is latent, the genome is stably maintained without new virus production. B cell differentiation to plasma cells lead to sporadic reactivation in submucosal sites, but what triggers reactivation is unknown. During latency, macrophages and dendritic cells have a less stable form of latency, with strong tendencies to reactivate (118, 119). Epithelial and fibroblast infections are predominantly lytic *in vitro*. *In vivo*, virus behaviour in these cell types is still not well characterized. B cell infection seeds MHV-68 to the bone marrow (120). Whether it infects myeloid stem cells in the bone marrow to establish a more stably persistent myeloid infection is unknown. Immature B cells isolated

from the bone marrow have shown to exhibit high frequencies of stable latent infection. Interestingly, circulating mature B cells detected in the BM, 15, 42 and 48 days post i.n or i.p infection show that developing B cells harbor viral genome through persistent infection and then immigrate to the periphery and seed tissues (120).

1.4.3.2 Immune response to MHV-68

The normal immune response to MHV-68 will be addressed with emphasis on $CD8^+$, $CD4^+$, antibody response and IFN-γ which indirectly or directly influence responses required to develop vaccine strategies against EBV.

1.4.3.3 $CD8^+$ T cell responses

In $CD4^+$ T cell depleted or $CD4^+$ deficient mice, $CD8^+$ T cells have little effect on lymphoid infection and provide no protection against lytic infection (112, 116, 121). This is despite large numbers of $CD8^+$ T cells responding to lytic epitopes p56 and p79 (122). Similar to EBV, MHV-68 expresses a number of immune evasion genes, particularly K3 and M3 that interfere with virus clearance during lytic infection (123, 124). K3 is a viral gene that encodes a zinc-finger-containing protein. It reduces the half-life of newly synthesised MHC I molecules, hence blocking antigen presentation to $CD8^+$ T cells, while M3 binds a board spectrum of host chemokines which may block recruitment of $CD8^+$ T cells into lymphoid organs. These inhibitory effects restrict $CD8^+$ cytotoxic T lymphocytes, particularly during expansion of latently infected B cells (123, 124). The long-term importance of $CD8^+$ T cells was addressed by infecting beta-2-microglobulin-deficient mice. These mice had increased lymphoid infection and developed B cell lymphomas (125). MHV-68 was not present in all tumours, a sharp contrast to EBV where essentially all tumour cells have EBV genomes. These studies show that $CD8^+$ T cells are required to limit latent infection during lytic infection and are subjected to multiple viral evasive strategies similar to those described for EBV.

1.4.3.4 $CD4^+$ T cell responses

A major function for $CD4^+$ T cells is to provide B cell help in the production of virus-neutralising antibody responses (103, 126). $CD4^+$ T cells can also direct effector functions via cytokine secretion (IFN-γ and TNF-alpha) and kill infected cells via fas/fas-ligand interaction (121, 127). However, a further complication with MHV-68 is the observed exploitation of $CD4^+$ T cell help to drive non-specific B cell lymphoproliferation following *in*

vivo infection (103, 128, 129). This effect was ablated in CD40L deficient mice and in chimeric mice lacking MHC II specifically in B cells (128), implying $CD4^+$ T cells require cognate antigen binding to drive B cell maturation and proliferation. The specificities of $CD4^+$ T cells that drive virus-specific and non-specific B cell proliferation are unknown. Furthermore, how $CD4^+$ T cells control infection at the site of entry- the nasal neuroepithelium is also not yet characterised.

In the lungs of immunocompetent BALB/c mice, virus is cleared after 7 to 10 days while in $CD4^+$ T cell depleted mice, virus is cleared after 10 to 20 days (112). In $CD4^+$ and $CD8^+$ depleted mice, MHV-68 infection is fatal (112), demonstrating that $CD4^+$ and $CD8^+$ T cells are important in controlling lytic infection. In the spleen, virus replication in $CD4^+$ T cell depleted mice is reduced but there is no effect on long term latency while in $CD8^+$ T cell depleted mice, virus titer in the spleen increased. This was attributed to B cell driven lymphoproliferation (112, 129). Using a C57BL/6 C2D mice genetically deficient for the H-$1A^b$ gene (lacks classical $CD4^+$ T cells), $CD8^+$ T cells were found to control acute lytic replication in the lungs but were unable to control long term infection compared to wild type mice (103, 116). These mice also had reduced splenomegaly and a low-grade, chronic lytic infection because of their lack of antibody response. This study further showed that, for effective control of chronic infection, $CD4^+$ and $CD8^+$ T cells are both important.

A mechanism of how $CD4^+$ T cells control infection was demonstrated in B cell deficient mice. Neutralising IFN-γ in these mice diminished $CD4^+$ T cell response and increased lytic infection that increased mortality (121). This showed that in the absence of B cells, mice could recover from MHV-68 and keep the infection latent. It was only when IFN-γ was neutralised that mice began to die. Since IFN-γ is important for $CD4^+$ T cell effector function, direct $CD4^+$ T cell engagement with infected cells may be the important arm in dealing with gammaherpesvirus infections.

This was further shown in IFN-γ receptor-deficient BALB/c mice (130). However, the absence of IFN-γ in C57BL/6 mice had no effect on latency (131) potentially due to difference in their genetic background or complex unknown interaction between MHV-68 and IFN-γ in C57BL/6 mice (132).

1.4.3.5 Antibody

Antibody mediated control of MHV-68 could be important when virus reactivates from latency and undergoes lytic infection. Thus, preformed antibody to MHV-68 is likely to block lytic infection (132). Adoptive transfer of neutralising and non-neutralising antibody during lytic infection in normal mice and in B cell deficient mice, reduced lytic infection (126, 133). This was mediated by IgG Fc receptor dependent cytotoxicity (133) suggesting that, antibody targets epithelial cell infection.

1.4.3.6 Vaccine strategies in animal models

1.4.3.7 Glycoprotein subunit vaccines

The first vaccination in BALB/c mice to model EBV gp350 used a recombinant vaccinia virus expressing MHV-68 glycoprotein gp150. Glycoprotein gp150 is a positional homologue of gp350 and is expressed during lytic infection (134, 135). This vaccine provided no protection against persistent infection but protected mice against virus induced mononucleosis (136) consistent with EBV gp350 vaccination outcomes in humans and in primate models.

1.4.3.7.1 $CD4^+$ T cell specific epitopes

Subunit MHV-68 vaccines that target $CD4^+$ T cell lymphocytes was trialled. Vaccination with $gp150_{67–83}$ peptide was found to stimulate $CD4^+$ T cells but showed minimal protection against lytic infection in the lungs of C57BL/6 mice (137) and had no protection against latency in BALB/c or C57BL/6 (136-138). The fact that latency was not controlled suggests this peptide is either not abundantly expressed during lytic infection to prime $CD4^+$ T cells or it is not expressed by infected B cells during latency.

1.4.3.7.2 $CD8^+$ T cell specific epitopes

Vaccination against MHV-68 $CD8^+$ T cell lytic epitopes $gB_{604-612}$, $ORF6_{487-495,}$ $ORF61_{524-531}$ and p56 provided acute protection in the lungs of C57BL/6 mice against lytic infection (137, 139). Virus replication in lymphoid organs (MLN and spleen) of p56 vaccinated C57BL/6 mice was delayed, but long-term infection was not prevented (139). An attempt to vaccinate against M2, a latently expressed protein, to protect against long-term infection failed (140).

1.4.3.8 Live attenuated MHV-68 vaccine

Using a similar approach to varicella zoster virus, a live attenuated MHV-68 engineered by removing latency associated genes was highly effective at reducing lytic infection and long term latent loads in both BALB/c and C57BL/6 mice (141-143). Protection was long lived, suggesting $CD4^+$, $CD8^+$ and B cells were are all important. Disrupting this T cell-B cell balance likely impairs protection.

1.4.3.9 Vaccine vectors

Controlling persistent infection requires live attenuated vaccine as demonstrated for varicella zoster virus. The use of cytomegaloviruses as vaccine vectors against HIV has gathered momentum. A live attenuated RhCMV vaccine expressing multiple proteins of SIV (Gag, Rev-Tat-Nef and Env) provided robust life-long SIV-specific $CD4^+$ and $CD8^+$ effector memory T cells even in $RhCMV^+$ macaques. The macaques upon repeated intrarectal challenge, showed resistance to acquisition of SIV compared to controls (144). Interestingly, a recombinant adenovirus vaccine expressing the same proteins provided no protection (145). The $CD8^+$ T cell responses elicited in the RhCMV/SIV vectors, particularly to gag, derive from unconventional antigen presentation via unconventional MHC –E and is under the genetic control of CMV (146, 147).

The vaccine results described above have shown that targeting lytic or latent epitopes alone do not work in preventing MHV-68 infection. Inducing virus-specific antibody only limits the severity of disease in both humans and in animal models. Notably, a live attenuated ORF73 mutant protected mice against persistent infection via an unknown mechanism of action. ORF73 is a latency associated viral gene that regulates viral gene expression and maintains MHV-68 genome as episomes in latently infected dividing B cells (148-153). Further *in vivo* studies of how live attenuated vaccine vectors work is a timely and tractable strategy to evaluate their potential as vaccine candidates.

CHAPTER 2: MATERIALS AND METHODS

2.1 Reagents and consumables

Reagents were purchased from the following companies: Qiagen, Fisher Scientific, Invitrogen, Roche, Sigma-Aldrich (sigma), Thermo Scientific and Mirus. Materials for cell culture and plastic ware were purchased from BD Biosciences, Corning and Sigma. Molecular biology reagents and enzymes were obtained from Roche, Clontech, Southern Biotec, New England BioLabs and Promega.

2.2 Media and solutions

Some solutions were prepared by Research assistants Kimberley Bruce and Clara Lawler

Table 1: Reagents

Name	**Company**	**Composition**
Luria-Bertani (LB) broth	Sigma	40 g of LB powder in 2 L water
2xTY broth	In house	16 g Tryptone, 10 g Yeast extract, NacI 5 g in 1 L pH 6.8
Antibiotics for selection	Sigma	12.5 µg/mL or 10 µg/mL of Chloramphenicol, Kanamycin, Puromycin and Zeocin
Agar	Sigma	Variable
DMEM	Sigma	Dulbecco's Modified Eagle's Medium (DMEM), supplemented with 2 mM glutamine, 100U/mL penicillin, 100 µg/mL streptomycin and 10% fetal calf/bovine serum
RPMI	Sigma	RPMI 1640 medium supplemented with 10% heat-inactivated fetal calf serum, 2 mM L-glutamine, 25 mM HEPES (pH 7.2), 50 µM 2-mercaptoethanol, penicillin (100 U/mL), and streptomycin (100 µg/mL).
CCMB buffer	In house	11.8 g $CaCL_2$, 4.0 g $MnCL_2$, 2.0 g $MgCL_2$, 0.7 g KCL, 100mL glycerol, 1 L water and filter sterilise
2xTY glycerol	In house	16 g Tryptone, 10 g Yeast extract, NacI 5 g +7% (w/v) glycerol

Freezing solution	In house	10% DMSO and 90% heat inactivated FBS/FCS
Carboxymethylcellulose (CMC)	In house	15 g High viscosity CMC + 15 g Low viscosity CMC + 400 mL water + 600 mL PBS, autoclaved at 121^{o}C for 15 minutes
PBS	In house	PBS tablets dissolved in water and autoclaved
0.1% Tween-20/PBS (PBS/T)	In house	2 mL Tween-20, 200 mL 10X PBS and 1798 mL water
0.05% Tween-20/PBS (PBS/T)	In house	1mL Tween-20, 200mL 10X PBS and 1799 mL water
TE buffer	In house	1X of 10X (108g Tris base and 55g of boric acid in 900mL water and 0.5M EDTA (pH 8.0) and adjusted to 1L with water
TAE buffer	In house	1X of 50X (242 g of Tris base and 37.2 g of $Na_2EDTA.(2H_2O)$ in 900 mL water and 57.1 mL of glacial acetic acid, final volume adjusted to 1 L with water)
0.1% thiol Blue	In house	1 g thiol blue in 1 L water
4% PFA/PBS	In house	Dilute 1/4 (4%PFA) in X volume of PBS
1% agarose	In house	0.5 g agarose in 50 mL TBEE

2.3 Bacteria

2.3.1 Bacterial strain

Escherichia coli DH10B (Invitrogen) was used to propagate the BAC^{+} ORF73 deletion mutant (BAC^{+} Δ73) obtained from the UK.

2.3.2 Growth and storage

Liquid cultures of *E.coli* containing plasmids pA M3 sOVA and BAC^{+} Δ73 were grown in LB broth containing kanamycin or chloramphenicol antibiotics at 30^{o}C or 37^{o}C respectively on an orbital shaker at 180 rpm. These cultures were further used for DNA extractions. Bacterial stocks for long-term storage were derived from overnight cultures as above and stored at -80^{o}C in 1 mL 2xTY broth containing 7% (v/v) glycerol. Bacteria were streaked

onto nutrient agar plates and grown overnight at either 30ºC, 37ºC or 42ºC. Single colonies were then picked for subsequent manipulation.

2.4 Making recombinant BAC$^+$ Δ73 mutant using BAC technology

2.4.1 Construction and analysis of shuttle vector and BAC plasmid DNA

Plasmid DNA (containing pA M3 sOVA) was extracted using QIAGEN Miniprep kit from *E.coli* grown on LB broth containing kanamycin. To check for sucrose sensitivity and presence of kanamycin resistant gene in the pA M3 sOVA plasmid, colonies were grown on agar plate containing either 50% sucrose or kanamycin. BAC plasmid DNA was isolated from *E.coli* cultures using an alkaline lysis procedure involving phenol-chloroform, DNA was precipitated with isopropanol, washed with 70% ethanol and resuspended in Tris buffer (10 mM Tris-HCI-1mM EDTA, pH 7.5). 10 µL of purified plasmid DNA was digested using EcoRI, run on 1% agarose gel in TBEE buffer for 1 hr at 110V. 42 µL BAC plasmid DNA was digested using EcoRI and BstEII restriction enzymes and run on 0.8% agarose in TAEE buffer overnight at 30 V.

2.4.2 Preparation of competent DH10B *E.coli* containing BAC$^+$ Δ73

5 mL overnight culture of DH10B *E.coli* containing BAC$^+$ Δ73 were grown in LB broth containing chloramphenicol at 37ºC with shaking was diluted 1/100 and further grown at 37ºC with shaking until log phase. The bacteria were pelleted at 908 x g for 15 minutes at 4ºC. The pellet was resuspended in pre-chilled CCMB buffer- ¼ of the starting culture volume. The bacteria were then incubated on ice for at least 3 hrs. After incubation, the bacteria were pelleted at 4ºC and resuspended in CCMB buffer- 1/12 of the starting culture volume. Aliquots of 100 µL were snap frozen on dry ice and stored at -80ºC for future use.

2.4.3 Recombination MHV-68 BAC$^+$ Δ73 sOVA

For transformation, 100 ng purified psk pA sOVA M3 plasmid DNA which contains the recA gene that allows for replication in recA deficient DH10B *E.coli* and SacB, a negative selection marker in sucrose containing agarose was electroporated into competent *E.coli* DH10B containing the BAC$^+$ Δ73 mutant using heat shock (30 min on ice, 42ºC for 90 secs, on ice 2 minutes). 900 µL of SOB broth were added to the transformed bacteria and cells were incubated for 30 minutes at 30ºC with shaking. 100 µL of the transformed bacterial culture were then plated onto chloramphenicol and kanamycin containing agar

plates and incubated overnight at 30^{o}C. Colonies were replated on chloramphenicol-kanamycin containing or kanamycin containing plates and grown overnight at 42^{o}C. Colonies picked from chloramphenicol-kanamycin plates were again replated on chloramphenicol-sucrose, kanamycin-chloramphenicol and chloramphenicol plates overnight at 30^{o}C. Colonies picked from chloramphenicol-sucrose plate were plated onto chloramphenicol and kanamycin containing plates and grown on LB broth containing chloramphenicol. Plasmid DNA from single cultured colonies were extracted as mentioned above to analyse mutants.

2.4.4 Reconstitution MHV-68 BAC^{+} Δ73 sOVA

BHK-21 cells were transfected with 3 µg of BAC DNA (clone 2, 6, 13, 14, 21 and 24) using TransIT®-LT1 transfection reagent. Briefly, BHK-21 cells were seeded in six well plates in complete DMEM medium overnight at 37^{o}C, 5% CO_2. Complete DMEM medium was replaced with DMEM (containing no streptomycin or penicillin) and incubated for 30 minutes at 37^{o}C, 5% CO_2. 2 mL warm Opti-MEM was added in 2 mL labelled test tubes. To these tubes, 13 µL of lipid mix was added and left for 1 minute at room temperature (RT) and 300 µL of this mix added to labelled 1.5 mL test tubes containing 10 µL of 300 ng/µl BAC plasmid DNA (clone 2, 6, 13, 14, 21 and 24) and incubated for 30 minutes at RT. After 30 minutes, 310 µL of total mix was added to each six well plate and incubated for 2 days. After 2 days, the BHK-21 cells were split. After 3 days, plaques expressing the GFP formed in clones 13, 14 and 21 and complete CPE was observed a day later. Supernatant and cells of reconstituted BAC^{+} Δ73 sOVA recombinant virus constructs (Clones 13, 14 and 24) were harvested by scrapping off cells in 2 mL cryovials using 1 mL pipette tips and stored in -80^{o}C as stocks.

2.4.5 Removal of BAC cassette

To remove the BAC cassette sequence, 2x10^{5} NIH-3T3 expressing Cre were seeded in six well plates and infected with 1 µL or 10 µL of BAC^{+} Δ73 sOVA (clones 13 and 14). After 5 days, the cells were monitored for GFP expression and CPE. Absence of GFP expression confirmed loss of loxP-flanked by the BAC/eGFP cassette removed by Cre recombinase. Wells with complete CPE were harvested by scrapping cells and supernatant in 1.5 mL cryovials and stored in -80^{o}C as master stocks.

2.5 Mice

2.5.1 Facility

C57BL/6 (IA $^{+/-}$), C57BL/6 back crossed (IA $^{-/-}$) (MHC II^{-}), BALB/c, F1 (C57BL/6 crossed with BALB/c), CD169-DTR (diphtheria toxin receptor) and DO11.10 transgenic mice were either bred or housed at the UQ Biological facility at Australian Institute for Bioengineering and Nanotechnology (AIBN), University of Queensland Centre for Clinical Research (UQCCR), School of Chemistry and Molecular Biosciences (SCMB) and Herston Medical Research Centre (HMRC). All procedures and experiments were approved by the University of Queensland Animal Ethics Committee in accordance with the Australian National Health and Medical Research Council guidelines (projects 301/13 and 479/15).

2.5.2 Infections

6 to 12 week old adult male and female mice were sex matched and infected via the intranasal route (i.n) under anaesthesia (isoflurane) with $3x10^4$ (p.f.u/30 µL) in DMEM to study lower respiratory tract infection or without anaesthesia with $1x10^5$ (p.f.u/5 µL) to study upper respiratory tract infection in parallel where necessary. For vaccination or to directly study splenic infection, mice were injected via the intraperitoneal (i.p) route with 10^4-10^6 (p.f.u/100µL). Adoptive transfer was performed by intravenous injection (i.v).

2.5.3 *In vivo* depletions and anti-IFN-γ administration

CD4$^+$ and CD8$^+$ T cells were depleted using rat anti-mouse CD4 clone GK1.5 and rat anti-mouse CD8α clone 2.43 at 200 µg/mouse by i.p injection at 96 hrs, 48 hrs before infection and at the time of infection and every 48 hrs until the time of harvest. IFN-γ clone XMG1.2 was administered via i.p injection (200 µg/mouse) at the time of infection and every 48 hrs until the time of harvest. Depletions were confirmed by either flow cytometry or histology using rat anti-mouse CD4 (RM4-4) and rat anti-mouse CD8β (H35-17.2) and rat anti-mouse IFN-γ XMG1.2.

2.6 Mammalian cell culture

2.6.1 Cell lines

Cells and cell lines used or generated in this thesis are described in the table below

Table 2: Cell and cell lines

Cells	Description
BHK-21	Syrian hamster fibroblast cell line obtained from rapidly growing primary culture of newborn hamster kidney tissue (154).
MEF	Fibroblast cell line isolated from mouse embryos in house by Helen Farrell and is stored in liquid nitrogen. Routinely used for MCMV plaque assays or immunofluorescence.
NIH-3T3	Embryonic immortalised fibroblasts (ATCC). This cell line is used to propagate MCMV.
NIH-3T3 CRE	Embryonic fibroblast cell line that expresses a Cre-recombinase. It is used for the removal of the intervening DNA as Cre-recombines paired loxP sites (155).
BALB/c-3T3	Fibroblast cell line isolated from BALB/c mouse used as a negative control for MHC II expression.
BALB/c-3T3-C2TA	Transduced with C2TA transactivator using retrovirus
RAW 264.7	A monocyte/macrophage cell line isolated from a tumor induced by Abelson murine leukemia virus in adult male BALB/c mice (ATCC).
RAW 264.7 (RAW-C2TA)	Transduced with C2TA transactivator using retrovirus to express MHC II. This is used to study effects of infection on MHC II and characterise recombinant OVA viruses in an antigen presentation assay.
NMuMG	An epithelial cell line isolated from the mammary gland of NAMRU female mouse (ATCC).
293T	An epithelial cell line that is a highly transfectable human cell line derived from the 293-human embryonic kidney (HEK) cell line by insertion of the temperature sensitive gene for SV40 T antigen (American Type culture collection- ATCC).
DO11.10 $CD4^+$ T cell hybridoma cells	A fusion of BW5147 cells with a T cell expressing a T cell receptor that recognises $OVA_{323-339}$ in the context of $I\text{-}A^d$. It is useful to detect expression of the OVA epitope (156).
Cell lines	

BALB/c-3T3-C2TA-M78 4	Transduced with M78 amplified from K181 viral DNA using retrovirus.
BALB/c-3T3-C2TA-M78 2	Transduced with M78 amplified from a plasmid expressing M78 using retrovirus.
RAW-C2TA-M78 4	Transduced with M78 amplified from K181 viral DNA using retrovirus.
RAW-C2TA-M78 2	Transduced with M78 amplified from a plasmid expressing M78 using retrovirus.
RAW-C2TA-M78 Clone E6	Clone generated from the parent line RAW-C2TA-M78 2.

2.6.2 Cell culture

Cells were maintained in Dulbecco's Modified Eagle's Medium, supplemented with 2 mM glutamine, 100 U/mL penicillin, 100 µg/mL streptomycin and 10% fetal calf/bovine serum using flat tissue 75 cm or 150 cm culture flasks. Primary cells particularly for interferon gamma (IFN-γ) responses were maintained in RPMI 1640 medium supplemented with 10% heat-inactivated fetal calf serum, 2 mM L-glutamine, 25 mM HEPES (pH 7.2), 50 µM 2-mercaptoethanol, penicillin (100 U/mL), and streptomycin (100 µg/mL). Cells were passaged by washing confluent monolayers with PBS, detached by incubation with 0.25% (w/v) trypsin/0.004% (w/v) EDTA for 2 minutes at 37^{o}C. Macrophage cells were occasionally detached by scrapping off cells using a scrapper. For trypsin-based detachment, reaction was stopped by adding complete 10% DMEM, and the cells were centrifuged at 536 x g for 5 minutes. The cell pellet was resuspended in fresh complete 10% DMEM and seeded in a new flask at either 1/5 or 1/10 or 1/20 of the total volume.

2.7 Viruses

Viruses used in this thesis are described. All MHV-68 viruses used were derived from strain MHV-68 (102) and MCMV from K181 Perth strain. Unless otherwise stated, all the MHV-68 and vaccinia recombinant viruses were provided by Dr Philip Stevenson, MCMV OVA^{+} viruses by Alec Redwood and MCMV WT and mutants by Helen Farrell and Dr Nicholas Davis-Poynter.

Table 3: Viruses used in the thesis

Gamma-herpesvirus	Description
WT MHV-68	Lacks the loxP-flanked BAC/GFP cassette removed from by passing through NIH-3T3-CRE cells (157).
WT eGFP+ MHV-68	Retains the BAC cassette (155, 157).
WT gM eGFP+ MHV-68	Expresses GFP attached to the C terminus of gM (158).
ORF73- eGFP+ M3 sOVA	Retains the BAC cassette. GFP expression is driven by the M3 promotor (unpublished data described in chapter 5).
ORF73- eGFP- M3 sOVA	Lacks the BAC cassette removed by passing through NIH-3T3-CRE cells. GFP expression is also driven by the M3 promotor (unpublished data described in chapter 5).
WT M3 mOVA MHV-68	Expresses a fusion protein of OVA with the transferrin receptor transmembrane domain, which is efficiently processed and presented to both CD4 and CD8 T cells (159).
WT M3 sOVA MHV-68	Expresses full-length OVA, including its signal sequence under the M3 lytic promotor (160).
WT IiOVA MHV-68	Expresses OVA323-339 peptide in place of the CLIP peptide of mouse invariant chain. OVA323-339 is driven by ORF73 (160).
EFla-eGFP MHV-68	BAC-negative eGFP expressing virus. GFP is expressed under a cellular promoter for polypeptide chain elongation factor 1 alpha (EF1a). Expression is independent of lytic or latent infection (161).
Beta herpesvirus	
WT	K181 Perth strain.
β-gal recombinants	
WT	Expresses β-gal from the M33 intron driven by HCMV IE1 promoter (unpublished).
M78^{-}	Expresses β-gal cassette under the HCMV IE1 protomer at genomic coordinate 111681 within M78 ORF disrupting M78 expression (162).

M33^{-}	Expresses β-gal cassette flanked by HCMV IE1 promoter and poly(A) signals inserted in the M33 coding region (163).
gO^{-}	Expresses β-gal cassette within the gO ORF disrupting M74 (unpublished).
gL^{-}	Expresses β-gal cassette under the control of HCMV promoter inserted within gL ORF by homologous recombination (164).
M131^{-}	Expresses β-gal within the m131 ORF driven by the HCMV IE promoter (165).
M78_CΔ155	Made by inserting β-gal cassette in the ORF of M78 (M78-), then using M78 null as the parent to generate recombinant M78_cΔ155 (162).
HA tagged	
HAM78 (REV)	M78^{-} revertant that express N-terminal HA-tagged onto M78 via homologous recombination (162).
HAM78 cΔ155	Express N-terminal HA-tagged onto M78 via homologous recombination. The virus lacks 155 amino acids from the C-terminus (162).
GFP	
WT	Expresses GFP from the M131 intron under the HCMV IE promoter (166).
M78^{-}	Made by homologues recombination, deleting ORF (coordinates 111084-112499) and expresses GFP from the M131 intron under the HCMV IE promoter.
Independent mutants	
M131^{-}1	Has a premature stop codon in the m131 ORF (165).
M78 orf deletion	Made by homologues recombination, deleting ORF (coordinates 111084-112499) (unpublished).
Vaccinia virus	
Vaccinia gH/gL	Expresses MHV-68 glycoprotein gH/gL.
Vaccinia control	Expresses an irrelevant protein.

2.8 Preparation of virus stocks

2.9 MHV-68

Virus stocks were prepared by infecting BHK-21 cells at a multiplicity of infection (MOI) 0.01 for 4 to 5 days or until CPE was complete. The cells were frozen, thawed and virions pelleted down by ultracentrifugation (33,000 x g, 2 hrs at 4ºC) using Beckman Coulter Avanti-J-26 XP1 centrifuge, and supernatants discarded. Virus pellet was resuspended in 6 mL 10% or 2% complete DMEM and spun down using a low speed centrifugation (245 x g for 5 min at 4°C) to remove cellular debris. Supernatants were stored in aliquots at −80°C. Virus titers were determined by plaque assay on BHK-21 cells.

2.10 MCMV

2.10.1 Working stocks

Virus stocks were prepared by infecting NIH-3T3 cells in 6 well plates at a MOI 0.01 for 3 days or until CPE was complete. The cells were frozen, thawed and supernatant added to a 175 flask. After 3 days, the flask was frozen, thawed and supernatants were centrifuged at low speed (581 x g for 30 minutes) to pellet cells. Supernatants were stored as working stocks and tittered by plaque assay on MEFs.

2.10.2 Concentrated clean stocks

To prepare concentrated stocks, a 175 cm^2 flask of NIH-3T3 cells were infected at MOI 0.01 for 3 days or until CPE was complete. The cells were frozen, thawed and supernatant added to six 175 cm^2 flasks. After 3 days, the flasks were frozen, thawed and supernatants and cells were ultracentrifuged to pellet virions (33,000 x g for 2 hrs at 4ºC) using Beckman Coulter Avanti-J-26 XP1 centrifuge, and supernatants discarded. Virus pellet was resuspended in 6 mL 2% complete DMEM and spun down at low speed (545 x g for 5 minutes at 4°C) to remove cellular debris. Supernatants were stored in aliquots at −80°C and titer determined by plaque assay on MEFs.

2.10.3 Virion detection stocks

To prepare concentrated stocks, a 175 cm2 flask of NIH-3T3 cells were infected at MOI 0.01 for 3 days or until CPE was complete. The cells were frozen, thawed and supernatant added to six 175 cm2 flasks. After 3 days, the flasks were frozen, thawed and supernatants and cells were ultracentrifuged to pellet virions (33,000 x g for 2 hrs at 4°C)

using Beckman Coulter Avanti-J-26 XP1 centrifuge, and supernatants discarded. Virus pellet was resuspended in 6 mL complete DMEM and spun down using a low speed centrifugation (545 x g for 5 minutes at 4°C) to remove cellular debris. Supernatants were stored in aliquots at −80°C. Virus titers were determined by plaque assay on monolayer of MEF cells. Briefly, ten-fold MCMV serial dilutions were added onto MEFs. After 60 minutes of incubation at 37°C, 5% CO_2, complete DMEM medium containing 0.3% CMC was added. After 3 days, cells were fixed in 1%PFA/PBS and stained with 0.1% toluidine blue solution to determine plaque numbers.

2.11 In vitro growth kinetics

2.12 Multi-step growth kinetics- low multiplicity of infection

2.12.1 MHV-68

BHK-21 and RAW-C2TA cells were infected in suspension with BAC^- WT or BAC^- Δ73 sOVA at low MOI 0.01. The production of infectious virus was monitored over a course of seven days. At different times post infection, cells and supernatants were harvested and stored at -80ºC. 500 µL of ten-fold MHV-68 serial dilutions were added onto BHK-21 cells. After 2 hrs of incubation at 37°C, 5% CO_2, complete DMEM medium containing 0.3% CMC was added. After 4 days, cells were fixed in 1% PFA/PBS and stained with 0.1% toluidine blue solution to determine plaque numbers. Virus titer was determined by multiplying the number of plaques by the dilution factor and then by the ratio of volume plated in 1 mL (plaques x dilution factor x 1 mL/0.5 mL).

2.12.2 MCMV

Monolayers of RAW 246.7 and RAW-C2TA cells were infected in triplicates in 24 well plates with WT or $M78^-$ at low MOI 0.01 for 1 hr at 37ºC 5% CO_2. The cells were then washed twice in PBS and fresh 2% complete DMEM medium added. The production of infectious virus was monitored over a course of seven days. At different times post infection, cells and supernatants were harvested and stored at -80ºC for later analysis by plaque assay.

2.13 Multi-step growth kinetics- high multiplicity of infection

2.13.1 MCMV

Monolayers of RAW-C2TA were infected in triplicates in 24 well plates with WT or $M78^-$ at high MOI 1 and centrifuged (536 x g for 30 minutes). The cells were incubated for 1 hr at

37ºC 5%CO_2. After 1 hr, culture media was aspirated, and the cells were incubated in citric acid for 1 minute and washed twice in PBS. 2% complete DMEM medium was added and the cells were incubated at 37ºC 5% CO_2. Production of infectious virus was monitored over a course of 48 hrs. At different times post infection, cells and supernatants were harvested and stored at -80ºC for later analysis by plaque assay.

2.14 Single-step growth kinetics

2.14.1 MCMV

Monolayers of BHK-21, MEFs, NMuMG, NIH-3T3 and RAW-C2TA (seeded at 10^6 cells/well) were left uninfected or infected at different MOI (0.1, 0.3 and 1) with WT GFP or $M78^-$ for 18 hrs at 37ºC 5% CO_2. For RAW-C2TA cells, infection was enhanced by centrifugation (536 x g for 30 minutes) and left for 24, 48 and 72 hrs. To determine level of infection, the cells were washed once in PBS, scrapped off using a pipette and centrifuged (500 x g for 5 minutes). The cell pellets were then resuspended in 200 µL ice-cold PBS and analysed using BD Accurri C6 flow cytometer.

2.15 Viral infectivity assays

2.16 Plaque assay- measure of lytic virus

At different times post infection, organs of interest from infected mice were harvested in 1 mL 10% complete DMEM, frozen at -80ºC, thawed at 37ºC and homogenised in stainless steel strainers or tissue glass dounce homogenizers.

2.16.1 MHV-68

For MHV-68, ten-fold serial dilutions of organ homogenates were co-cultured with BHK-21 cells. After 1 to 2 hrs of incubation at 37°C, 5% CO_2, 10% complete DMEM medium containing 0.3% CMC was added. After 4 days, cells were fixed in 1% PFA/PBS for 1 hr or overnight and stained with 0.1% toluidine blue solution to determine plaque numbers.

2.16.2 MCMV

For MCMV, homogenates prepared as above were briefly centrifuged (8,000 x g for 1 minute) to pellet debris. 200 µL of five-fold serial dilutions of organ homogenates were then added onto monolayers of MEFs seeded overnight in 24 well plates and centrifuged (536 x g for 30 minutes at 28ºC). After centrifugation, the cells were incubated for 1 hr at

37°C, 5% CO_2. After 1-hr incubation at 37°C, 5% CO_2, the medium was aspirated and fresh 2% complete DMEM medium containing 0.3% CMC was added. After 3 days, cells were fixed in 1% PFA/PBS and stained with 0.1% toluidine blue solution to determine plaque numbers.

2.17 Infectious centre assay- measure of latently infected reactivating cells

Latent virus was measured by infectious centre assay, a measure for B cell reactivation in permissive cells. Briefly, for MHV-68, at different times post infection, harvested organs were homogenised in 1 mL complete DMEM using stainless steel strainers. Ten-fold serial dilution of homogenates were co-cultured with BHK-21 cells for 1 to 2 hrs and 4 mLs of 0.3% CMC was then added. After 4 days, the medium was aspirated, and wells fixed in 1% PFA/PBS for 1 hr or overnight and stained in 0.1% toluidine for plaque counting.

2.18 Determining virus titer in infected cells and tissues

Virus titer was determined by multiplying the number of plaques by the dilution factor and then by the ratio of volume plated in 1 mL to determine virus titer per organ per mouse or per mL. Formulae (no of plaques *dilution factor)/ (volume plated/1 mL)

2.19 DNA extraction protocols

2.19.1 Plasmid DNA extraction- miniprep

5 mL overnight cultures of *E.coli* grown in LB broth were centrifuged 908 x g for 15 minutes at RT to pellet cells. DNA was extracted according to manufacturer's instructions (QIAGEN). Briefly, pelleted *E.coli* was resuspended in 250 µL buffer P1 and transferred to a 1.5 mL microfuge tube. 250 µL buffer P2 was then added and mixed by inverting the tube gently 4 to 6 times. 350 µL buffer N3 was then added and again mixed by inverting the tube 4 to 6 times and centrifuged for 10 minutes at 11,000 x g. 800 µL of supernatant was added to a spin column and centrifuged for 60 secs at 11,000 x g. The flow through was discarded and the column was washed with 500 µL buffer PB and centrifuged at 11,000 x g, 60 secs. The flow through was discarded and washed again in 750 µL buffer PE and centrifuged at 13000 for 1 minute to remove residual wash buffer. To elute DNA, 50 µL Buffer EB (10 mM Tris-CI, pH 8.5) was added, left to stand for a minute and centrifuged (11,000 x g for 1 min). The plasmid DNA was then used for subsequent manipulations.

2.19.2 BAC DNA extraction- Alkaline/SDS lysis

200 µL ice-cold P1 (50 mM Tris-Cl, pH 8.0, 10 mM EDTA, 100 µg/mL RNase A) was added to 5 mL overnight cultures of *E.coli* cell pellet and left at RT for 30 minutes. 300 µL P2 (200 mM NaOH, 1% SDS) was then added, the tube was inverted to mix and left to incubate for 5 minutes at RT. 300 µL ice-cold P3 (3.0 M potassium acetate, pH 5.5) was then added, to mix the tubes were inverted a few times and left on ice for 5 to 10 minutes. The samples were then centrifuged (11,000 x g, 10 minutes) and the supernatant was transferred to a new 1.5 mL tube and 500 µL phenol/chloroform added. To mix, the tube was inverted a few times and left at RT for 2 minutes, then centrifuged (11,000 x g, for 5 minutes). The aqueous phase was transferred to a new 1.5 mL tube and 800 µL RT isopropanol added and inverted a few times to mix and left to incubate for 5 minutes at RT and then centrifuged (11,000 x g, for 10 minutes). The supernatant was discarded, and the white pellet washed in 70% ethanol and then centrifuged (11,000 x g, 5 minutes). The ethanol was aspirated, and the pellet left to air dry at RT for 30 minutes. The pellet was then resuspended in 100 µL 10 mM Tris-HCI, pH 8.5.

2.19.3 Viral DNA extraction from cell free virion stocks

Viral DNA from working or concentrated cell free virion stocks was extracted using NucleoSpin® DNA extraction kit (MACHEREY-NAGEL). Briefly, 500 µL of virus (MCMV WT, MCMV mOVA, MCMV sOVA, Vaccinia IiOVA, MHV-68 sOVA, MHV-68 mOVA, MHV-68 IiOVA, MHV-68 Δ73 sOVA and MHV-68 WT) was added to 1.5 mL tubes and spun down (1hr, 11,000 x g at 4^{o}C). Supernatant was discarded, and viral pellet resuspended (200 µL lysis buffer T1, 25 µL Proteinase K solution, 200 µL binding buffer B3), vortex and incubated at 70^{o}C for 10 minutes to denature DNA. 210 µL 100% ethanol was then added, vortexed and applied to NucleoSpin® Tissue Column and centrifuged (11,000 x g, for 1 min). Flow through was discarded and 500 µL of wash buffer (BW) added and centrifuged (11,000 x g, for 1 min). This was repeated using 600 µL of wash buffer (BW). The NucleoSpin® Tissue Column was dried (11,000 x g, 1 min), 100 µL Buffer BE added and incubated for 1 min at RT. DNA was eluted in 1.5 mL tube (11,000 x g, 1 min) and resuspended in TE buffer. DNA yield was determined using nanodrop.

2.19.4 Genomic DNA extraction from tissues

Genomic DNA was extracted from mouse tissues using a wizard genomic DNA extraction kit according to manufacturer's instructions (Promega). Briefly, 300 µL of thawed tissue homogenates from the nose (N), salivary glands (SG), lungs (L), lymph modes (MLN and CLN), spleen (SP) and bone marrow (BM) was added to 1.5 mL labelled test tubes. To this, 600 µL of ice-cold Nuclei lysis solution (120 µL 0.5M EDTA solution pH 8.0, 500 µL of Nuclei lysis solution, 17.5 µL 20mg Proteinase K) was added and incubated at 55^{o}C for 3-hrs. The homogenate was vortexed once every 1 hr and allowed to cool to RT for 5 to10 minutes. Once cooled, 200 µL of Protein Precipitation Solution was added and vortexed vigorously at high speed for 20 seconds and incubated on ice for 5 minutes. The sample was then centrifuged for 4 minutes at 11,000 x g, and 600 µL of supernatant containing DNA was carefully removed and transferred to a new 1.5 mL test tube containing 600 µL of RT isopropanol. The sample was mixed by inverting the tube several times until white thread-like strands of DNA forming a visible mass was observed. DNA was pelleted by centrifugation at 11,000 x g for 1 minute. The pellet was washed in 600 µL RT 70% molecular grade ethanol by inverting the tube several times and centrifuged at 11,000 x g for 1 minute. 70% ethanol was gently aspirated using a pipette and the DNA pellet left to air dry on a clean absorbent paper for 15 to 30 minutes. 100 µL rehydration solution was added to the DNA pellet and incubated overnight at 4^{o}C.

2.19.5 Genomic DNA extraction from blood

Genomic DNA from blood of infected mice was extracted using Promega DNA extraction kit according to manufacturer's instructions. Briefly, 150 to 300 µL of blood was collected in 1.5 mL test tubes containing 20 µL 0.5M EDTA to prevent clotting. The tube was gently rocked to thoroughly mix the blood and then 900 µL of cell lysis buffer was added. The tube was inverted 5-6 times and incubated at RT for 10 minutes to lyse red blood cells. The tubes were then centrifuged for 20 seconds at 11,000 x g. The supernatant was discarded and the whole process was repeated twice or until white pellets were observed. The pellet was then resuspended in 300 µL of nuclei lysis. To lyse the white blood cells, the solution was pipetted 5 to 6 times and incubated at 37^{o}C for 1 hr until clumps were disrupted. The solution was allowed to cool at RT for 5 to 10 minutes. Once cooled, 300 µL of Protein Precipitation Solution was added and vortexed vigorously at high speed for 20 seconds and then centrifuged for 3 minutes at 11,000 x g. 300 µL of the supernatant containing DNA was carefully removed and transferred to a new 1.5 mL test tube

containing 300 µL of RT isopropanol. The sample was mixed by inverting the tube several times until white thread-like strands of DNA forming a visible mass was observed. DNA was pelleted by centrifugation at 11,000 x g for 1 minute. The pellet was washed in 300 µL RT 70% molecular grade ethanol by inverting the tube several times and centrifuged at 11,000 x g for 1 minute. 70% ethanol was gently aspirated using a pipette and the DNA pellet left to air dry on a clean absorbent paper for 15 to 30 minutes. 100 µL rehydration solution was added to the DNA pellet and incubated overnight at 4^{o}C.

2.20 RNA extraction protocol

$1x10^6$ to $2x10^6$ RAW-C2TA, thioglycollate stimulated peritoneal macrophage cells and NIH-3T3 were left uninfected or infected with WT or M78$^-$ GFP at different MOI. Infection of RAW-C2TA and thioglycollate stimulated macrophage was enhanced by centrifugation (536 x g for 30 minutes at 28^{o}C). After 18 hrs (NIH-3T3) or 24 hrs (peritoneal macrophages) or 48 hrs (RAW-C2TA), culture media was aspirated, and cells were harvested in PBS. 100-200 µL was reserved to determine level of infection by quantifying GFP expression using flow cytometry. The remaining cells were pelleted (500 x g for 5 minutes). RNA was extracted using Trizol reagent according to manufacturer's instructions (Life Technology- Invitrogen). Briefly, 400 µL Trizol reagent was added to cell pellet and pipetted up and down several times to homogenise and left to incubate for 5 minutes at RT. 200 µL chloroform was added to the lysate, vortexed for 15 seconds and incubated at RT for 3 minutes. The samples were then centrifuged for 15 minutes at 11,000 x g at 4^{o}C. The colourless aqueous phase was transferred to a new 1.5 mL test tube containing 500 µL RT isopropanol, incubated for 10 minutes at RT and then centrifuged for 10 minutes at 11,000 x g at 4^{o}C. The supernatant was discarded, and the white gel-like pellet washed in 400 µL 70% ethanol by inverting the tube few times and centrifuged at 8,000 x g at 4^{o}C for 5 minutes at 4^{o}C. The supernatant was discarded using a pipette and left to air dry for 10 minutes at 37^{o}C. The pellet was resuspended in 20 to 50 µL water by pipetting up and down and incubated at 55^{o}C on a heat block for 15 minutes. 2 µL aliquot was then analysed for nucleic acid concentration using nanodrop.

2.20.1 DNase 1 treatment

50 ng to 1000 ng RNA was treated with DNase 1 (RNase free) prior to RT-PCR according to manufacturer's instructions (New England BioLabs). Briefly, 50 ng 10 µg RNA was added to 10 µL 10X DNase buffer (100 mM Tris-HCI, 25 mM MgCI2, 5 mM CaCI2 pH 7.6,

at 25°C), 1 µL (DNase 2U/µL) and water to a volume of 100 µL. The samples were mixed and incubated at 37°C for 10 minutes. DNase 1 was inactivated by adding 1 µL 0.5 M EDTA (filtered using a 0.2 µM filter) to a final concentration 5 mM and incubated for 10 minutes at 75°C.

2.20.2 Single strand cDNA synthesis using reverse transcriptase

First strand cDNA synthesis was performed using ProtoScript II First Strand cDNA Synthesis Kit according to manufacturer's instructions (New England BioLabs). Briefly, 1 to 4 µL of DNase treated template RNA (10 ng-1000 ng) was added to 10 µL 2X reaction mix, 2 µL oligo $d(T)_{23}$ VN (50 µM), 2 µL of 10X enzyme mix and 2 µL to 4 µL of nuclease free water, to a total reaction volume of 20 µL. Control samples had no enzyme. The samples were mixed and incubated at 42°C in a water bath or heat block for 1 hr. To inactivate the enzyme, the samples were further incubated for 5 minutes at 80°C, then kept on ice, and stored at -20°C for later analysis.

2.21 Spectrophotometry of nucleic acid

2 µL DNA or RNA or DNase 1 treated RNA was quantified using nanodrop to determine DNA concentration. To equilibrate the machine, 2 µL of RNase-free water was applied and 2 µL rehydration buffer or water used to blank. 2 µL of genomic DNA, RNA or DNase 1 treated RNA was then quantified in ng/µL. Purity index 260/280 ratio was automatically determined during analysis.

2.22 Transcription analysis using PCR

MHC II, beta-2-microglobulin, M33 and IE1 were amplified in a 25 µL reaction to check specificity of the reverse transcriptase. 5 to 10 µL of 1/5 or 1/100 diluted cDNA synthesis with or without reverse transcriptase, 2.5 µL 10X buffer, 0.5 µL dNTPs (10 mM), 0.5 µL each of forward and reverse primers (10 µM), 0.125 µL Taq DNA polymerase. Water was added to a final reaction volume of 25 µL. The samples were run as follows (95°C 1 min, 35 cycles at 95°C 15 secs, 55°C 15 sec, 72°C 30 secs, then 72°C for 7 minutes and 4°C indefinitely. 10 to 25 µL of PCR reaction was mixed in 2-5 µL 1X blue loading dye and run on a 1.5% agarose gel in TAE buffer at 70 to 110V. Bands were visualised using Carestream Gel Logic 212 Pro.

Table 4. RNA primer list

RNA primers to target genes	sequence
M33 Forward	5'GAAACTTCTTAACCTTTCCAACGG 3'
M33 Reverse	5' TCAGGATGATCACCGTGTTGATG 3'
IE1 Forward	5'CGATGCGCTCGAAGATATCATTG 3'
IE1 Reverse	5'AACCGTCCGCTGTGACCTGAC 3'
Beta-2-m Forward	5' GAGACTGATACATACGCCTGCAG 3'
Beta-2-m Reverse	5' TAGACCAAAGATGAGTAACTGCATC 3'
MHC II	5'CATCCACACAGCTTATTAGGAATG3'
MHC II	5'GATGCCGCTCAACATCTTGCTC3'

2.23 Polymerase Chain Reaction (PCR)

Ovalbumin or M78 genes were amplified using PCR in 100 µL reaction (Taq DNA polymerase 1 µL, 10X buffer 10 µL, dNTPs (10 mM) 2 µL, purified DNA 5 µL, forward primer (100 µM) 1 µL, reverse primer (100 µM) 1 µL and 80 µL water). The samples were run as follows (95^{o}C 5 minutes, 30 cycles at 95^{o}C 1min, 55^{o}C 1 min, 72^{o}C 1 min 30 secs, then 72^{o}C 10 minutes and 4^{o}C indefinitely). 10 µL 2 log DNA ladder, amplified PCR products mixed in 8 µL orange loading dye were run on 1% agarose gel (0.5 g LE agarose, 50 mL TBEE buffer, 110V). Bands were visualised using Carestream Gel Logic 212 Pro.

Table 5. PCR primer list

PCR primers to target genes	Sequence
OVA 1 Forward	5'CAAATAAATAAGGTTGTTCGCTTT3'
OVA 2 Reverse	5'CATCCACTCCAGCCTCTGCTG3'
OVA 3 Forward	5'TGCAGATGAGTGACCAGATTGG3'
M78 Forward	5'AAAGAATTCGTCGCCATGCCGACTTCATCGTG3'
M78 Reverse	5'AAAAGATCTCAGACAACAGAGGAGGAGGTAGGC3'
HAM78 Forward (independent)	5'GTCGAATTCTCGCCATGCCGTACCCATAC3'

2.24 Quantitative real-time PCR (QPCR)

Genomic DNA was diluted to 5 ng/µL and a serial dilution of plasmid DNA of varying concentrations containing either K3 (MSCV GFP K3 plasmid) or M78 (B129) was used to generate a standard curve based on calculated copies per reaction. To detect MHV-68 in tissues, K3 primers were used to amplify K3 in MHV-68 infected tissues while M78 to detect MCMV infected tissues. For cellular controls, primers to mtitin was used to amplify connectin from genomic DNA of infected mice tissues. Water was used as no template control. The reaction was performed in a final volume of 20 µL as follows; 10 µL 2X Syber green (Roche), 1.2 µL of primer mix (Forward and Reverse at 10 µM), 6.8 µL sterile water and 2 µL genomic (10 ng) or plasmid DNA of varying dilutions as standards or water. Amplification and real-time green fluorescence detection was performed using Rotor gene 6000 (Corbett Research) using a two-step amplification process using the following protocol: an initial denaturation and polymerase activation step of 10 minutest at 95^{o}C, followed by 40 cycles of denaturation at 95^{o}C for 10 secs, annealing at 60^{o}C for 15 secs and extension at 72^{o}C for 20 secs then melt curve generation 95^{o}C for secs, 60^{o}C for 5 secs and 72^{o}C for 5 secs. The threshold cycle value for each run, and the number of viral DNA copies and cellular DNA copies per sample were obtained using Rotor Gene Software series 1.7.87. Viral load was quantified as the ratio of viral copies/cellular copies per reaction per sample.

Table 6. QPCR primer list

QPCR primers to target genes	**Sequence**
M78 Forward	5’ATCGAGCGTGAGGTACAGGT3’
M78 Reverse	5’CCTAGGGAGCCTCATCCTCT3’
K3 Forward	5’TCTTTGTGGGCTGCTGGGTCG3’
K3 Reverse	5’GGCTGTGCTGATGATAGTGATG3’
mtitin Forward	5’AAAACGAGCAGTGACGTGAGC3’
mtitin Reverse	5’TTCAGTCATGCTGCTAGCGC3’

2.25 Gel electrophoresis

Amplified PCR products or restriction digest products for diagnostics were run on 0.8-1.5% gel in either TAE or TBE buffer supplemented with ethidium bromide (TAEE or TBEE) for DNA visualisation.

2.26 Western blot

NIH-3T3 or RAW-C2TA cells were infected (1 PFU/cell, 24 hrs) with wild type or mutant MCMV or MHV-68 or recombinant OVA MCMV and MHV-68 viruses or left uninfected. For OVA detection, supernatants and floating dead cells were centrifuged at 4^{o}C for 1 hr at 11,000 x g to remove FCS. Supernatant was stored at -20^{o}C as secreted fraction. The pellet was then washed once in PBS and resuspended in lysis buffer (150 mM NacI, 1% Triton x-100, 50 mM Tris-HCl pH 8.0) supplemented with a cocktail of protease inhibitor (SIGMA) or 1 mM PMSF and incubated on ice for 30 minutes. After 30 minutes, the lysate was either centrifuged at 11,000 x g, for 15 minutes to extract the cytoplasmic fraction or left without centrifugation as whole cell lysate. The cytoplasmic or whole cell lysates were stored at -20^{o}C for later analysis. For virions, infected cells were ultracentrifuged at 33,000 x g for 2 hrs at 4^{o}C. The supernatant was discarded, and the pellet resuspended in 2% complete DMEM and centrifuged at 545 x g for 5 minutes. The supernatant was either stored at -80^{o}C or further spun at 21,000 x g for 1 hr to pellet virions. The supernatant was discarded, and the pellet resuspended in 200 µL PBS and stored at -20^{o}C.

To detect OVA or viral proteins, secreted, cytoplasmic and whole cell fractions and virion were mixed in 3X Laemmli's buffer [(4% w/v SDS, 20% glycerol v/v, 10% v/v 2-mercaptoethanol, 0.01% w/v bromophenol blue and 125 mM Tris-HCI pH 6.8)] at a ratio 1:1. For OVA, samples were boiled at 95^{o}C for 5 minutes while virions, cell lysate or whole cell lysate fractions for M78 detection were incubated at 42^{o}C for 5 minutes. All samples were resolved by 10-12.5% SDS-PAGE (3.75 mL 1.5M Tris-HCI, pH 8.8, 4.2 mL 30:1 Acrylamide base, 2.05 mL deionised water, 50 µL 10% APS, 5 µL TEMED and 100 µL 10% SDS) on a 4% stacking gel (1mL 1M Tris-HCI, pH 6.8, 1 mL 30:1 Acrylamide base, 5 mL ionised water, 5 µL TEMED and 100 µL 10% APS) using a power Pac 1000 (Bio-Rad) gel system in SDS-PAGE running buffer (25 mM Tris-HCI, 12 mM glycine, 0.1% w/v SDS) at 174V for 30 to 40 minutes. The membrane was then transferred onto 0.45 µM PVDF membrane (activated in methanol for 1 minute) at a constant current 250 mA for 1 hr. The membrane was blocked in 10% skim milk/PBST for 1 hr at RT with gentle rocking and

probed with a number of antibodies; rabbit anti-OVA pAb (Abcam), rabbit anti-M78, rabbit anti-MCMV, rabbit serum, rat anti-beta-actin and mouse anti-IE1 (chroma 101) in 5%skim milk/PBST overnight at 4^{o}C followed by three times wash in PBST and detection in IRDye® 800CW Goat-anti-Rabbit Antibody IgG (H+L) (LI-COR) or rabbit anti-rat or goat anti-mouse IgG antibodies in 5%skim milk/PBST. Membrane bands were detected using LI-COR odyssey infrared imager.

2.27 Generation of RAW-C2TA and BALB/c-3T3-C2TA expressing cell lines

M78 was amplified from K181 viral DNA and from B53 plasmid that has an HA- tagged M78 to generate an independent M78 clone. M78 was amplified using two sets of DNA polymerases as follows; 3 µL of (15.89 ng/µL viral DNA) or 1 µL (1 ng or 5 ng plasmid DNA), 20 µL 5X Q5 buffer, 2 µL 10 mM dNTP, 5 µL 10 µM Forward and Reverse, 1 µL Q5 DNA polymerase and water to a final volume of 50 µL. OneTaq DNA polymerase was also used for amplification as follows; 20 µL 5X OneTaq buffer, 2 µL 10 µM dNTP, 2 µL 10 µM Forward and Reverse, 0.5 µL One Taq polymerase, 3 µL (15.89 ng/µL viral DNA) or 1 µL (1 ng or 5 ng) plasmid DNA and water to volume of 100 µL. The PCR reaction was performed as follows: 95^{o}C 5 minutes, 35 cycles of 95^{o}C 30 secs, 55^{o}C 30 secs, 72^{o}C 1 min 45 secs and 7 minutes extension at 72^{o}C, and indefinitely at 4^{o}C.

2.27.1 PCR purification

Q5 PCR amplified products were purified as follows according to the manufactures instructions (MACHEREY-NAGEL); Briefly, 100 µL of PCR product was mixed in 200 µL NT1 by pipetting up and down and then added to a NucleoSpin column and centrifuged (11,000 x g, for 30 secs). The flow through was discarded and 700 µL of NT3 was added and centrifuged (11,000 x g, 30 secs). This was repeated, and the silica membrane was dried by centrifugation (11,000 x g, for 1 min). 30 µL of elution buffer was then added to the column, left to stand at RT for 1 minute and centrifuged (11,000 x g, for 1 min). Eluted DNA was quantified using nanodrop and prepared for subsequent manipulation.

2.27.2 Restriction digest

The purified M78 PCR products were then digested with Bg1II and then with EcoRI in a 40 µL reaction as follows; 30 µL PCR purified templates, 4 µL Buffer 3.1, 3 µL BgIII and 3 µL water. The reaction was performed at 37^{o}C on a water bath for 2 hrs, then PCR purified as above. 30 µL PCR purified BgIII digested product was then digested with EcoRI-HF as

follows; 30 µL PCR purified templates, 4 µL EcoRI Cutsmart buffer, 3 µL EcoRI-HF and 3 µL water. The reaction was performed at 37ºC in a water bath for 2 hrs. The MSCV vector was also digested as follows; 3 µL vector (1697.03 ng/µl), 4 µL 10X Cutsmart buffer, 2 µL EcoRI-HF and 2 µL BamHI-HF and 29 µL water. The reaction was performed at 37ºC for 1 hr and half. 10 µL loading dye was then added to the 40 µL digested products and run on a gel. Bands corresponding to 1.4kb (M78) and 7kb MSCV vector were excised and gel purified. Nucleic acid concentration was determined by nanodrop. Ligation was then performed in a 20 µL reaction as follows; 8 µL of (48.62 ng/µL) MSCV vector, 8 µL of (57.95 ng/uL or 61.75 ng/uL) insert or water (no insert control), 2 µL of DNA ligase buffer and 2 µL T4 DNA ligase and mixed by pipetting up and down and incubated overnight at 16ºC. To inactivate the enzyme, the samples were incubated at 65°C for 10 minutes.

2.27.3 Transformation

50 µL of competent DH5α *E.coli* were thawed on ice and 1 µL of 1/20 dilution (100 ng) of ligation added. The tubes were gently flicked to mix and left on ice for 30 min, 42ºC for 90 seconds and then on ice for 2 minutes. 900 µL of 2TY broth (no antibiotic) was added and incubated for 40 minutes at 37ºC with shaking at 4500 rpm. The bacteria were then plated on 100 µg/ml ampicillin enriched agar plates overnight at 37ºC. Single colonies were then picked and grown on agar and in 10 mL LB broth containing ampicillin. The bacteria were then pelleted at 908 x g for 15 minutes and plasmid DNA extracted using alkaline lysis as described above and DNA concentration quantified by nanodrop.

2.27.4 To confirm ligation and transformation

Plasmid DNA extracted above were digested with EcoRI-HF and XhoI in a 50 µL reaction as follows; 5 µL of 1 to 3 µg plasmid DNA, 5 µL Cutsmart buffer, 2 µL EcoRI-HF RE, 2 µL XhoI RE and 36 µL water to diagnose presence of M78 in the MSCV vector. The samples were incubated at 37ºC for 2 hrs and 10 µL was run on a 1% agarose gel. Positive Plasmid DNA clones were used for transfection.

2.27.5 Transfection

$1x10^6$ 293T cells were seeded in 10 cm culture dish overnight. Transfection was performed according to manufacturer's instructions (MIRUS). Briefly, transfection reagent consisting of 500 µL Optimum and 20 µL transfect Lipid (TransIT®-LT1) was mixed in 1.5 mL tube by gently pipetting up and down. 2 µg of retrovirus packing plasmids PC143N and

PVSVG were then added. To these separate tubes, 1 µg positive DNA clones isolated from transformed *E.coli* generated from either independent M78 clone 2, M78 clone 4 or MSCV vector as control were then added and incubated at RT for 30 minutes. The mix was then added to seeded 293T cells and left to incubate at 37ºC, 5% CO_2 for 24, 48 and 72 hrs for retroviral virions to form.

2.27.6 Transduction of BALB/c-3T3-C2TA and RAW-C2TA

$1x10^6$ BALB/c-3T3-C2TA or RAW-C2TA cells were seeded in 10 cm culture dish overnight. The culture media was removed and 5 mL complete medium containing 10 µg/mL polybrene was added to the cells and 24-hr culture supernatant from retroviral transduced 293T cells filtered through 0.45 µM filter was then added to the cells for a final concentration of 5 µg/mL polybrene. This process was repeated at 48 and 72 hrs post retroviral transfection to maximise retroviral transduction of target cells. The cells were then selected in complete medium containing 10 µg/mL puromycin. Media was changed accordingly and selected resistant cells were frozen in 10% DMSO 90% FCS.

2.28 Generation of clones by limiting dilution

Continuous passage of RAW-C2TA led to loss of MHC II expression resulting in a mixture of MHC II high and MHC II low cells. M78 expressing RAW-C2TA were also found to unequally express M78. To isolate high expressing MHC II or M78 expressing clones, 200 µL of 1/1000 dilution of $4x10^6$ cells/mL RAW-C2TA or RAW-C2TA-M78 cells were added to 96 well plates. This was then diluted 10-fold, and finally 3-fold in 10% complete DMEM containing zeocin or puromycin, a selectable marker for MHC II and M78 expressing cells respectively. The cells were incubated at 37ºC 5%, CO_2 and monitored for growth. Media was changed accordingly. Individual clones were then cultured to scale in 6 well plates and assessed for MHC II and M78 expression using a 96 well immunofluorescence staining format. Briefly, cells were scrapped using a pipette and counted using a hemocytometer, and $2x10^4$ cells from each individual clone was seeded in a 96 well plate and left to adhere for 4 hrs. The cells were then washed twice in PBS and fixed in 1%PFA/PBS for 1 hr and permeablised in 0.1%tritonX-100/PBS for 15 minutes. To detect MHC II or M78, the cells were washed twice in PBS, blocked in 2% normal goat serum (NGS) in PBS for 1 hr and stained with rat anti-MHC II (M5/114) or rabbit anti-M78 sera for 1 hr. The cells were then washed in PBS, stained with Alexa Fluor 594 goat anti-rat or Alexa Fluor 488 goat anti-rabbit in 2%NGS/PBS for 1 hr and then washed. The plates

were viewed under a fluorescence microscope. Clones positive for MHC II or M78 expression were further cultured to scale and analysed for MHC II expression using flow cytometry or M78 using microscopy. Clones expressing 95 to 100% MHC II or M78 were frozen. RAW-C2TA clones were tested for their ability to secrete nitric oxide (NO_2) and present $OVA_{323-339}$ peptide to simulate $CD4^+$ T cell hybridomas to secrete IL-2. M78 expressing RAW-C2TA were further manipulated by microscopy to determine MHC II redistribution.

2.29 NO_2 test

10^6 cells (RAW-C2TA clones, NSO, BALB/c-3T3, and BALB/c-3T3-3T3-C2TA) were seeded in 24 well plates and left to adhere. The cells were then treated with 250 µL (1 mg/ml) LPS or left untreated and incubated overnight at 37^{o}C, 5%CO_2. NO_2 release was detected according to manufactures (Sigma) instructions. Briefly, 80 µL of culture medium from each well was added to 96 well plate in duplicates. $NaNO_2$ standard solution 100 µM (0.1 nmole/µL) was added as 0, 20, 40 and 80 µL in duplicates. Solution buffer was then added to each sample well and standards to bring the reaction volume to 100 µL. 50 µL of Griess reagent A was then added to the wells and left to incubate at room temperature (RT) for 5 minutes, then 50 µL of Griess reagent B was added and incubated for another 10 minutes on a horizontal shaker. Absorbance was read at 570 nm using POLARstar® Omega Plate Reader Spectrophotometer (BMG Labtech; ex 400 nm, em 505 nm; 37°C)

2.30 Antigen presentation assay

I-A^d-restricted, $OVA_{323–339}$-specific DO11.10 CD4+ T cell hybridoma cells respond to ovalbumin by expressing the $OVA_{323-339}$-specific T cell receptor (Tcr) (156). This receptor binds $OVA_{323-339}$ peptide complex presented on MHC class II (1-A^d/1-A^b) by antigen presenting cells (pAPCs) (156). To test CD4+ T cell stimulation, uninfected BT3 and RAW C2TA cells were incubated with ten-fold serial dilution of $OV_{A323-339}$ peptide in the presence of $OVA_{323–339}$-specific DO11.10 hybridoma cells. To determine presentation of $OVA_{323-339}$ peptide in infected cells, the following procedures were employed;

2.30.1 BALB/c-3T3-C2TA

$3×10^4$ H2d BALB/c-3T3-C2TA cells were left uninfected or were infected MOI 0.3 with WT or OVA-expressing MCMV or MHV-68 recombinants in the presence of $3×10^4$ I-Ad-restricted, $OVA_{323–339}$-specific DO.11.10 hybridoma cells. Uninfected controls were co-

cultured in the presence of $OVA_{323–339}$ peptide. After 24 hrs, supernatants were harvested and assayed for IL-2 by ELISA.

2.30.2 RAW-C2TA

$3×10^4$ H2d RAW C2TA cells were left uninfected or were infected MOI 2 with WT or OVA-expressing MHV-68 recombinants or with 1 P.F.U/cell WT or OVA-expressing MCMV. After 96 hrs, $3×10^4$ I-Ad-restricted, $OVA_{323–339}$-specific DO.11.10 hybridoma cells were added to each well. Uninfected controls had 10-fold serial dilutions of $OVA_{323–339}$ peptide. After 24-48 hrs, supernatants were harvested and assayed for IL-2 by ELISA.

2.31 Enzyme-linked immunosorbent assay (ELISA)

2.31.1 IL-2

96 well EIA/RIA flat bottom without lid High Binding Polystyrene non-sterile (Corning Incorporated, NY) plates were coated with rat anti-mouse IL-2 mAb (clone JES6–1A12, BD-Pharmingen) overnight at 4°C in 50 mM $NaHCO_3$ pH 7.6 overnight at 4°C. The plates were then washed five times in 0.1% PBS/Tween-20 and blocked in 2%BSA/PBST (1hr, 37°C). Captured IL-2 was detected with biotinylated mAb JES6–5H4 (BD-Pharmingen) (1hr, 37°C), washed five times in PBST and incubated with streptavidin-conjugated alkaline phosphatase (BD-Pharmingen) for 1hr at 37°C, washed five times with 0.1%Tween-20/PBS and developed using nitro-phenyl-phosphate substrate (Sigma) (30 minutes, RT) in the dark. Absorbance was read at 405 nm using SPECTRA MAX 190 ELISA plate reader (Bio-strategy).

2.31.2 Preparation of sera from mouse blood

Blood was collected in 1.5 mL tubes from alert mice by tail bleed or from the peritoneum cavity during surgery. Briefly, for tail bleeds, mice were exposed to mild heat using a heat lamp to increase blood circulation. 5 mm of tail was then cut using a razor and blood was collected in 1.5 mL test tubes. During surgery, blood was collected from the peritoneum cavity following excision of the main blood vessel that supplies the abdominal organs. The blood was allowed to clot at RT for 2 to 4 hrs. After clotting, the blood was centrifuged at high speed (11,000 x g for 1 minute). Top layer sera were transferred to a new tube and stored at -20°C for later analysis.

2.31.3 IgM and IgG

96 well EIA/RIA flat bottom without lid High Binding Polystyrene non-sterile (Corning Incorporated, NY) plates were either coated with MHV-68 or MCMV lysate or OVA (Abcam) overnight at 4ºC in 50 µL 50 mM $NaHCO_3$ pH 7.6 overnight at 4ºC. The plates were then washed five times in 0.1% PBS/Tween-20. For MHV-68 or MCMV specific antibody, plates were blocked in 2%BSA/PBST (1hr, 37ºC) while OVA-specific response plates were blocked in 10%skim milk/PBST. Sera were diluted 1/00 in PBS and then serially diluted 3-fold in either 2%BSA/PBST or 5%skim milk/PBST. 100 µL was then added to each well in each respective plate and incubated for 2 hrs at 37ºC. The plates were then washed four times in PBST and incubated with 50 µL of either goat anti-mouse IgM (Southern Biotech) or IgG (SIGMA) conjugated alkaline phosphatase for 1 hr at 37ºC, washed five times in PBST and developed using nitro-phenyl-phosphate substrate (Sigma) (30 minutes to 2 hrs at RT) in the dark. Absorbance was read at 405 nm using Spectramax 190 ELISA plate reader (Bio-strategy).

Table 7. IL-2 ELISA detection antibodies

IL-2 detection	Manufacturer and batch	Reactivity/isotope	Stock (mg/mL)	Working concentration
Anti-Mouse IL-2 (JES6-1A12)	BD Pharmingen 554424	Rat IgG2a	0.5	1:500
Recombinant IL-2	BD Pharmingen 550069	Mouse	0.2	1:1000- serial dilution starting 1:128 to 1:2048
Biotin Anti-Mouse IL-2 (JES6-5H4)	BD Pharmingen 554426	Rat IgG2b	0.5	1:2000
AKP streptavidin	BD Pharmingen 554065		1	1:2000-5000
Antibody detection				
Ovalbumin	Millipore AB1225	Rabbit pAb	10	1:400
MHV-68 lysate	In house	Mouse	N/A	1:400

MCMV lysate	In house	Mouse		1:400
IgM	Southern Biotech 1021-04	Goat	N/A	1:2000
IgG	Sigma 051M4891	Goat	N/A	1:2000
IgG1	Southern Biotech 1070-04	Goat	N/A	1:2000
IgG2a	Southern Biotech 1080-04	Goat	N/A	1:2000
IgG2b	Southern Biotech 1090-04	Goat	N/A	1:2000

2.32 The Enzyme-Linked Immunospot assay (ELISPOT)

2.32.1 Coating plates

96 well plate IP sterile white plates 0.45 µM Hydrophobic High Protein Binding Immobilon-P PVDF membrane (Merck Millipore, Ireland) were activated in 50 µL 70% ethanol for 2 minutes, washed four times in 200 µL PBS and coated with 50 µL rat anti-mouse IFN-γ mAb (clone R4-6A2; BD-Pharmingen) in PBS and left overnight at 4^{o}C. On the day of the assay, the plates were washed five times in PBS and blocked in complete RPMI medium until target cells were prepared for incubation.

2.32.2 Ficoll plaque gradient lymphocyte isolation

Uninfected and infected spleens, lymph nodes, lungs or noses were harvested, homogenised and single cell suspensions were graded on ficoll-paque density gradient media and centrifuged (20 minutes at 281 x g at 20^{o}C) to separate serum, lymphocytes, monocytes and blood. The lymphocyte fraction was washed once in PBS (8 minutes at 281 x g at 20^{o}C) and again in complete DMEM (5 minutes at 245 x g at 20^{o}C) and resuspended in complete RPMI medium.

2.32.3 $CD4^{+}$ T cell enrichment using Mouse Depletion Dynabeads

To enrich $CD4^{+}$ T cells, Ficoll plaque gradient isolated lymphocytes above were resuspended in isolation buffer (2%FCS/PBS supplemented with 2 mM EDTA) and

enrichment of $CD4^+$ T cells performed using manufactures instructions (Invitrogen). Briefly, 500 µL-1 mL leucocytes (10^7-10^9 cells) were incubated in 100 µL heat inactivated FCS supplemented with 50 µL antibody mix which contains a cocktail of rat monoclonal antibodies against mouse CD8, CD45R (B220), CD11b (Mac1), Ter-119 and CD16/CD32 (Life technologies). The cells were then mixed and incubated at 4°C for 20 minutes. After incubation, the cells were washed in isolation buffer and centrifuged (5 to 8 minutes at 500 x g at 4°C). The cell pellet was resuspended in 1 mL isolation buffer and incubated with 500 µL pre-washed Mouse Depletion Dynabeads (are superparamagnetic polystyrene beads of 4.5 µM diameter) coated with a polyclonal sheep anti-rat IgG antibody and incubated for 15 minutes at RT with gentle tilting. 4 mLs isolation buffer was then added to the bead bound cells, resuspended by pipetting using a pipette and placed in a magnet for 2 minutes. Supernatant containing the untouched $CD4^+$ T cells were transferred to a new tube, centrifuged (5 minutes at 245 x g at 4°C), resuspend in RMPI medium and counted.

For ovalbumin specific IFN-γ response, naïve target cells were either left untreated or incubated with 5 µM $OVA_{323-339}$ peptide (InvivoGen) or 10 µM $OVA_{257-264}$ (InvivoGen) or infected with MHV-68 mOVA (MOI 3) in suspension. The cells were then irradiated at 2000 rads using a GC220 irradiator. For virus specific responses, naïve target cells were infected with MCMV (MOI 1) or MHV-68 (MOI 3) in suspension and irradiated as above. Infected target cells were left to incubate for 2 hrs at 37°C, 5% CO_2. After 2 hrs, the cells were washed once in PBS and in complete RPMI medium. The cells were then resuspended in complete RPMI medium and 100 µL of $2x10^5$ cells were then added to the coated and blocked 96 well plate and incubated at 37°C, 5%CO_2 until effector cells were ready. 100 µL of 3-fold serial dilutions ($1x10^5$ to $1x10^4$) $CD4^+$ T cell enriched or unenriched effector cells from MHV-68 mOVA, MHV-68 or MCMV WT or $M78^-$ infected mice were then added to the seeded target cells respectively. The plates were incubated at 37°C, 5%CO_2 for 48 hrs. After 48 hrs, the wells were washed twice in deionised water for 3 to 5-minute intervals, three times in 0.05% Tween-20/PBS (PBST) and captured IFN-γ was detected with biotinylated rat anti-mouse IFN-γ mAb (clone XMG1.2; BD-Pharmingen) in 10% FCS/PBS at RT for 2 hrs. The wells were then washed four times in PBS/T and streptavidin-conjugated alkaline phosphatase (BD-Pharmingen) supplemented in 10% FCS/PBS was added and left to incubate at RT for 1hr. The wells were then washed four times in PBST and three times in PBS. Parafilm was applied to the bottom of the plate and the membrane bound plate firmly attached onto the parafilm to minimise background. 50 µL of 5-bromo-4-chloro-3-indolyl phosphate/nitro-blue tetrazolium substrate (Sigma-Aldrich

Co. LLC) dissolved in water was then added to each well and left to develop at RT. The reaction was stopped by washing the wells in running water. The plates were then left to air dry overnight and spots were manually enumerated using a dissecting microscope. Background spots from uninfected wells were averaged and subtracted from spots in treated wells.

Table 8. IFN-γ detection peptides and antibodies

IFN-γ detection	Manufacturer and batch	Reactivity /isotope	Stock (mg/mL)	Working concentration
$OVA_{323-339}$	InvivoGen	vac-isq	1	1:100
$OVA_{257-264}$	InvivoGen	vac-sin	1	1:100
Anti-Mouse IFN-γ (R4-6A2)	BD Pharmingen 551216	Rat IgG1	1	1:1000
Biotin Anti-Mouse IFN-γ (XMG1.2)	BD Pharmingen 554410	Rat IgG1	0.5	1:2000
AKP streptavidin	BD Pharmingen 554065		1	1:4000

2.33 Immunohistochemistry

Organs were fixed in PLP mixture (1% formaldehyde, 10 mM sodium periodate, 75 mM L-lysine) for 18 hrs at 4ºC. The organs were then placed in 30% sucrose at 4ºC for 18 hr. The tissue samples were then frozen in OCT embedding medium. 5 µM tissue sections of lungs, spleens, salivary glands or lymph nodes were cut using a cryostat (manufacturer) air dried overnight at RT, washed three times in phosphate-buffered saline (PBS), blocked in 5% NGS/0.3% Triton X-100 for 1 hr at RT, followed by a combination of primary monoclonal or polyclonal antibodies diluted in 2%NGS/0.3%triton X-100/PBS for 18 hrs at 4ºC. After an overnight incubation, the sections were washed three times in PBS and incubated for 1hr at RT with a combination of secondary antibodies and DAPI to stain nucleus in 2%NGS/0.3%Triton X-100/PBS. Sections were then mounted onto microscope coverslips in Prolong Gold and visualised using laser confocal or an epifluorescence microscope. Antibodies and concentrations are tabled in the appendix section.

2.34 Immunofluorescence

Coverslips were sterilised in 70% ethanol and placed in 24 well plates, washed twice in PBS and $2x10^5$ cells in 500 µL 10% complete DMEM were seeded and left to adhere for 4 hrs or overnight at 37ºC 5%CO_2. The cells were then infected with MHV-68 BAC^+ or BAC^- WT or OVA-recombinant MHV-68 viruses or WT or recombinant MCMV OVA expressing viruses (MOI 0.3, 18 hrs). The culture medium was discarded, washed twice in PBS and fixed in 2%PFA/PBS for 1hr at RT with gentle agitation, washed twice in PBS and permeablised in 0.1% triton-x100/PBS for 15 minutes. Non-specific binding was blocked using 2%NGS/PBS for 1 hr at RT. A combination of primary antibodies diluted in 2%NGS/PBS were added to the cells and incubated for 1 hr at RT with gentle rocking or overnight at 4ºC. Cells were then washed twice in PBS and incubated in a combination of secondary antibodies and DAPI for nuclei stain in 2%NGS/PBS for 1 hr at RT. Cells were then washed twice with PBS and three times in water before mounting coverslips onto microscope slides with Prolong Gold. The slides were cured overnight, nailed polished around the rim. Antibodies and concentrations are tabled in the appendix section.

Table 9. Primary antibody list

			Working concentration			
Primary antibodies	Manufacture and Batch	Stock (mg/mL)	WB	IHC	IF	FACS
Rabbit pAb anti-MHV-68 IgG	In house	-	1:10000	1:10000	1:10000	
Rabbit pAb anti-ovalbumin IgG	Millipore AB1225	10	1:5000	-	1:5000	-
Rabbit pAb anti-ovalbumin IgG	Abcam 181688	1	1:4000	1:4000	1:4000	
Rabbit pAb anti-MCMV IgG	In house	-	1:0000	1:16000	1:16000	
Rabbit pAb anti-M78 IgG	In house	-	1:400	-	1:8000	-
Mouse anti-IE1 (chroma101) IgG1	In house	-	1:5	1:10	1:10	1:5
Rat mAb anti-α-Tubulin (P-16) IgG_{2a}	Biorad MCA77G	0.5	1:2000	NA	NA	NA
Biotin Rat mAb anti-CD44 (IM7) IgG1	BD Pharmingen 553132	0.5	NA	NA	1:1000	1:500
Rat anti-MHC II (M5/114.15.2) IgG2b	BD Pharmingen 556999	0.5	1:1000	1:1000	1:1000	1:1000
Armenian hamster anti-CD11c (HL3) IgG1	BD Pharmingen 553799	0.5		1:500		
Rat mAb anti-F4/80 (3C137) IgG2b	Santa Cruz 71086	0.1		1:100		
Rat mAb anti-CD68 (FA-11) IgG2a	Abcam 53444	1		1:1000		
Goat pAb anti-SPC (M-20) IgG	Santa Cruz 7706	0.2		1:200		

Rat mAb anti-CD206 (MR5D3) IgG2a	Biorad MCA2235	0.25		1:250		
Chicken anti-β-gal IgY	Abcam 9361	0.25	-	1:1000	1:1000	1:1000
Rat mAb anti-CD169 IgG2a	Biorad MCA884	0.2	-	1:200	-	-
Goat pAb anti-podoplanin IgG	R&D Systems AF 3244	0.2	-	1:200	-	-
Rat mAb anti-CD45R RA3-6B2 IgG2a	Santa Cruz 19597	0.2	-	1:100	-	-
Rat anti-mouse CD4 (L3T4- GK1.5) IgG2b	BD Pharmingen 553727	0.5	-	1:500	-	-
Mouse anti-mouse DO-11.10 Clonotypic TCR (KJ1-26) IgG2a	BD Pharmingen 551771	0.5	-	1:500	-	-
Biotin conjugate mouse anti-mouse DO-11.10 TCR (KJ1-26) IgG2a	Thermo Scientific MA5-17661	0.1	-	1:100	-	-
Biotin Mouse anti-mouse H-2D (d) (34-2-12)	BD Pharmingen 553578	0.5	-	1:1000	1:1000	1:500

Table 10. Secondary antibody list

			Working concentration			
Secondary antibodies	Manufacture and Batch	Stock (mg/mL)	WB	IHC	IF	FACS
Alexa Fluor 594 donkey anti-rat IgG (H+L)	Life Technologies A21209	2	-	1:2000	1:2000	-
Alexa Fluor 568 goat anti-rat IgG (H+L)	Abcam 175476	2	-	1:2000	1:2000	-
Alexa Fluor 568 goat anti-rabbit IgG (H+L)	Invitrogen A11011	2			1:2000	
Alexa Fluor 594 goat anti-rat IgM (µ chain)	Life Technologies A21213	2	-	1:2000	1:2000	1:2000
TRITC goat anti-Armenian Hamster IgG (H+L)	Abcam 5741	1	-	1:1000	-	-
Alexa Fluor 647 goat pAb to Armenian Hamster IgG	Abcam 173004	2	-	1:2000	-	-
Alexa Fluor 647 goat anti-rat IgG (H+L)	Life Technologies A21247	2	-	1:2000	1:2000	1:2000
Alexa Fluor 647 donkey anti-rat IgG (H+L)	Abcam 150155	2	-	1:2000	1:2000	-
Alexa Fluor 647 goat anti-mouse IgG1 (γ1)	Life Technologies A21206	2	-	1:2000	-	1:2000
Alexa Fluor 488 goat anti-rat IgG (H+L)	Life Technologies A11006	2	1:10000	1:2000	1:2000	-

Alexa Fluor 488 donkey anti-rabbit IgG (H+L)	Invitrogen A21206	2	-	1:2000	1:2000	-
Alexa Fluor 488 goat anti-rabbit IgG (H+L)	Life Technologies A11008	2	1:10000	1:2000	1:2000	-
Alexa Fluor 488 goat anti-chicken IgY (H+L)	Abcam 150173	2	-	1:2000	1:2000	1:2000
Alexa Fluor 488 goat anti-mouse IgG1 (γ1)	Life Technologies A21121	2	-	1:2000	1:2000	1:2000
Dylight 800 Conjugated rabbit anti-rat IgG (H+L)	Rockland	1	1:10000 -20000	-	-	-
IRDye® 680RD Goat pAb anti-mouse IgG (H + L)	LI-COR C30117-01	1	1:10000 -20000	-	-	-
IRDye® 800CW Goat pAb anti-mouse IgG (H + L)	LI-COR C30409-07	1	1:10000 -20000	-	-	-
Oregon Green 488 goat pAb anti-mouse IgG (H+L)	Life Technologies 011033	2	-		1:2000	
DAPI	Life Technologies	1	-	1:1000	1:1000	-

2.35 Microscopy

2.35.1 Epi-fluorescence

Coverslips were viewed on a Nikon fluorescence microscope using 40X or 100X (oil immersion) objective. The microscope is equipped with the blue (330-380 nm), green (465-495) and red (540-580 nm) channels.

2.35.2 Confocal laser

For more detailed images, coverslip or tissue mounts were viewed on ZEISS LSM 710 Confocal microscope using 40X, and oil immersion objectives 63X and 100X. The microscope is equipped with 405, 561 and 633 lasers that can be switched on or off using the ZEN2012 software. Multi-tracking was used to randomly take pictures of multiple sections within tissues for cell counting.

2.36 Image analysis

Images were processed and analysed in image J or using ZEN2012. To determine number of infected cells or cells expressing cell type markers of interest, images were analysed using the cell counter plugin. Nuclei staining was used to determine total number of cells per field of view.

2.37 Flow cytometry

2.37.1 Genotyping

C57BL/6 MHC II knockout mice ($IA^{-/-}$) were genotyped using flow cytometry. Briefly, the mice were exposed to mild heat using a heat lamp to increase blood follow. 5 mm of tail was then cut, and blood was collected in 1.5 mL test tubes containing 50 µL (400 µg/mL) heparin sulphate or 20 µL of 0.5 M EDTA, pH 6.8. To lyse red blood cells, 1 mL ammonium chloride lysis buffer was added to the tubes and incubated at 37^{o}C for 15 to 30 minutes or until reddish colour was observed. The cells were then centrifuged for 5 minutes at 500 x g. The supernatant was discarded, and the cell pellet was washed twice in PBS and double stained for $CD4^{+}$ and $CD8^{+}$ T cells as described in the flow cytometry section for primary cells below.

2.37.2 Primary cells

10^6 lymphocytes isolated from blood as above, or spleens and lymph nodes were washed twice in PBS and stained in 2% FCS/PBS containing a cocktail of antibodies in the presence of mouse Fc receptor block purified rat anti-mouse CD16/CD32 clone 2.4G2 for 1 hr at 4^{o}C. The cells were then washed twice in PBS and resuspended in 200 µL ice-cold PBS for analysis on BD Accurri C6 flow cytometer. Flow cytometry antibodies used are described in the appendix section of the thesis.

2.37.3 Immortalised cells

10^6 cells were seeded in six well plates and left uninfected or infected with MHV-68 or MCMV WT or number of mutants expressing different reporter genes.

For surface staining, the cells were scrapped, washed twice in PBS, counted and stained with a combination of directly conjugated antibodies or unconjugated antibodies in 2%FCS/PBS or 2%NGS/PBS for 1 hr at 4^{o}C in the presence or absence of purified rat anti-mouse CD16/CD32 Fc block. Cells directly stained with fluorophore-conjugated antibodies were washed twice in PBS and resuspended in PBS for later analysis or manipulated further for intracellular staining as described in the subsequent section below. For unconjugated antibody labelled cells, the cells were washed twice in PBS and incubated with either phycoerythrin (PE) or PerCP-Cy5.5 conjugated streptavidin to detect biotinylated antibodies or Alexa Fluor secondary antibodies to rat or mouse in 2%FCS/PBS or 2%NGS/PBS for 1 hr at 4^{o}C. The cells were then washed twice in PBS and resuspended in 200 µL ice-cold PBS for later analysis.

For intracellular staining, cells stained above, or unstained cells were fixed in 2%PFA/PBS for 30 minutes at RT, washed twice in PBS and incubated in 0.5% saponin/PBS for 15 minutes at RT. To detect infected cells, the cells were stained in antibodies to hamster anti-β-gal to detect recombinant MCMV viruses expressing β-gal, or monoclonal mouse anti-mouse IE1 sera to detect IE1 or polyclonal rabbit anti-HA to detect HA tagged MCMV viruses in combination with antibodies to MHC II, CD44 or MHC I (if previously unstained) diluted in 2%NGS/0.5%saponon/PBS incubated for 1hr at RT. The cells were then washed twice in 0.5%saponin/PBS and incubated with secondary antibodies against their respective primary targets in 2%NGS/0.5%saponin/PBS for hr at 4^{o}C. The cells were then washed once in 0.5%saponin/PBS, once in PBS and resuspended in 200 uL ice-cold PBS

and analysed on a multicolour flow cytometer or BD Accurri C6 flow cytometer. Propidium iodide (1mg/mL, batch MKBP1360V, Sigma) was used to detect and gate out dead cells using the PE 575/25 nm channel. GFP expressing viruses were detected directly.

Table 11. Flow cytometry antibodies

Flow cytometry antibodies	Manufacture and Batch	Isotype	Stock (mg/mL)	Working concentration
FITC Rat anti-mouse CD4 GK1.5	BD Pharmingen	Rat		1:500
FITC Rat Anti-Mouse CD4 (RM4-4)	BD Pharmingen 553055	Rat IgG2b	0.5	1:500
Alexa Fluor 488 Rat anti-mouse CD4 (RM4-5)	BD Pharmingen 557667	Rat IgG2a	0.2	1:200
FITC Rat Anti-Mouse CD71 (C2/C2F2)	BD Pharmingen 561936	Rat IgG1	0.5	1:500
PE Rat Anti-Mouse CD11b (M1/70)	BD Pharmingen 553311	Rat IgG2b	0.2	1:200
PE Hamster Anti-Mouse CD69 (H1.2F3)	BD Pharmingen 553237	Armenian Hamster IgG1	0.2	1:200
PE Rat anti-mouse CD62L MEL-14	BD Pharmingen 553151	Rat IgG2a	0.2	1:200
PE Rat anti-mouse CD8β (H35-17.2)	BD Pharmingen 550798	Rat IgG2b	0.2	1:500
PE Rat anti-mouse CD19 ID3	BD Pharmingen	Rat		1:500
PE streptavidin	BD Pharmingen 554061	N/A	0.5	1:500
Propidium Iodide	Sigma-Aldrich MKBP1360V	DNA	10	1:1000
PerCP Cy5.5 Rat anti-mouse I-A/I-E (M5/114.15.2)	BD Pharmingen 562363	IgG2b	0.2	1:200
PerCP Cy5.5 streptavidin	BD Pharmingen 554061	N/A	0.5	1:500

PerCP Cy5.5 Rat anti-mouse CD8α (53-6.7)	BD Pharmingen 551162	Rat IgG2a	0.2	1:200
Alexa Fluor 647 Rat anti-mouse CD19 (ID3)	BD Pharmingen 557684	Rat IgG2a	0.2	1:200
Alexa Fluor 647 Rat anti-mouse 1-A/1-E M5/114.15.2	BD Pharmingen 562367	Rat IgG2b	0.2	1:100
Alexa Fluor 647 mouse anti-mouse DO.11.10 clonotypic TCR KJ-126	BD Pharmingen 562524	Mouse IgG2a	0.2	1:500
Biotin Rat anti-mouse CD86 (GL1)	BD Pharmingen 553690	Rat IgG2a	0.5	1:500
Purified Rat anti-mouse Cd16/CD32 (2.4G2)	BD Pharmingen 553142	Rat IgG2b	0.5	1:500
BV241 Rat anti-mouse CD71 (C2/C2F2)	BD Horizon 562716	Rat IgG1	0.2	1:200

2.38 Statistical analysis

Data analysis was performed in GraphPad Prim 6 or excel. Unpaired 2 tailed student t-test was performed. For multiple analysis, Bonferroni-Dunn post-test was performed to correct for multiple comparisons. Statistical analysis was performed on $\log_{10}$ transformed data. Fischer exact test was also performed on counted cells or percentage data obtained from flow cytometry analysis.

CHAPTER 3: MCMV AS A LIVE-ATTENUATED PERSISTENT VACCINE VECTOR.

3.1 Results

3.1.1 Characterisation of recombinant OVA$^+$ MCMV viruses

To use ovalbumin as model antigen, recombinant OVA$^+$ MCMV viruses were characterised. MCMV OVA viruses, express membrane bound (mOVA) or secreted (sOVA) forms of ovalbumin from the viral genome. In MCMV mOVA, transferrin receptor is fused to the C-terminus of OVA (unpublished). This directly targets OVA to the endocytic pathway for efficient processing and presentation as $OVA_{323-339}$ peptide to CD4$^+$ T cells (160). The sOVA virus has an intact signal sequence. OVA is expressed as a soluble cytoplasmic protein and secreted from infected cells (160). The HCMV IE promoter drives OVA expression in both viruses. *In vivo*, MCMV mOVA or sOVA is expected to prime CD4$^+$ and CD8$^+$ T cells via MHC II epitope $OVA_{323-339}$ and MHC I epitope $OVA_{257-264}$ respectively.

3.1.2 *In vitro* characterisation of MCMV recombinant OVA viruses

To confirm the presence of ovalbumin in MCMV OVA viruses, viral DNA was extracted from infected NIH-3T3 cells and the OVA sequence amplified using two sets of primers (OVA 1 and OVA 2, 900 bps) or (OVA 2 and OVA 3, 430 bps) by PCR (Table 5). Bands of approximately 900 and 430 bps were detected in mOVA and sOVA respectively (Fig. 3.1a). WT was negative for either OVA bands, confirming primer specificity.

To determine whether ovalbumin was expressed, NIH-3T3 cells were infected with MCMV mOVA or sOVA at MOI 1 for 48 hrs or left uninfected. Cell culture (secreted) and cell lysate (cytoplasmic) fractions were then denatured (95^{o}C for 5 minutes) and resolved on a 10-12.5% SDS-PAGE gel, transferred to methanol activated PVDF membrane and blotted for OVA. A single band of 43 KDa, consistent with the size of OVA was detected in the cell culture fraction derived from sOVA- infected cells, while mOVA was negative (Fig. 3.1b). Both cell lysate fractions stained positive for OVA (Fig. 3.1b) similar to purified OVA as positive control. MCMV mOVA had an additional slower migrating band consistent with a glycosylated form of OVA (indicated by the asterisk). To confirm OVA expression, MEFs were infected at MOI 2 with MCMV mOVA or sOVA or left uninfected. The cells were then fixed, permeablised and stained for OVA or MCMV lytic antigens by indirect immunofluorescence. In mOVA and sOVA infected MEFs, infected cells stained positive for lytic antigens and expressed ovalbumin (Fig. 3.1c).

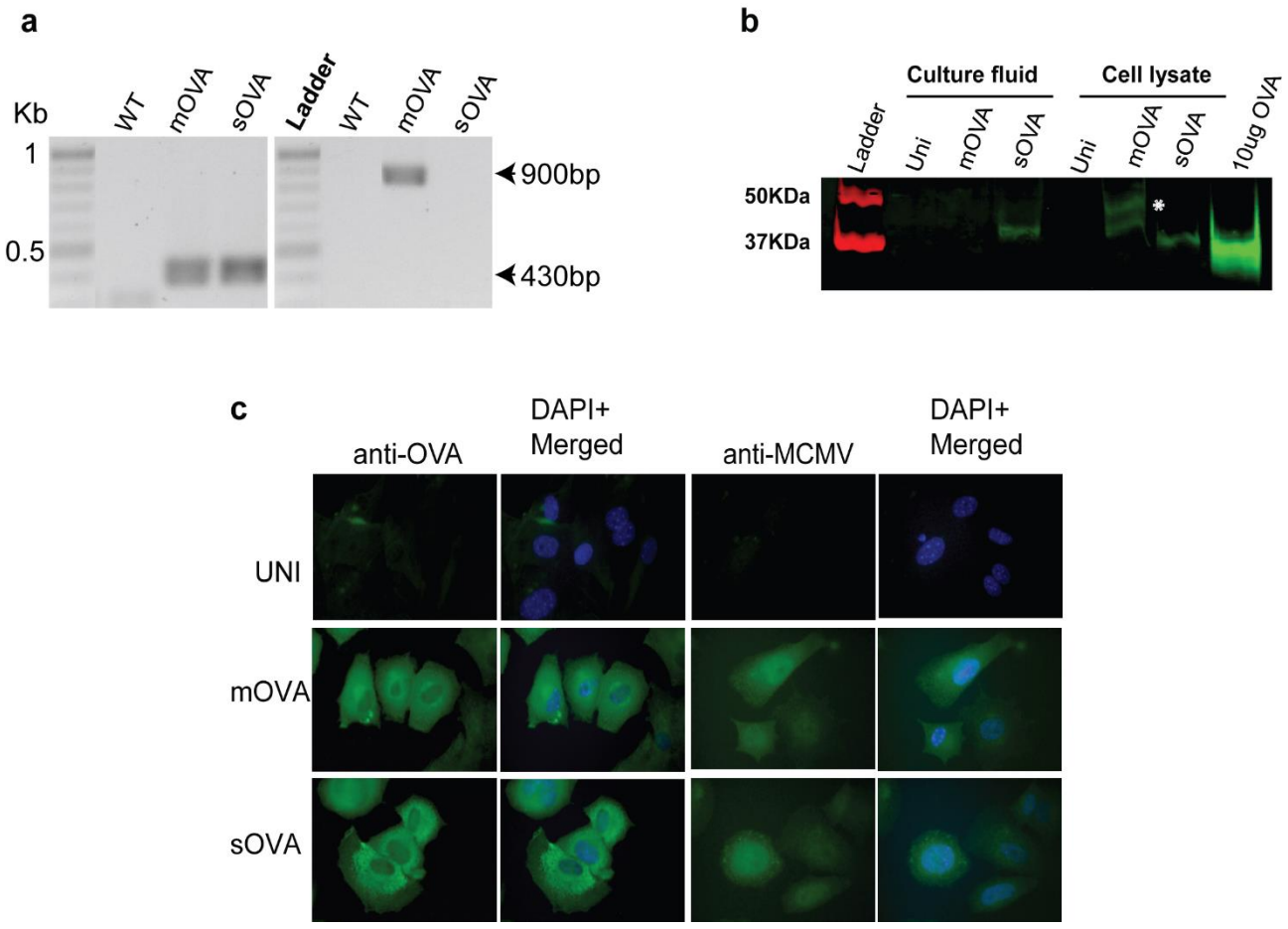

Fig. 3. 1. *In vitro* characterisation of recombinant MCMV ovalbumin viruses.

a) Viral DNA extracted from infected 3T3 cells was amplified for OVA using two sets of primers and the products ran on a 1% agarose gel. Bands of 0.9 Kb and 0.43 Kb were detected. **b)** $1x10^6$ 3T3 cells were left uninfected or infected (MOI 1, 18 hrs) with MCMV OVA expressing viruses in 24 well plates. Cell lysate and culture media supernatant were diluted in 3X Laemmli buffer and resolved by SDS-PAGE and were analysed by immunoblotting with polyclonal rabbit anti-OVA. A band of 43 KDa was detected. **c)** MEFs infected at MOI 2 overnight were fixed and stained for OVA and lytic antigens. Cell nuclei was stained with DAPI. All images were captured at X 63 magnification. Data are representative of 3 independent experiments.

To determine whether MCMV OVA$^+$ infected cells would present OVA$_{323-339}$ peptide to stimulate OVA$_{323-339}$-specific CD4$^+$ T cell hybridomas *in vitro*, MHC class II$^+$ RAW-C2TA and BALB/c-3T3-C2TA cells were used as antigen presenting cells. Since OVA$_{323-339}$-specific CD4$^+$ T cell hybridomas secrete IL-2 following engagement with OVA$_{323-339}$ (160), IL-2 levels in co-cultures were used as a marker of T cell stimulation. BALB/c-3T3-C2TA cells were left uninfected or infected at MOI 0.3 with either OVA$^+$ MCMVs or WT MCMV in the presence of CD4$^+$ T cell hybridomas. After 24 hrs, IL-2 in culture medium was analysed by ELISA. CD4$^+$ T cells in MCMV mOVA infected cells secreted more IL-2 than in sOVA relative to uninfected cells incubated in the presence of 1 µM OVA$_{323-339}$ peptide (Fig. 3.2a). No IL-2 secretion was observed in uninfected or WT infected cells (Fig. 3.2a). The experiment was repeated using RAW-C2TA cells. MCMV mOVA again stimulated CD4$^+$ T cells to secrete high levels of IL-2 compared to MCMV sOVA relative to uninfected cells incubated in the presence of 1 µM OVA$_{323-339}$ peptide (Fig. 3.2b). This suggests that MCMV mOVA stimulates CD4$^+$ T cells better than sOVA *in vitro*.

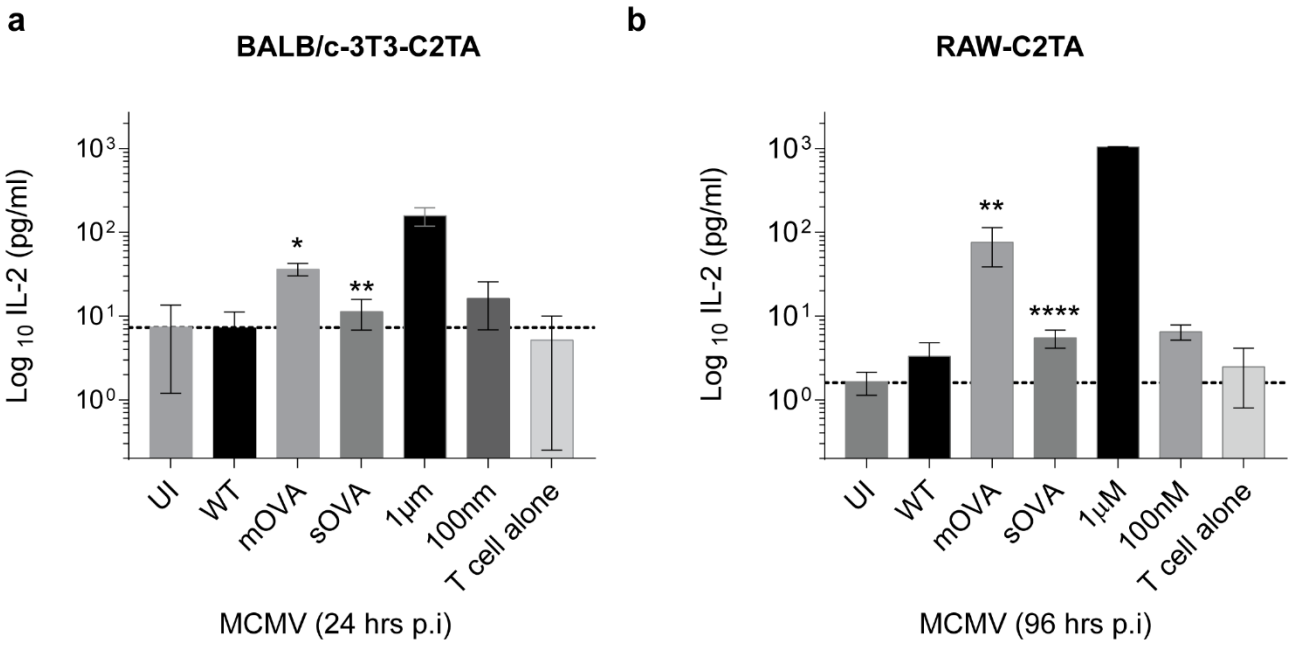

Fig. 3. 2. MCMV OVA viruses induce IL-2 secretion.

a) 3x10^4 BALB/c-3T3-C2TA cells were either left uninfected or infected (MOI 0.3, 24 hrs) with WT or MCMV OVA in the presence of 3x10^4 OVA$_{323-339}$ peptide CD4$^+$ T cell hybridomas. 24 hrs later, supernatants were assayed for IL-2 secretion using ELISA. **b)** 3x10^4 RAW-C2TA cells were either left uninfected or infected (MOI 1, 96 hrs) with WT or MCMV OVA. 3x10^4 OVA$_{323-339}$ peptide CD4 T cell hybridomas were then added and IL-2 was assayed using ELISA after 24 hrs. Error bars show ± SEM from the mean of duplicate

cultures from 3 independent experiments. Dotted line shows limit of detection relative to uninfected cells. Difference in IL-2 was determined using unpaired 2-tailed t-test. 1 µM was used for comparison. (* p>0.05; ** p<0.01; *** p<0.001; **** p<0.0001). Dotted line shows limit of IL-2 detection and error bars show ± SEM (n=2-4 per group).

3.1.3 *In vivo* replication kinetics of recombinant MCMV OVA virus

Live attenuated vaccines are required to be latency deficient but should be immunogenic for the host to mount an immune response (143). 6-8 weeks old C57BL/6 mice were anesthetized and infected via the i.n route with $3x10^4$ plaque forming units per mouse (p.f.u/mouse) of WT, MCMV mOVA or MCMV sOVA. Four days post infection, replication in the lungs and salivary glands was determined by plaque assay. Infectious virus was detected in the lungs of WT (mean titer 3.2) and MCMV sOVA (mean titer 2.9) infected mice although the latter was modestly lower (Fig. 3.3, p<0.05). In contrast, MCMV mOVA was severely attenuated (mean titer 1.7, p<0.001). At this early time point, no virus was found in the salivary glands of mice infected with either WT, MCMV mOVA or sOVA (Fig. 3.3). Eight days post infection, virus was detected in the salivary glands and lungs of WT infected mice by plaque assay, but not in sOVA or mOVA infected samples (Fig. 3.3). The results show that, MCMV mOVA and sOVA caused lytic replication at site of inoculation but failed to spread to the salivary glands. This provided an excellent *in vivo* model for a live attenuated vaccine using ovalbumin as model antigen. Accordingly, the effectiveness of MCMV sOVA as a live attenuated vaccine against a challenge with recombinant MHV-68 was tested in preliminary experiments.

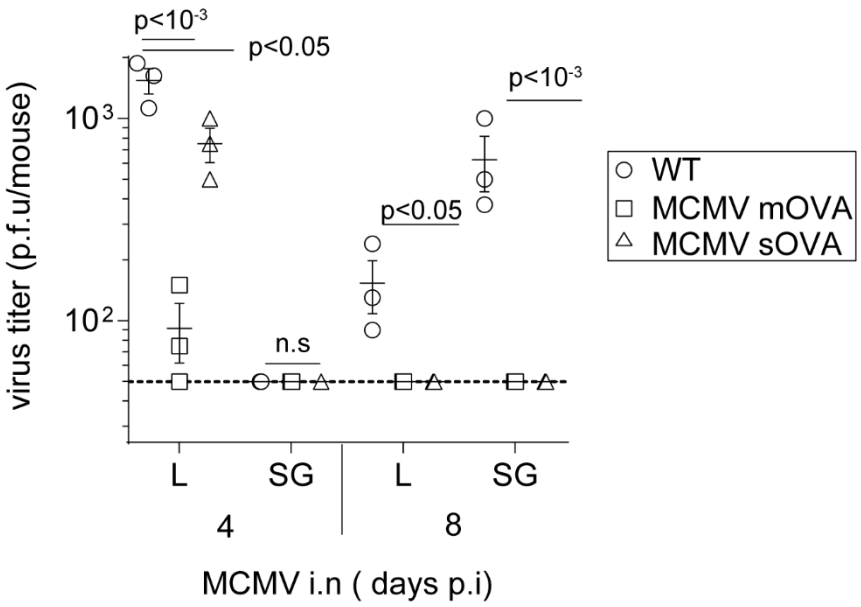

Fig. 3. 3. MCMV OVA viruses are defective in SG colonisation.

C57BL/6 mice were infected i.n under anaesthesia with 10^5/p.f.u WT, MCMV mOVA or MCMV sOVA in 30 µL DMEM. After 4 and 8 days post infection, virus replication in the lungs and salivary glands were determined by plaque assay on MEFs. Each symbol represents titres from individual mice. Difference in mean was determined using unpaired 2 tailed t-test with Bonferroni-Dunn correction for multiple comparison with WT as control. ns 'not significant' ($p>0.05$). Dotted line shows limit of detection and error bars show ± SEM (n=3 per group).

3.2 MCMV sOVA as a model live attenuated vaccine vector to secreted ovalbumin

3.2.1 Does MCMV sOVA protect against MHV-68 M3 sOVA lytic infection?

The aim of this experiment was to determine whether vaccinating mice with MCMV sOVA would protect against a subsequent challenge with MHV-68 M3 sOVA. Recombinant MHV-68 M3 sOVA expresses ovalbumin under the M3 promoter, a highly expressed lytic protein (160). 6-8 weeks old BALB/c mice were vaccinated with 10^5 p.f.u/mouse of MCMV mOVA or MCMV sOVA via the i.p route or left unvaccinated as control. To confirm infection, antibody to MCMV and OVA was determined by ELISA 14 and 21 days post i.p injection.

3.2.2 Antibody response to MCMV and ovalbumin

IgM and IgG2a responses to MCMV were detected in MCMV mOVA and MCMV sOVA infected mice but not in unvaccinated mice at both 14 and 21 days post vaccination (Fig. 3.4a, c). MCMV sOVA infected mice had slightly lower IgM and IgG2a levels at day 21 to MCMV mOVA (Fig. 3.4a, b, $p<0.001$). Interestingly, MCMV mOVA but not sOVA-infected mice showed a rising OVA-specific IgG2a response (Fig. 3.4e, $p<0.001$). There was no IgG1 response to either MCMV or OVA at either day 14 or 21 post vaccination (Fig. 3.4c, d).

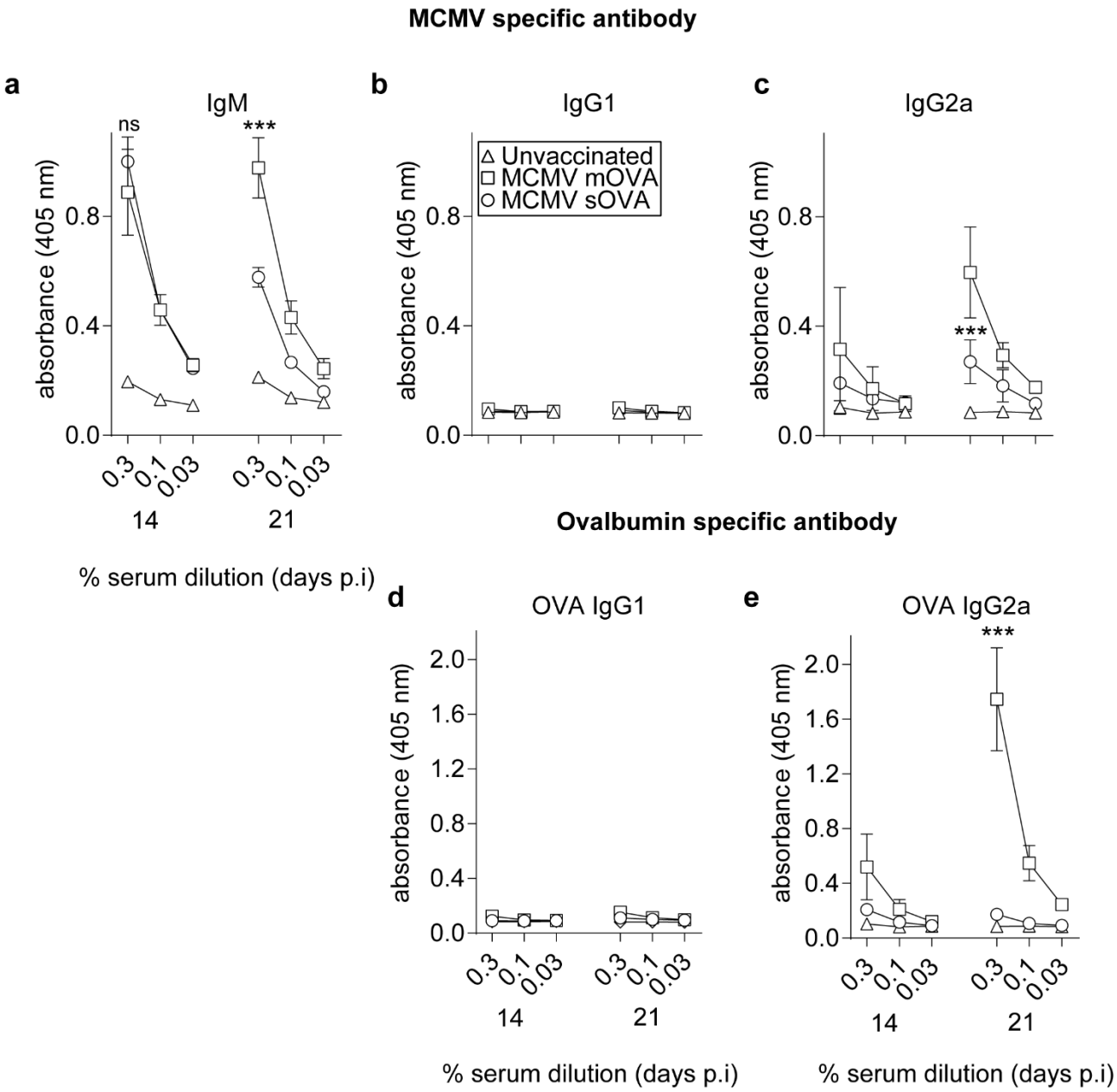

Fig. 3. 4. MCMV and OVA-specific primary antibody response following i.p infection.

6-8 week old BALB/c mice were vaccinated via the i.p route with 10^5 p.f.u/100 µL of MCMV mOVA or sOVA or left unvaccinated. 14 and 21 days post vaccination, antibody levels to MCMV (**a, b** and **c**) and OVA (**d** and **e**) were determined by ELISA. For virus (**a-c**) and OVA (**d-e**) specific IgM, IgG1 and IgG. Absorbance was read at 405 nm. Error bars show ± SEM (n=2 per group) in duplicates. Data was analysed using unpaired student 2 tailed t-test (ns, p>0.05; * p<0.05; ** p<0.01; *** p<0.001, **** p<0.0001). MCMV mOVA was used to compare differences.

3.2.3 Response to MHV-68 M3 sOVA in MCMV sOVA and mOVA vaccinated mice

Thirty-three days post vaccination, BALB/c mice were challenged with MHV-68 sOVA via i.n infection with or without anaesthesia to model lower and upper respiratory tract infection. Six days later, blood, noses and lungs were harvested. Aged-matched unvaccinated mice had low IgM and IgG to MHV-68 and OVA consistent with a primary infection while MCMV mOVA and sOVA vaccinated mice had elevated levels of IgG but not IgM to OVA (Fig. 3.5a-b). There was no significant difference in virus titer between vaccinated and unvaccinated controls (Fig. 3.5c, $p>0.05$). Taken together, this showed that neither MCMV mOVA nor sOVA vaccination conferred protection or reduced lytic MHV-68 M3 sOVA infection.

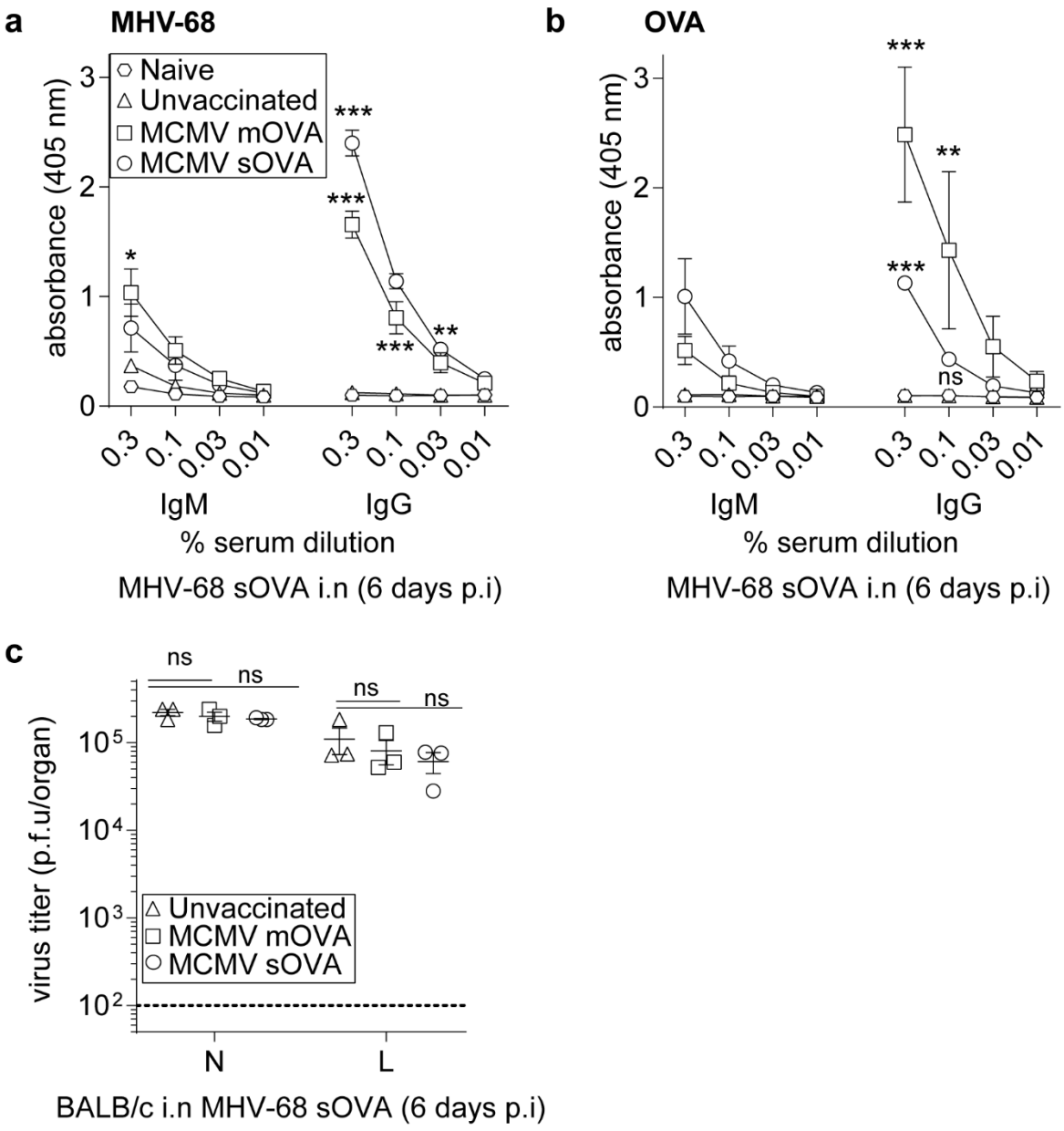

Fig. 3. 5. Immune response to MHV-68 sOVA following intranasal infection.

a, b) Adult BALB/c vaccinated with MCMV mOVA, MCMV sOVA or left unvaccinated were challenged with 10^4-10^5 p.f.u/mouse. 6 days post challenge MHV-68 and OVA-specific antibody responses in the serum were measured by ELISA. Absorbance was read at 405 nm. The error bars show ± SEM (n=3 per group). Data was analysed using unpaired student 2 tailed t-test (ns, $p>0.05$; * $p<0.05$; ** $p<0.01$; *** $p<0.001$). Unvaccinated mice were used for comparison. **c)** Lungs and noses were tittered on BHK cells. Each data point represents virus titer per mouse error bars show ± SEM from the mean (n=3 per group). Difference in mean between unvaccinated and vaccinated groups was determined by multiple unpaired 2 tailed t-test using Bonferroni Dunn correction for multiple comparisons. ns 'not significant', $p > 0.05$. Dotted line shows limit of detection.

3.2.4 Does adoptive transfer of $OVA_{323-339}$ transgenic $CD4^+$ T cells protect BALB/c mice against MHV-68 infection?

To understand how $CD4^+$ T cells control lytic infection in the nose or lung, $OVA_{323-339}$-specific $CD4^+$ T cells were isolated from lymph nodes and spleens of naïve DO11.10 transgenic mice and enriched for $CD4^+$ T cells using magnetic beads. $2x10^6$ $OVA_{323-339}$-specific DO11.10 $CD4^+$ T cells were then transferred to naïve BALB/c mice ("treated") via intravenous injection via the lateral tail vein. These mice were then primed with MCMV sOVA. Control mice that did not receive DO11.10 $OVA_{323-339}$-specific $CD4^+$ T cells ("untreated"), were either primed with MCMV sOVA or MCMV WT. Seventeen days post priming, splenocytes from treated and untreated mice were stained for CD4 and KJ1-26 to detect DO11.10 $OVA_{323-339}$-specific $CD4^+$ T cells and activation markers CD62L and CD69 to determine activation status of these cells. Splenocytes from treated and not untreated mice primed with MCMV sOVA stained positive for KJ1-26 (Fig. 3.6- red circle). This confirmed adoptive transfer of naïve DO11.10 $OVA_{323-339}$-specific $CD4^+$ T cells worked. Surprisingly, the cells expressed $CD62L^{hi}$ and $CD69^{lo}$, a profile of naïve $CD4^+$ T cells.

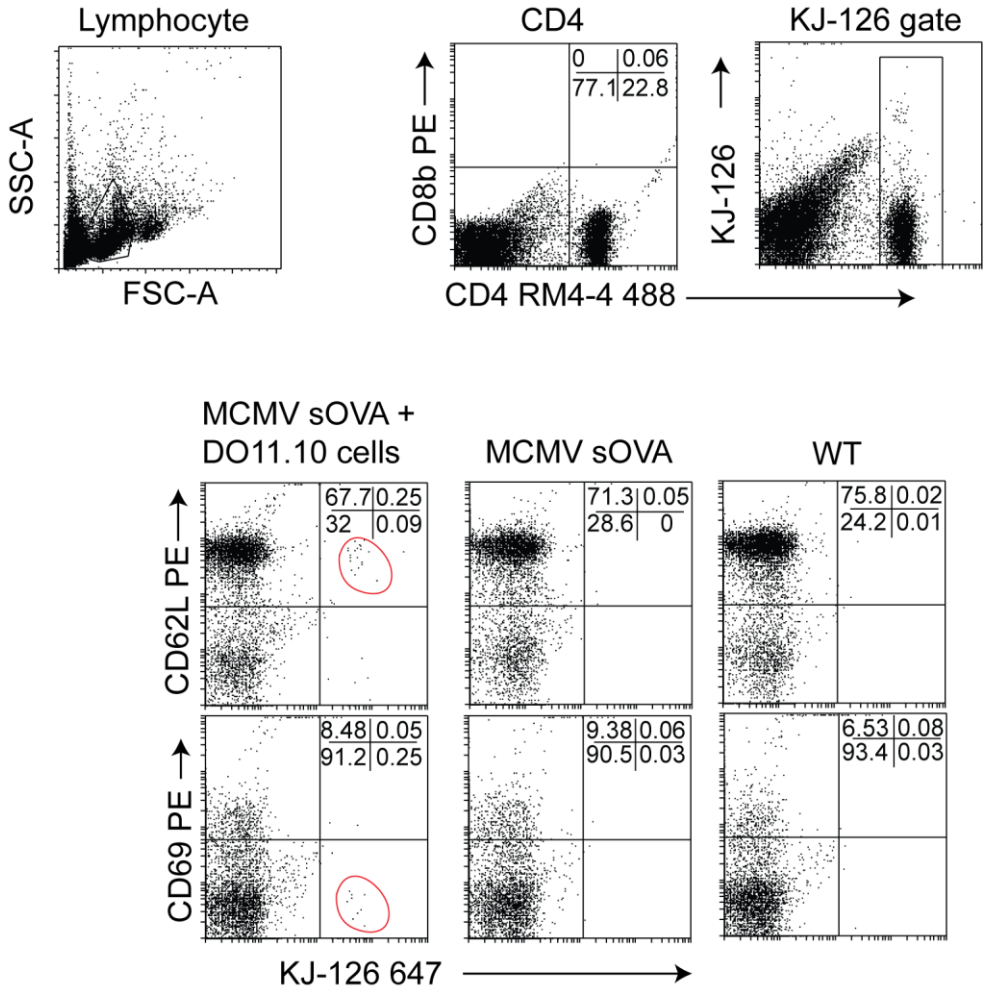

Fig. 3. 6. Presence of adoptively transferred DO11.10 CD4⁺ T cells in treated BALB/c mice.

6-8 week old naïve BALB/c mice were injected i.v with 2 x 10^6 naïve DO11.10 $OVA_{323-339}$-specific $CD4^+$ T cells or left untreated and infected via the i.p route with 10^5 p.f.u/mouse of MCMV sOVA and WT. After 17 days, splenocytes were stained for $CD4^+$ T cells (Alexa Fluor 488 rat anti-mouse CD4 4.4), KJ1-26 $CD4^+$ T cells (Alexa Fluor 647 mouse anti-mouse DO11.10 Tcr), CD62L (PE rat ant-mouse CD62L) or CD69 (PE). KJ1-26^+ $CD4^+$ T cells were found in mice that received DO11.10 $OVA_{323-339}$-specific $CD4^+$ T cells shown in red.

To determine whether treated mice would protect against MHV-68 infection, the remaining treated and untreated groups were challenged via the i.n route with MHV-68 M3 mOVA. Seven days post infection, organs of interest were harvested, and virus titer determined by plaque assay. There was no difference in lytic virus between treated and untreated groups in either the nose or lung (Fig. 3.7b, $p>0.05$). Mediastinal lymph nodes and superficial cervical lymph nodes and spleen titers also showed no significant differences (Fig. 3.7c).

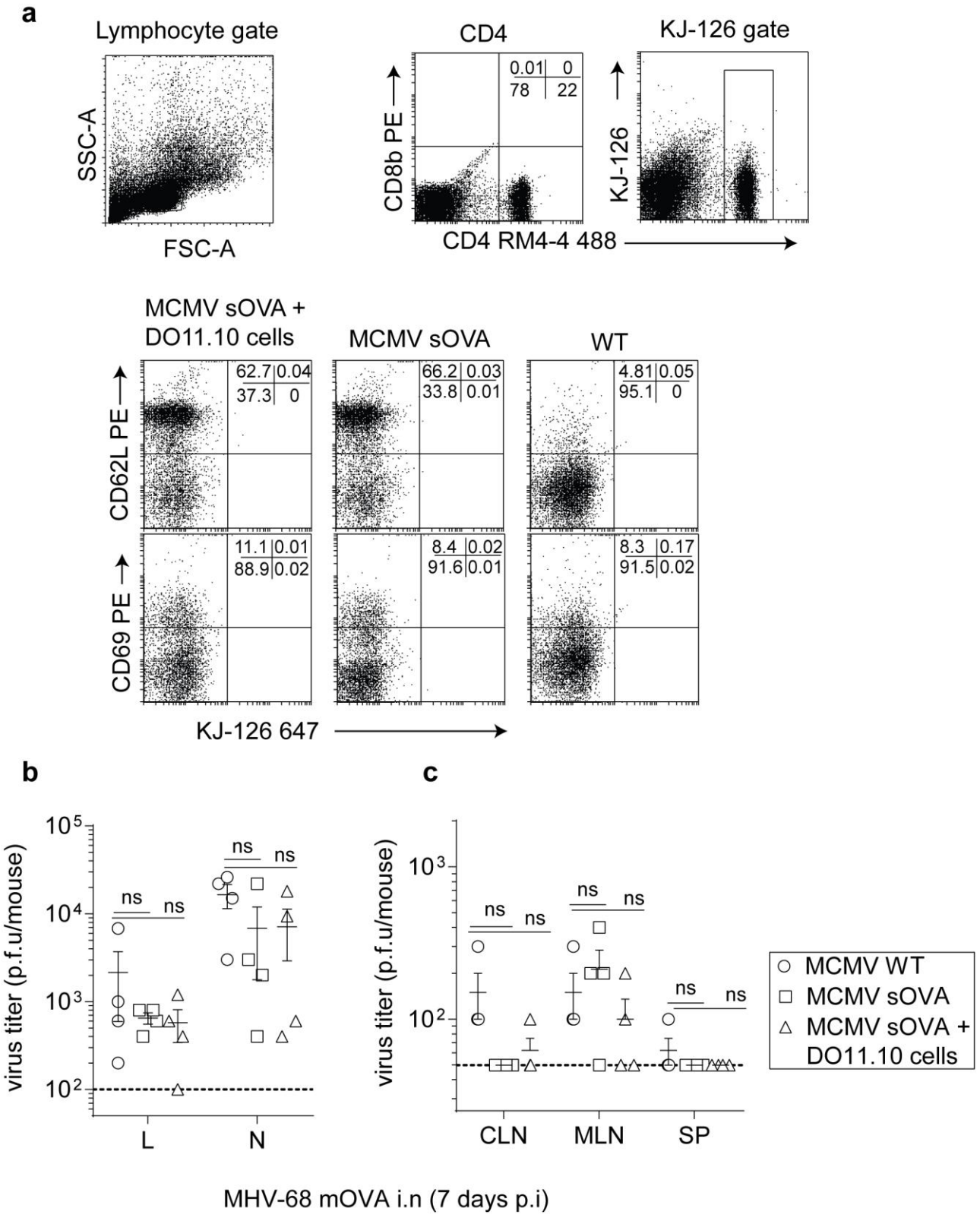
a
Lymphocyte gate
SSC-A
FSC-A
CD4
CD8b PE
CD4 RM4-4 488
0.01
0
78
22
KJ-126 gate
KJ-126
MCMV sOVA +
DO11.10 cells
MCMV sOVA
WT
CD62L PE
CD69 PE
62.7
0.04
37.3
0
66.2
0.03
33.8
0.01
4.81
0.05
95.1
0
11.1
0.01
88.9
0.02
8.4
0.02
91.6
0.01
8.3
0.17
91.5
0.02
KJ-126 647
b
c
virus titer (p.f.u/mouse)
ns
L
N
CLN
MLN
SP
MCMV WT
MCMV sOVA
MCMV sOVA +
DO11.10 cells
MHV-68 mOVA i.n (7 days p.i)

Fig. 3. 7. Absence of adoptively transferred DO11.10 CD4$^+$ T cells in treated BALB/c.

Remaining BALB/c mice in **figure 3.6** were challenged with MHV-68 mOVA via the i.n route with 1x10^5 p.f.u/mouse without anaesthesia for nose infection and 3x10^4 p.f.u/mouse under anaesthesia for lung infection. **a)** Seven days post challenge, splenocytes were again stained for CD4$^+$ T cells (Alexa 488 CD4 4.5), KJ126 CD4$^+$ T cells (Alexa 647 KJ126), CD62L (PE) or CD69 (PE) and analysed by flow cytometry. **b)** Virus titer in lungs and noses of day 7 infected mice was determined by plaque assay on BHK-21 cells. **c)** Infectious center assay was performed on SCLN, MLN and spleen homogenates on BHK-21 cells. Each data point represents virus replication per mouse and error bars show ±SEM (n=4 per group). Difference in mean was determined using multiple unpaired 2-tailed t-test using Bonferroni Dunn correction for multiple comparisons. Significance was taken as $p< 0.05$, ns 'not significant', and $p > 0.05$.

Flow cytometry analysis showed absence of CD4$^+$KJ126$^+$ cells in treated mice that had previously stained positive (Fig. 3.7a). This was also observed 11 days post challenge (Fig. 3.8b). At this time point, there was no difference in infectious virus in the SCLN, MLN or spleen between treated and untreated groups (Fig. 3.8c). This suggests that secreted OVA was not efficiently processed or presented to stimulate and expand DO11.10 OVA$_{323-339}$-specific CD4$^+$ T cells. To exclude absence of MHC II epitope within the MCMV mOVA sequence, MCMV mOVA and sOVA viral DNA were amplified for OVA using primer set (OVA 2 and OVA 3). The 430 bp fragment (Fig. 3.1a) was gel purified and sequenced. Sequence results showed MHC I (SIINFEKL-red) and MHC II (ISQAVHAAHAEINEAGR-green) epitope sequences were present in both MCMV mOVA and sOVA viral DNA (Fig. 3.9).

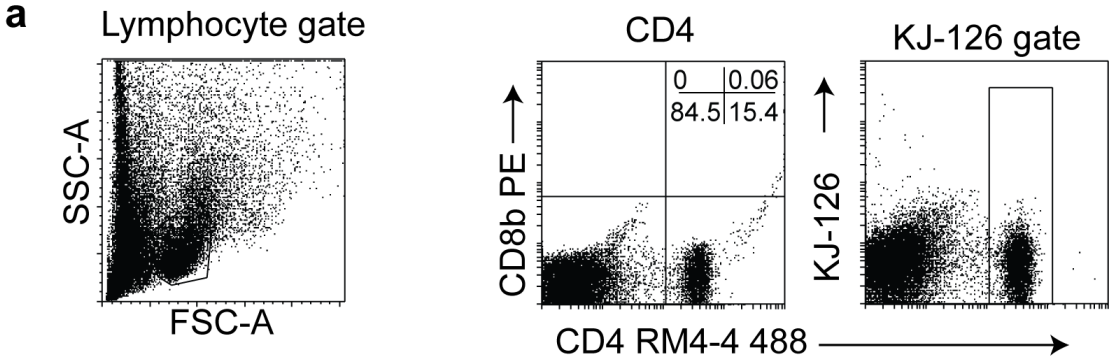
a
Lymphocyte gate
SSC-A
FSC-A
CD4
0
0.06
84.5
15.4
CD8b PE
CD4 RM4-4 488
KJ-126 gate
KJ-126

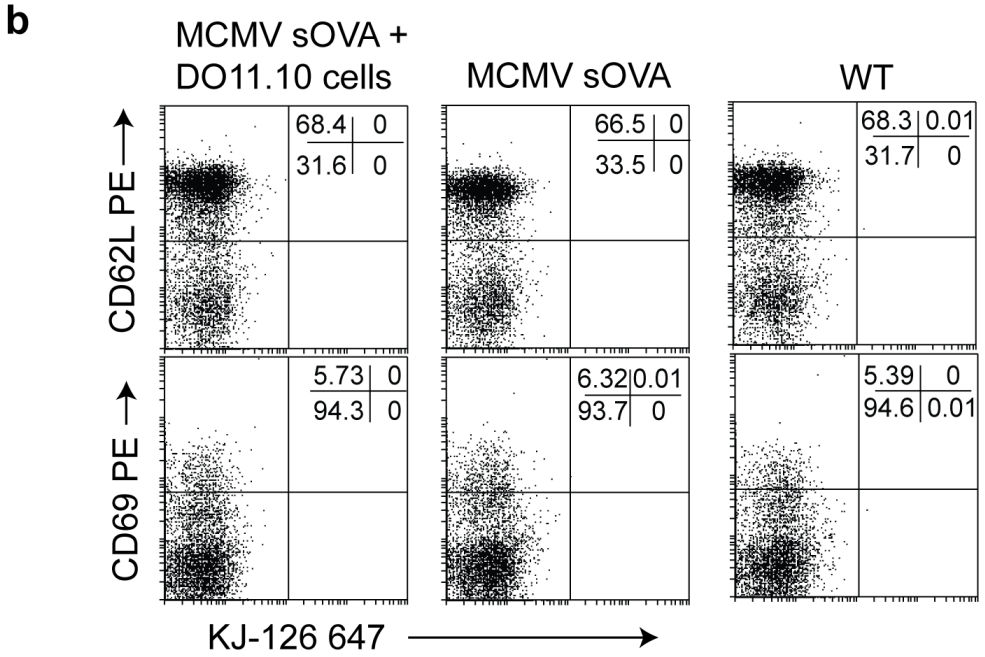
b
MCMV sOVA +
DO11.10 cells
MCMV sOVA
WT
68.4
0
31.6
0
66.5
0
33.5
0
68.3
0.01
31.7
0
5.73
0
94.3
0
6.32
0.01
93.7
0
5.39
0
94.6
0.01
CD62L PE
CD69 PE
KJ-126 647

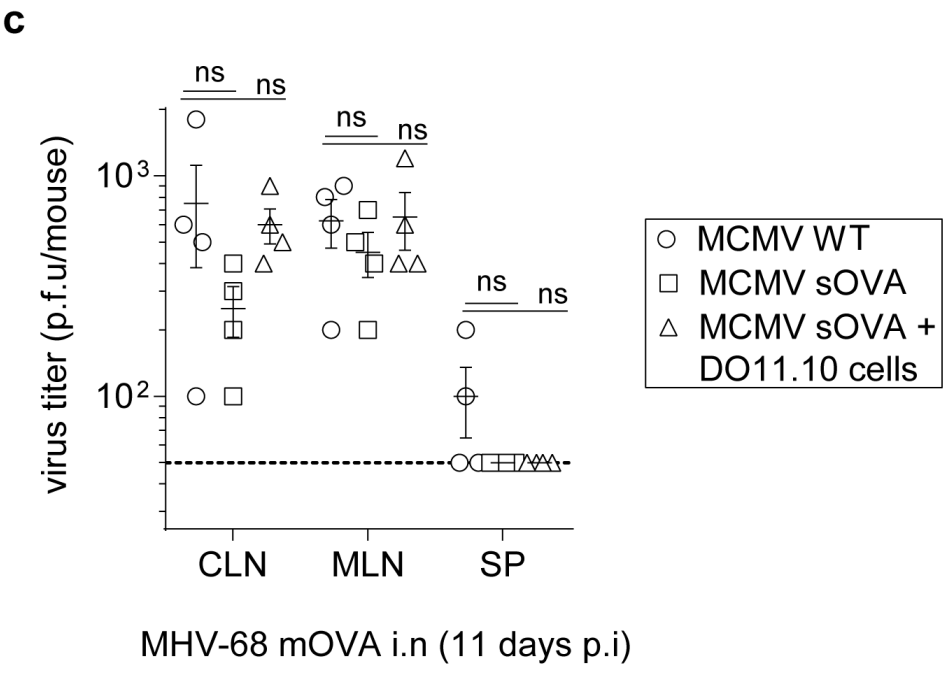
c
ns
ns
ns
ns
ns
ns
10^3
10^2
virus titer (p.f.u/mouse)
CLN
MLN
SP
MCMV WT
MCMV sOVA
MCMV sOVA +
DO11.10 cells
MHV-68 mOVA i.n (11 days p.i)

Fig. 3. 8. MCMV sOVA priming does not stimulate OVA-specific DO11.10 CD4$^+$ T cells.

BALB/c mice challenged as **in figure 3.7** were sacrificed after 11 days. **a, b)** splenocytes were stained for CD4$^+$ T cells (Alexa 488 CD4 4.5), KJ126 CD4$^+$ T cells (Alexa 647 KJ126), CD62L (PE) or CD69 (PE) and analysed by flow cytometry. **c)** Infectious center assay was performed on SCLN, MLN and spleen homogenates on BHK-21 cells. Each data point represents virus titer per mouse (n=4 per group) and error bars show ±SEM. Difference in mean was determined using multiple unpaired 2-tailed t-test with Bonferroni Dunn correction for multiple comparisons. ns 'not significant' p > 0.05.

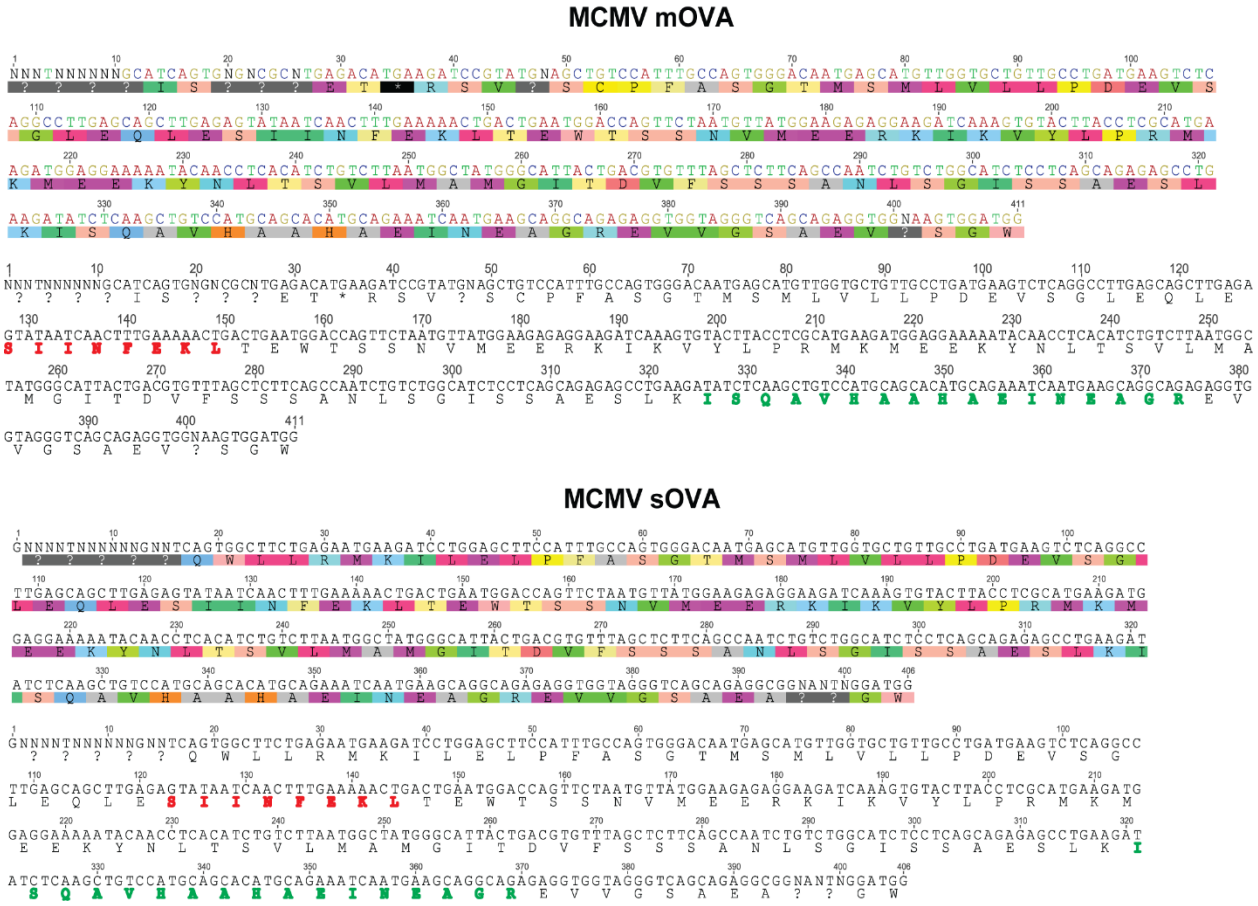

Fig. 3. 9. MHC I and MHC II epitopes in MCMV mOVA and sOVA.

MCMV mOVA and sOVA viral DNA extracted from infected 3T3 cells was amplified for OVA using primers spanning the MHC I and MHC II epitopes. The 430bp bands were excised, and sequenced. Red shows MHC I epitope and green MHC II.

3.3 MCMV mOVA, a model live attenuated vaccine vector to induce $CD4^+$ T cell immunity.

The failure of MCMV sOVA to expand adoptively transferred DO11.10 $OVA_{323-339}$-specific $CD4^+$ T cells in BALB/c mice, suggested that sOVA was perhaps not efficiently presented. To directly test a $CD4^+$ T cell vaccine against MHV-68, MCMV mOVA was used. This virus stimulated $OVA_{323-339}$-specific $CD4^+$ T cell hybridomas *in vitro* (Fig. 3.2a, b). *In vivo*, it is expected to induce $OVA_{323-339}$ $CD4^+$ T cell responses as well as $OVA_{257-264}$-specific $CD8^+$ T cell responses. Thus, to study how $CD4^+$ T cells control MHV-68 mOVA infection, C57BL/6 and BLAB/c mice were vaccinated in parallel with MCMV WT or MCMV mOVA virus. C57BL/6 vaccination was to control for OVA-specific $CD8^+$ T cell response as OVA priming stimulates robust $OVA_{257-264}$ specific memory $CD8^+$ T cells. Fifty-one days post priming, mice were tail bled to measure antibody response to OVA then challenged with MHV-68 mOVA. MHV-68 mOVA has a transferrin receptor linked to the C-terminus of OVA that directs OVA to the endocytic pathway for efficient processing and presentation of $OVA_{323-339}$ peptide in infected myeloid cells or B cells. MHV-68 M3 promoter drives ovalbumin expression predominately during lytic infection (160).

3.3.1 BALB/c vaccination restricts lytic mucosal infection but not lymphoproliferative disease

Antibody response to OVA in MCMV mOVA and MCMV WT primed mice showed predominately IgG response to OVA in the former confirming ovalbumin vaccination status (Fig. 3.10a). Lytic replication of MHV-68 mOVA in the nose (N) and lung (L) of MCMV mOVA vaccinated mice was reduced compared to MCMV WT (Fig. 3.10b, $p<0.001$). Expansion of B cells in the lymph nodes (lymphoproliferation) was significantly enhanced particularly in the superficial lymph node (CLN) of MCMV mOVA vaccinated mice compared to WT (Fig. 3.10d, $p<0.05$). In the mediastinal lymph node (MLN) and the spleen (SP), where B cell expansion causes lymphoproliferation and splenomegaly was no different between MCMV mOVA and WT vaccinated mice respectively (Fig. 3.10d, $p>0.05$). Antibody confirmed MHV-68 and OVA-specific IgG response in MCMV mOVA and MCMV WT vaccinated mice (Fig. 3.10e-f). The latter had lower IgG to OVA and higher IgM to MHV-68 mOVA suggesting primary response compared to MCMV mOVA vaccinated group (Fig. 3. 10f).

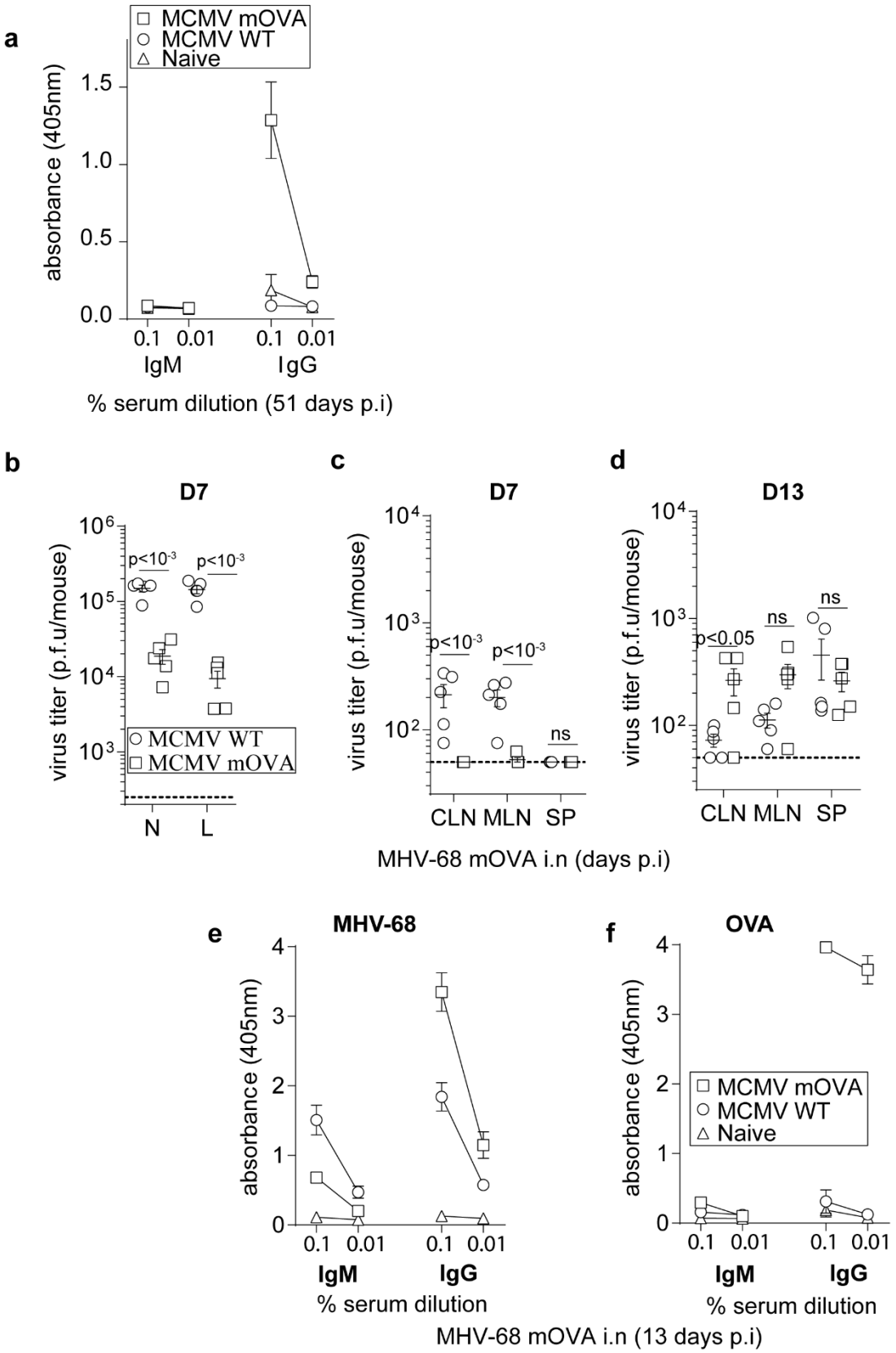
a
MCMV mOVA
MCMV WT
Naive
absorbance (405nm)
1.5
1.0
0.5
0.0
0.1 0.01 0.1 0.01
IgM IgG
% serum dilution (51 days p.i)
b
D7
virus titer (p.f.u/mouse)
p<10-3 p<10-3
MCMV WT
MCMV mOVA
N L
c
D7
p<10-3 p<10-3 ns
CLN MLN SP
d
D13
p<0.05 ns ns
CLN MLN SP
MHV-68 mOVA i.n (days p.i)
e
MHV-68
absorbance (405nm)
0.1 0.01 0.1 0.01
IgM IgG
% serum dilution
f
OVA
MCMV mOVA
MCMV WT
Naive
IgM IgG
% serum dilution
MHV-68 mOVA i.n (13 days p.i)

Fig. 3. 10. MCMV mOVA vaccination primes OVA-specific CD4$^+$ T cells.

Adult BALB/c mice were vaccinated via i.p injection with 10^6 p.f.u/mouse with MCMV mOVA or WT virus. After 51 days, IgM and IgG antibody response to OVA was determined by ELISA. The error bars show ± SEM (n=5 per group). The mice in **a** were then challenged with MHV-68 mOVA via the i.n route with $1x10^5$ p.f.u/mouse without anaesthesia for nose infection and $3x10^4$ p.f.u/mouse under anaesthesia for lung infection. **b)** Plaque assay was performed on noses and lungs after 7 days and infectious center assay **(c, d**) on SCLN, MLN and spleen after 7 and 13 days post challenge on permissive BHK-21 cells. Each data point represents virus titer per mouse (n=5 per group) and error bars show ±SEM. Mean difference was determined using multiple unpaired 2-tailed t-test using Bonferroni Dunn correction for multiple comparisons. ns 'not significant', $p > 0.05$. **e, f**) MHV-68 and OVA-specific antibody responses at day 13 post challenge was measured by ELISA. The error bars show ± SEM (n=5 per group). Data are representative of 2 independent experiments.

3.3.2 How do CD4$^+$ T cells restrict MHV-68 mOVA lytic infection in BALB/c?

3.3.2.1 IFN-γ response to OVA

IFN-γ has been shown to be the major cytokine secreted by CD4$^+$ T cells in response to MHV-68 infection (121). To measure IFN-γ response to OVA, BALB/c mice vaccinated with MCMV mOVA were challenged with MHV-68 mOVA. Seven days p.i, mice were depleted or not of CD4$^+$ and/ or CD8$^+$ T cell lymphocytes. Naïve target splenocytes were then infected with MHV-68 mOVA or incubated with 5 µM $OVA_{323-339}$ or 10 µM $OVA_{257-264}$ peptide or left untreated as control. Effector cells from undepleted, CD4$^+$ T cell depleted, CD8$^+$ T cell depleted, or CD4$^+$ and CD8$^+$ depleted mice were then co-cultured with the treated and untreated feeder cells and IFN-γ secretion measured. Only effector cells from undepleted and CD8 depleted mice secreted IFN-γ upon re-stimulation with MHV-68 mOVA and $OVA_{323-339}$ peptide (Fig. 3.11). IFN-γ to MHV-68 mOVA was highly variable between mice. The IFN-γ response was specific, since the $OVA_{257-264}$ peptide provided little stimulation to undepleted or CD4$^+$ T cell depleted effector cells (Fig. 3.11). Taken together, these results suggest that IFN-γ response to OVA or MHV-68 in BALB/c mice was predominately CD4$^+$ T cell dependent. Differences between mice in the level of MHV-68 mOVA infection could account for the variability of the IFN-γ response.

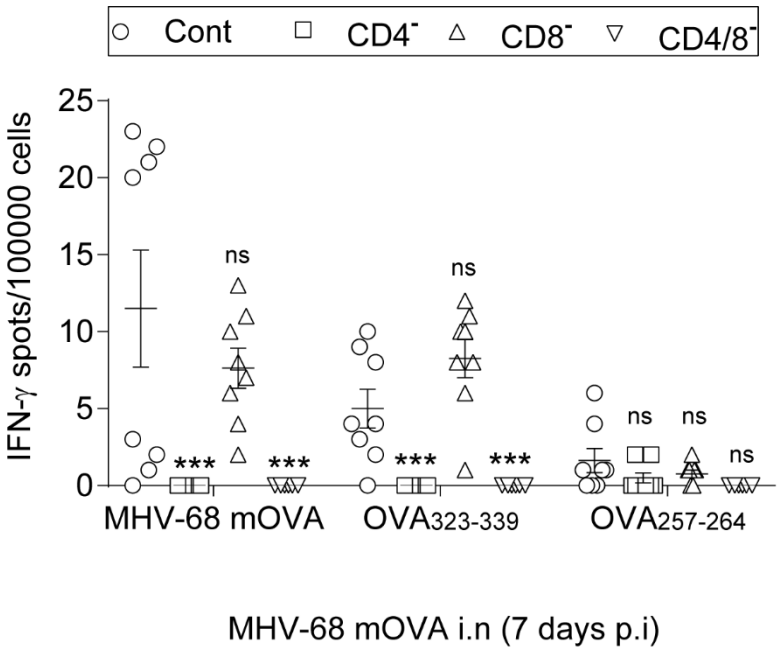

Fig. 3. 11. Frequency of IFN-γ producing T lymphocytes.

Adult BALB/c mice vaccinated by i.p injection with MCMV mOVA **as in fig. 3.10** were depleted of T lymphocytes or left undepleted and then challenged via the i.n route with MHV-68 mOVA. Seven days post challenge, the frequency of IFN-γ producing T cells in splenocytes of undepleted, $CD4^+$ T cell depleted, $CD8^+$ T cell depleted and $CD4^+$ and $CD8^+$ depleted mice upon stimulation with MHV-68 mOVA, $OVA_{323-339}$ or $OVA_{257-264}$ or uninfected target cells was determined by ELISPOT. Each symbol represents the number of spots per $1x10^5$ effector cells from which the mean number of spots of uninfected target cells were subtracted. The error bars show difference in spots between mice in quadruplicates (n=2 per group). Data was analysed using multiple t-test (ns, $p>0.05$; * $p<0.05$; *** $p<0.001$). Undepleted (Cont) IFN-γ spots was used to compare response between $CD4^+$, $CD8^+$ and $CD4/8^+$ depleted effector T lymphocytes.

3.3.2.2 Adoptive transfer of $CD4^+$ T cell $OVA_{323-339}$

To better characterise the contribution of $CD4^+$ T cells in limiting lytic infection, DO11.10 $OVA_{323-339}$-specific $CD4^+$ T cells were adoptively transferred to naïve BALB/c mice as previously described. Subsequently, mice were primed with MCMV mOVA by i.p injection. After 14 days, the mice were challenged with MHV-68 mOVA or MHV-68 WT. Seven days post challenge organs of interest were harvested. First, splenocytes were processed and stained KJI-26 as before to determine whether DO11.10 $OVA_{323-339}$-sepcific $CD4^+$ T cells expanded. These cells were undetectable by flow cytometry (results not shown). Infectious virus was then determined by plaque assay. MHV-68 mOVA lung and nose titers were significantly reduced compared to MHV-68 WT (Fig. 3.12a). Lytic antigen staining showed infection in MHV-68 mOVA infected lungs was localised compared to WT infected lung where infection was dispersed throughout the tissue (Fig. 3.12b-c). Infected cells in both groups expressed podoplanin and were negative for CD68 suggesting type 1 alveolar epithelial cells. $CD4^+$ T cells are seen proximal to infected cells (Fig. 3.12c).

a

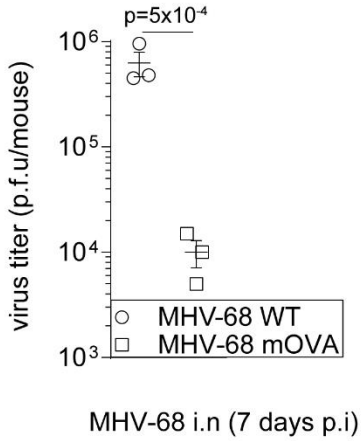
p=5x10-4
virus titer (p.f.u/mouse)
10^6
10^5
10^4
10^3
MHV-68 WT
MHV-68 mOVA
MHV-68 i.n (7 days p.i)

b

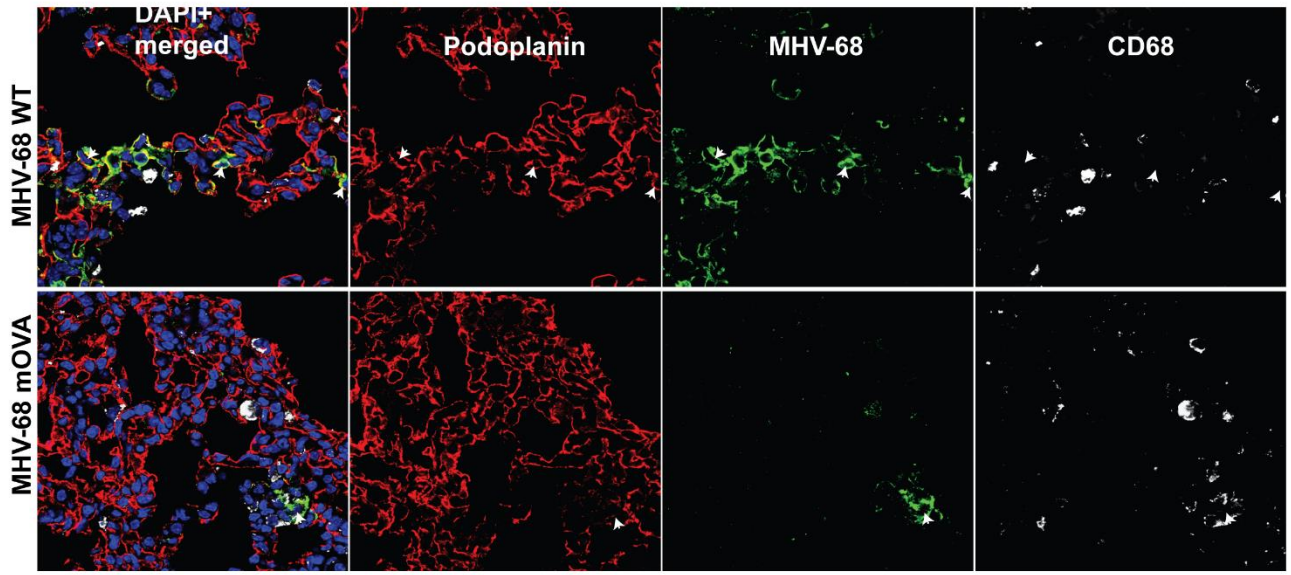
DAPI+ merged
Podoplanin
MHV-68
CD68
MHV-68 WT
MHV-68 mOVA

c

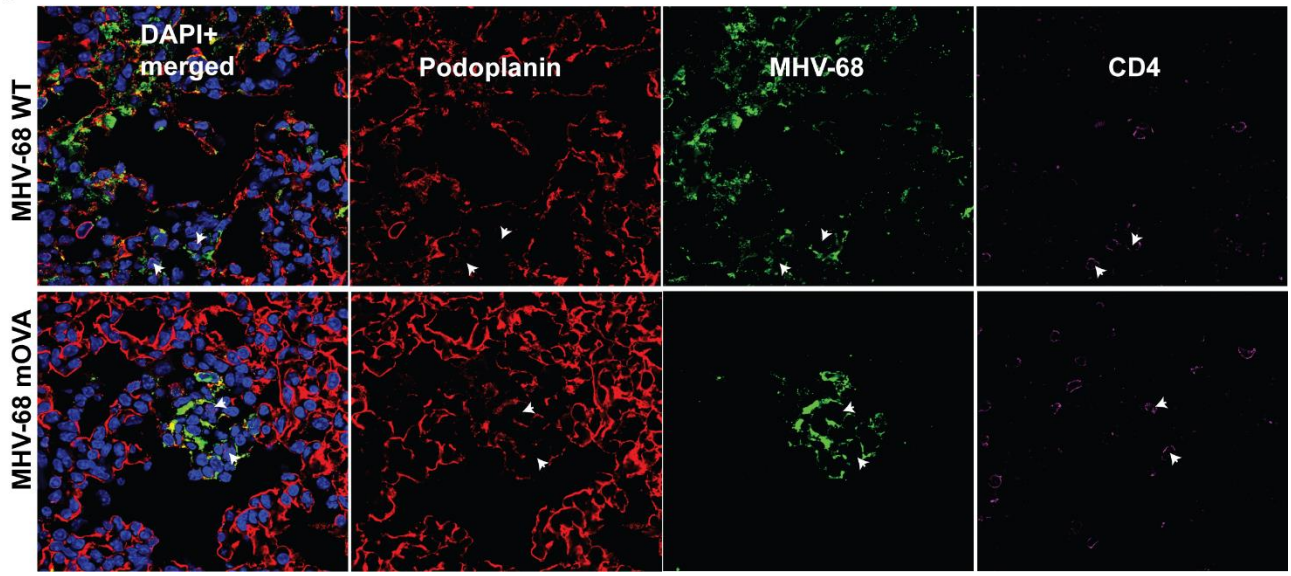
DAPI+ merged
Podoplanin
MHV-68
CD4
MHV-68 WT
MHV-68 mOVA

Fig. 3. 12. OVA primed $CD4^+$ and $CD8^+$ T cells control lytic infection.

Adult BALB/c mice were adoptively transferred naïve $2x10^6$ $OVA_{323-339}$-specific $CD4^+$ T cells from DO11.10 transgenic mice by i.v injection and primed with $1x10^5$ p.f.u/200µL MCMV mOVA via the i.p route. After 14 days, the mice were then infected via the i.n route with MHV-68 WT or MHV-68 mOVA. **a)** Virus titer in the lungs was determined by plaque assay 7 days post infection. Each data point represents virus titer per mouse (n=3 per group) and error bars show ± SEM. Difference in mean was determined using multiple unpaired 2 tailed t-test using Bonferroni Dunn correction for multiple comparisons. ns 'not significant', $p > 0.05$. **b, c)** MHV-68 WT and MHV-68 mOVA lungs were stained for MHV-68 lytic antigens and for podoplanin, CD68 and CD4. Arrows show podoplanin and $CD4^+$ T cells. $CD4^+$ T cells are seen proximal to infected cells. All images were taken at X63 magnification.

3.3.3 DO11.10 transgenic mice are heterogeneous

To understand why $OVA_{323-339}$-specific KJ1-26^+CD4^+ T cells were undetectable, DO11.10 transgenic mice were genotyped. The mice were found to be heterogeneous for the clonotypic marker KJ1-26 that recognises $OVA_{323-339}$ Tcr (Fig. 3.13a). As expected BALB/c splenocytes were negative for KJ1-26 (Fig. 3.13b). This implies the reduction in lytic replication and restriction of infected cells by $CD4^+$ T cells observed in MHV-68 mOVA infected mice is the result of the action of endogenously primed $CD4^+$ T cell clones. Previous reports have shown that, BALB/c ($H\text{-}2^d$) mice primed with OVA generated distinct clones of $CD4^+$ T cells in response $OVA_{323-339}$ peptide stimulation compared to DO11.10 transgenic mice. It was then postulated that in BALB/c mice, $OVA_{323-339}$ could be presented in three different forms, potentially generating three distinct T cell epitopes (167).

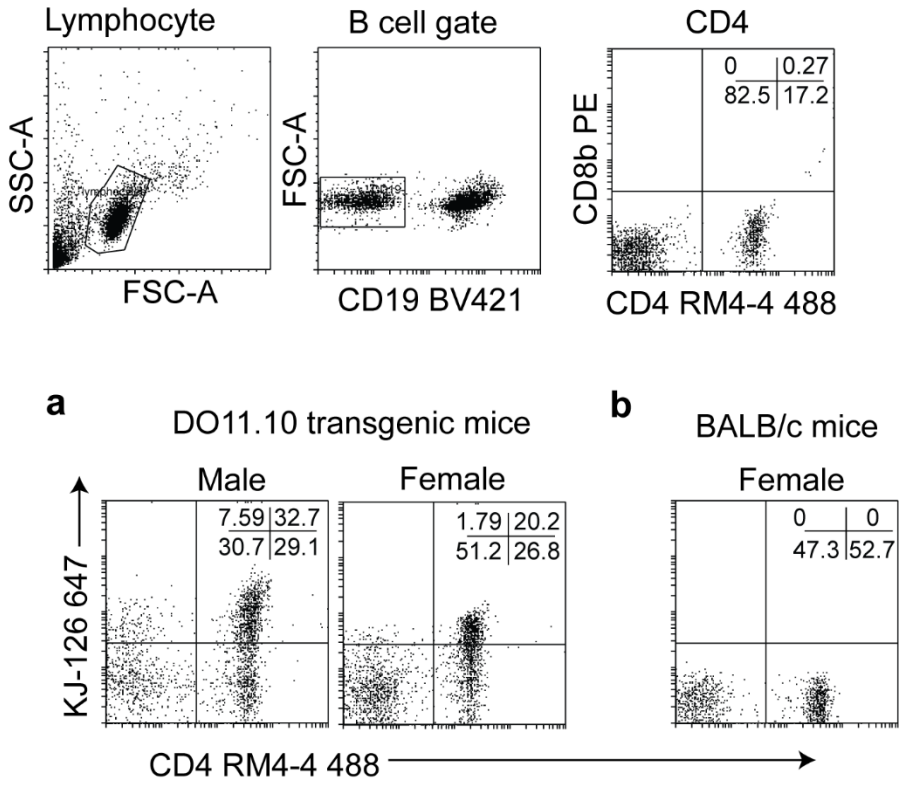

Fig. 3. 13. OVA$_{323-339}$-specific DO11.10 transgenic mice are heterogeneous.

Splenocytes from DO11.10 transgenic mice and BALB/c were harvested, homogenised and single cell suspensions stained. DO11.10 splenocytes were stained with rat anti-mouse CD19 BV421, CD4$^+$ T cells using rat anti-mouse CD4 clone RM4-4 fluorescein or double stained with CD4$^+$ and KJ1-26 647. CD19 was used to gate out B cells. DO11.10 transgenic mice **(a)** had KJ1-26 high and low cells while BALB/c mice **(b)** stained negative for KJ1-26 cells.

3.3.4 C57BL/6 vaccination confers protection against mucosal infection and short-term lymphoproliferative disease

Ovalbumin priming of C57BL/6 mice stimulates memory $OVA_{257-264}$ specific $CD8^+$ T cells. Thus, to control for $CD8^+$ T cell response and determine how $CD4^+$ T cells reduced MHV-68 mOVA infection in BALB/c mice, MCMV mOVA and MCMV WT primed C57BL/6 were tail bled fifty-one days post priming and challenged with MHV-68 mOVA. Antibody response to OVA in MCMV mOVA and MCMV WT primed mice showed predominately IgG response to OVA in the former confirming ovalbumin vaccination (Fig. 3.14a). During lytic infection, MHV-68 mOVA nose and lung infection was controlled in MCMV mOVA vaccinated mice compared to MCMV WT (Fig. 3.14b). Lymphoproliferation and splenomegaly which occurs 13 to 18 days post infection was controlled at day 13 in MCMV mOVA vaccinated mice but not MCMV WT (Fig. 3.14d). During persist infection which occurs from 21 days, MCMV mOVA vaccination failed to control long term persistent infection of B cells in the lymph node and spleen (Fig. 3.14e) despite elevated levels of IgG to OVA (Fig. 3.14g-h).

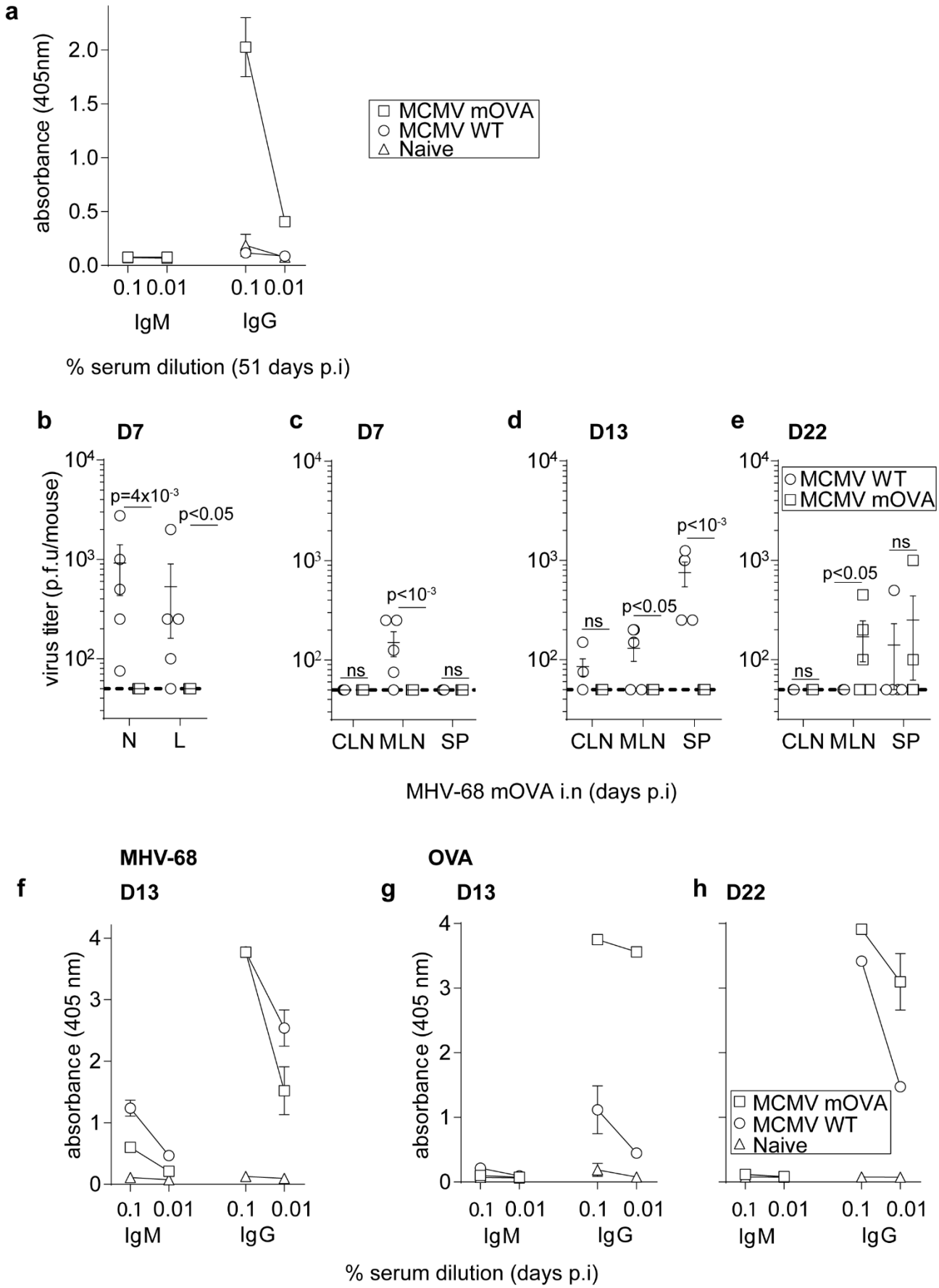
a
absorbance (405nm)
2.0
1.5
1.0
0.5
0.0
0.1 0.01
IgM
0.1 0.01
IgG
MCMV mOVA
MCMV WT
Naive
% serum dilution (51 days p.i)
b
D7
virus titer (p.f.u/mouse)
p=4x10-3
p<0.05
N
L
c
D7
p<10-3
ns
ns
CLN MLN SP
d
D13
p<10-3
p<0.05
ns
CLN MLN SP
e
D22
MCMV WT
MCMV mOVA
p<0.05
ns
ns
CLN MLN SP
MHV-68 mOVA i.n (days p.i)
MHV-68
OVA
f
D13
absorbance (405 nm)
0.1 0.01
IgM
0.1 0.01
IgG
g
D13
absorbance (405 nm)
0.1 0.01
IgM
0.1 0.01
IgG
h
D22
MCMV mOVA
MCMV WT
Naive
0.1 0.01
IgM
0.1 0.01
IgG
% serum dilution (days p.i)

Fig. 3. 14. MCMV mOVA primes OVA-specific CD8$^+$ T cells.

Adult C57BL/6 mice were vaccinated via the i.p route with 10^6 p.f.u/mouse with MCMV mOVA or WT. After 51 days, IgM and IgG response to OVA were determined by ELISA. **a)** Absorbance was read at 405 nm. The error bars show ± SEM (n=5 per group). The mice in **a** were then challenged with MHV-68 mOVA via the i.n route with $1x10^5$ p.f.u/mouse without anaesthesia for nose infection and $3x10^4$ p.f.u/mouse under anaesthesia for lung infection. **b)** 7 days post challenge, virus titer in the nose and lung was determined by plaque assay and by infectious centre assay on SCLN, MLN and spleen after 7 (**c**), 13 (**d**) and 22 (**e**) days. Each data point represents virus titer per mouse (n=5 per group) and error bars ±SEM of the mean. Difference in mean was determined using multiple unpaired 2 tailed test using Bonferroni Dunn correction for multiple comparisons. ns 'not significant', $p > 0.05$. **f, g** and **h)** MHV-68 and OVA-specific antibody response in the serum at day 13 and 21 post challenge was measured by ELISA. The error bars show ± SEM (n=5 per group). Data are representative of 2 independent experiments.

3.3.5 To understand T cell mediated immune control of MHV-68 mOVA using F1 mice

The vaccination response to MHV-68 mOVA in BALB/c and C57BL/6 mice showed neither CD4$^+$ nor CD8$^+$ T cells alone were effective at controlling infection. To understand how CD4$^+$ and CD8$^+$ T cells coordinate the control MHV-68 infection, BALB/c mice were crossed with C57BL/6 mice. Adult F1 offspring were then vaccinated with MCMV mOVA or MCMV WT. One-month post vaccination, the mice were tail bled to measure antibody to MCMV and OVA and the challenged via the i.n route with MHV-68 mOVA. Antibody to MCMV was predominately IgG in MCMV WT and MCMV mOVA vaccinated mice suggesting persistent infection meanwhile while antibody to OVA was predominately IgG in the former and not the latter, confirming ovalbumin vaccination status (Fig. 3.15a). After 7 days post challenge, lytic infection in the nose and lung of MCMV mOVA vaccinated mice was reduced compared to MCMV WT (Fig. 3.15b, $p<0.01$). To understand how lytic infection was reduced, MCMV mOVA vaccinated F1 mice were depleted of T cell lymphocytes or not and challenged with MHV-68 mOVA. Seven days post challenge, lytic infection in the nose and lung of undepleted, CD4$^+$ and CD4 and/ or CD8$^+$ depleted mice was determined by plaque assay. T lymphocyte depletion was confirmed by flow cytometry (Fig. 3.15d). The results show that neither CD4$^+$ nor CD8$^+$ T cells alone were sufficient to control infection at the lungs and the nose (Fig. 3.15c). However, depleting both CD4$^+$ and

$CD8^+$ T cells increased virus infection (Fig. 3.15c, $p<0.01$). This suggests that primed $CD4^+$ and $CD8^+$ T cells are both necessary to restrict lytic replication.

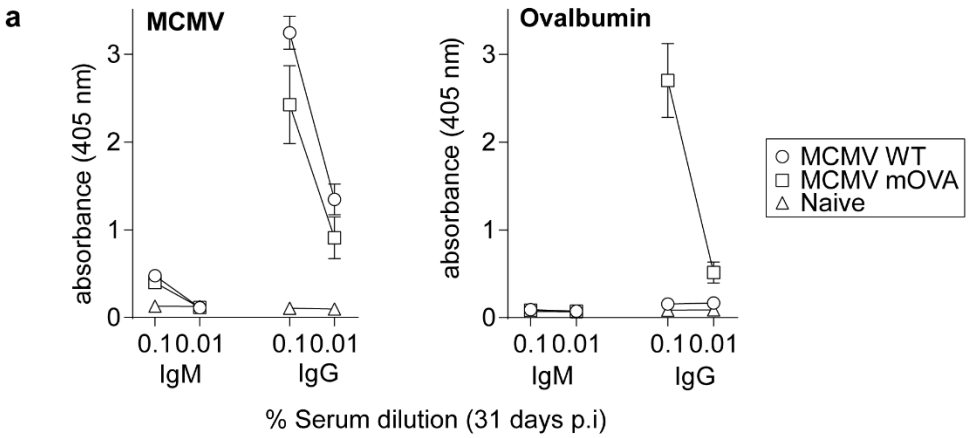
a
MCMV
Ovalbumin
absorbance (405 nm)
MCMV WT
MCMV mOVA
Naive
0.1 0.01
IgM
IgG
% Serum dilution (31 days p.i)

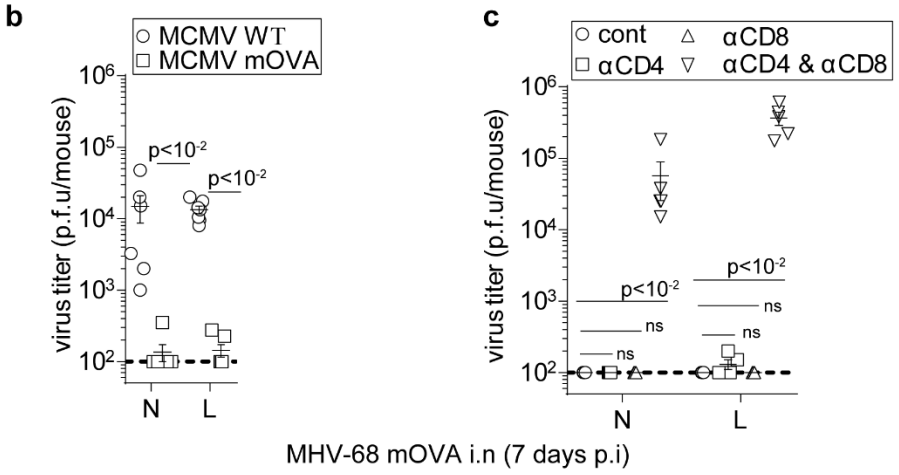
b
c
MCMV WT
MCMV mOVA
cont
αCD8
αCD4
αCD4 & αCD8
virus titer (p.f.u/mouse)
p<10-2
ns
N
L
MHV-68 mOVA i.n (7 days p.i)

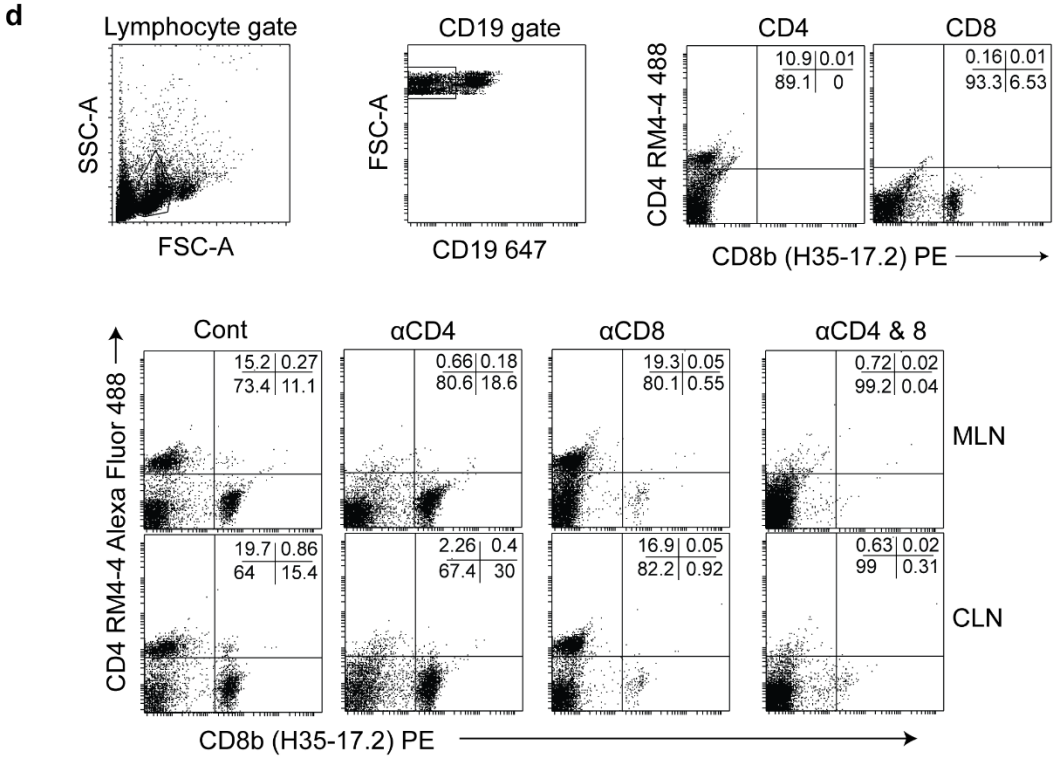
d
Lymphocyte gate
SSC-A
FSC-A
CD19 gate
CD19 647
CD4
CD8
CD4 RM4-4 488
CD8b (H35-17.2) PE
Cont
αCD4
αCD8
αCD4 & 8
CD4 RM4-4 Alexa Fluor 488
MLN
CLN

Fig. 3. 15. Lytically primed OVA-specific $CD4^+$ T cells restrict lytic infection.

a) Adult F1 mice were vaccinated i.p with 10^6 p.f.u/mouse with MCMV mOVA or WT. After 31 days, IgM and IgG antibody response to MCMV and OVA were determined by ELISA. Error bars show ± SEM (n=5 per group). **b)** The mice in **a** were then challenged with MHV-68 mOVA via the i.n route with $1x10^5$ p.f.u/mouse without anaesthesia for nose infection and $3x10^4$ p.f.u/mouse under anaesthesia for lung infection. Plaque assay was performed on noses and lungs after 7 days. **d)** T cell lymphocytes were depleted in MCMV mOVA vaccinated mice in **a** at 96 hrs, 48 hrs and at time of infection with MHV-68 mOVA via i.n with $3x10^4$-$1x10^5$ p.f.u/mouse and every 48 hrs until termination at day 7. Virus titer was then determined by plaque assay in **c**. T lymphocyte depletion in **d** was determined by staining lymphocytes from SCLN, MLN and spleen for $CD4^+$ and $CD8^+$ T cells and CD19 to gate out B cells. Each data point in **b** and **c** represents virus replication per mouse (n=5-6 per group) and error bars show ± SEM. Data was determined using multiple t-test with Bonferroni Dunn correction for multiple comparisons. ns 'not significant', $p > 0.05$.

3.3.6 F1 mice fail to control latent infection

To determine whether $CD4^+$ T cells would rescue persistent infection observed in C75BL/6 mice, F1 mice were vaccinated as above, and infection was monitored over a course of 100 days. Seven days post infection, virus was detected in the MLN of MCMV WT but MCMV mOVA vaccinated mice (Fig. 3.16a). At day 13, a period of acute lymphoproliferation, lymph node virus titers measured by infectious centre assay in MCMV mOVA vaccinated mice was reduced while in the spleen it was controlled compared to MCMV WT (Fig. 3.16b). At day 18 and day 22 post infection, a period of extensive B cell expansion (splenomegaly), the level of virus in the lymph node and spleen was comparable between MCMV mOVA and MCMV WT vaccinated mice (Fig. 3.16c-d, $p>0.05$). This was also observed by qPCR at day 30, day 72 and day 100 in the spleen (Fig. 3.16e-g).

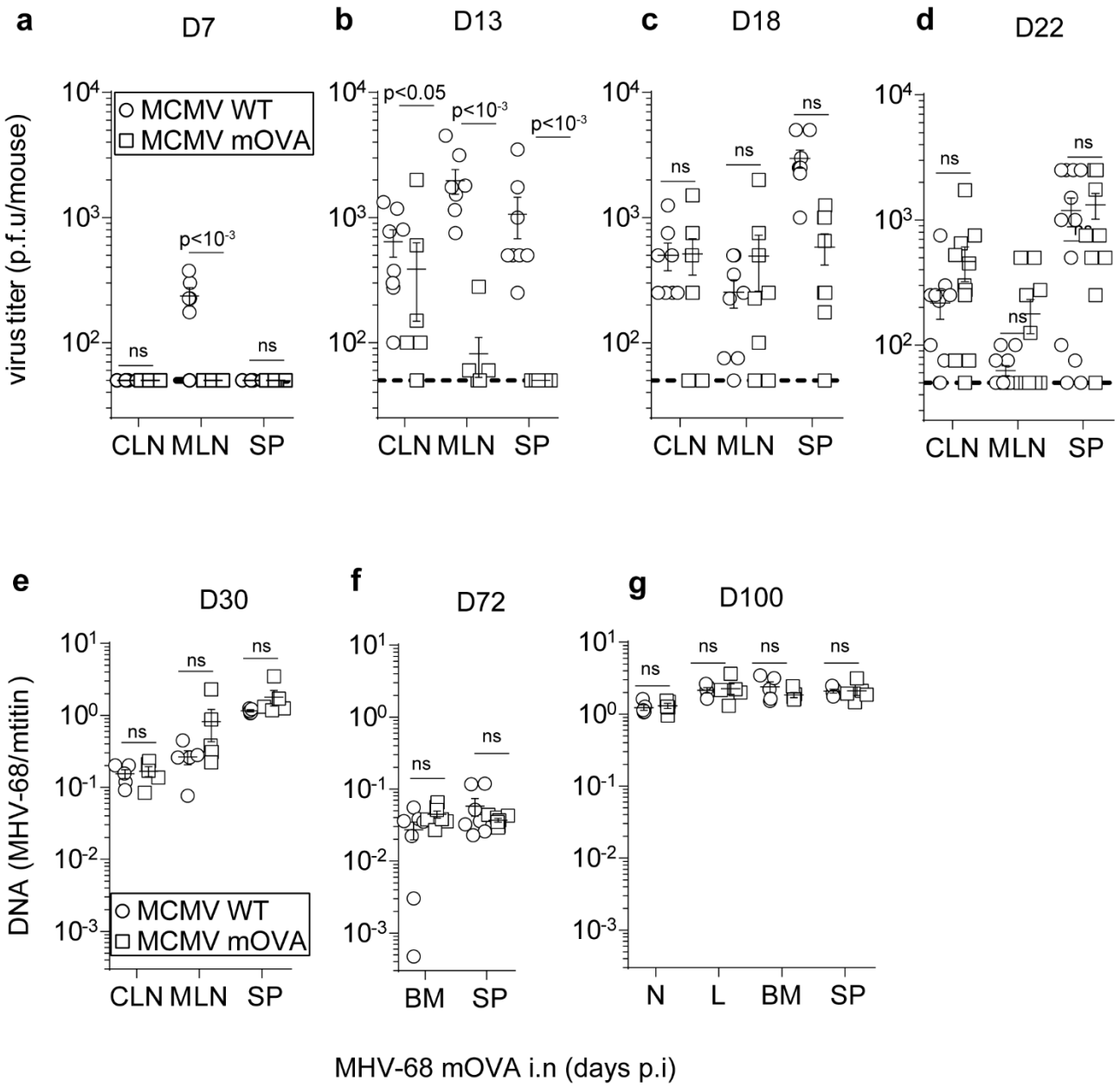

Fig. 3. 16. Lytically primed OVA-specific CD4$^+$ T cells restrict acute but not long-term infection

Adult F1 mice vaccinated and challenged as in **Fig. 3.15** were monitored over a course of 100 days. Infectious virus in **a**, **b**, **c** and **d** was determined by infectious center assay. Viral load in **e**, **f** and **g** was determined by QPCR. Each data point represents the ratio of K3 viral copies normalised to mtitin cellular copies per mouse tissue (n=5-6 per group). Error bars show ± SEM. Multiple unpaired 2 tailed t-test with Bonferroni Dunn post-test correction was used to analyse difference in means. ns 'not significant', $p > 0.05$.

Viral DNA was also detected in the bone marrow of mice at day 72 and day 100 (Fig. 3.16f-g) and in the nose and lung at the latter time point. There was no difference between MCMV mOVA and WT groups (Fig. 3.16d-g, $p>0.05$). This suggests that MHV-68 evades host immune response and recirculates in latently infected cells between peripheral and non-periphery sites to establish persistent infection in the host. Antibody to OVA was abundantly produced throughout infection but was ineffective at neutralising MHV-68 mOVA (Fig. 3.17a). Thus, cytotoxic T cell lymphocyte response to infected cells that present OVA is probably more effective, than neutralisation in C57BL/6 or F1 mice.

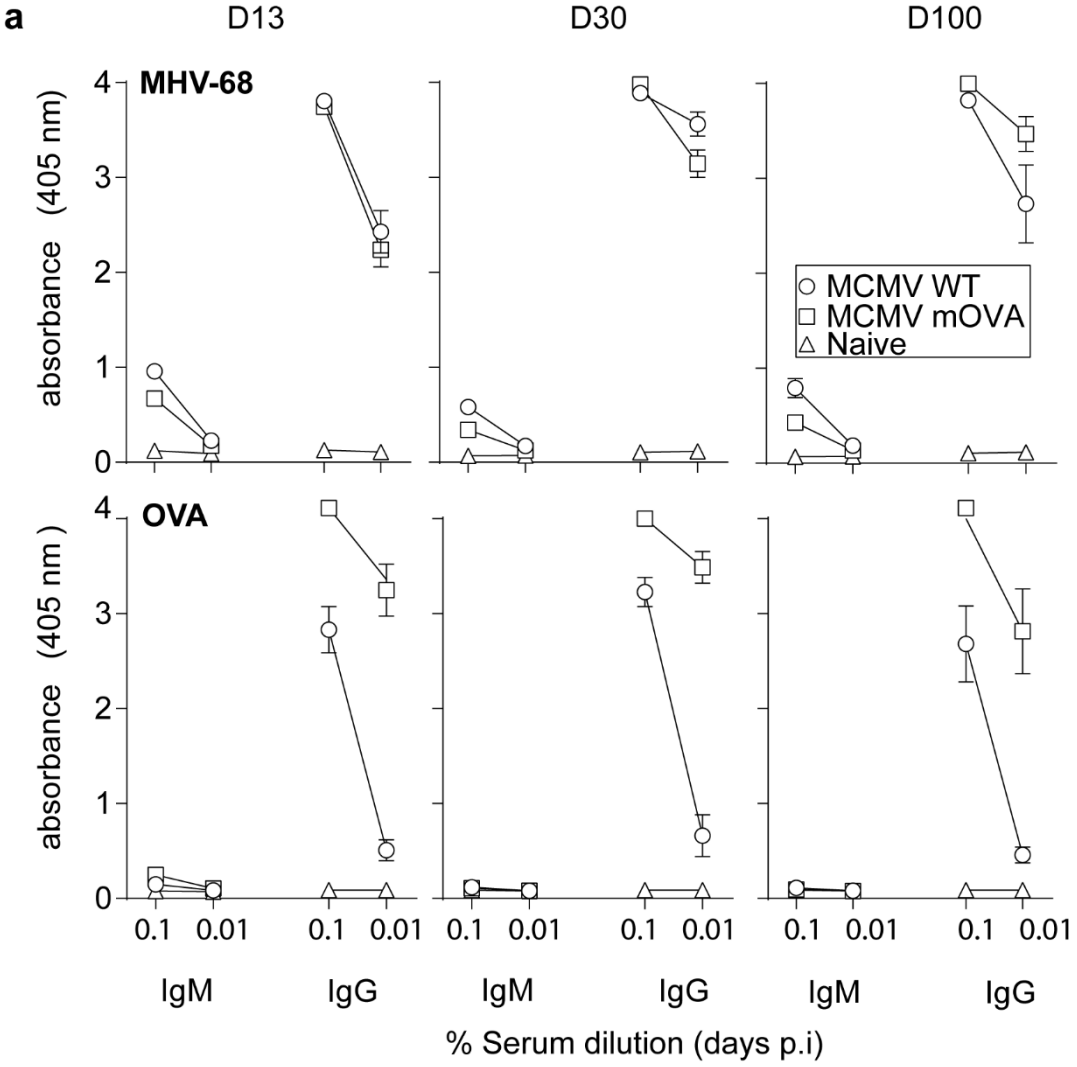

Fig. 3. 17. F1 mice retain elevated levels of OVA-specific antibody IgG.

Adult F1 mice vaccinated and challenged as in **Fig. 3.16** were analysed for IgM and IgG antibody response to MHV-68 and OVA after 13, 30 and 100 days post infection by ELISA. Absorbance was read at 405 nm. Error bars show ± SEM (n=5 per group).

3.3.7 Primed lytic $CD4^+$ T cells restrict splenomegaly in MHV-68 IiOVA infected mice

$CD4^+$ T cells have been shown to be important during latency. To determine whether primed $CD4^+$ T cells can limit B cell proliferation in the spleen (splenomegaly), BALB/c mice were vaccinated with MCMV mOVA and MCMV WT. The mice were then challenged with MHV-68 IiOVA. MHV-68 IiOVA expresses $OVA_{323-339}$ in tandem with IRES downstream of ORF73 to translate the epitope when the promoter is active (160). During latency, $OVA_{323-339}$ is then presented in the context of 1-A^d/1-A^b by infected antigen presenting cells (160). During lytic infection, there was no difference in virus titer in the nose, lungs or lymphoid organs between MCMV mOVA and MCMV WT vaccinated mice (Fig. 3.18a). The presence of relatively high titer virus in the lymph nodes and spleen at day 7 (Fig. 3.18b) suggests virus replication was unrestricted at mucosal sites. By day 13, a period of lymphoproliferation and onset of splenomegaly, MCMV mOVA vaccinated mice had reduced infectious virus in the spleen suggesting reduced splenomegaly compared to MCMV WT (Fig. 3.18c). In the lymph nodes, there was no difference in virus titer between MCMV mOVA and WT mice (Fig. 3.18c) suggesting lymphoproliferation was comparable. Thus, the results suggest that, lytically primed $CD4^+$ T cells can reduce splenomegaly when the $OVA_{323-339}$ epitope is expressed during latency.

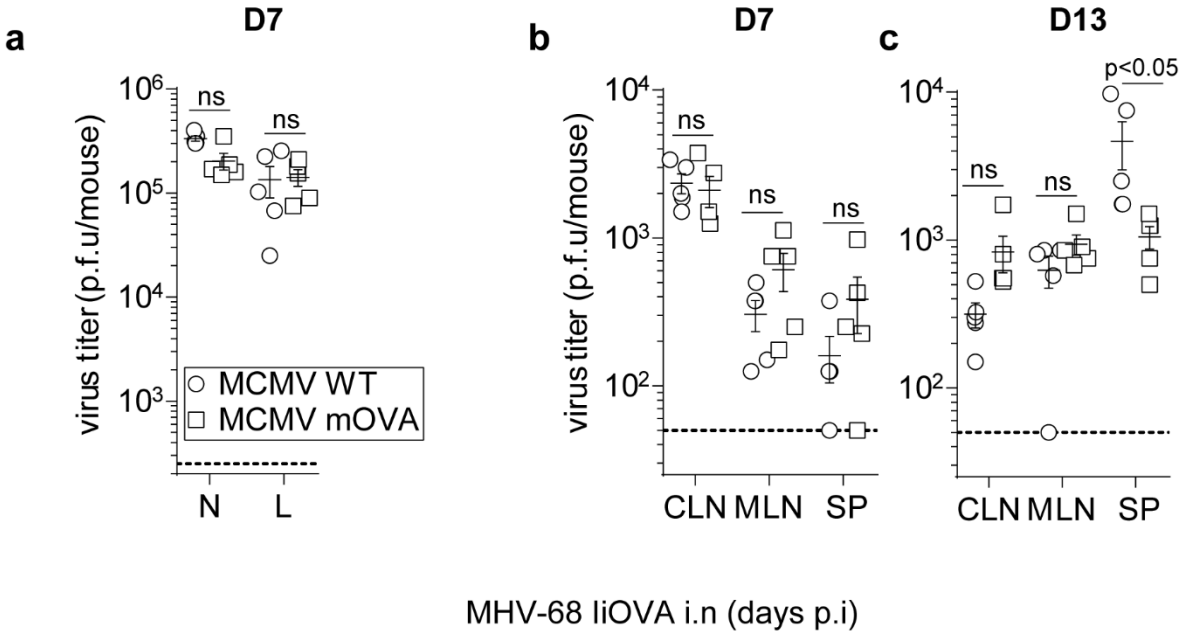

Fig. 3. 18. Lytically primed OVA-specific CD4⁺ T cells restrict splenomegaly.

Adult BALB/c mice were vaccinated via the i.p route with 10^6 p.f.u/mouse with MCMV mOVA or WT. After 51 days, the mice were challenged with MHV-68 liOVA via the i.n route with $1x10^5$ p.f.u/mouse without anaesthesia for nose infection and $3x10^4$ p.f.u/mouse under anaesthesia for lung infection. Virus titer in the nose and lung in **a** was determined by plaque assay after 7 days and infectious center assay on SCLN, MLN and spleen in **b** and **c** after 7 and 13 days post challenge. Each data point represents virus titer per mouse (n=5 per group) and error bars show SEM from the mean. Difference in mean was determined using multiple unpaired 2 tailed t-test using Bonferroni Dunn post-test. ns 'not significant', $p > 0.05$.

3.4 Can pre-existing antibody restrict mucosal infection?

To address whether antibody was required to control MHV-68 infection, BALB/c were vaccinated with vaccinia virus expressing MHV-68 glycoprotein gH/gL and an irrelevant non MHV-68 glycoprotein for a month. To confirm antibody response to gH/gL, sera from vac control and gH/gL vaccinated BALB/c was assayed on CHO expressing gH/gL (CHO gH/gL) or CHO cells and analysed by flow cytometry.

3.4.1 gH/gL antibody in BALB/c mice controls MHV-68 infection

Flow cytometry results showed BALB/c vaccinated with vac gH/gL, shown as dotted line, bound to gH/gL expressing CHO cells, while vac control did not bind to gH/gL expressing CHO cells (Fig. 3.19b). Vac gH/gL vaccination restricted MHV-68 lytic infection in the nose but not the lung (Fig. 3.19c). Lymphoproliferation in the lymph nodes and splenomegaly in the spleens was also controlled in vac gH/gL vaccinated mice compared to vac control (Fig. 3.19d-e, $p<0.001$)

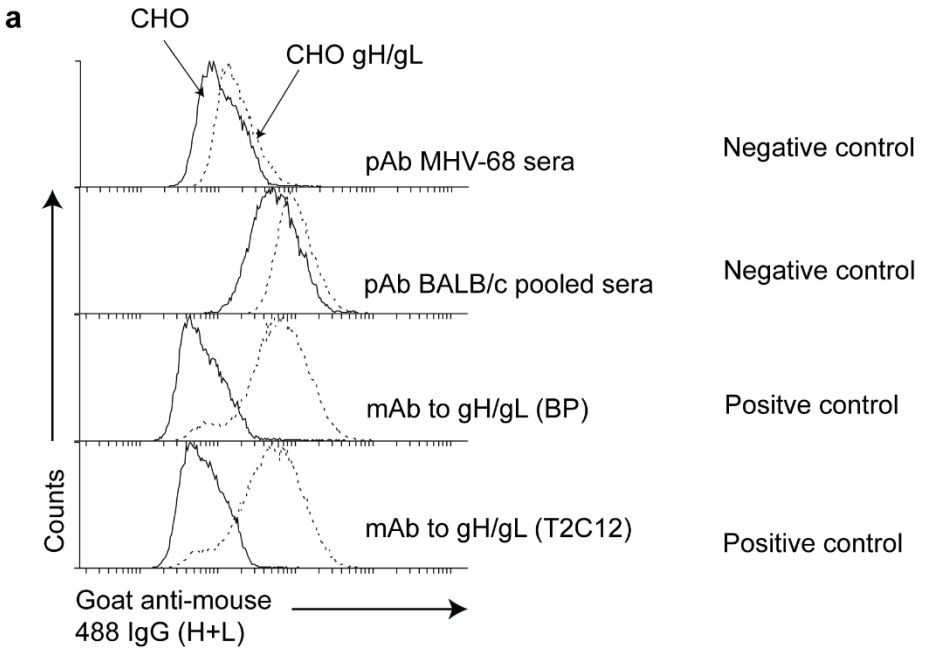
a
CHO
CHO gH/gL
pAb MHV-68 sera
Negative control
pAb BALB/c pooled sera
Negative control
mAb to gH/gL (BP)
Positve control
mAb to gH/gL (T2C12)
Positive control
Counts
Goat anti-mouse
488 IgG (H+L)

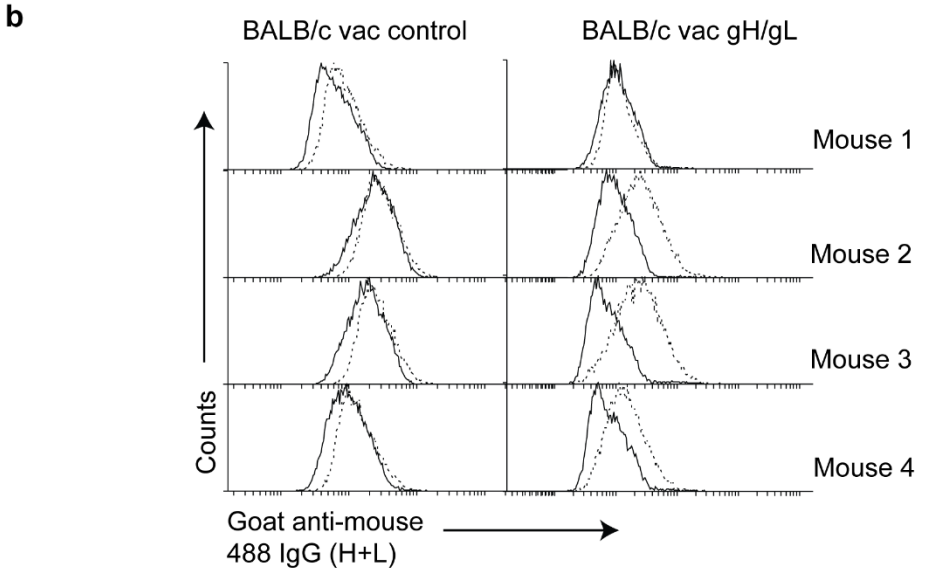
b
BALB/c vac control
BALB/c vac gH/gL
Mouse 1
Mouse 2
Mouse 3
Mouse 4
Counts
Goat anti-mouse
488 IgG (H+L)

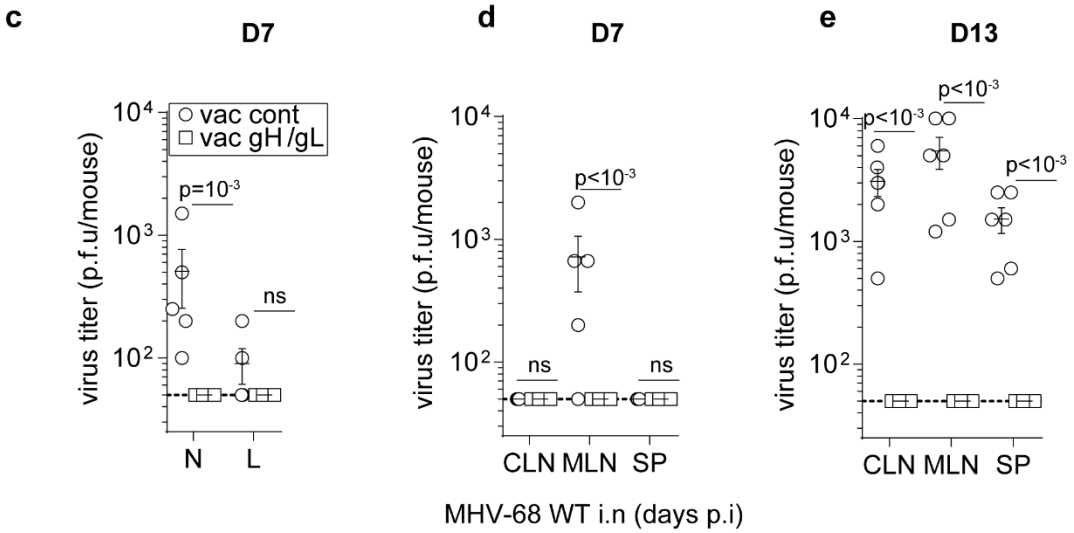
c
D7
vac cont
vac gH/gL
p=10-3
ns
virus titer (p.f.u/mouse)
N
L
d
D7
p<10-3
ns
ns
CLN MLN SP
e
D13
p<10-3
p<10-3
p<10-3
CLN MLN SP
MHV-68 WT i.n (days p.i)

Fig. 3. 19. Pre-existing gH/gL controls acute lytic infection and B cell lymphoproliferation.

a, b) Adult BALB/c mice were vaccinated i.p with 10^6 p.f.u/mouse recombinant vaccinia virus expressing gH/gL or irrelevant protein. After a month, the mice were tail bled and antibody to gH/gL was determined by immunofluorescence using CHO cells expressing gH/gL or irrelevant protein. Bound antibody was detected using goat anti-mouse Alexa Fluor 488 IgG (H+L) and analysed by flow cytometry. **c-e**) The mice were then challenged i.n with MHV-68 via the i.n route with $1x10^5$ p.f.u/mouse without anaesthesia for nose infection and $3x10^4$ p.f.u/mouse under anaesthesia for lung infection. Virus titer in the nose and lung in **c** was determined by plaque assay and reactivating virus in **d** and **e** was determined by infectious center assay. Each data point represents reactivating virus per mouse organ (n=5-6 per group) and error bars show ± SEM. Multiple unpaired 2 tailed t-test with Bonferroni Dunn correction post-test was used to analyse difference in means. ns 'not significant', $p > 0.05$.

3.4.2 gH/gL antibody in C57BL/6 mice fails to control MHV-68 infection

To determine whether antibody was also required to control MHV-68 infection in C57BL/6 mice, the mice were vaccinated with vaccinia virus expressing MHV-68 glycoprotein gH/gL and an irrelevant non MHV-68 glycoprotein for a month. To confirm antibody response to gH/gL, sera was analysed on CHO cells expressing gH/gL or not by flow cytometry. Vac gH/gL vaccinated C57BL/6 sera bound gH/gL expressing CHO cells while vac control sera did not (fig. 3.20b). However, there was considerable variability between mice. The mice were then infected i.n with MHV-68 WT. After seven days post infection, vac gH/gL vaccinated mice failed to restrict MHV-68 nose and lung infection (fig. 3.20c, $p>0.05$). Lymphoproliferation in the lymph node of vac gH/gL vaccinated mice was controlled by day 13 (fig. 3.20d-e). Splenomegaly in the spleen of vac gH/gL vaccinated mice was increased compared to vac control at day 7 and reduced by day 13 (fig. 3.20d-e). In summary, pre-existing antibody to gH/gL is more effective in BALB/c mice than in C57BL/6 mice.

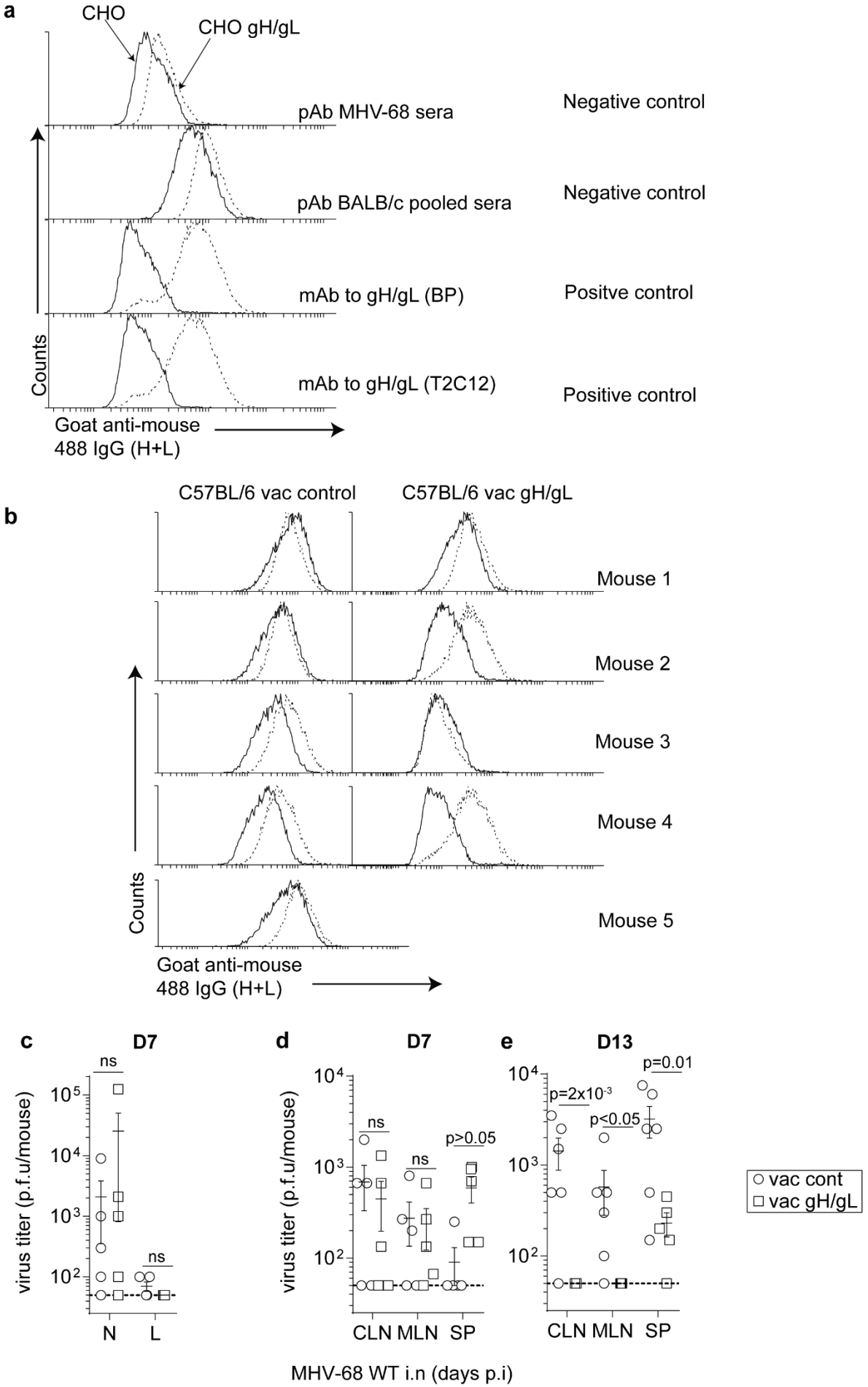
a
CHO
CHO gH/gL
pAb MHV-68 sera
Negative control
pAb BALB/c pooled sera
Negative control
mAb to gH/gL (BP)
Positve control
mAb to gH/gL (T2C12)
Positive control
Counts
Goat anti-mouse
488 IgG (H+L)
b
C57BL/6 vac control
C57BL/6 vac gH/gL
Mouse 1
Mouse 2
Mouse 3
Mouse 4
Mouse 5
Counts
Goat anti-mouse
488 IgG (H+L)
c
D7
ns
ns
virus titer (p.f.u/mouse)
N
L
d
D7
ns
ns
p>0.05
CLN MLN SP
e
D13
p=0.01
p=2x10-3
p<0.05
CLN MLN SP
vac cont
vac gH/gL
MHV-68 WT i.n (days p.i)

Fig. 3. 20. Pre-existing gH/gL fails to control lytic infection and B cell lymphoproliferation.

a, b) Adult C57BL/6 mice were vaccinated i.p with 10^6 p.f.u/mouse recombinant vaccinia virus expressing MHV-68 glycoproteins gH/gL or an irrelevant protein. After a month, the mice were tail bled and antibody to gH/gL was determined by immunofluorescence using CHO cells expressing gH/gL or irrelevant protein. Bound antibody was then detected using goat anti-mouse Alexa Fluor 488 IgG (H+L) and analysed by BD Accurri C6 flow cytometer. **c-e)** The mice were then challenged i.n with MHV-68 via the i.n route with $1x10^5$ p.f.u/mouse without anaesthesia for nose infection and $3x10^4$ p.f.u/mouse under anaesthesia for lung infection. Virus titer in the nose and lung in **c** was determined by plaque assay and reactivating virus in **d** and **e** was determined by infectious center assay. Each data point represents reactivating virus per mouse organ (n=5-6 per group) and error bars show ± SEM. Data analysis was performed using multiple unpaired 2 tailed t-test with Bonferroni Dunn post-test for multiple comparisons. ns 'not significant', $p > 0.05$.

3.5 Discussion

Vaccination with MCMV mOVA showed OVA-specific $CD4^+$ T cells reduced lytic infection in the nose and lungs of BALB/c mice but failed to control lymphoproliferation or splenomegaly during latency. Lytic infection was restricted by IFN-γ through OVA-specific T lymphocytes responding to the $OVA_{323-339}$ peptide, and not $OVA_{257-264}$, a $CD8^+$ T cell epitope. This is consistent with the described role of $CD4^+$ T cells in controlling MHV-68 infection in the lung via IFN-γ in B-cell deficient mice (121, 168). This was confirmed in DO11.10 transgenic mice in which $OVA_{323-339}$ specific $CD4^+$ T cells were found to restrict lytic infection and reduced latency but failed to prevent latency when MHV-68 mOVA was given i.p (159). These results show that, $CD4^+$ T cells play a role early during infection but are limited as infection progresses. Moreover, $CD4^+$ T cells are also known to drive proliferation of latently infected B cells in lymph nodes and spleen (116, 129, 169). MCMV mOVA primed mice had elevated virus titers compared to control mice suggesting $CD4^+$ T cell help. Whether primed $OVA_{323-339}$ $CD4^+$ T cells are the same subset of memory $CD4^+$ T cells driving B cell proliferation and splenomegaly remains to be determined.

The effective control of MHV-68 mOVA lytic and acute lymphoproliferation in C57BL/6 replicated previous observations using OT1/B6 and OT1/RAG systems (170) despite MHV-68 interference with MHC I antigen presentation (171, 172). This showed the SIINFEKL epitope in MCMV mOVA was presented to and recognised by cytotoxic $CD8^+$ T cells inducing a robust cytotoxic response. This robust response failed to prevent persistent infection consistent with previous results. Interestingly, OT-1 specific $CD8^+$ T cells was found to decrease in number 22 days post infection, a time which coincided with re-emergence of virus replication (170). This decline in $CD8^+$ T cells was attributed to lack of $CD4^+$ T cell help but could also reflect the role of $CD4^+$ T cells long term (122, 170). Re-emergence of infectious virus was observed 22 days after challenge in our vaccine model despite the presence of $CD4^+$ T cells in primed C57BL/6 immunocompetent mouse. Why this occurs is unknown. It is possible that MHV-68 evades primed $CD4^+$ T cells by transcriptional regulation of viral antigen expression in latently infected B cells. This was somewhat the case when primed MCMV mOVA mice were challenged with MHV-68 IiOVA that expressed $OVA_{323-339}$ peptide in tandem with ORF73. Lytically primed $CD4^+$ T cells reduced splenomegaly. This showed that OFR73 could be modulating expression of viral antigens on latently infected germinal center B cells (150, 173). What $CD4^+$ T cells see as

antigen during lytic infection is perhaps transcriptionally silent in latency or in latently infected B cells and only when reactivation occurs, are these cells effective. This selective viral gene expression in B cells is perhaps a strategy to sacrifice myeloid cells as targets since they have less stable forms of latency and are prone to reactivate (150).

The contribution of $CD4^+$ and $CD8^+$ T cells in controlling MHV-68 infection is well characterised (122, 174-176). This was tested in F1 mice, which in theory should generate proportionate $CD4^+$ and $CD8^+$ T cell responses to OVA. MCMV mOVA vaccinated F1 mice restricted lytic MHV-68 mOVA infection in the nose and lung. Virus clearance was dependent on primed $CD4^+$ and $CD8^+$ T cells as depleting both led to elevated virus titers in these mice (175). Antibody in this setting provided no protection, probably because OVA is not a viral protein, and neutralisation is thus ineffective. The underlining challenge in vaccine design against EBV is limiting persistent infection as demonstrated by reduced infectious mononucleosis. MHV-68 viral DNA was still detectable by real time PCR in the bone marrow and spleen at day 72 and in the nose, lung and in lymphoid tissue after 100 days. MHV-68 infection of the bone marrow occurs around 12 to 15 days post i.n or i.p infection and persists long term (116, 120, 177). EBV and KSHV have been detected in the bone marrow of AIDS patients and in transplant patients of the latter (178, 179). The bone marrow is thought to function as a site for haematopoiesis and activation of naïve or memory immune cells (120). Thus, access to the bone marrow through either trafficking of virions or by circulating mature B cells or reactivating cells or directly via the blood suggests an important strategy to replenish peripheral sites by infected immature B cells that seed to the spleen to undergo maturation (120). Therefore, early intervention at site of entry could limit bone marrow colonisation which in turn could limit persistence.

Antibody is important in preventing or reducing primary infection. The role of immune sera and monoclonal antibodies in reducing MHV-68 infection has previously been explored and found to reduce lytic infection via IgG Fc receptor engagement (133). However antibody coated virions were also found to be taken up via FcR mediated endocytosis by FcR^+ myeloid cells which was gp150 dependent (180). In the absence of gp150, post exposure to polyclonal gH/gL elicited by vaccinia virus vaccination blocked FcR^- mediated infection (181). This protective result was replicated in BALB/c but not in C57BL/6 mice when given vac gH/gL i.p and challenged with MHV-68 i.n. The mechanism of action of gH/gL neutralising antibody occurs by inhibiting endocytosis or membrane fusion in fibroblasts or epithelial cells (182-184). Monoclonal gH/gL can to some extent enhance

FcR^+ myeloid cell infection (180, 184). The fact that BALB/c mice revealed protection implies less epithelial /fibroblast infection and more myeloid infection where MHV-68 is less lytic. Although this is plausible, it is limited by the assay performed in this thesis. Perhaps, identifying infected cells by histology to determine the ratio of epithelial/fibroblast to myeloid cells would provide a better insight into the molecular mechanism of protection as Rosa and colleagues showed to some extent that gH/gL monoclonal antibody shifts MHV-68 infection from epithelial or fibroblasts to FcR^+ myeloid cells were infection is latent (180). Whether this is strain dependent remains to be determined.

MHV-68 is not known to inhibit NK cell antibody dependent cellular cytotoxicity. However, Alder and colleagues showed that MHV-68 can escape NK cell mediated immune surveillance by upregulating CEACAMI expression on lung alveolar epithelial cells (185). CAECAMI is an inhibitory receptor expressed by several cells including NK cells (185). MHV-68 infection of CAECAMI knockout mice showed faster clearance than in wild type mice. Depletion of NK cells in CAECAMI knockout mice showed much higher lung titers than undepleted CAECAMI knock out mice confirming that expression of CAECAMI either inhibits or initiates NK-cell killing. It is possible, that in C57BL/6 mice, infected cells are more resistant to NK-cell killing via induction of CAECAMI expression on infected epithelial cells. Whether this mechanism restricts antibody mediated cellular cytotoxicity remains to be investigated.

CHAPTER 4: MURINE CYTOMEGALOVIRUS DEGRADES MHC CLASS II TO COLONIZE THE SALIVARY GLANDS

Full title

Murine cytomegalovirus degrades MHC class II to colonize the salivary glands

Short title

MCMV M78 degrades MHC class II

Author list

Joseph Yunis[1], Helen E. Farrell[1], Kimberley Bruce[1], Clara Lawler[1], Stine Sidenius[1], Orry Wyer[1], Nicholas Davis-Poynter[1,2] and Philip G. Stevenson.[1,2,3]

Affiliations

[1]School of Chemistry and Molecular Biosciences, University of Queensland, Brisbane, Australia.

[2]Child Health Research Center, University of Queensland, South Brisbane, Australia.

[3]Correspondence: Dr Philip Stevenson; School of Chemistry and Molecular Biosciences, University of Queensland, St Lucia, 4072, Queensland, Australia; email: p.stevenson@uq.edu.au

Abstract

Cytomegaloviruses (CMVs) establish persistent, systemic myeloid cell infections in immunocompetent hosts. Persistence implies immune evasion, and CMVs evade $CD8^+$ T cells by inhibiting MHC class I-restricted antigen presentation. The myeloid cells that CMVs colonize can also interact with $CD4^+$ T cells via MHC class II (MHC II). Human CMV (HCMV) attacks the MHC II presentation pathway *in vitro*. What role this evasion might play in host colonization is unknown. We show that Murine CMV (MCMV) down-regulates MHC II via M78, a multi-membrane spanning viral protein that captured MHC II from the cell surface for pH-dependent degradation in lysosomes. M78-deficient MCMV down-regulated MHC I but not MHC II. After intranasal inoculation, it showed a severe defect in salivary gland (SG) colonization that was associated with MHC II expression on infected cells and was significantly rescued by $CD4^+$ T cell loss. Therefore, MCMV requires $CD4^+$ T cell evasion by M78 to colonize the SG, its main site of long-term shedding.

Author summary

Human cytomegalovirus is the commonest infectious cause of harm to unborn children. Vaccines have not stopped it establishing chronic, systemic infections. Murine cytomegalovirus (MCMV) provides an accessible model to understand why. We show that MCMV evades $CD4^+$ T cells via its M78 protein, and that this helps infection to spread despite the immune response. Thus, while $CD4^+$ T cells are important for host defence, viral evasion limits their capacity to act alone in controlling infection.

Introduction

Herpesviruses pre-date adaptive immunity, and in response to its evolution have acquired counter-balancing mechanisms of evasion. Persistent, productive infections result, with high prevalence in most populations and consequently significant disease burdens. Congenital infection by HCMV is a serious public health problem that motivates vaccine development. Vaccines to date have blunted acute infection but have not prevented viral persistence or transmission.

CMVs have extensive arsenals of immune evasion genes. To improve infection control we must understand what limits these set on immune function. This requires animal models. The most accessible is MCMV. Like HCMV, MCMV attacks MHC class I to evade $CD8^+$ T cells. This promotes SG infection [1]; similar evasion by Rhesus CMV helps to re-infect immune hosts [2]. HCMV also attacks MHC II, reducing interferon-γ (IFNγ)-dependent induction [3] and triggering MHC II degradation via US2 [4], US3 [5] and pp65 [6]. The rationale for evading $CD4^+$ T cells through attack on MHC II is less clear than for $CD8^+$ T cells and MHC I: MHC II can present cell-endogenous antigens after autophagy [7] but presents mainly exogenous antigens so presenting cells need not be infected; and while $CD4^+$ T cells can induce target cell apoptosis [8], they are much less effective killers than $CD8^+$ T cells. To understand the importance of MHC II attack by CMVs we must measure its impact *in vivo*.

Analysis of how MCMV might evade $CD4^+$ T cells has focussed on cytokines: low MHC II expression on infected cells is attributed to IFNγ inhibition [9] and IL-10 induction [10] reducing MHC II transcription. The viral genes responsible have not been identified. M27 reduces IFNγ signalling through STAT-2, but from day (d) 7 of infection $M27^-$ MCMV is no less attenuated in IFNγ receptor-deficient than in wild-type mice [11], arguing against significant $CD4^+$ T cell evasion. We show that MCMV, like HCMV, degrades MHC II in infected cells. For MCMV this required M78, a multi-membrane spanning viral protein with homology to chemokine receptors but without canonical signalling motifs. $M78^-$ MCMV propagates poorly in cultured macrophages and poorly colonizes the SG [12-14]. Cells infected by $M78^-$ but not wild-type (WT) MCMV retained MHC II *in vivo*, and $CD4^+$ T cell loss significantly reversed the M78-dependent defect in SG colonization. Therefore $CD4^+$ T cell evasion is an important M78 function that is necessary for MCMV to colonize its main site of long-term shedding.

Results

MCMV degrades MHC II in infected cells.

Most myeloid cells express MHC II inducibly rather than constitutively. IFNγ induces MHC II expression but also inhibits MCMV replication [15, 16]. To track viral effects on MHC II without this complication, we induced MHC II in RAW-264 monocytes (normally MHC II^-) by expressing the MHC II transactivator (C2TA), which acts down-stream of IFNγ [17]. RAW-C2TA cells were constitutively MHC II^+. When they were exposed to MCMV-GFP, GFP^+ cells lost MHC II but not CD44 or CD71 (Fig.1a). Immunostaining cells exposed to β-galactosidase $(\beta gal)^+$ MCMV (Fig.1b) similarly showed normal or increased MHC II expression in βgal^- (uninfected) cells and MHC II loss in strongly βgal^+ cells. In weakly βgal^+ cells MHC II was clumped and internalized, suggesting that this was an intermediate stage in down-regulation.

Antibody IBL5/22, which recognizes a conformation-independent MHC II epitope, gave equivalent results to antibody M5/114 (Fig.1c), so MCMV caused MHC II degradation rather than just denaturation. MCMV also reduced MHC II on thioglycollate-induced peritoneal macrophages of BALB/c and C57BL/6 mice (Fig.1d). Thus, the degradation did not depend on constitutive C2TA expression, and applied across at least 2 MHC II haplotypes.

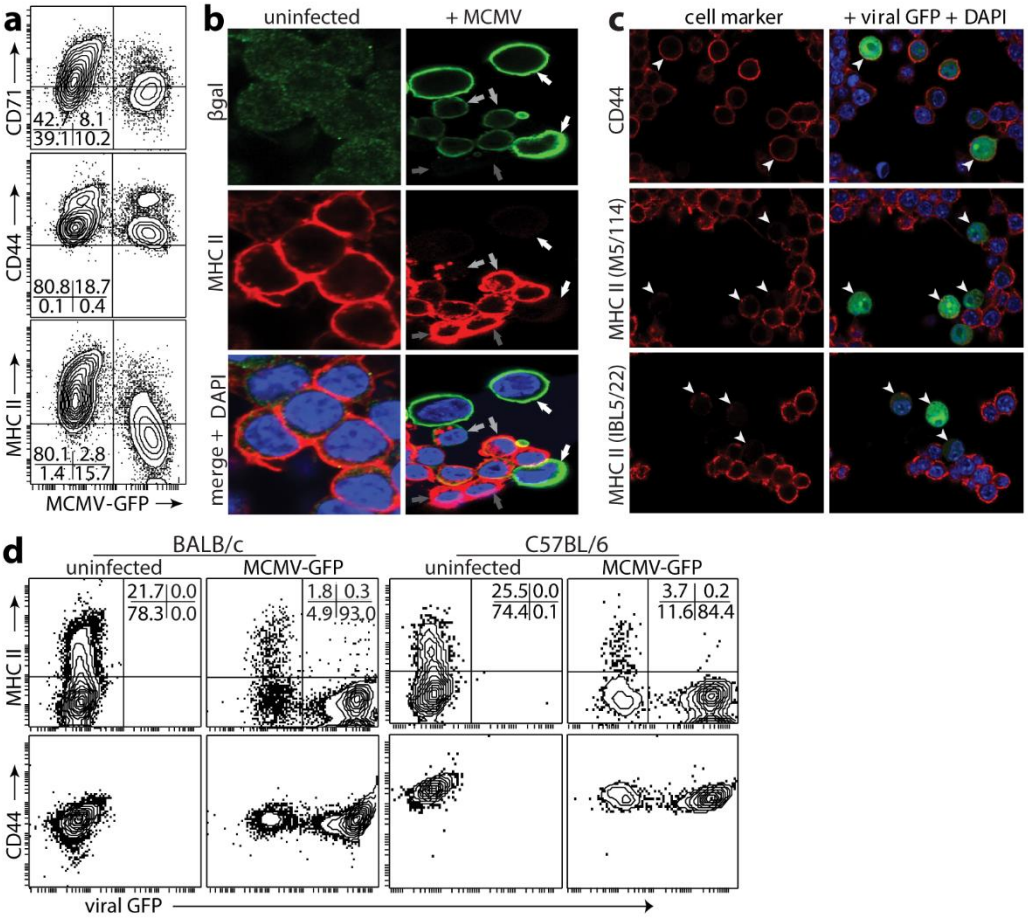

Figure 1. MCMV degrades MHC II.

a. RAW-C2TA cells infected with MCMV-GFP (0.5 p.f.u. / cell, 48h) were analysed for surface MHC II by flow cytometry. Mean fluorescence intensity was >10-fold lower on GFP^+ cells than on GFP^-. CD44 and CD71 mean fluorescence intensity of GFP^+ cells was reduced <2-fold. Numbers show % cells in each quadrant. Each data set represents at least 3 experiments.

b. RAW-C2TA cells were uninfected or infected with MCMV-βgal (1 p.f.u. / cell, 72h), then fixed, permeabilized and stained for βgal and MHC II. White arrows show example MHC II^- infected cells; dark grey arrows show MHC II^+ uninfected cells in the same cultures; light grey arrows show weakly $βgal^+$ cells with MHC II in internal vesicles. Significantly fewer $MCMV^+$ cells (<10%, n>200) than $MCMV^-$ cells (>90%, n>200) were MHC II^+ ($p<10^{-4}$ by Fisher's exact test). >100 weakly $βgal^+$ cells showed MHC II redistribution.

c. RAW-C2TA cells were infected as in **b**. MHC II^+ cells were identified with conformation-dependent (M5/114) and -independent (IBL5/22) antibodies. Arrows show example

infected cells. Significantly fewer GFP^+ (<15%, n>100) than GFP^- cells (>90%, n>100) were $M5/114^+$ and $IBL5/22^+$ ($p<10^{-4}$ by Fisher's exact test).

d. Peritoneal macrophages were recovered from BALB/c or C57BL/6 mice 72h after i.p. thioglycollate. Non-adherent cells were discarded. The remaining cells were infected or not with MCMV-GFP (1 p.f.u. / cell, based on total cell numbers before adherence). 48h later surface MHC II and CD44 were analysed by flow cytometry. Numbers show % total cells in each quadrant, collecting >5000 cells. In uninfected cultures, macrophages were 22% (BALB/c) and 26% (C57BL/6) MHC II^+. In infected cultures, GFP^- macrophages were 27% (BALB/c) and 24% (C57BL/6) MHC II^+, while GFP^+ macrophages were 0.3% (BALB/c) and 0.2% (C57BL/6) MHC II^+ ($p<10^{-4}$ by X^2 test).

MCMV removes MHC II from the cell surface and degrades it in acidic endosomes

Unlike RAW-C2TA cells, MCMV-infected fibroblasts expressing C2TA preserved MHC II (Fig.2a). This result suggested that MHC II degradation might require macrophage-specific, acidic endosomes. To test the need for low pH, we exposed infected RAW-C2TA cells to ammonium chloride or bafilomycin, which inhibit endosomal acidification. Both treatments significantly rescued MHC II expression (Fig.2b-c). By contrast the proteasome inhibitor MG-132 had no effect (Fig.2d-e).

Complete MHC II loss from infected cells suggested that in addition to any effect on nascent protein, MCMV removed mature MHC II from the plasma membrane. To test this idea, we incubated RAW-C2TA cells with an MHC II-specific antibody (1h, 4ºC), using excess antibody to minimize cross-linking and using rat antibodies to avoid binding by MCMV Fc receptors. We then washed off unbound antibody, infected the cells or not overnight (18h, 37ºC), then added a fluorescently labelled secondary antibody (1h, 4ºC) and assayed its binding by flow cytometry (Fig.2f). Thus, we assayed MHC II that was on the plasma membrane before infection (for primary antibody binding) then retained there (for secondary antibody binding). We also stained MHC II on uninfected cells without a 37ºC incubation (1h, 4ºC) (t=0h). The surface MHC II of uninfected RAW-C2TA cells was similar at t=0h and t=18h, indicating that its turnover is normally slow. By contrast MCMV-infected (GFP^+) cells showed a marked loss of surface-tagged MHC II over 18h. Therefore, MCMV removed MHC II from the plasma membrane of infected cells. As RAW-C2TA cells maintained surface MHC II for at least 18h, reduced synthesis - for example through transcriptional suppression - could not explain the down-regulation. Minimal MHC II down-regulation by MCMV in BALB/c-3T3-C2TA cells (Fig.2a) and rescue by bafilomycin

(Fig.2b-e) also argued against transcriptional suppression making a significant contribution.

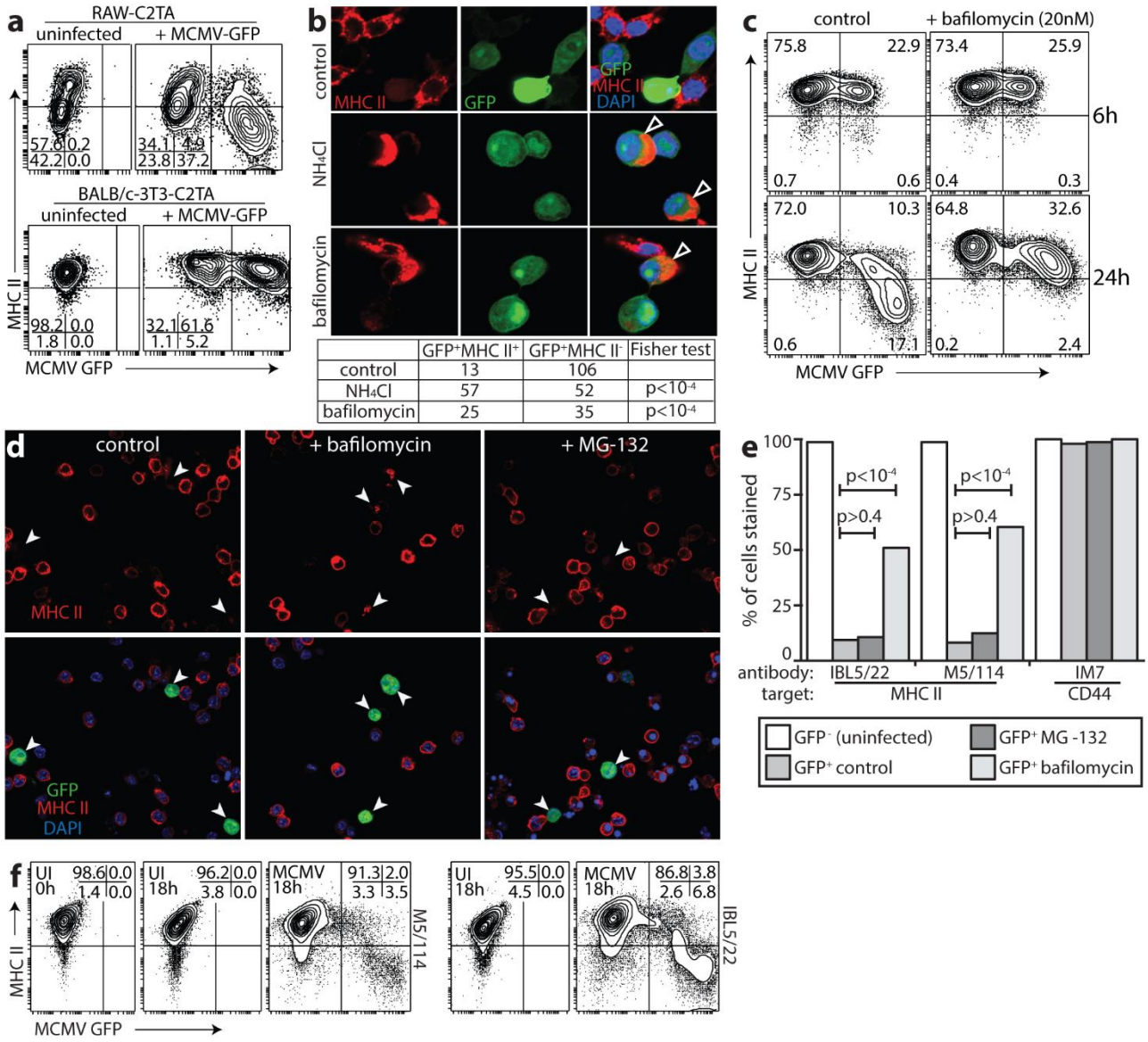

Figure 2. Viral MHC II degradation occurs in low pH endosomes.

a. RAW-C2TA and BALB/c-3T3-C2TA cells were infected or not with MCMV-GFP (3 p.f.u. / cell and 0.5 p.f.u. / cell respectively, as MCMV more efficiently infects fibroblasts than RAW-264 cells). 18h later surface MHC II was assayed by flow cytometry. Unlike RAW-C2TA macrophages, infected 3T3-C2TA fibroblasts retained MHC II expression.

b. RAW-C2TA cells infected or not with MCMV-GFP (1 p.f.u. / cell, 24h) were exposed (18h) to 100mM ammonium chloride, 20nM bafilomycin or medium alone (control), then

fixed, permeabilized and stained for MHC II. Viral GFP was visualized directly. Nuclei were stained with DAPI. Arrows show cells with rescued MHC II. The table quantitates MHC II expression for GFP^+ cells.

c. RAW-C2TA cells were infected with MCMV-GFP (3 p.f.u. / cell, 2h). Then bafilomycin (20nM) was added or not (control), and the cells cultured for a further 6h or 24h. They were then stained for MHC II with Alexa647-conjugated mAb M5/114 and analysed by flow cytometry. Virus-expressed GFP was assayed directly. Numbers show the % of total cells in each quadrant.

d. RAW-C2TA cells were infected with MCMV-GFP (1 p.f.u. / cell, 72h), treated with bafilomycin (20nM) or the proteasome inhibitor MG-132 (50μM), and 18h later stained for MHC II. Arrows show example infected cells. The MHC II rescued by bafilomycin had an endosomal distribution. MG-132 gave no rescue. The graph in **e** shows total cell counts across at least 10 fields of view (>200 cells per bar). Statistical comparison was by Fisher's exact test.

f. RAW-C2TA cells were incubated (1h, 37^{o}C) with M5/114 or IBL5/22 rat mAbs to MHC II, washed to remove unbound antibody, infected (MCMV, 18h) or not (UI, 18h) with MCMV-GFP (2 p.f.u. / cell), cultured overnight (18h, 37^{o}C), stained at 4^{o}C with anti-rat IgG pAb and analysed by flow cytometry. Control untreated cells (UI, 0h) were stained in parallel for surface MHC II using M5/114 and anti-rat IgG pAb without overnight culture.

MHC II degradation by MCMV requires M78

MHC II loss from the cell surface, and the intracellular distribution of the MHC II rescued by ammonium chloride or bafilomycin (Fig.2), argued that MCMV initiates MHC II degradation by relocalizing it to endosomes. The MCMV M78 is highly endocytic [13], so we tested its contribution, infecting RAW-C2TA cells with WT or $M78^-$ MCMV (Fig.3). $M78^-$ MCMV is reported to grow normally in fibroblasts and poorly in macrophages [12, 14]. We found impaired infectious virus production in RAW-264 cells after low multiplicity of infection, with less defect after higher multiplicity infection (Fig.3a). There was no difference between MHC II^+ and MHC II^- RAW-264 cells. There was no obvious defect in RAW-264 cell infection as measured by viral β-gal expression (Fig.3b), or by flow cytometry of viral GFP expression (S1a Figure), and RAW-C2TA cells infected by WT or $M78^-$ MCMV showed no obvious difference in viral or MHC II transcription (S1b-c Figure).

Flow cytometry of WT MCMV-infected cells showed a marked loss of both surface (non-permeabilized), and total (permeabilized) MHC II (Fig.3b). $M78^-$ MCMV infection little affected either. MHC II loss from peritoneal macrophages also required M78 (Fig.3c).

Identifying infected cells by immunofluorescent staining with a polyclonal anti-MCMV antibody (Fig.3d) or with an IE1-specific antibody (Fig.3e) confirmed that MHC II loss was M78-dependent. We also tested bone marrow-derived macrophages (Fig.3f). When uninfected, approximately 30% of these were MHC II^+; when infected with WT or $M78^+$ REV MCMV, expression decreased to <5%; and when infected with $M78^-$ MCMV there was no decrease.

Flow cytometry of cells infected with an independent $M78^-$ mutant (Fig.3g) confirmed that MHC II loss was M78-dependent. MHC I loss was contrastingly M78-independent. In $H2^d$ cells this depends primarily on m06, which degrades MHC I in lysosomes [18]. Therefore, M78 was not required for all MCMV-driven, lysosome-dependent protein degradation. As $M78^+$ MCMV down-regulated neither CD71 (Fig.1a), which cycles through early endosomes, nor CD44, neither did M78 generally promote glycoprotein endocytosis and loss.

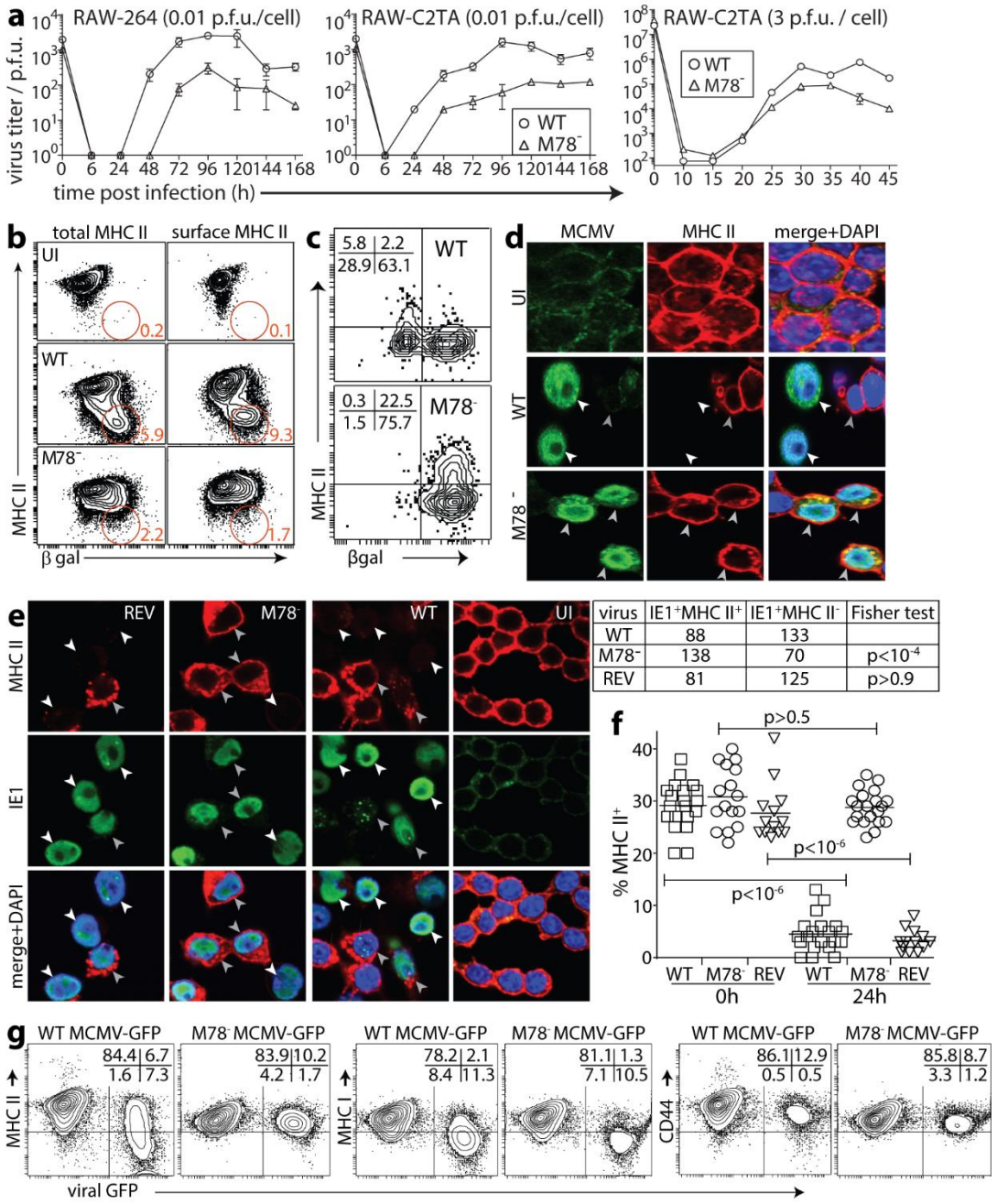

Figure 3. MHC II degradation by MCMV requires M78.

a. RAW-264 and RAW-C2TA cells were infected at low multiplicity (0.01 p.f.u. / cell, 1h) and washed x3 in PBS. RAW-C2TA cells were also infected at high multiplicity (3 p.f.u. / cell) by centrifuging virus onto the cells (536 x *g*, 30min), then washed x 3 in PBS. The cells were cultured in complete medium, and at each time point, triplicate cultures were plaque-assayed for infectious virus. Symbols show mean ± SEM. Time=0 shows the calculated virus input. M78^{-} MCMV had similar growth defects in MHC II^{+} and MHC II^{-} cells.

b. RAW-C2TA cells were infected with WT or M78^{-} βgal^{+} MCMV (1 p.f.u. / cell, 72h), or left uninfected (UI), then stained for surface MHC II (non-permeabilized) before fixation, permeabilization and staining for βgal; or fixed, permeabilized then stained for MHC class II plus βgal (permeabilized). MHC II either just at the cell surface (non-permeabilized) or also in the cell (permeabilized) was assayed by flow cytometry. Numbers show % total cells in each gated region. This was significantly less for M78^{-} than for WT MCMV ($p<10^{-4}$ by X^2 test.) Total βgal^{+} cell numbers were comparable.

c. Peritoneal macrophages from thioglycollate-treated BALB/c mice were infected with WT or M78^{-} βgal^{+} MCMV (1 p.f.u. / cell, 48h), then fixed, permeabilized, stained with antibodies to MHC II and βgal, and analysed by flow cytometry. Numbers show % total cells in each quadrant. Significantly more GFP^{+} cells were MHC II^{+} with M78^{-} than with WT MCMV ($p<10^{-4}$ by X^2 test).

d. RAW-C2TA cells infected as in **b** were fixed, permeabilized, stained for MHC II and for MCMV antigens with polyclonal immune serum, then imaged by confocal microscopy. For WT MCMV, white arrows show infected cells and the grey arrow an uninfected cell. For M78^{-} MCMV, arrows show infected cells. M78^{-} but not WT infected cells showed MHC II^{+}MCMV^{+} vesicles just below the plasma membrane. Significantly fewer MCMV^{+} cells were MHC II^{+} for WT (4/59 cells) than for M78^{-} infection (62/69 cells) ($p<10^{-4}$ by Fisher's exact test).

e. RAW-C2TA cells were infected with WT, M78^{-} or revertant (REV) viruses (1 p.f.u. / cell, 72h), or left uninfected (UI). They were then fixed, permeabilized and stained for MHC II plus MCMV IE1. White arrows show infected cells that have lost MHC II expression; grey arrows show cells that retain it. Where WT and REV-infected cells retained some MHC II, corresponding presumably to an earlier stage of infection, it showed an altered, endosomal distribution. The table gives total counts for >30 fields of view per sample.

f. Macrophages grown from bone marrow cells were infected with WT, REV or M78^{-} MCMV (2 p.f.u. / cell, 24h), then fixed and stained for MHC II. Symbols show counts for individual fields of view. Bars show means. WT and REV infections caused significant MHC II^{+} cell loss; M78^{-} infection did not.

g. RAW-C2TA cells were infected with WT or M78^{-} (deletion mutant) MCMV-GFP (1 p.f.u. / cell, 72h), then analysed by flow cytometry for surface glycoproteins. % total cells in each quadrant is shown. M78 disruption significantly reduced loss of MHC II ($p<10^{-4}$ by X^2 test) and not MHC I. CD44 was maintained.

M78 relocalizes MHC II to endosomes

RAW-C2TA cells expressing M78 via retroviral transduction showed some MHC II loss but much less than that of infected cells (Fig.4a). Both MCMV-infected RAW-C2TA cells (Fig.4b) and RAW-C2TA cells transduced with an $M78^+$ retrovirus (Fig.4c, 4d) expressed M78 in internal vesicles - previous studies have identified it in early endosomes [13]. In transduced cells, CD44 remained on the plasma membrane whereas MHC II relocalized to $M78^+$ vesicles. MCMV-infected bone marrow-derived macrophages (Fig.4e) and RAW-C2TA cells transiently transfected with an M78 expression plasmid (Fig.4f) similarly showed MHC II / M78 co-localization in vesicles.

Surprisingly, despite M78-transduced cells being readily obtained and despite retroviral transduction generally giving uniformly strong recombinant gene expression [19], M78-transduced RAW-C2TA cells showed variable M78 expression (Fig.4d), as did RAW-C2TA-M78 cell clones and an independently-derived RAW-C2TA-M78 line (Fig.4g). Cells with strong M78 expression redistributed MHC II, but puromycin-resistant cells that expressed less M78 had less effect on MHC II. To understand why, we tracked M78 from the cell surface. We infected RAW-C2TA cells with MCMV expressing HA-tagged M78 (4h, 37^{o}C), labelled them with HA-specific rabbit IgG and MHC II-specific rat IgG (1h, 4^{o}C), washed off excess antibody, then incubated the cells at 37^{o}C for different times before fixation, permeabilization and staining with anti-rabbit IgG and anti-rat IgG labelled secondary antibodies. M78 tagged by antibody at the infected cell surface was rapidly endocytosed (Fig.4h). It co-localized with MHC II in internal vesicles, then became undetectable, as did surface-tagged MHC II (Fig.4i). Transfected HA-M78 was also lost rapidly, whereas transfected HA-CCR5 was preserved (Fig.4j). Therefore, rapid M78 and MHC II endocytosis appeared to be accompanied by M78 degradation, and in infected cells also by MHC II degradation.

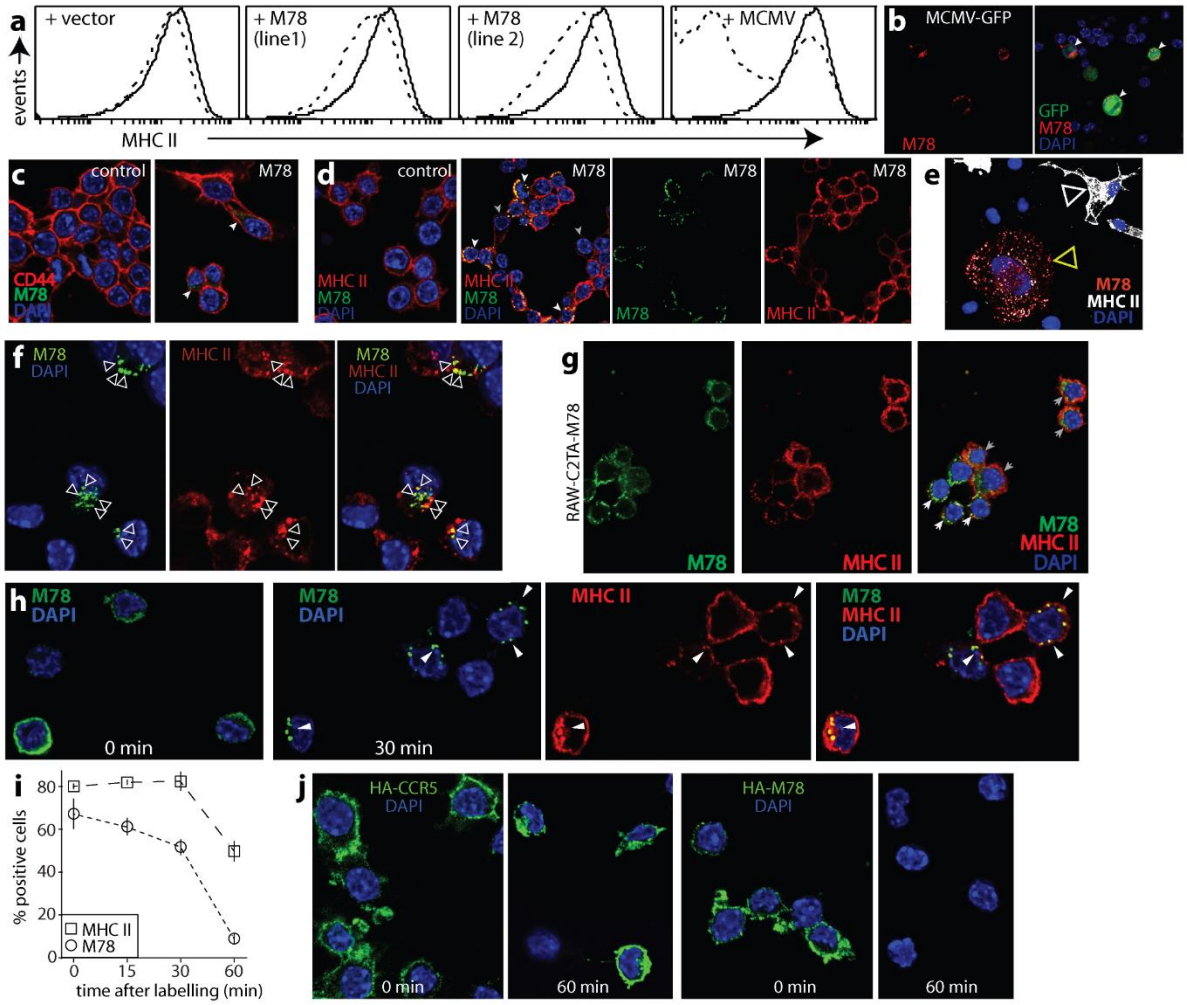

Figure 4. M78 relocalizes MHC II.

a. Cloned RAW-C2TA cells were transduced with vector alone or with M78 (line 1 and line 2), or infected with MCMV-GFP (+ MCMV, 1 p.f.u. / cell, 72h), then stained for MHC II (dashed lines). Solid lines show uninfected, untransduced RAW-C2TA cells. The biphasic population with MCMV corresponds to GFP^+ ($MHC\ II^-$) and GFP^- ($MHC\ II^+$) cells. M78 transfection had much less effect than MCMV infection on cell surface MHC II expression.

b. MCMV-GFP-infected RAW-C2TA cells were stained for M78. GFP was visualized directly. Nuclei were stained with DAPI. Arrows show example of infected cells with M78 in vesicles.

c. Untransduced (control) and M78-transduced RAW-C2TA cells were stained for M78 and CD44. Arrows show M78 staining, which did not co-localize with CD44.

d. M78-transduced RAW-C2TA cells were stained for M78 and MHC II. M78 occupied intracellular vesicles, as did MHC class II in $M78^+$ cells. White arrows show examples of co-localization. Grey arrows show $M78^-$ cells with MHC II on the plasma membrane.

e. Macrophages grown from bone marrow were infected with WT MCMV (1 p.f.u. / cell, 24h), then fixed and stained for M78 and MHC II. The white arrow shows a typical uninfected MHC II^+ cell. The yellow arrow shows a typical infected cell with MHC II in vesicles. >80% of vesicles were $M78^+MHC\ II^+$, <20% were $M78^+MHC\ II^-$ and <1% were $M78^-MHC\ II^+$ (n>300). Thus, there was significant endosomal M78 / MHC II co-localization ($p<10^{-4}$ by Fisher's exact test).

f. RAW-C2TA cells were transfected with a plasmid expressing HA-tagged M78. 3d later they were fixed, permeabilized and stained for M78 and MHC II. Nuclei were stained with DAPI. Arrows show examples of M78 and MHC II co-localizing in internal vesicles.

g. Cloned RAW-C2TA-M78 cells were stained for MHC II and M78. White arrows show $M78^+$ cells with MHC II in vesicles; grey arrows show cells with diffuse M78 staining and MHC II not relocalized. M78/MHC II co-localization was observed in >30% of transduced cells (n>500) and not in untransduced controls.

h. RAW-C2TA cells were infected with HA-$M78^+$ MCMV (4h, 37^{o}C), incubated with rabbit anti-HA and rat anti-MHC II IgG (1h, 4^{o}C), then washed and incubated at 37^{o}C for the times indicated before fixation, permeabilization and staining with anti-rat (red) and anti-rabbit (green) antibodies. Nuclei were stained with DAPI. Stainings show the change in distribution of surface-labelled M78 from 0 to 30min, and at 30min M78 co-localization with internalized MHC II (yellow, arrows).

i. Summary of staining results from **h** shows similar kinetics of surface-labelled M78 and MHC II loss. Cells were scored as stained or not regardless of internalization. Each point shows mean ± SEM of 5 fields of view and >100 cells counted.

j. RAW-C2TA cells were transfected with plasmid expressing HA-tagged M78, or HA-tagged CCR5 as a control. 3d later they were incubated with rabbit anti-HA IgG (1h, 4^{o}C), then washed and either fixed and permeabilized at once (0 min) or first incubated at 37^{o}C (60 min). All cells were then stained with for rabbit IgG (green). Nuclei were stained with DAPI. HA-CCR5 detection was maintained over 60min, whereas HA-M78 detection was lost.

$CD4^+$ T cell loss significantly rescues *in vivo* infection by $M78^-$ MCMV

As M78 was necessary for MCMV-driven degradation of MHC II, $M78^-$ MCMV provided an opportunity to understand what $CD4^+$ T cell evasion contributes to host colonization *in vivo*. We gave mice intranasal (i.n.) WT or $M78^-$ MCMV (Fig.5). After 1-3d few WT-infected lung cells expressed MHC II, whereas many of those infected by $M78^-$ MCMV did so (Fig.5a, 5b). Therefore, M78 also down-regulated MHC II *in vivo*.

M78 has been studied as an MCMV gene of unknown function: $M78^-$ MCMV given intraperitoneally (i.p.) shows reduced liver, spleen and SG infections [12]; given i.n. it shows reduced lung and SG infections [14]. Rat CMV lacking its M78 homolog (R78) is also attenuated *in vivo* [20]. Plaque assays of infectious virus and QPCR of viral DNA showed normal acute lung infection. This reflected presumably that macrophages are not a major source of acute virus production in the lungs [26]. However, $M78^-$ MCMV was cleared faster from the lungs, and showed a marked defect in SG infection (Fig.5c).

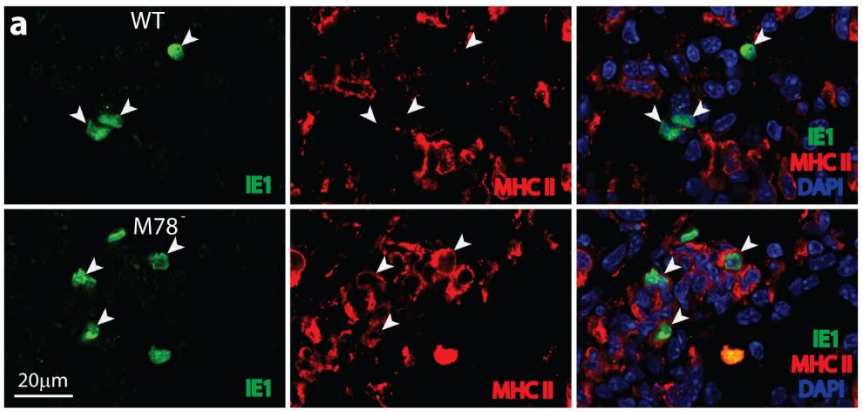

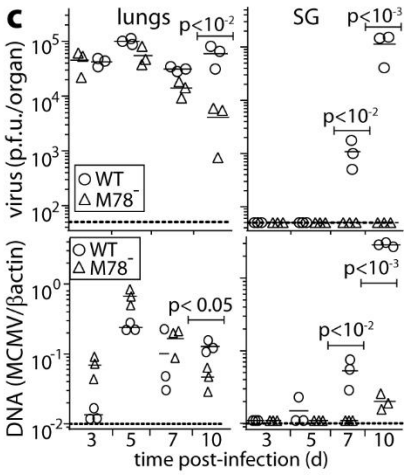

b IE1+ cells		day 1		day 3		day 5	
		MHC II+	MHC II-	MHC II+	MHC II-	MHC II+	MHC II-
virus	WT	1	32	2	34	2	13
	M78-	11	20	36	43	16	64
Fisher test		$p<10^{-3}$		$p<10^{-4}$		p=0.7	

Figure 5. M78$^-$ MCMV replication *in vivo*.

a. BALB/c mice were given i.n. WT or M78$^-$ MCMV ($3x10^4$ p.f.u.). 3d later lung sections were stained for MCMV IE1 and MHC II. Nuclei were stained with DAPI. Arrows show infected cells.

b. Quantitation of staining as in **a**, for sections from 3 mice. Few WT infected cells were MHC II$^+$. At d1 and d3, significantly more M78$^-$-infected cells were MHC II$^+$.

c. Mice were infected as in **a**. Lungs and salivary glands were plaque-assayed for infectious virus, and QPCR-assayed for viral genomes relative to cellular (βactin) genomes. Bars show means, other symbols show individual mice. Dashed lines show assay sensitivity limits. Significant differences are indicated.

Antibody responses to M78^{-} MCMV were significantly lower than those to WT infection (Fig.6a), consistent with M78^{-} viral loads being lower. ELIspot assays (Fig.6b-c) showed no obvious difference in CD4^{+} T cell response between M78^{-} and WT MCMV. We assessed the functional contribution of CD4^{+} T cells to M78^{-} MCMV attenuation by infecting BALB/c mice depleted of T cell subsets (Fig.6d). CD8^{+} T cell depletion increased M78^{-} MCMV titers in the lungs at d10. However, it increased WT titers by a similar amount ($p>0.5$). It did not significantly affect SG infection. Therefore M78^{-} MCMV attenuation was not due to better control by CD8^{+} T cells.

CD4^{+} T cell depletion did not alter lung infection. However, it increased SG infection by M78^{-} MCMV. Some M78-dependent defect remained relative to WT, but unlike with CD8^{+} T cell depletion there was a significant relative increase in M78^{-} virus titers ($p<0.04$). CD4^{+} T cell depletion also increased M78^{-} viral genome loads relative to WT (Fig.6e). Therefore CD4^{+} T cell evasion appeared to be an important *in vivo* M78 function.

To confirm this result, we infected MHC II-deficient C57BL/6 mice (IA$^{-/-}$) with WT, M78^{-} mutant or M78^{+} revertant (REV) viruses (Fig.6f-g). At d10, virus titers in the lungs and SG of immunocompetent mice (IA$^{+/-}$) were significantly lower for M78^{-} MCMV than for WT or REV. IA$^{-/-}$ lungs showed higher M78^{-} plaque titers, and the increase in M78^{-} titer with CD4^{+} T cell loss (IA$^{-/-}$ mice) was significantly greater than for WT or REV MCMV ($p<0.05$). CD4^{+} T cell loss also increased M78^{-} titers in SG, relative to both WT and REV ($p<0.004$), as well as M78^{-} viral DNA loads ($p<0.01$). To exclude a generally greater effect of CD4^{+} T cell depletion on low level SG colonization, we compared our untagged M78 deletion mutant (M78^{-}I) with M131^{-} MCMV [21], which also poorly colonizes SG (Fig.6h). Again M78^{-} titers in SG showed a greater defect relative to WT in IA$^{+/-}$ than in IA$^{-/-}$ mice ($p<0.01$), indicating significant rescue by CD4^{+} T cell loss. By contrast M131^{-} titers in SG showed a greater defect relative to WT in IA$^{-/-}$ mice. Nor did CD4^{+} T cell depletion rescue SG infection by i.n. M33^{-} MCMV (Fig.6i). Therefore CD4^{+} T cell loss specifically rescued SG infection by M78^{-} MCMV.

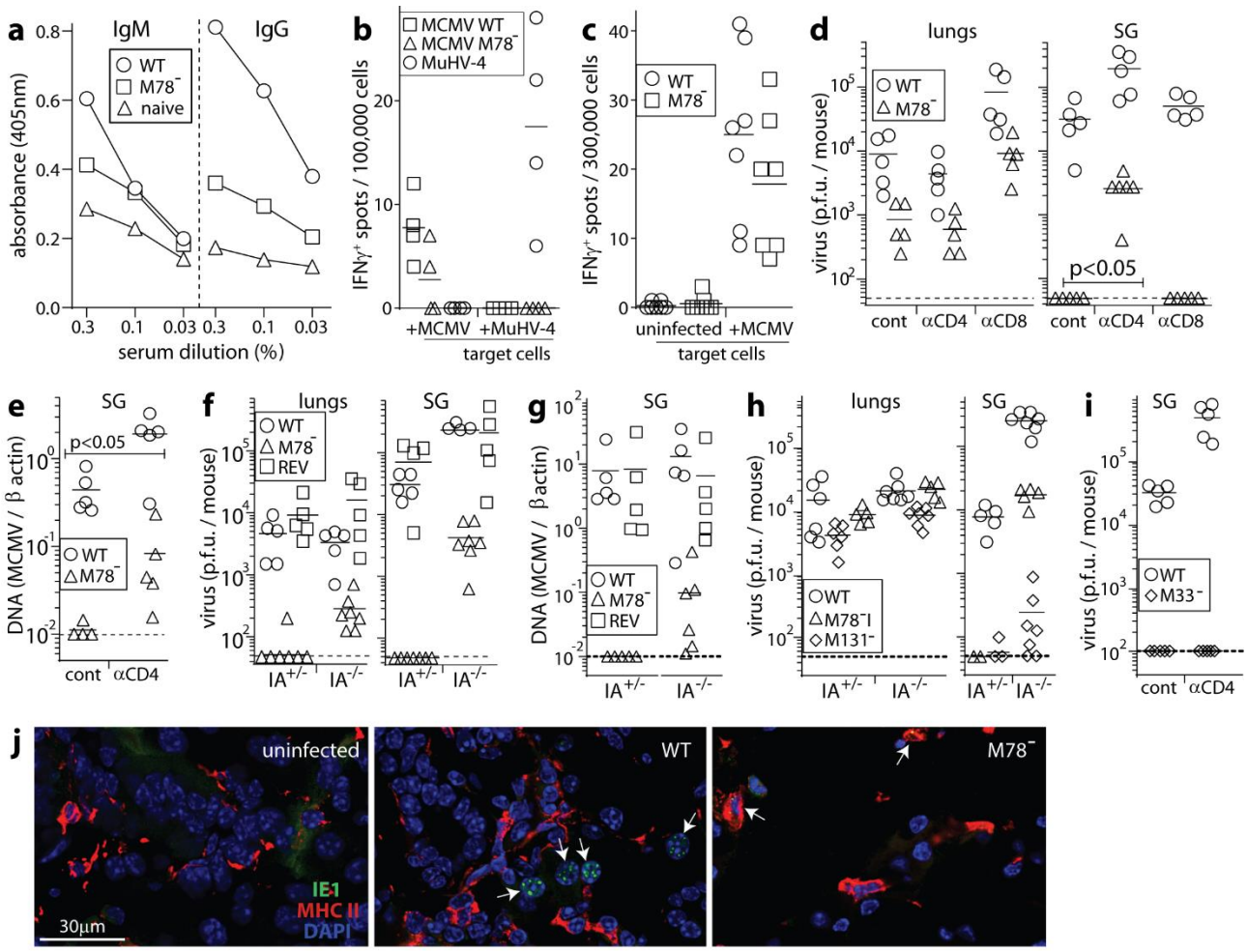

Figure 6. Significant M78$^-$ MCMV rescue by CD4$^+$ T cell loss.

a. C57BL/6 mice were given WT or M78$^-$ MCMV i.n. (3x10^4 p.f.u.). 56d later sera were assayed for MCMV-specific IgG and IgM by ELISA. Naive = age-matched, uninfected controls. Each point shows the mean of results for 7 mice. M78$^-$ MCMV elicited significantly less IgG response than WT ($p<0.01$).

b. C57BL/6 mice were given WT or M78$^-$ MCMV, or as a control MuHV-4 i.n. (3x10^4 p.f.u.). 56d after MCMV infection or 10d after MuHV-4 infection, CD4$^+$ T cells were purified from splenocytes, pooled from 2 mice per group, by depleting other cells with magnetic beads (Untouched mouse CD4 cell kit, Thermofisher). IFNγ production in response to MCMV-exposed or MuHV-4-exposed naive syngeneic spleen cells (1 p.f.u. / cell) was measured by ELIspot assay. Symbols show replicate wells, bars show means.

c. C57BL/6 mice were given WT or M78$^-$ MCMV i.n. (3x10^4 p.f.u.). 56d later IFNγ production by splenocytes exposed to uninfected or MCMV-exposed naive syngeneic spleen cells was measured by ELIspot assay. Symbols show individual mice, bars show means. CD4$^+$ T cell responses to WT and M78$^-$ MCMV were not significantly different.

d. BALB/c mice were depleted of $CD4^+$ or $CD8^+$ T cells (αCD4, αCD8) or left undepleted (cont), then given i.n. WT or $M78^-$ MCMV ($3x10^4$ p.f.u.). 10d later lungs and SG were plaque assayed for infectious virus. Symbols show individuals, bars show means. In lungs, immune depletions did not significantly change the ratio of WT to $M78^-$ titers. In SG, $CD4^+$ T cell depletion significantly reduced this ratio.

e. Viral DNA loads of SG in **d** were determined by QPCR. Again $CD4^+$ T cell depletion significantly reduced the ratio of WT to $M78^-$ infection, that is significantly reversed the $M78^-$ infection defect.

f. Immunocompetent ($IA^{+/-}$) and MHC II^- ($IA^{-/-}$) C57BL/6 mice were given WT, $M78^-$ or revertant (REV) MCMV i.n. ($3x10^4$ p.f.u.). At d10 lungs and SG were plaque-assayed for infectious virus. Symbols show individual mice, bars show means. For both lungs ($p<0.05$) and SG ($p<0.01$), $CD4^+$ T cell loss ($IA^{-/-}$ mice) significantly increased $M78^-$ plaque titers relative to WT or REV.

g. For the mice in **f**, $CD4^+$ T cell loss significantly increased $M78^-$ viral DNA loads in SG relative to WT or REV ($p<0.05$).

h. $IA^{-/-}$ and $IA^{+/-}$ mice were given i.n. WT, $M131^-$ or M78 deletion mutant ($M78^-$I) MCMV. At d10 lungs and SG were plaque assayed for infectious virus. Symbols show individuals, bars show means. The ratio of $M78^-$I/WT salivary gland titers was significantly higher in $IA^{-/-}$ than $IA^{+/-}$ mice ($p<0.01$), while the ratio of $M131^-$/WT salivary gland titers was reduced.

i. BALB/c mice were depleted of $CD4^+$ T cells as in **d**, then given WT or $M33^-$ MCMV i.n.. After 10d SG were plaque assayed for infectious virus. Symbols show individuals, bars show means. $CD4^+$ T cell depletion increased WT MCMV SG infection but failed to rescue SG infection by $M33^-$ MCMV.

j. BALB/c mice were depleted of $CD4^+$ T cells and given WT or $M78^-$ MCMV i.n. as in **d**. At d10 salivary gland sections were stained for MHC II and MCMV IE1. UI = uninfected control. Arrows show example infected cells (speckled nuclear IE1 staining). These cells were all MHC II^- with WT MCMV and MHC II^+ with $M78^-$ MCMV. Images are representative of 6 mice per group.

SG cells infected by M78$^-$ but not WT MCMV are MHC II$^+$

SG contain MHC II$^+$ interstitial cells, but acinar cells are MHC II$^-$ [22] (Fig.6j, uninfected). Therefore, MHC II degradation should not promote acinar cell infection directly. However myeloid cells disseminate MCMV, and for at least 2 weeks after i.n. MCMV >80% of infected cells in the SG are CD11c$^+$ (myeloid) rather than Aquaporin V$^+$ (acinar). At d10 after WT infection of CD4$^+$ T cell-depleted mice, all infected cells (n>100, counting samples from 6 mice) were MHC II$^-$ (Fig.6j, WT), but those infected by M78$^-$ MCMV were MHC II$^+$ (Fig.6j, M78$^-$). Without CD4$^+$ T cell depletion, no M78$^-$ infected cells were seen. Therefore, M78 promoted SG colonization by guarding disseminating infected myeloid cells against CD4$^+$ T cell engagement.

Discussion

M33 of MCMV [23], and UL33 and US28 of HCMV [24] encode chemokine receptor homologs that signal constitutively. M78 and its equivalents in HCMV (U78) and rat CMV (R78) have not been shown to signal, nor to bind chemokines, implying that they have other functions. M78 relocalized MHC II to endosomes and was required for MCMV-driven MHC II degradation. $M78^-$ MCMV also produced less infectious virus than did WT MCMV from $MHC\ II^+$ and $MHC\ II^-$ RAW-264 cells, so MHC II degradation is unlikely to be the only M78 function. However, $CD4^+$ T cell loss significantly rescued poor SG infection by $M78^-$ MCMV. Therefore M78-dependent $CD4^+$ T cell evasion made a demonstrably important contribution to host colonization.

MCMV reaches the SG via infected, migratory dendritic cells [25-27]. With WT MCMV, these cells lacked detectable MHC II. With $M78^-$ MCMV, infected cells were not seen in SG of immunocompetent mice. However, $CD4^+$ T cell loss led to the appearance of $MHC\ II^+$ infected cells. Thus, M78 promoted SG infection by acting in infected myeloid cells, presumably protecting them against $CD4^+$ T cell engagement. Impaired virus production by $M78^-$ infected myeloid cells might also impair infection transfer to SG acinar cells, but the primary defect seemed to be in infected myeloid cells reaching the SG. While infected myeloid cells spread i.n. MCMV from the lungs to new sites, type 2 alveolar epithelial cells appear to be the main source of infectious virus in the lungs [28]. Thus, normal acute lung infection by $M78^-$ MCMV was consistent with a myeloid cell-focussed defect. M78 could be considered a myeloid cell-specific infection module, which couples $CD4^+$ T cell evasion to virus production in myeloid cells and so increases systemic infection spread.

Despite MHC II degradation by CMVs, $CD4^+$ T cells play an important role in infection control [29, 30]. Effective antigen presentation by MCMV-infected dendritic cells may be possible even when MHC II is undetectable by immunostaining. Alternatively, protective $CD4^+$ T cells could act indirectly, responding to antigen on uninfected presenting cells. Such a scheme is suggested by MHC II presenting mainly cell-exogenous rather than cell-endogenous antigens, and by MCMV disrupting a range of presenting functions in infected cells [31, 32]. The failure of M78 disruption to increase MCMV-specific $CD4^+$ T cell responses was consistent with uninfected presenting cells driving most $CD4^+$ T cell priming. It follows that primed, protective $CD4^+$ T cells may not directly recognize CMV-infected cells, but rather recruit and activate other anti-viral effectors with independent modes of recognition, for example NK cells.

What then does MHC II degradation in infected cells achieve? Because MCMV exploits normal dendritic cell migration to spread [26], infected cells are likely to encounter $CD4^+$ T cells in lymph nodes. CD4+ T cell recognition of MHC II plus antigen on infected dendritic cells would not necessarily lead to killing, as $CD4^+$ T cells primarily activate rather than kill engaged presenting cells. $CD8^+$ T cell evasion is more important for infected cell survival. However, $CD4^+$ T cell-derived cytokines have anti-viral effects [16], and $CD4^+$ T cell engagement would reduce the migration of infected myeloid cells and so would reduce infection spread. Increased $CD4^+$ T cell engagement would also promote local antibody responses and innate effector recruitment. Thus, MHC II expression on infected myeloid cells, even if presenting mainly non-viral antigens, would open up a new front of host defence, with more precise targeting of recruited effectors to infected cells. By removing MHC II from the surface of infected myeloid cells, M78 isolated them from any $CD4^+$ T cell engagement, promoting systemic infection spread and making MCMV-infected cells harder for $CD4^+$ T cell-dependent defences to find.

Materials and Methods

Mice. BALB/c, C57BL/6 and $IA^{-/-}$ mice [33] were infected i.n. at 6-12 weeks old ($3x10^4$ p.f.u. in 30μL, under anaesthesia). We depleted $CD4^+$ / $CD8^+$ T cells with mAbs GK1.5 / 2.43 (Bio X Cell, 200μg/mouse/48h, from 96h pre-infection). Flow cytometry of spleen cells showed that the depletions were >95% complete (S2 Figure). Embryonic fibroblasts were obtained from 15–17d old embryos harvested from pregnant out-bred CD1 mice.

Ethics statement. Experiments were approved by the University of Queensland Animal Ethics Committee (projects 301/13, 391/15 and 479/15) in accordance with the Australian code for the care and use of animals for scientific purposes, from the Australian National Health and Medical Research Council.

Plasmids. M78 was amplified from K181 MCMV with Q5 polymerase (New England Biolabs), adding *Mfe*I and *Sal*I sites to its 5' and 3' ends, ligated into pMSCV-IRES-PURO [34] and verified by DNA sequencing. Expression plasmids for HA epitope-tagged-M78 and CCR5 are described [13]. Each HA tag was N-terminal and so extracellular when the protein spanned the plasma membrane.

Cells. Peritoneal macrophages were obtained by peritoneal lavage 48h after i.p. 3% Brewer's thioglycollate. B cells were removed by adherence to plastic and washing with PBS. Recovered cells were >90% $F4/80^+CD19^-$. Macrophages were grown from bone marrow by culture with M-CSF-1 (10ng/ml, Peprotech). These cells, mouse embryo-derived fibroblasts, NIH-3T3 (American Type Culture Collection (ATCC) CRL-1658), 293T (ATCC CRL-3216), RAW-264 cells (ATCC TIB-71), RAW-264 cells transduced with the human MHC II transactivator to induce MHC II (RAW-C2TA) [35], BALB/c-3T3 and BALB/c-3T3 cells transduced with C2TA, were grown in Dulbecco's modified Eagle's medium with 2mM glutamine, 100IU/ml penicillin, 100μg/ml streptomycin and 10% fetal calf serum (complete medium). Retroviral transduction was by transfecting 293T cells with pMSCV-M78-PURO and a packaging plasmid [34], adding supernatants to cells with hexadimethrine bromide (10μg/ml), then selecting with puromycin (10μg/ml). RAW-C2TA cells were transfected by electroporation.

Viruses. We used MCMV strain K181. Variants expressing GFP from the M131 intron (MCMV-GFP) [28] or βgal from the M33 intron (MCMV-βgal) [36]; with a premature stop codon in M131 ($M131^-$) [21]; with a βgal cassette replacing M33 ($M33^-$) [37]; with a βgal

expression cassette at genomic coordinate 111681 (Genbank GU305914) disrupting M78 ($M78^-$); and a revertant with an N-terminal HA epitope tag on M78 (REV) [13] are described. An independent M78 mutant ($M78^-$I) was made by homologous recombination, deleting the ORF (coordinates 111084-112499). This mutation was also recombined into MCMV-GFP. Viruses were grown in NIH-3T3 cells. Viruses were plaque assayed on embryonic fibroblasts [28]. Statistical comparison was by Student's 2-tailed unpaired t test unless otherwise stated.

Immunostaining. Organs were fixed in 1% formaldehyde-10mM sodium periodate-75mM L-lysine (24h, 4^{o}C), equilibrated in 30% sucrose (18h 4^{o}C), then frozen. 6μM sections were blocked with 0.3% Triton X-100 / 5% normal goat serum, then incubated (18h, 4^{o}C) with mAbs to MHC II (rat, M5/114) and MCMV IE1 (mouse IgG_1, CROMA101) [38]. Sections were washed x3 in PBS, incubated (1h, 23^{o}C) with Alexa 488-goat anti-mouse IgG_1 and Alexa 568-goat anti-rat IgG pAb plus DAPI (1μg/ml), then washed x3 in PBS, and mounted in ProLong Gold (Life Technologies). Cultured cells were adhered to coverslips, then fixed (2% formaldehyde, 30min), blocked in PBS / 0.1% Triton-X100 / 1% bovine serum albumin, then stained with antibodies to MHC II (M5/114 or IBL5/22), CD44 (rat mAb IM7, MCMV IE1 (CROMA101), βgal (chicken pAb, AbCam), MCMV (rabbit pAb), and M78 (rabbit pAb) [13]. Cells were washed x3 in PBS / 0.1% Tween-20, incubated with combinations of Alexa488-goat anti-chicken IgG pAb, Alexa488-goat anti-mouse IgG_1, Alexa488- or Alex568-goat anti-rabbit pAb and Alexa568-goat anti-rat IgG pAb, plus DAPI (1μg/ml), then washed x3 in PBS / 0.01% Tween-20, x2 in PBS and mounted ProLong Gold. GFP fluorescence was visualized directly. Images were acquired with a Zeiss LSM510 microscope and analyzed with ImageJ.

Flow cytometry. Cells were detached from plates, blocked with 1% BSA / 1μg/ml anti-CD16/32 (2.4G2), incubated (1h, 4^{o}C) with antibodies to MHC II (APC-mAb M5/114), CD44 (biotin-IM7), MHC class I (biotin-34-5-8S), CD71 (biotin-C2, BD Biosciences), washed x2 in PBS, then incubated with fluorescein-streptavidin, washed x2 in PBS and analysed on an Accuri flow cytometer. GFP fluorescence was measured directly. To detect βgal, cells were fixed in 2% PFA after surface staining, then permeabilized in 70% ethanol, washed x2 and incubated with chicken anti-βgal followed by Alexa488-goat anti-chicken IgG pAb (AbCam). To test $CD4^+$ and $CD8^+$ T cell depletions, spleen cells were stained with antibodies to CD4 (fluorescein-RM4-4), and CD8β (phycoerythrin-H35-17.2) (BD Biosciences).

Quantitative PCR. DNA was extracted from organs or blood (Wizard Genomic DNA Purification, Promega). MCMV coordinates 111218-111461 were amplified (LightCycler 480 SYBR green, Roche Diagnostics) and converted to genome copies by comparison with plasmid DNA amplified in parallel. Cellular DNA was quantified in the same samples by amplification of a □-actin gene segment. Viral DNA loads were normalized by cellular DNA loads.

RT-PCR. RNA was extracted from cells (Ambion) and reverse-transcribed with an oligo-dT primer (New England Biolabs). MHC II, β2M cellular cDNAs and IE1 and M33 viral cDNAs were then amplified by PCR. To distinguish cDNA from genomic DNA, each primer pair spanned an intron. The primers were (5' to 3'): MHC II - GATGCCGCTCAACATCTTGCTC and CATCCACACAGCTTATTAGGAATG; β_2M - TAGACCAAAGATGAGTAACTGCATC and GAGACTGATACATACGCCTGCAG; IE1 - AACCGTCCGCTGTGACCTGAC and CGATGCGCTCGAAGATATCATTG; M33 - TCAGGATGATCACCGTGTTGATG and GAAACTTCTTAACCTTTCCAACGG. PCR products were separated by electrophoresis on 2% agarose gels and visualized by staining with ethidium bromide.

Acknowledgements

Prof. Geoff Hill (Queensland Institute of Medical Research) kindly provided MHC II-deficient mice.

References

1. Lu X, Pinto AK, Kelly AM, Cho KS, Hill AB. Murine cytomegalovirus interference with antigen presentation contributes to the inability of CD8 T cells to control virus in the salivary gland. J Virol. 2006;80: 4200-4202.

2. Hansen SG, Powers CJ, Richards R, Ventura AB, Ford JC, Seiss D, et al. Evasion of CD8+ T cells is critical for superinfection by cytomegalovirus. Science. 2010;328: 102-106.

3. Miller DM, Cebulla CM, Rahill BM, Sedmak DD. Cytomegalovirus and transcriptional down-regulation of major histocompatibility complex class II expression. Semin Immunol. 2001;13: 11-18.

4. Tomazin R, Boname J, Hegde NR, Lewinsohn DM, Altschuler Y, Jones, TR, et al. Cytomegalovirus US2 destroys two components of the MHC class II pathway, preventing recognition by $CD4^+$ T cells. Nat Med. 1999;5: 1039-1043.

5. Hegde NR, Tomazin RA, Wisner TW, Dunn C, Boname JM, Lewinsohn DM, et al. Inhibition of HLA-DR assembly, transport, and loading by human cytomegalovirus glycoprotein US3: a novel mechanism for evading major histocompatibility complex class II antigen presentation. J Virol. 2002;76: 10929-10941.

6. Odeberg J, Plachter B, Branden L, Soderberg-Naucler C. Human cytomegalovirus protein pp65 mediates accumulation of HLA-DR in lysosomes and destruction of the HLA-DR alpha-chain. Blood. 2003;101: 4870-4877.

7. Strawbridge AB, Blum JS. Autophagy in MHC class II antigen processing. Curr Opin Immunol. 2007;19: 87-92.

8. Shresta S, Pham CT, Thomas DA, Graubert TA, Ley TJ. How do cytotoxic lymphocytes kill their targets? Curr Opin Immunol. 1998;10: 581-587.

9. Heise MT, Connick M, Virgin HW. Murine cytomegalovirus inhibits interferon gamma-induced antigen presentation to CD4 T cells by macrophages via regulation of expression of major histocompatibility complex class II-associated genes. J Exp Med. 1998;187: 1037-1046.

10. Redpath S, Angulo A, Gascoigne NR, Ghazal P. Murine cytomegalovirus infection down-regulates MHC class II expression on macrophages by induction of IL-10. J Immunol. 1999;162: 6701-6707.

11. Zimmermann A, Trilling M, Wagner M, Wilborn M, Bubic I, Jonjic S, et al. A cytomegaloviral protein reveals a dual role for STAT2 in IFN-γ signaling and antiviral responses. J Exp Med. 2005;201: 1543-1553.

12. Oliveira SA, Shenk TE. Murine cytomegalovirus M78 protein, a G protein-coupled receptor homologue, is a constituent of the virion and facilitates accumulation of immediate-early viral mRNA. Proc Natl Acad Sci USA. 2001;98: 3237-3242.
13. Sharp EL, Davis-Poynter NJ, Farrell HE. Analysis of the subcellular trafficking properties of murine cytomegalovirus M78, a 7 transmembrane receptor homologue. J Gen Virol. 2009;90: 59-68.
14. Davis-Poynter N, Yunis J, Farrell HE. The Cytoplasmic C-Tail of the Mouse Cytomegalovirus 7 Transmembrane Receptor Homologue, M78, Regulates Endocytosis of the Receptor and Modulates Virus Replication in Different Cell Types. PLoS One. 2016;11: e0165066.
15. Presti RM, Popkin DL, Connick M, Paetzold S, Virgin HW. Novel cell type-specific antiviral mechanism of interferon gamma action in macrophages. J Exp Med. 2001;193: 483-496.
16. Lucin P, Pavić I, Polić B, Jonjić S, Koszinowski UH. Gamma interferon-dependent clearance of cytomegalovirus infection in salivary glands. J Virol. 1992;66: 1977-1984.
17. Chang CH, Fontes JD, Peterlin M, Flavell RA. Class II transactivator (CIITA) is sufficient for the inducible expression of major histocompatibility complex class II genes. J Exp Med. 1994;180: 1367-1374.
18. Wagner M, Gutermann A, Podlech J, Reddehase MJ, Koszinowski UH. Major histocompatibility complex class I allele-specific cooperative and competitive interactions between immune evasion proteins of cytomegalovirus. J Exp Med. 2002;196: 805-816.
19. Boname JM, de Lima BD, Lehner PJ, Stevenson PG. Viral degradation of the MHC class I peptide loading complex. Immunity. 2004;20: 305-317.
20. Kaptein SJ, Beisser PS, Gruijthuijsen YK, Savelkouls KG, van Cleef KW, Beuken E, et al. The rat cytomegalovirus R78 G protein-coupled receptor gene is required for production of infectious virus in the spleen. J Gen Virol. 2003;84: 2517-2530.
21. Fleming P, Davis-Poynter N, Degli-Esposti M, Densley E, Papadimitriou J, Shellam G, et al. The murine cytomegalovirus chemokine homolog, m131/129, is a determinant of viral pathogenicity. J Virol. 1999;73: 6800-6809.
22. Steiniger B, Falk P, Lohmüller M, van der Meide PH. Class II MHC antigens in the rat digestive system. Normal distribution and induced expression after interferon-gamma treatment in vivo. Immunology. 1989;68: 507-513.
23. Sherrill JD, Miller WE. G protein-coupled receptor (GPCR) kinase 2 regulates agonist-independent Gq/11 signaling from the mouse cytomegalovirus GPCR M33. J Biol Chem. 2006;281: 39796-39805.

24. Waldhoer M, Kledal TN, Farrell H, Schwartz TW. Murine cytomegalovirus (CMV) M33 and human CMV US28 receptors exhibit similar constitutive signaling activities. J Virol. 2002;76: 8161-8168.
25. Farrell HE, Bruce K, Lawler C, Oliveira M, Cardin R, Davis-Poynter N, et al. Murine Cytomegalovirus Spreads by Dendritic Cell Recirculation. MBio. 2017;8: e01264.
26. Stoddart CA, Cardin RD, Boname JM, Manning WC, Abenes GB, Mocarski ES. Peripheral blood mononuclear phagocytes mediate dissemination of murine cytomegalovirus. J Virol. 1994;68: 6243-6253.
27. Farrell HE, Lawler C, Tan CS, MacDonald K, Bruce K, Mach M, et al. Murine Cytomegalovirus Exploits Olfaction To Enter New Hosts. MBio. 2016;7: e00251.
28. Farrell HE, Lawler C, Oliveira MT, Davis-Poynter N, Stevenson PG. Alveolar Macrophages Are a Prominent but Nonessential Target for Murine Cytomegalovirus Infecting the Lungs. J Virol. 2015;90: 2756-2766.
29. Carneiro-Sampaio M, Coutinho A. Immunity to microbes: lessons from primary immunodeficiencies. Infect Immun. 2007;75: 1545-1555.
30. Jonjić S, Mutter W, Weiland F, Reddehase MJ, Koszinowski UH. Site-restricted persistent cytomegalovirus infection after selective long-term depletion of $CD4^+$ T lymphocytes. J Exp Med. 1989;169: 1199-1212.
31. Loewendorf A, Krüger C, Borst EM, Wagner M, Just U, Messerle M. Identification of a mouse cytomegalovirus gene selectively targeting CD86 expression on antigen-presenting cells. J Virol. 2004;78:13062-13071.
32. Andrews DM, Andoniou CE, Granucci F, Ricciardi-Castagnoli P, Degli-Esposti MA. Infection of dendritic cells by murine cytomegalovirus induces functional paralysis. Nat Immunol. 2001;2: 1077-1084.
33. Grusby MJ, Johnson RS, Papaioannou VE, Glimcher LH. Depletion of $CD4^+$ T cells in major histocompatibility complex class II-deficient mice. Science. 1991;253: 1417-1420.
34. Boname JM, Stevenson PG. MHC class I ubiquitination by a viral PHD/LAP finger protein. Immunity. 2001;15: 627-636.
35. Smith CM, Rosa GT, May JS, Bennett NJ, Mount AM, Belz GT, et al. $CD4^+$ T cells specific for a model latency-associated antigen fail to control a gammaherpesvirus in vivo. Eur J Immunol. 2006;36: 3186-3197.
36. Davis-Poynter NJ, Lynch DM, Vally H, Shellam GR, Rawlinson WD, Barrell BG, et al. Identification and characterization of a G protein-coupled receptor homolog encoded by murine cytomegalovirus. J Virol. 1997;71: 1521-1529.

37. Davis-Poynter NJ, Lynch DM, Vally H, Shellam GR, Rawlinson WD, Barrell BG, Farrell HE. Identification and characterization of a G protein-coupled receptor homolog encoded by murine cytomegalovirus. J Virol. 1997;71: 1521-1529.
38. Trgovcich J, Stimac D, Polić B, Krmpotić A, Pernjak-Pugel E, Tomac J, et al. Immune responses and cytokine induction in the development of severe hepatitis during acute infections with murine cytomegalovirus. Arch Virol. 2000;145: 2601-2618.

Supporting figures

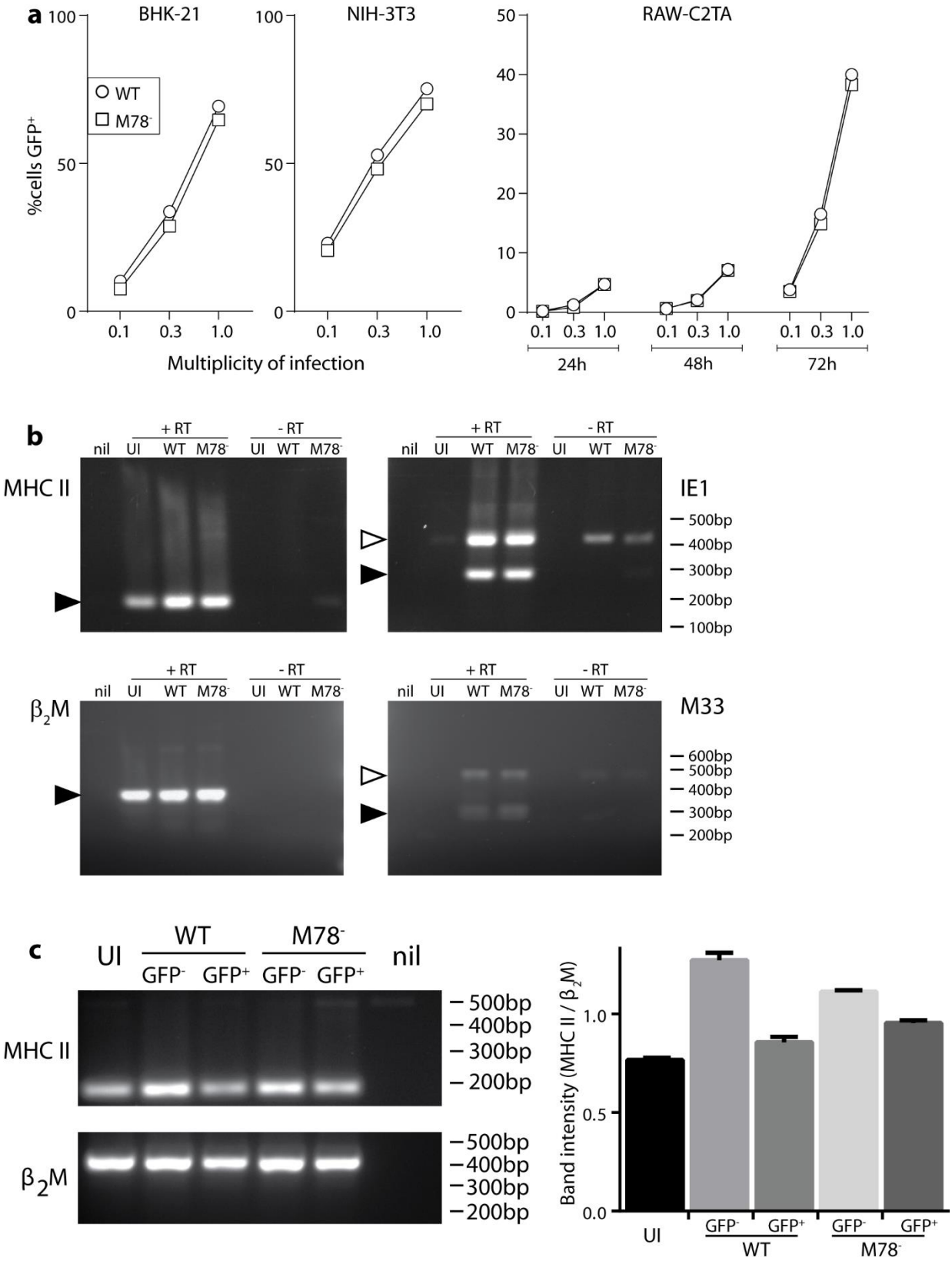

Supporting figure 1. Normal M78$^-$ MCMV infection of RAW-C2TA cells.

a. BHK-21, NIH-3T3 cells and RAW-C2TA cells were infected with GFP$^+$ WT or GFP$^+$ M78$^-$ MCMV at different multiplicities. GFP expression was then quantified by flow cytometry, after 18h for BHK-21 and NIH-3T3 cells, and after 24, 48 and 72 hrs for RAW-C2TA cells. No significant difference in infection was observed between WT and M78$^-$ MCMV.

b. RAW-C2TA cells were infected with WT or M78$^-$ MCMV (3 p.f.u. / cell, 72h). RNA was then harvested, reverse transcribed with an oligo-dT primer and used to amplify MHC II, β_2-microglobulin (β_2M), the MCMV IE1 or the MCMV M33. Each primer set spanned an intron. The filled arrow shows the predicted size of the product amplified from spliced cDNA, and the open arrow that amplified from unspliced cDNA or genomic DNA. For MHC II and β_2M, unspliced product was not seen as it would be very large. -RT = control samples without reverse transcription. UI = uninfected. No difference was observed in IE1 or M33 transcription, or in MHC II induction.

c. RAW-C2TA cells were infected with GFP$^+$ WT or GFP$^+$ M78$^-$ MCMV (3 p.f.u. / cell, 72h) then flow cytometrically sorted into GFP$^+$ and GFP$^-$ fractions. RNA was extracted, reverse-transcribed and amplified by PCR as in **b**, using primers for MHC II and β_2M. nil = no template control. MHC II band intensity is shown, normalised by β_2M band intensity for the same sample (mean ± SEM of triplicate samples). MHC II induction was evident in the GFP$^-$ cells of infected cultures. GFP$^+$ cells showed no MHC II transcriptional shut-down.

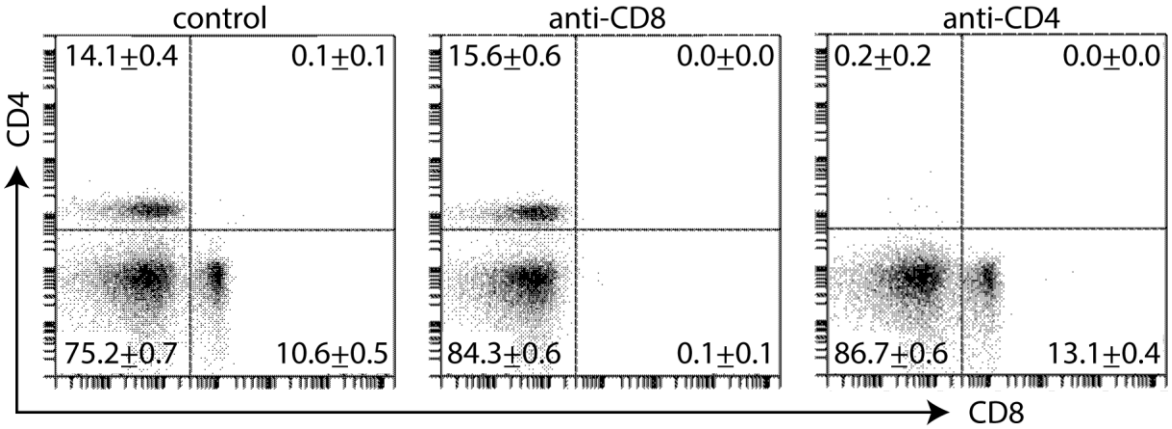

Supporting Figure 2. T cell depletion.

Mice were given i.p. every 48h 200µg protein G-purified anti-CD8α (2.43) or anti-CD4 (GK1.5) mAb, starting 96h before infection. Control = no antibody. Spleens taken at 10 days post-infection were analysed for CD4$^+$ and CD8$^+$ T cells by flow cytometry with antibodies to CD4 (RMA4-4 and CD8β (mAb H35-17.2). Numbers show mean ± SEM of FSC/SSC-gated lymphocytes for 5 mice.

4.1 Unpublished supporting research data.

4.1.1 Characterising BALB/c-3T3-C2TA and RAW-C2TA cells

BALB/c-3T3 and RAW 264.7, which are normally MHC class II negative, were transduced with the C2TA transactivator using a retrovirus. MHC I and MHC II were constitutively expressed in these cells (Fig. 4.1a-b) and were able to present $OVA_{323-339}$ peptide to stimulate DO11.10 hybridoma $CD4^+$ T cells to secrete IL-2 (Fig. 4.1c). Parent cell lines BALB/c-3T3 and RAW 264.7 were deficient in presenting $OVA_{323-339}$ peptide as expected.

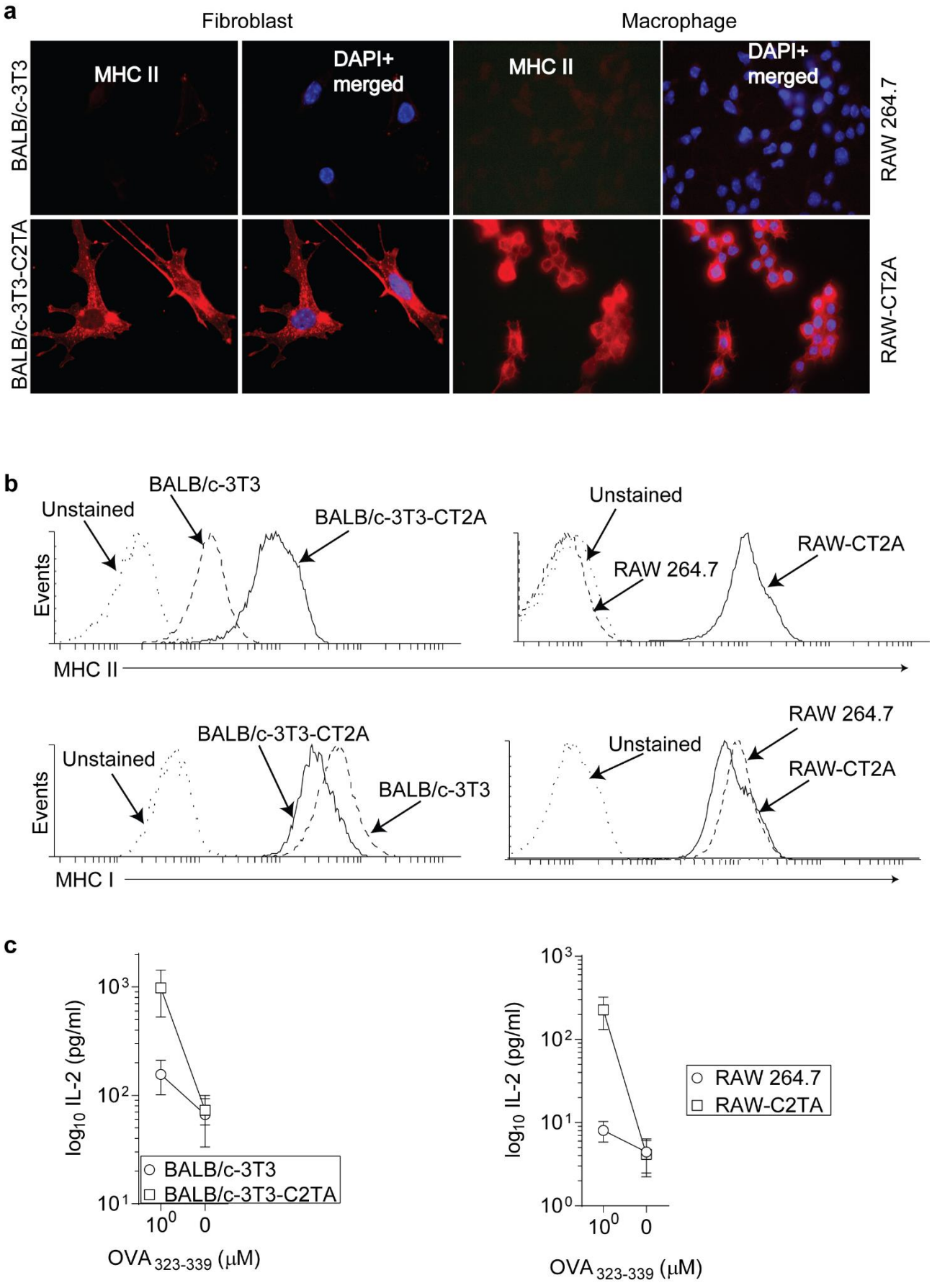
a
Fibroblast
Macrophage
MHC II
DAPI+ merged
MHC II
DAPI+ merged
BALB/c-3T3
BALB/c-3T3-C2TA
RAW 264.7
RAW-CT2A
b
Unstained
BALB/c-3T3
BALB/c-3T3-CT2A
Events
MHC II
Unstained
RAW 264.7
RAW-CT2A
Unstained
BALB/c-3T3-CT2A
BALB/c-3T3
Events
MHC I
Unstained
RAW 264.7
RAW-CT2A
c
log10 IL-2 (pg/ml)
10^3
10^2
10^1
BALB/c-3T3
BALB/c-3T3-C2TA
10^0
0
OVA 323-339 (μM)
log10 IL-2 (pg/ml)
10^3
10^2
10^1
10^0
RAW 264.7
RAW-C2TA
10^0
0
OVA 323-339 (μM)

Fig. 4. 1. BALB/c-3T3-C2TA and RAW-C2TA constitutively express MHC II.

Untransduced and MHC II transduced BALB/c-3T3 and RAW 264.7 cells were fixed, permeablised and blocked in 2%NGS/PBS (RT, 1 hr). MHC II was stained using rat anti-MHC II- M5/114 (4^{o}C,18 hrs) and detected using Alexa Fluor goat anti-rat 594 and DAPI stained nucleus (RT, 1 hr). The cells were visualised on an epifluorescence microscope at 63X magnification**. b)** Cells in a were incubated in rat anti-mouse CD16/CD32 Fc block in combination with Alexa Fluor 647 rat anti-MHC II (M5/114) (4^{o}C, 1 hr). MHC I was stained using biotinylated mouse anti-MHC I (H-2D (d) (34-2-12) (4^{o}C, 1 hr) and detected using streptavidin PerCP Cy5.5 (4^{o}C, 1 hr). MHC II and MHC I expression was analysed on BD Accurri C6 flow cytometer. Data was visualised on weasel as in **b**. Arrows show expression profiles of expression. Dotted line shows unstained cells, dashed line; untransduced BALB/c-3T3 and RAW 264.7 cells and solid line; transduced BALB/c-3T3-C2TA and RAW-C2TA. Cells in a were co-cultured with CD4^{+} T cell hybridoma cells specific for OVA$_{323-339}$ peptide in the presence of 1 µM OVA$_{323-339}$ peptide or medium. After 24 hrs, IL-2 in culture was detected using ELISA. Data represents log IL-2 (pg/ml) of duplicate cultures. Error bars difference in mean. Data are representative of 3 independent experiments.

4.1.2 Generation of uniform MHC II expressing clones

Continuous culture of RAW-C2TA cells, led to MHC II high and MHC II low populations (data not shown). To generate high expressing MHC II clones, RAW-C2TA cells was serially diluted to generate individual clones that were maintained in zeocin, a selection marker for MHC II expressing cells. Individual clones were then screened for MHC II expression by immunostaining using a 96 well format. Positive clones were further expanded and analysed by flow cytometry. The results showed RAW-C2TA clones 2 and 7 had 64-75% MHC II expression while clones 6, 9 11 and 12 had 91-98% expression (Fig. 4.2a). Parent RAW-C2TA line (mixed) had 14.7% and the untransduced RAW 264.7, had no MHC II expression (Fig. 4.2a). Similarly, BALB/c-3T3-C2TA had 99% MHC II expression compared to 12% in BALB/c-3T3. To determine whether the RAW-C2TA clones would stimulate I-A^{d}-restricted OVA$_{323–339}$-specific DO11.10 hybridoma cells to secrete IL-2, BALB/c-3T3, BALB/c-3T3-C2TA, NSO and RAW-C2TA clones 7, 9 and 11 were co-cultured with OVA$_{323-339}$-specific DO11.10 hybridoma cells in the presence of 1 µM OVA$_{323-339}$ peptide or medium. BALB/c-3T3-C2TA and RAW-C2TA clones stimulated OVA$_{323-339}$ specific DO11.10 hybridoma cells to secrete IL-2 compared to BALB/c-3T3 and

NSO cells respectively (Fig. 4.2b). To confirm the RAW-C2TA clones were macrophages, clones 7, 9 and 11 were stimulated with or without LPS for 4 hrs and analysed for NO_2 secretion 24 hrs later. All RAW-C2TA clones secreted NO_2 except fibroblast cell lines BALB/c-3T3-C2TA and BHK-21 cells and NSO cells (Fig. 4.2c). RAW-C2TA clone 9 was used throughout this thesis as RAW-C2TA.

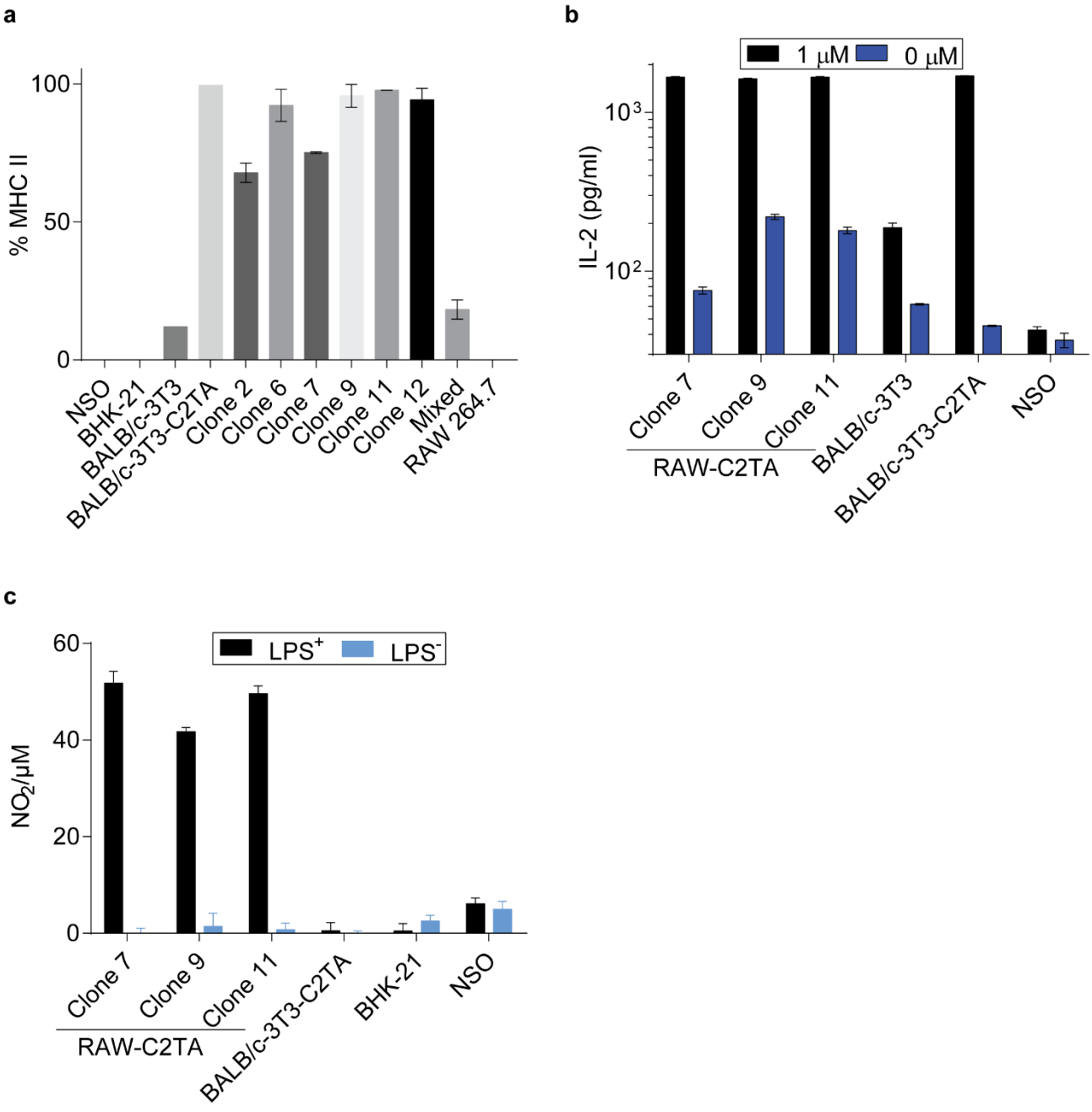

Fig. 4. 2. RAW-C2TA clones uniformly express MHC II and stimulate $CD4^+$ T cells.

a) Untransduced and MHC II transduced fibroblasts and macrophages were directly stained for MHC II using rat anti-MHC II- M5/114 (4ºC, 1 hr). MHC II was detected BD

Accurri C6 flow cytometerrri6 flow cytometer. Data was visualised and analysed on weasel. Bar graph represents percentage means of three independent experiments. Error bars show difference in means. Positive clones (>95%) were used for further analysis. **b)** RAW-C2TA positive clones in **a** and fibroblast cell lines BALB/c-3T3 and BALB/c-3T3-C2TA and NSO Cells were co-cultured with $CD4^+$ T cell hybridoma cells specific for $OVA_{323-339}$ peptide in the presence of 1 µM $OVA_{323-339}$ peptide or medium. After 24 hrs, IL-2 in culture was detected using ELISA. Data represents log IL-2 (pg/ml) of duplicate cultures. Error bars difference in mean. **c)** Cells in **b** were stimulated with LPS (10 µg/ml) or medium for 4 hrs, then washed and supplemented with fresh 10% complete medium. After 24 hrs, NO_2 in culture medium was detected using NO_2 kit. Absorbance was read at 570 nm using POLARstar® Omega Plate Reader Spectrophotometer. Data represents NO_2/µM of duplicate cultures. Error bars show difference in mean. Data are representative of 3 independent experiments.

4.1.3 MCMV restricted $CD4^+$ T cell stimulation *in vitro*

MCMV was previously shown to interfere with $CD4^+$ T cell stimulation *in vitro* by interfering with MHC II expression. Thus, RAW-C2TA cells were infected with WT or recombinant MCMV or MHV-68 expressing transferrin linked OVA (mOVA) from the viral genome or left uninfected. The cells were then co-cultured with DO11.10 $CD4^+$ T cell hybridomas and IL-2 was measured after an overnight incubation. $CD4^+$ T cell hybridomas in mOVA-recombinant MCMV infected wells secreted less IL-2 (1.32 ± 0.55) compared to in mOVA-recombinant MHV-68 infected wells (2.90 ± 0.122), a 1.58 ± 0.56 log difference (Fig. 4.3b, $p<0.001$). To determine whether this was macrophage specific, BALB/c-3T3-C2TA cells were infected overnight as above in the presence of DO.11.10 hybridoma cells and secreted IL-2 measured. Interestingly, $OVA_{323-339}$-specific $CD4^+$ cells in mOVA-recombinant MCMV infected wells secreted 1.38 ± 0.18 log IL-2 compared to 1.20 ± 0.25 in mOVA-recombinant MHV-68 infected wells, a -0.08 ± 0.31 log difference (Fig. 4.3a, $p>0.05$). The results suggested, the difference in IL-2 secretion could be macrophage specific and probably due to $CD4^+$ T cell restriction by MCMV. To test this hypothesis, BALB/c-3T3-C2TA cells were infected with recombinant MHV-68 expressing EF1a eGFP or MCMV GFP. There was no significant change in MHC II expression in MHV-68 EF1a eGFP or MCMV GFP infected cells (Fig. 4.4a). MHC I expression was slighted altered in MHV-68 EF1a eGFP infected cells compared to MCMV GFP where MHC I downregulation was more evident (Fig. 4.4b). The results demonstrate that, neither MHV-68 nor MCMV

affect MHC II expression in fibroblasts, which could explain the unaltered IL-2 response observed. In RAW-C2TA cells, GFP$^+$ MHV-68 Δ73 sOVA or gM eGFP infected RAW-C2TA cells expressed MHC II while MCMV GFP$^+$ cells downregulated MHC II (Fig. 4.4c). Both viruses downregulated MHC I but retained CD44 expression (Fig. 4.4d-e). Thus, direct infection rather than soluble factor contributed to downregulation of MHC II expression and was specific to MCMV.

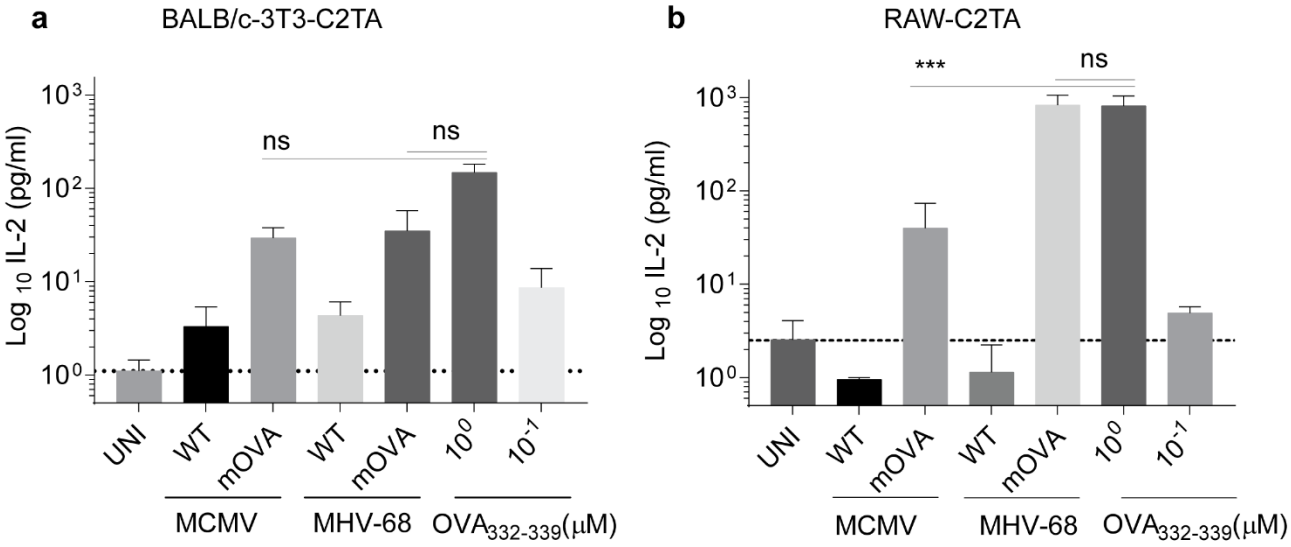

Fig. 4. 3. MCMV restricts CD4+ T cell stimulation in RAW-C2TA cells.

3x10^4 BALB/c-3T3-C2TA in **a** or RAW-C2TA cells in **b** were either left uninfected or infected with recombinant or WT MCMV or MHV-68. BALB/c-3T3-C2TA cells were infected at MOI 0.3 for 18 hrs in the presence of 3x10^4 CD4$^+$ T cell hybridoma cells. RAW-C2TA cells were infected at MOI 2 MHV-68 or 1 MCMV for 96 hrs, then 3x10^4 CD4$^+$ T cell hybridomas were added to the cells. Uninfected cells were incubated in OVA$_{323-339}$ peptide or medium. After 24 hrs post co-culture, culture medium of BALB/c-3T3-C2TA and RAW-C2TA was assayed for IL-2 using ELISA respectively. Error bars show mean difference of duplicate samples. Data was analysed using unpaired student 2 tailed t-test (ns, $p>0.05$; * $p<0.05$; *** $p<0.001$). Data are representative of 3 independent experiments.

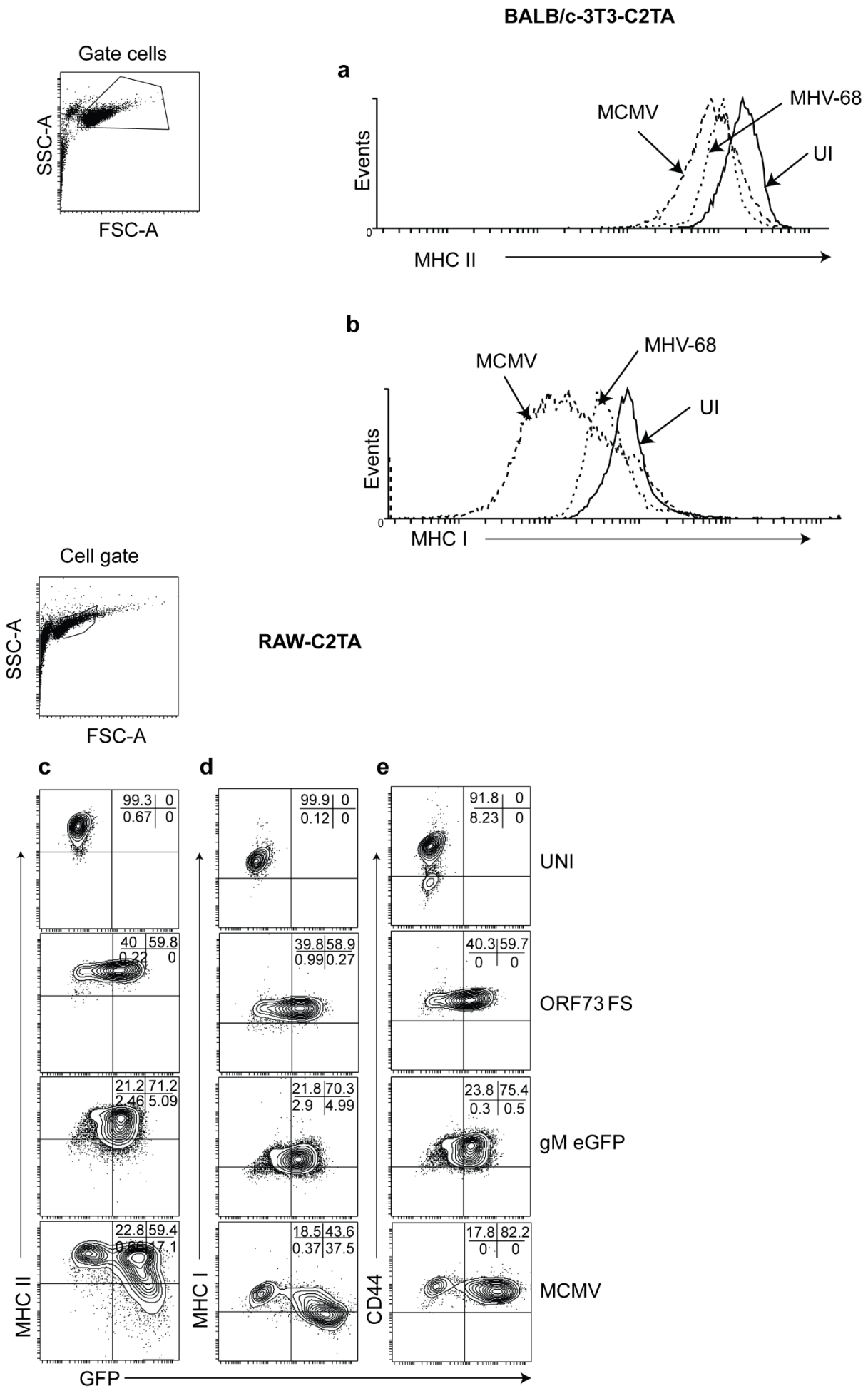
BALB/c-3T3-C2TA
Gate cells
SSC-A
FSC-A
a
Events
MCMV
MHV-68
UI
MHC II
b
Events
MCMV
MHV-68
UI
MHC I
Cell gate
SSC-A
FSC-A
RAW-C2TA
c
d
e
99.3 0
0.67 0
99.9 0
0.12 0
91.8 0
8.23 0
UNI
40 59.8
0.22 0
39.8 58.9
0.99 0.27
40.3 59.7
0 0
ORF73 FS
21.2 71.2
2.46 5.09
21.8 70.3
2.9 4.99
23.8 75.4
0.3 0.5
gM eGFP
22.8 59.4
18.5 43.6
0.37 37.5
17.8 82.2
0 0
MCMV
MHC II
MHC I
CD44
GFP

Fig. 4. 4. BALB/c-3T3-C2TA retain MHC II expression.

a, b) BALB/c-3T3-C2TA cells were left uninfected or infected with MCMV GFP or MHV-68 EF1a eGFP (MOI 0.3, 18 hrs). The cells were incubated in rat anti-mouse CD16/CD32 Fc block in combination with Alexa Fluor 647 rat anti-MHC II (M5/114) (4^{o}C, 1 hr). MHC I was stained using biotinylated mouse anti-MHC I (H-2D (d) (34-2-12) (4^{o}C, 1 hr) and detected using streptavidin PerCP Cy5.5 (4^{o}C, 1 hr). MHC II and MHC I expression was detected using BD Accurri C6 flow cytometer. Data was visualised on weasel and plotted on histogram. Dark firm line; uninfected, dotted line; MCMV and dashed line; MHV-68. **c)** RAW-C2TA cells were left uninfected or infected with MCMV GFP or MHV-68 gM eGFP or BAC^{+} Δ73 sOVA GFP (MOI 1, 48 hrs) by centrifugation (536 x g for 30 minutes). The cells were incubated in rat anti-mouse CD16/CD32 Fc block in combination with Alexa Fluor 647 rat anti-MHC II (M5/114) (4^{o}C, 1 hr). MHC I and CD44 was stained using biotinylated mouse anti-MHC I (H-2D (d) (34-2-12) and biotin anti-CD44 (IM7) (4^{o}C, 1 hr) and detected using streptavidin PerCP Cy5.5 (4^{o}C, 1 hr). MHC II (**c**), MHC I (**d**) and CD44 (**e**) expression was detected using BD Accurri C6 flow cytometer. Data was visualised and analysed on weasel. Data is representative of 3 independent experiments.

4.1.4 Confirmation of M78 expression in WT and absence in M78^{-} virus

To determine whether M78 was implicated in MHC II downregulation, absence of M78 expression in M78^{-} virus was determined by immunostaining and western blot. M78 was only detected in WT but not in M78^{-} viruses by microscopy (Fig. 4.5a). Both viruses expressed similar patterns of IE1 and MCMV lytic antigens on western blot (Fig. 4.5b).

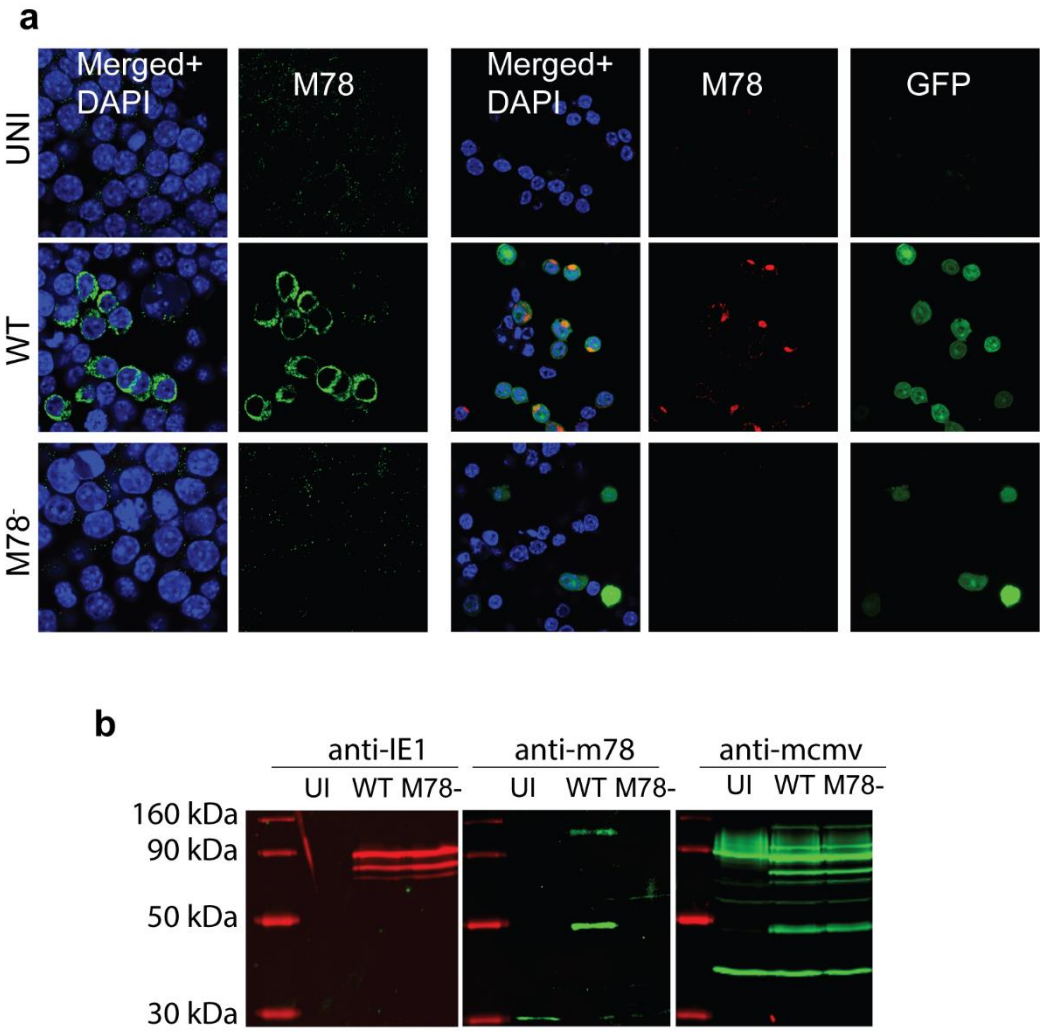

Fig. 4. 5. M78 deficient virus does not express M78.

RAW-C2TA cells were infected with WT or MCMV GFP (MOI 1, 48 hrs). The cells were fixed, permeablised and blocked in 2%NGS/PBS (RT, 1 hr) and stained with rabbit anti-M78 antibody (4ºC, 1 hr) and detected with Alexa Fluor goat anti-rabbit 488. DAPI stained nucleus. **b)** $1x10^6$ RAW-C2TA were infected with WT or $M78^-$ virus (MOI 1, 72 hrs). The cells were washed, lysed in 1% TritonX-100 lysis detergent and cytoplasmic fraction resolved in 10-12.5% SDS-PAGE on a 6% sacking gel, then transferred onto PVDF membrane and blocked with 10% skim milk/PBST (RT, 1hr) and blotted with anti-IE1, anti-M78 and anti-MCMV in 5% skim milk/PBST (4ºC, 18 hrs). The membrane was then washed and incubated in 5%skim milk/PBST containing IRDye® 800CW goat-anti-rabbit or rabbit anti-rat or IRDye® 680 CW goat anti-mouse (4ºC, 1 hr). Membrane bands were detected using LI-COR odyssey infrared imager. 75-90 kDa bands were observed with anti-IE1 for both viruses, 50-90 KDa bands in WT with anti-M78 and 40-160 kDa for both viruses with anti-MCMV. Data are representative of 2 independent experiments.

4.1.5 Kinetics of MHC II downregulation and degradation

To determine when MHC II downregulation occurred, RAW-C2TA cells were left uninfected or infected with MCMV WT MOI 1 or 10. MHC II expression was then monitored over a course of 24 hrs. Anti-MCMV sera was used to detect infected cells. MHC II expression was found to be altered as early as 6 hrs post infection particularly at MOI 10 in which MHC II clustered in the form of vesicles compared to uninfected cells (Fig. 4.6a). This was gradually lost as infection progressed. By 24 hrs, most infected cells completely lost MHC II expression regardless of MOI used compared to uninfected cells (Fig. 4.6a). To understand how MCMV downregulated MHC II, RAW-C2TA cells were incubated with MHC II- M5/114 and a monoclonal rat anti-mouse MHC II- IBL-5/22 to label surface MHC II. The cells were then infected with WT or M78^{-} GFP by centrifugation. After 2 hrs, unbound virions and excess labelling antibody were washed in PBS. The cells were then incubated for a further 18 hrs before surface labelled MHC II was detected using a rat monoclonal secondary antibody Alexa Fluor 647. The results show that surface labelled WT GFP^{+} but not M78^{-} infected cells lost MHC II expression (Fig. 4.6b). However, this difference was not significant (Fig. 4.6d, $p>0.05$).

4.1.6 Bafilomycin prevents MHC II endocytosis.

To determine whether inhibiting lysosomal acidification early during infection affects MHC II downregulation, RAW C2TA cells were infected with WT or M78^{-} GFP by centrifugation. After 2 hrs, unbound virions were washed and fresh medium bafilomycin was added. Controls had normal medium. After 6 or 24 hrs, surface MHC II was analysed. MHC II was unaltered at 6 hrs post infection (Fig. 4.6c). However, after 24 hrs, WT but not M78^{-} downregulated surface MHC II (Fig. 4.6c). This was inhibited in the presence of bafilomycin.

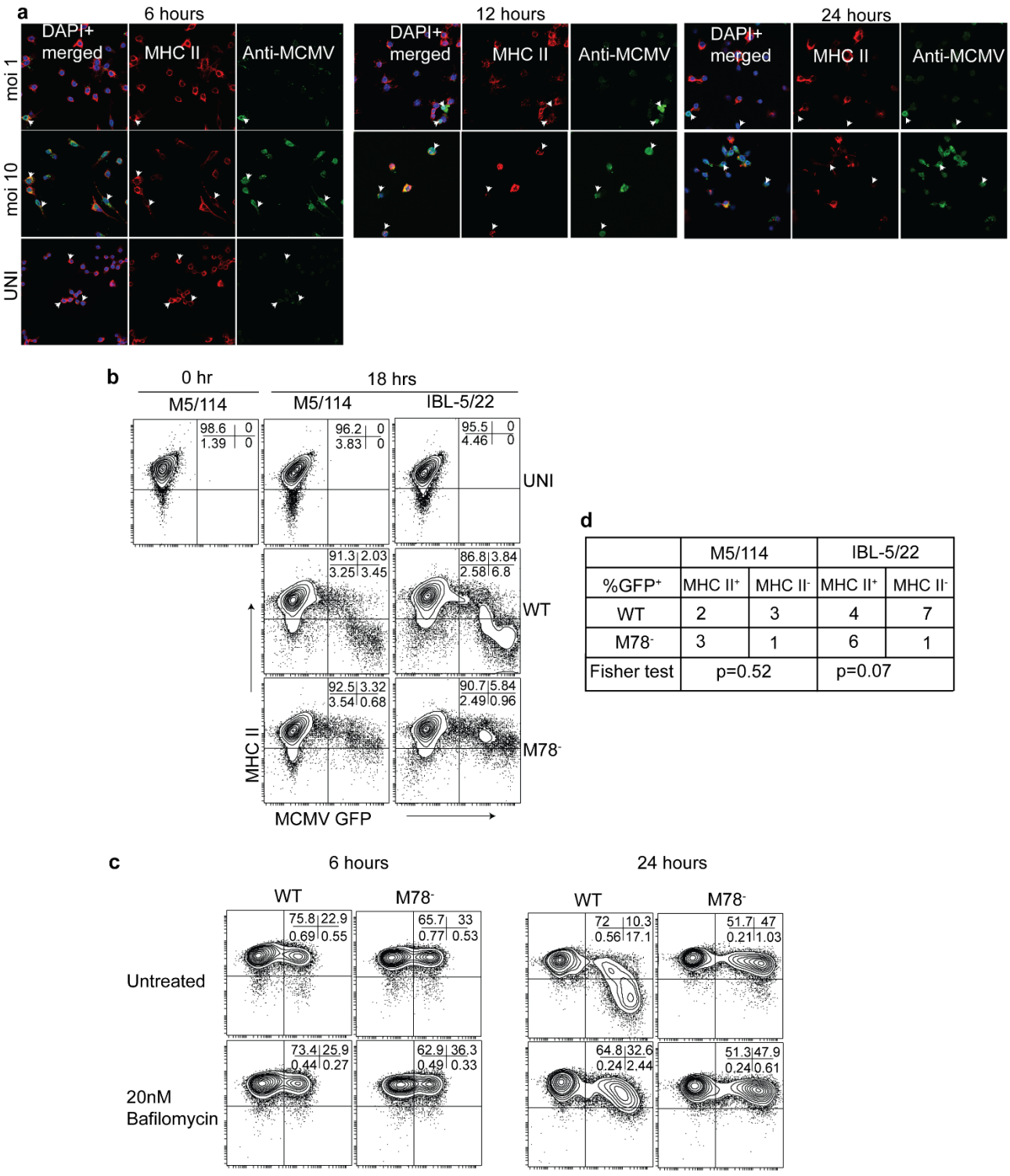

	M5/114		IBL-5/22	
%GFP+	MHC II+	MHC II-	MHC II+	MHC II-
WT	2	3	4	7
M78-	3	1	6	1
Fisher test	p=0.52		p=0.07	

Fig. 4. 6. MHC II downregulation is dose dependent and occurs as early as 6 hours p.i.

a) RAW-C2TA cells were left uninfected or infected with MCMV WT (MOI 1 or 10, for 6, 12 or 24 hrs). The cells were then fixed, permeablised and blocked in 2%NGS/PBS (RT, 1 hr). MHC II was stained using rat anti-MHC II- M5/114 and lytic antigens using rabbit anti-MCMV (4ºC,18 hr) and detected using Alexa Fluor goat anti-rat 594, Alexa Fluor goat anti-

rabbit 488 and DAPI to stain the nucleus (RT, 1 hr). The cells were visualised on confocal microscope at 40X magnification. Arrows show MHC II in vesicles or complete lost from the surface of infected cells. **b)** RAW-C2TA cells as in **A** were saturated with 10 µg/ml or 3 µg/ml MHC II M5/114 or IBL-5/22 antibody. Control cells were left untreated. The cells were then infected with WT or M78^{-} GFP by centrifugation (536 x g for 30 minutes). Infection was left to proceed for 2 hrs at 37^{o}C and unbound virions and unlabelled antibody washed. After 18 hrs, surface labelled MHC II was directly detected with Alexa Fluor goat anti-rat 647 in 2%FCS/PBS (4^{o}C, 1 hr). WT but not M78 GFP^{+} cells lost surface labelled MHC II and was independent of MHC II antibody used but not to significant levels. **c)** RAW-C2TA cells were infected with WT and M78^{-} GFP by centrifugation (536 x g for 30 minutes). Infection was left to proceed at 37^{o}C for 2 hrs. Fresh medium supplemented with or without 20 nM bafilomycin added. After 6 or 24 hrs, MHC II was directly detected with Alexa Fluor 647 rat anti-MHC II (M5/114) (4^{o}C, 1hr). At 6 hrs, MHC II expression was unaltered. By 24 hrs, WT but not M78 GFP^{+} cells downregulated MHC II and this was inhibited by bafilomycin. Data are representative of 2 independent experiments.

4.1.7 Characterising thioglycollate stimulated peritoneal macrophage cells

BALB/c or C57BL/6 mice were injected i.p with thioglycollate and after 96 hrs, mice were sacrificed and cells from the peritoneum cavity harvested and left to adhere at 37^{o}C 5%CO_2 for 4 hrs. The cells were then characterised by flow cytometry analysis. A tight gate was drawn on macrophage cells based on their FSC-A vs SSC-A profile (Fig. 4.7a). Adherent (enriched) and non-adherent (unenriched) cells were F4/80^{+}CD11b^{+}CD19^{-} and expressed MHC II$^{high/low}$.

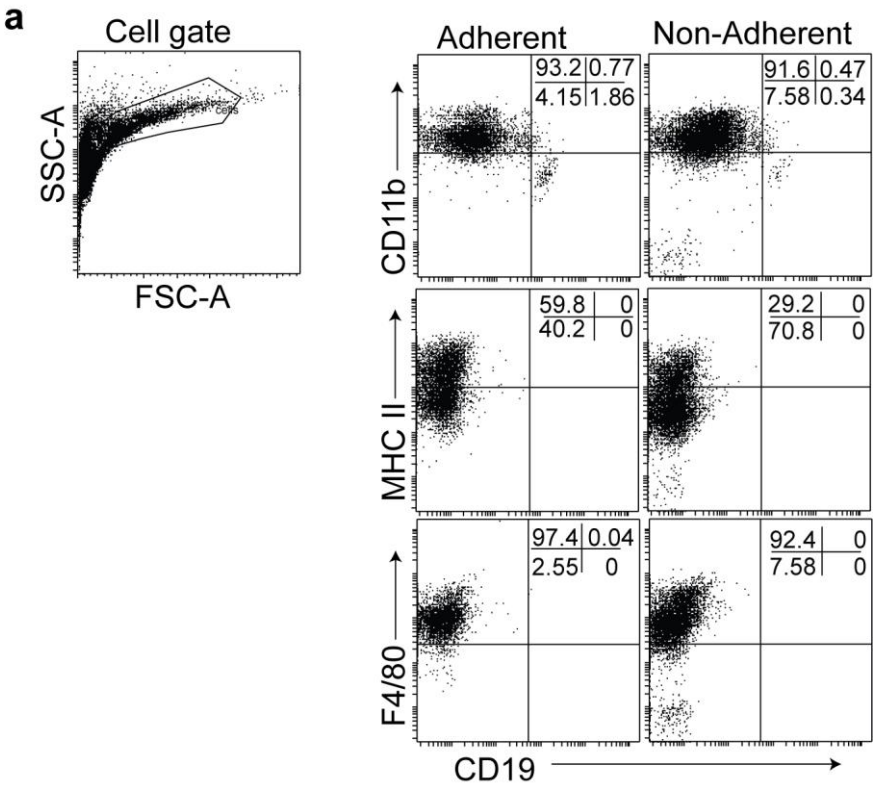

Fig. 4. 7. Characterising thioglycollate stimulated peritoneal macrophages.

C57BL/6 IA ($^{+/-}$) mice were injected i.p with thioglycollate. After 96 hrs, peritoneal cells were harvested, left to adhere and characterised by flow cytometry. The cells were incubated in 2%FCS/PBS (4^{o}C, 1 hr), with PE rat anti-mouse CD11b (M1/70) and Alexa Fluor 647 rat anti-mouse CD19 (ID3) and single stain with rat anti-MHC II (M5//14) and rat anti-F4/80 (3C137) (4^{o}C, 1 hr). The cells were then stained with Alexa Fluor 647 goat anti-rat (4^{o}C, 1 hr). Expression markers were detected on BD Accurri C6 flow cytometer. Data was analysed on weasel. Quadrants show percentages. Data is representative of 2 independent experiments.

4.1.8 M78 c-terminal domain is dispensable for MHC II degradation

The C-terminus of M78 was critical for rapid constitutive endocytosis of M78 and CCR5 (162, 186). To determine whether the C-terminus was required for MHC II downregulation, the C-terminal mutant lacking 155 amino acids from the C-terminus with an HA tag to the N-terminus of M78 (HAM78 cΔ155) was tested. Hemagglutinin expression was confirmed by western blot and immunostaining (Fig. 4.8a, b). This virus downregulated MHC II just like HAM78, a WT MCMV with an HA tag to the N-terminus of M78 by microscopy (Fig. 4.8c). IE1^{+} cells either lost or re-localised MHC II in vesicles. This was also associated with strong or weak IE1 expression as previously observed. Flow cytometry analysis further

showed the C-terminal mutant downregulated and degraded MHC II as WT based on surface (non-permeablised) and total MHC II (permeablised) expression while M78 retained expression (Fig. 4.8d). This showed a region upstream of M78 was required to downregulate and degrade MHC II.

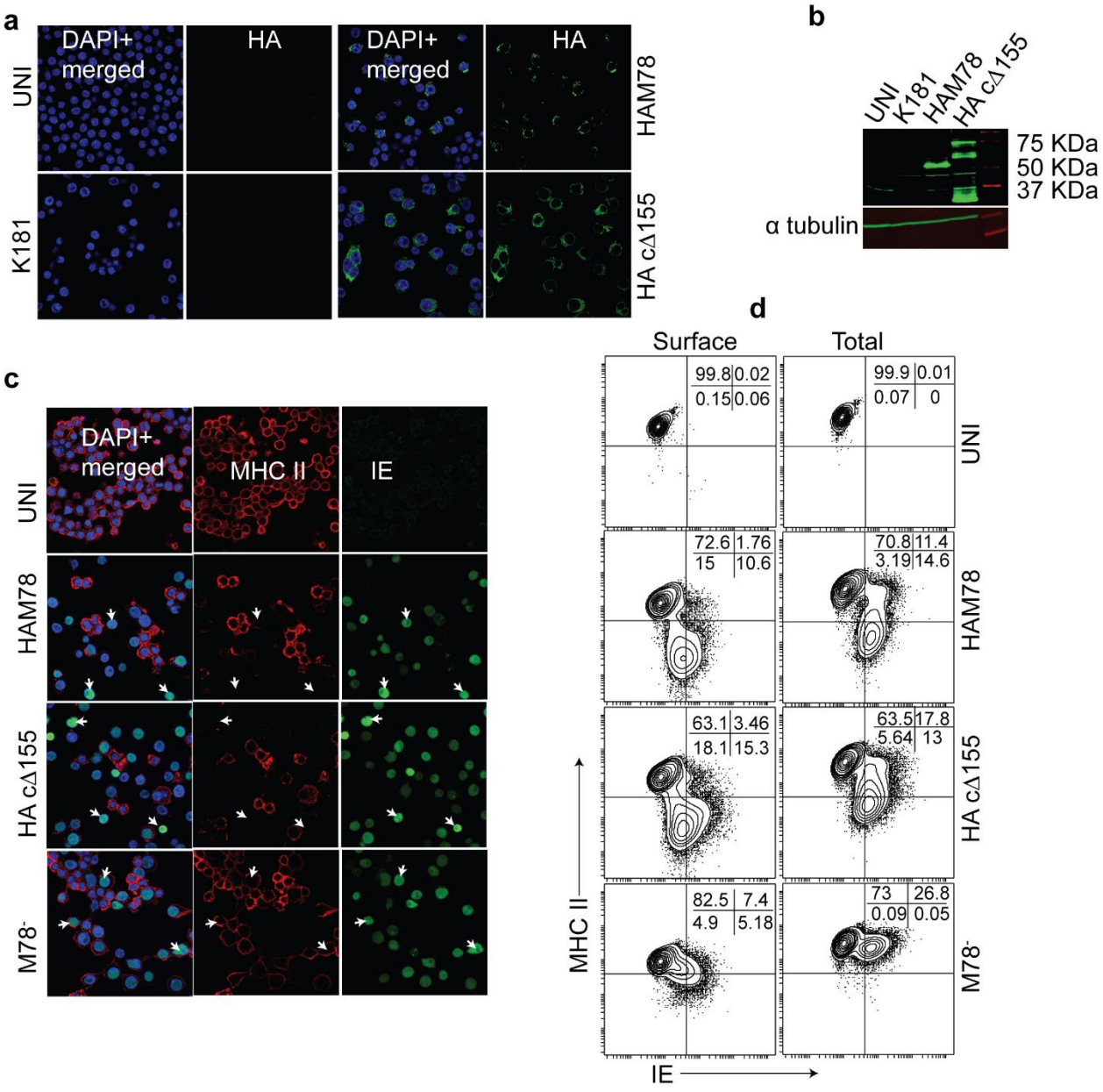

Fig. 4. 8. M78 C-terminus is dispensable for downregulation of MHC II.

a) RAW-C2TA cells were uninfected or infected with WT, HAM78 and HAM78 cΔ155 (MOI 1, 48 hrs). The cells were then fixed, permeablised and blocked in 2%NGS/PBS (RT, 1hr). HA was detected using rabbit anti-HA (4^{o}C, 1 hr) and visualised with Alexa Fluor goat anti-rabbit 488 and DAPI (RT, 1 hr). The cells were imaged at 63X objective on a laser confocal microscope. Arrows show HA expressing cells. Images are representative of 2

independent experiments. **b)** RAW-C2TA cells infected as in **a** were left for 72 hrs. Cell lysate were diluted in 3X Laemmli buffer and resolved by SDS-PAGE and were analysed by immunoblotting with anti-HA or anti-tubulin and detected with IRDye® 800CW goat-anti-rabbit or rabbit anti-rat. With anti-HA, 37-75 kDa bands were observed in HAM78 cΔ155 and a 50 KDa bands for HAM78, none for WT or UNI controls. Western blots are representative of 3 independent experiments. **c)** RAW-C2TA cells infected were uninfected or infected with HAM78, HAM78 cΔ155 and M78$^-$ virus by centrifugation (MOI 1, 48 hrs). The cells were fixed, permeablised and blocked in 2%NGS/PBS (RT, 1hr). MHC II was detected using rat anti-MHC II M5/114 in combination with mouse anti-IE1 using CHROMA101 (4^{o}C, 18 hrs), then with Alexa Fluor goat anti-rat 594, Alexa Fluor goat anti-mouse 488 and DAPI (RT, 1 hr). The cells were imaged at 63X on a laser confocal microscope. Arrows show IE1$^+$ cells positive for MHC II in M78$^-$ cells but not HAM78 or HAM78 cΔ155. **d)** Cells infected as in **c** were stained for surface (non-permeablised) or total (permeablised) MHC II using rat anti-MHC II-M5/114 Alexa Fluor 647. Infected cells were detected by intracellular staining for IE1 and detected with Alexa Fluor goat anti-mouse 488. Cells were then analysed on BD accuri6 flow cytometer and 30,000 events collected on gated live cells. Data was analysed on weasel and percentages shown in quadrants. IE1$^+$ cells on the lower right quadrants show MHC II was downregulated or degraded in HAM78, HAM78 cΔ155 but not M78$^-$ virus infected cells. Data are representative of 2 independent experiments.

4.1.9 Generating M78 expressing BALB/c-3T3-C2TA and RAW-C2TA cells

M78 full protein but not the C-terminal mutant was found to be critical for downregulation of MHC II. To determine whether the full-length protein alone was sufficient, two independent M78 clones were generated. One was amplified from MCMV K181 viral DNA and the other from B53 HAM78 expressing plasmid. The primers were flanked by restriction enzymes EcoRI (sense strand) and BgIII (anti-sense) for cloning. M78 was amplified using Q5 and Taq DNA polymerase and 1.4kb bands were detected on a 1% agarose gel (Fig. 4.9a). The Q5 amplified PCR products were digested with BgIII, PCR purified and then digested with EcoRI. The retrovirus expression vector was digested with EcoRI-HF and BamHI-HF. Competent DH5α *E.coli* cells were then transformed using heat shock, left to recover at 37^{o}C and grown in ampicillin-enriched media. Four independent clones were then cultured and miniprep DNA extracted. M78 insertion was confirmed in all clones amplified from

plasmid DNA and two from K181 viral DNA based on EcoRI and XhoI digest (Fig. 4.9c). All clones had the 1.2 kb M78 band.

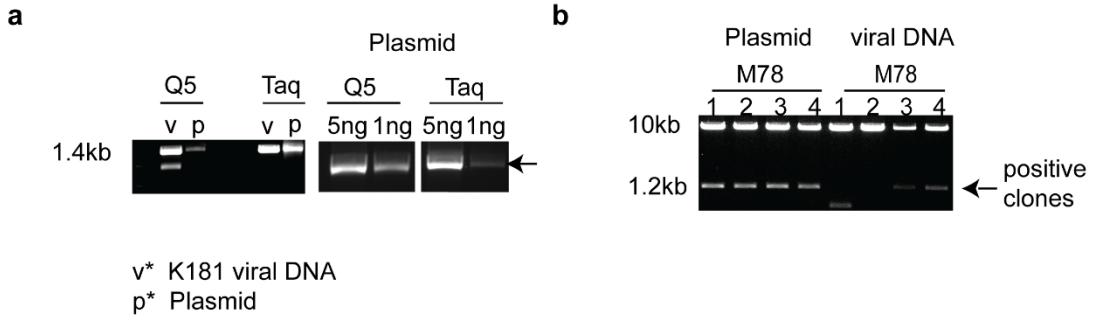

c

K181 viral DNA	**Concentration (ng/µl)**	
M78 clone 1	504.30	
M78 clone 2	495.50	
M78 clone 3	212.84	
M78 clone 4	355.58	← Positive
Plasmid		
Independent M78 clone 1	653.82	
Independent M78 clone 2	567.05	← Positive
Independent M78 clone 3	444.90	
Independent M78 clone 4	468.17	

Fig. 4. 9. Amplification of M78 from K181 viral DNA and HAM78 plasmid.

a) M78 was amplified using Q5 and Taq DNA polymerases from MCMV K181 viral DNA or B53 HAM78 plasmid. Arrow show 1.4kb band on a 1% agarose gel. **b)** Insertion of M78 into the puromycin-expressing vector was confirmed by EcoRI and XhoI double digest of miniprep plasmid DNA extracted from four individual colonies in **c**. All colonies from plasmid M78 1-4 showed 1.2kb band while clone 3 and 4 from K181 viral DNA were positive. Arrow in **c** shows positive clones used to generate M78 expressing cell lines.

To generate stable M78 expressing BALB/c-3T3-C2TA and RAW-C2TA cells, 293T cells were transfected using Optimum-transfect lipid with retroviral packing plasmids PVSVG and PC143N and M78 clone 4 (M78 1), or independent M78 clone 2 (M78 2) or an empty vector as control. After 48 hrs, supernatants from transfected 293T cells were filtered through a 0.45 µM filter and diluted in medium containing 10 µg/ml polypyrene to enhance virion attachment. This process was repeated at 72 hrs post transfection. The cells were then selected in medium containing puromycin. Resistant cells were fixed, permeablised and stained for M78 using anti-M78 sera. M78 1 and independent M78 2 expressed M78. M78 expression in RAW-C2TA and its redistribution of surface MHC II is described in the publication. In BALB/c-3T3-C2TA, M78 expression had no effect on surface MHC II by flow cytometry (Fig. 4.10). Immunostaining, showed M78 and MHC II co-localised in vesicles similar to infected cells (Fig. 4.10b). As previously observed in RAW-C2TA cells, M78 staining in BALB/c-3T3-C2TA was also variable despite puromycin resistance (Fig. 4.10b). The colocalisation of MHC II with M78 shows that M78 might interact with newly synthesised MHC II in fibroblasts before surface localisation while in macrophages M78 redistributes surface MHC II in vesicles.

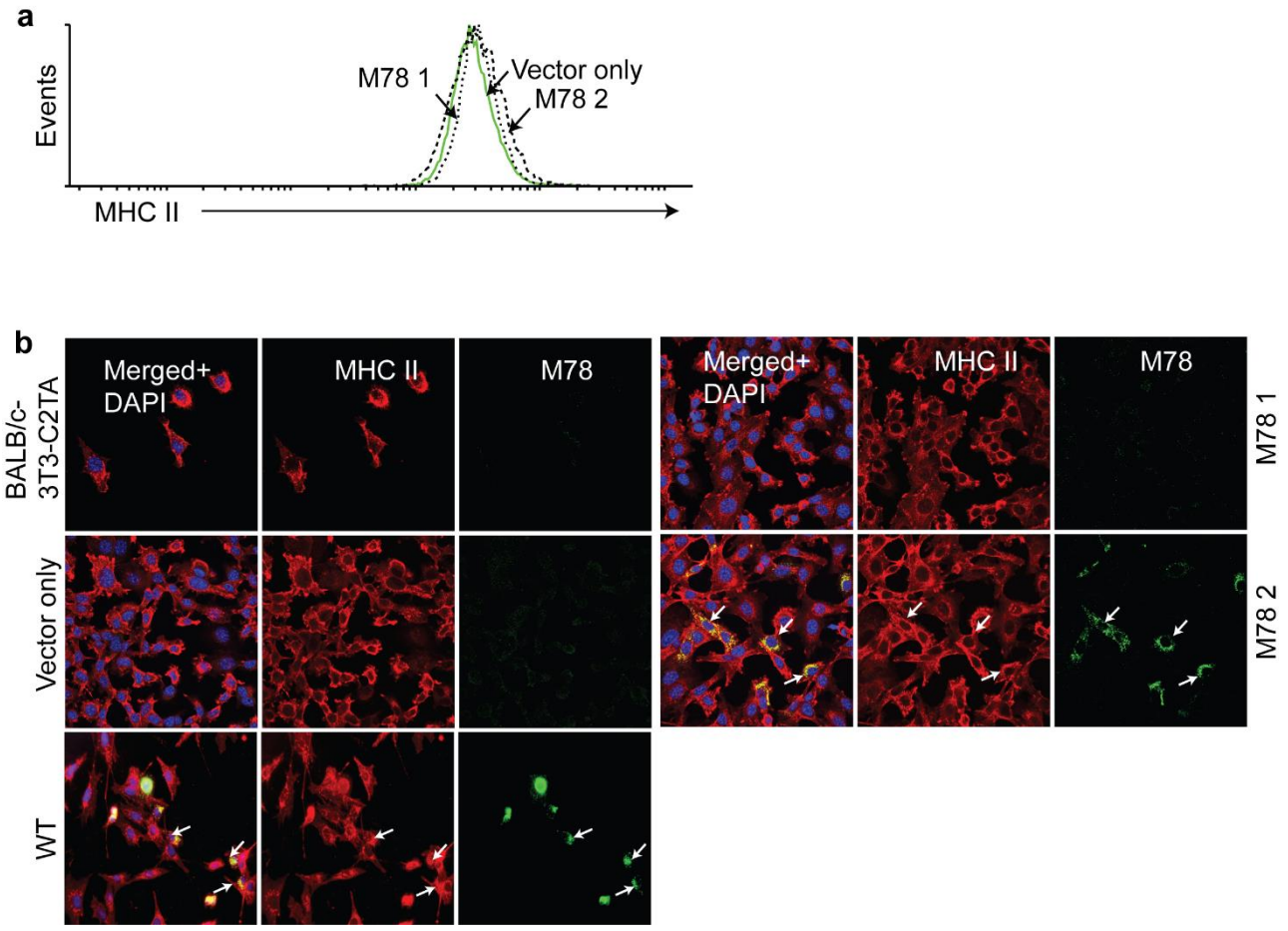

Fig. 4. 10. M78 localises with MHC II in the cytoplasm of BALB/c-3T3-C2TA.

a) Untransduced and transduced BALB/c-3T3-C2TA with vector only, M78 1 or M78 2 were directly stained for MHC II using Alexa Fluor 647 rat anti-MHC II (M5/114) (4^{o}C, 1hr) in combination with rat anti-mouse CD16/CD32 Fc block. The cells were analysed on BD Accurr6 flow cytometry and histogram generated on weasel. Solid green line shows transduced cells with vector only and dark dashed line M78 2 and dark dotted line M78 2. Data are representative of 3 independent experiments. **b)** Cells in **a** were fixed, permeablised, blocked in 2%NGS/PBS (RT, 1hr) and stained for MHC II (rat anti-MHC II-M5/114) and M78 (rabbit anti- M78) (4^{o}C, 1 hr) and detected using Alexa Fluor goat anti-rat 594 and Alexa Fluor goat anti-rabbit 488 (4^{o}C, 1hr). DAPI stained nucleus. WT Infected BALB/c-3T3 (MOI 0.3, 18 hrs) was used as control. The cells were visualised on confocal microscope at 63X magnification. Arrows show MHC II in M78 positive cells. Images are representative of 3 independent experiments.

4.1.10 Can complementing M78^{-} virus downregulate MHC II?

M78 expressing RAW-C2TA and untransduced RAW-C2TA cells were infected with WT and M78^{-} GFP. Flow cytometry analysis showed GFP^{+} WT infected cells downregulated MHC II while M78^{-} retained expression in untransduced RAW-C2TA (Fig. 4.11b) and in M78 transduced RAW-C2TA (Fig. 4.11d). This was also observed by microscopy (Fig. 4.11a-c). As expected both viruses downregulated MHC I but not CD44 in both cell lines (Fig. 4.11b-d).

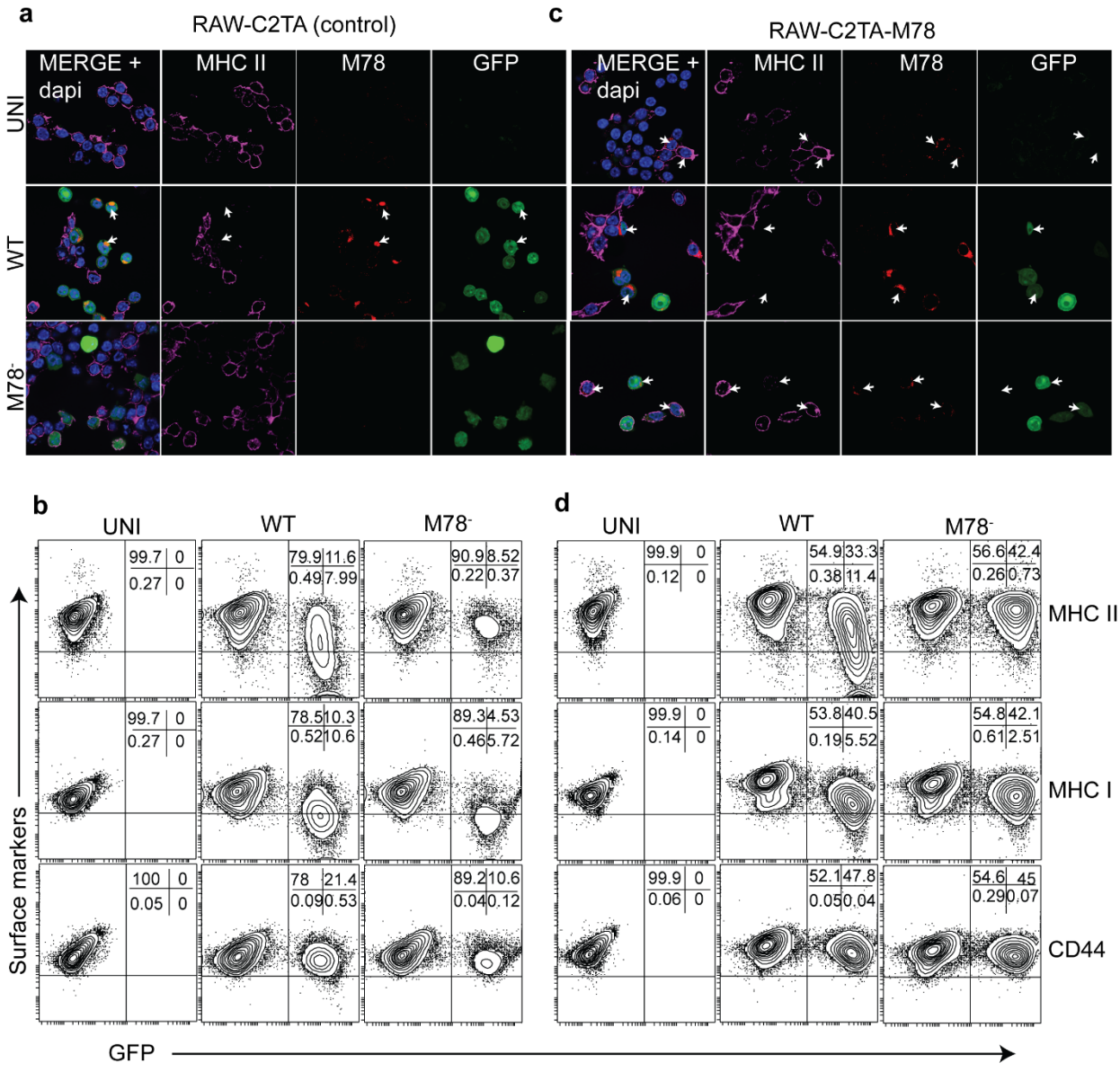

Fig. 4. 11. M78 expressing RAW-C2TA fail to complement M78$^-$ virus.

RAW-C2TA cells were infected with WT or M78$^-$ GFP by centrifugation (MOI 1, 48 hrs). The cells were fixed, permeablised and stained for MHC II (rat anti-MHC II) and M78 (rabbit anti-M78) and detected using Alexa Fluor goat anti-rat 647 and Alexa Fluor goat anti-rabbit 594. DAPI stained nucleus. Arrows show GFP$^+$ cells in WT and M78$^-$ infected cells. M78 is expressed in WT but not M78$^-$ infected cells except in M78 expressing cells. MHC II is lost in GFP$^+$ WT but not M78$^-$ virus in both cell lines. **b)** RAW-C2TA cells infected as in **a** were incubated in Fc block in combination with Alexa Fluor 647 rat anti-MHC II (M5/114) (4^{o}C, 1 hr). MHC I and CD44 was stained using biotin mouse anti-MHC I (H-2D (d) (34-2-12) and biotin anti-CD44 (IM7) (4^{o}C, 1 hr) and detected with streptavidin PerCP Cy5.5 (4^{o}C, 1 hr). Expression was detected using BD Accurri C6 flow cytometer on 30,000 events gated on live cells. Data was visualised and analysed on weasel. Quadrants show percentages. GFP$^+$ cells on the lower right quadrant show loss of surface MHC II in WT but not M78$^-$. MHC I and CD44 expression were comparable between viruses. Data are representative of 3 independent experiments.

4.1.11 Other candidate genes involved in MHC II downregulation

Having shown that M78 alone was not sufficient for MHC II downregulation in transduced cell lines, other candidates were tested; gL$^-$, gO$^-$, M131$^-$ and M33$^-$. All mutants analysed downregulated MHC II but not CD44 (Fig. 4.12a, b). gO$^-$ and gL$^-$ infected cells showed complete loss of MHC II expression. M78 expression and localisation was relatively similar between mutants and WT, that is, localised intracellular and in perinuclear regions in vesicles (186) (Fig. 4.12c). This showed that, absence of gL, gO or M131 had no effect on the localisation of M78 at least by microscopy. In summary, M78 requires an unknown gene to degrade MHC II.

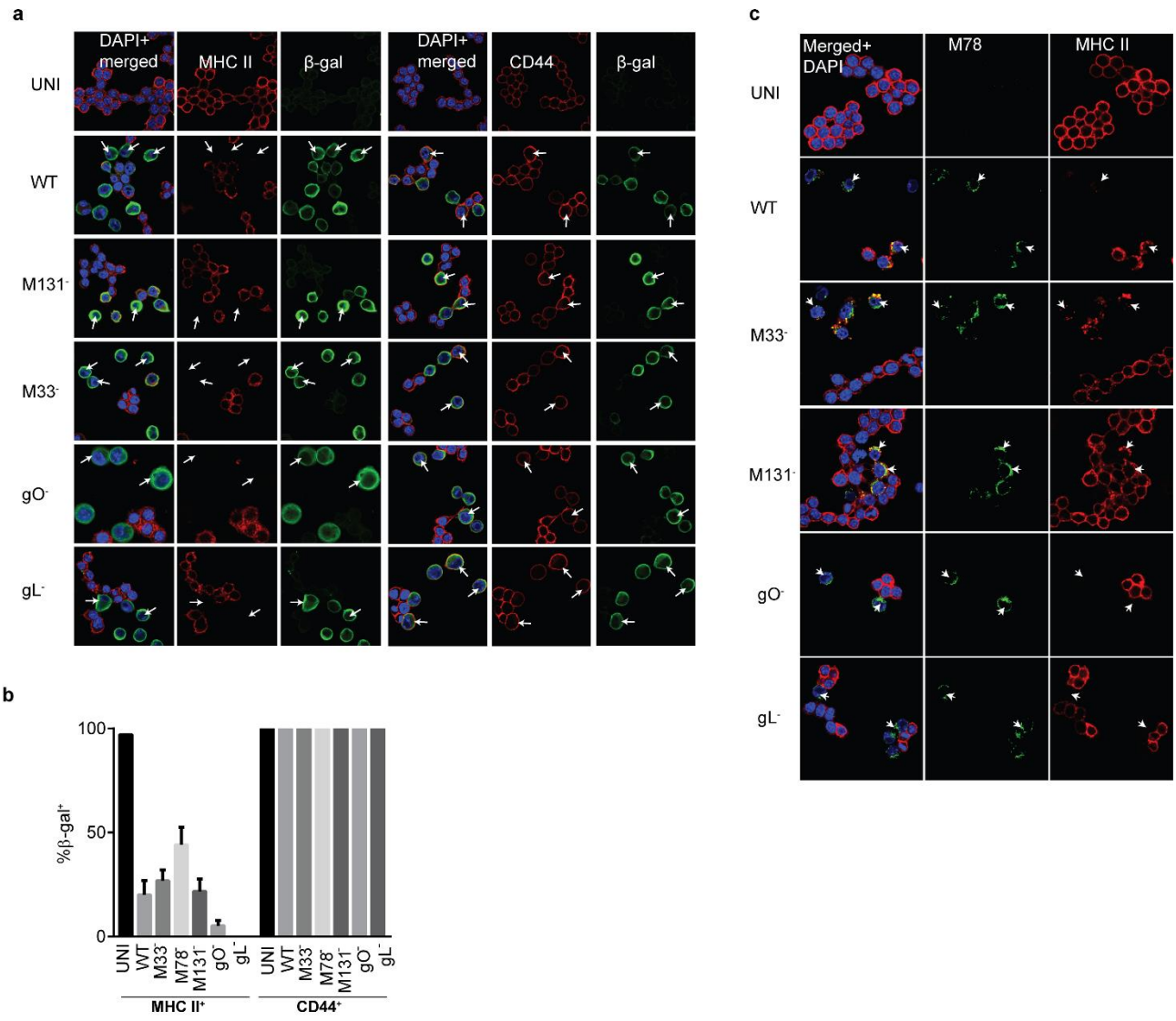

Fig. 4. 12. MCMV glycoprotein mutants downregulate MHC II.

RAW-C2TA cells were infected (MOI 1, 48 hrs) with β-gal expressing WT, M131^{-}, M33^{-}, gO^{-} and gL^{-} by centrifugation (536 x g for 30 minutes). The cells were fixed, permeablised and stained for MHC II (rat anti-MHC II-M5/114), CD44 (rat antii-CD44 IM7) and β-gal (chicken anti-β-gal) and detected using Alexa Fluor goat anti-rat 594 and Alexa Fluor goat anti-chicken 488. DAPI stained nucleus. The cells were visualised on confocal microscope at 63X magnification. Arrows show β-gal^{+} cells expressing MHC II or CD44**. b)** Percentage of β-gal^{+} cells expressing MHC II or CD44. Uninfected cells were used as controls. **c)** RAW-C2TA cells infected in as **a** were stained with rat anti-MHC II-M5/114 and rabbit anti-M78 and detected using Alexa Fluor goat anti-mouse 594 and Alexa Fluor goat anti-rabbit 488. DAPI stained nucleus. Cells were visualised as **a**. Arrows show M78 in perinuclear or intracellular areas, comparable in all infected cells. Images are representative of 2 independent experiments.

4.2 In vivo

4.2.1 M78 infects primary lung cells as WT and retains MHC II expression

To determine whether M78^{-} was impaired in infecting primary cells *in vivo*, immunocompetent BALB/c mice were infected via the i.n route with WT and M78^{-}. CHROMA101 staining for IE1 or anti-MCMV for lytic antigens detected infection and cell markers for resident macrophage, dendritic cells and type II alveolar epithelial cells, cell tropism. At day 1, 3 and 5, WT and M78^{-} infected similar cell types based on IE1^{+} cells (Fig. 4.13 a-c).

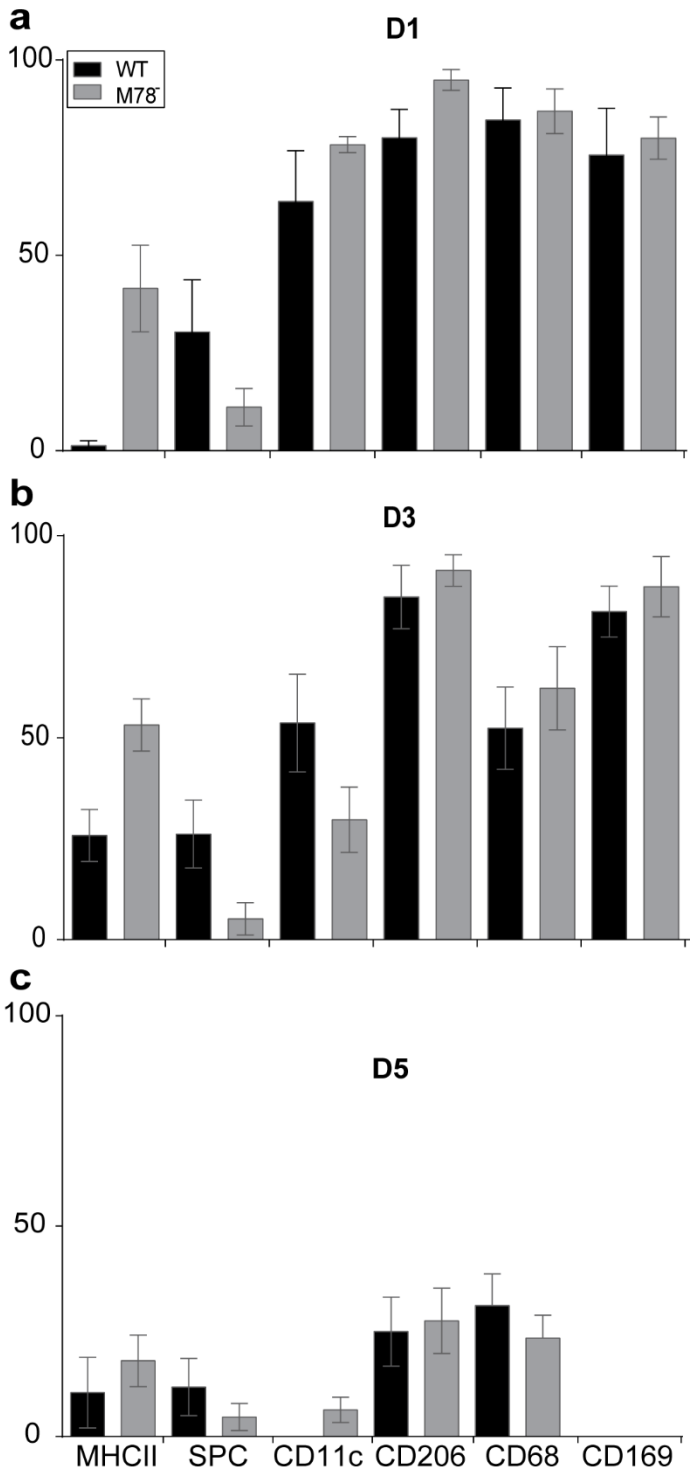

Fig. 4. 13. M78^{-} and WT infect similar cell types in BALB/c lung.

BALB/c were given WT or M78^{-} (3x10^{4} p.f.u/30µL) i.n under anaesthesia. After 1 **(a),** 3 **(b)**, and 5 **(c)** days p.i, lungs were stained with mouse anti-IE1 to identify infected cells and MHC II, macrophage cells (CD206, CD68, CD169), dendritic cells (CD11c) and type II alveolar epithelial cells (SPC). Nuclei were stained with DAPI. Ear bar graph represents percentage of IE1^{+} cells per field of view at 40X.

4.2.2 M78 targets MHC II expression in CD11c$^+$ cells

In the lungs, MHC II is expressed constitutively by type II alveolar epithelial cells (187-189). Naïve BALB/c lung stained for MHC II in combination with markers for CD11c and SPC showed MHC II in predominately SPC cells and a proportion of CD11c cells (Fig. 4.11a-b). Lytic antigen staining of day 3 lung revealed WT but not M78$^-$ infected CD11c lost MHC II expression (Fig. 4.14c-d).

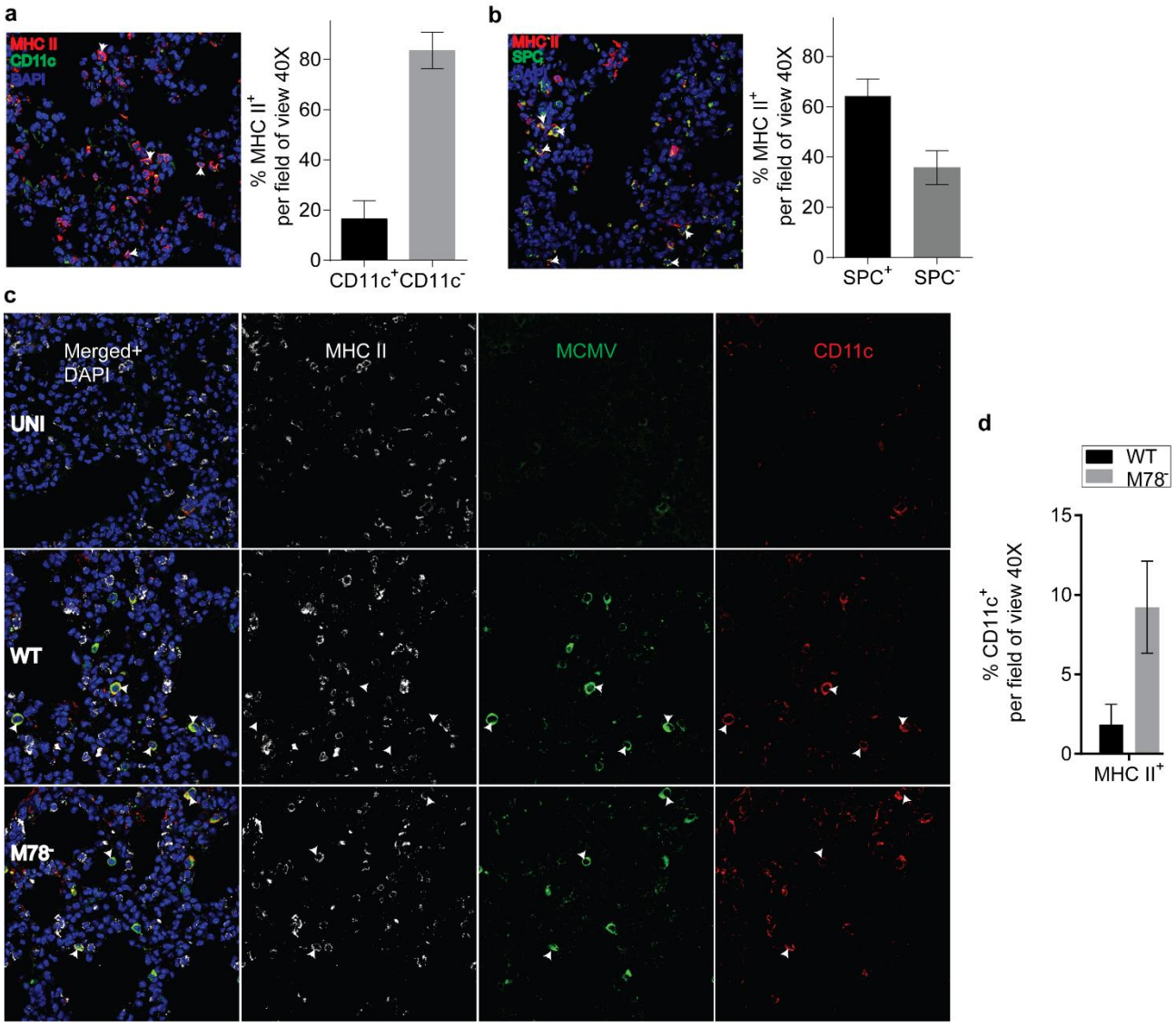

Fig. 4. 14. MCMV targets CD11c+ cells in the lung.

Naïve BALB/c lungs were stained for MHC II in combination with CD11c in **a** or SPC in **b**. Arrows show MHC II expressing CD11c$^+$ and SPC$^+$ cells. **c)** Day 3 BALB/c lungs in **Fig. 4.13** were stained with anti-MCMV sera to lytic antigens in combination with CD11c and

MHC II. Arrows show MHC II^{-}CD11c^{+} lytic antigen^{+} cells in WT but not M78^{-} infected lung shown in **d.**

4.2.3 Inhibiting IFN-γ partially rescues M78^{-} salivary gland defect

IFN-γ is known to restrict MCMV salivary gland infection. To determine whether anti-IFN-γ would rescue M78^{-} salivary gland defect, BALB/c were either left untreated or depleted of CD4^{+} T cells as previously described or by i.p injection with anti-IFN-γ at the time of infection via the intranasal route with WT and M78^{-} and every 48 hrs after infection until the experiment was terminated at day 15. In the lungs, M78^{-} virus titer was significantly lower than WT in CD4^{+} depleted and anti-IFN-γ treated mice (Fig. 4.15a). CD4^{+} T loss or anti-IFN-γ treatment had no effect on WT or M78^{-} lung infection suggesting lung infection control is independent of CD4^{+} T cell and IFN-γ (Fig. 4.15a). In the salivary glands, M78^{-} salivary gland defect in undepleted control mice was significantly greater than CD4^{+} depleted and anti-IFN-γ treated mice (Fig. 4.15a). This was also observed by QPCR (Fig. 4.15b). However, M78^{-} salivary gland replication failed to reach WT levels (Fig. 4.15a,b). Thus, the results show that MCMV can evade CD4^{+} T cells and IFN-γ response to colonise the salivary gland which is partially rescued by M78 deletion.

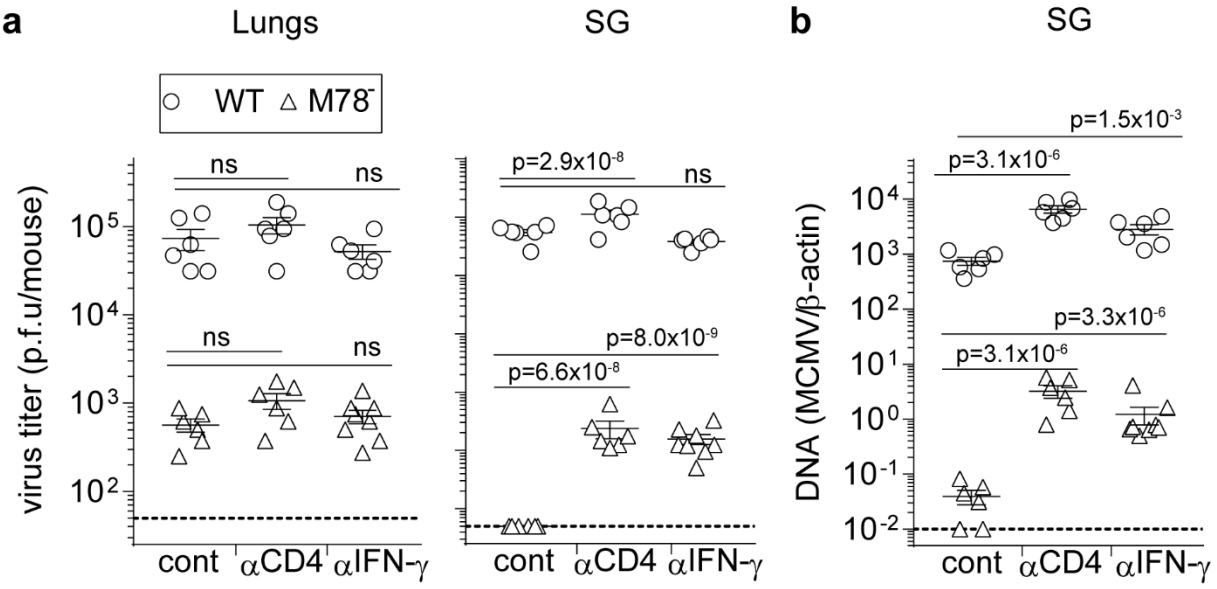

Fig. 4. 15. Anti-IFN-γ treatment partially rescues M78^{-} salivary gland defect.

a, b) BALB/c mice were depleted of CD4^{+} T cells or treated with anti-IFN-γ or left untreated and infected i.n with 3x10^{4} p.f.u/30µL WT or M78^{-} under anaesthesia. After 15 days, infectious virus in the lungs and salivary glands was determined. Symbols show individual

titers per mice and error bars show difference in mean values (n=5 per group). **b)** Viral load in the salivary of untreated, anti-IFN-γ treated and $CD4^+$ T cell depleted mice was determined by QPCR. Symbols represent viral genome copies for individual mice normalised to cellular copy number for each sample. Error bars show difference in mean values (n=5 per group). Data were analysed by unpaired 2-tailed student t-test with Bonferroni-Dunn post-test. $CD4^+$ T cell depletion and anti-IFN-γ treatment rescued $M78^-$ salivary gland defect but had no effect on the lungs.

4.2.4 $M78^-$ virus dissemination is restricted by $CD4^+$ T cells after i.p infection

$M78^-$ given i.p showed reduced liver, spleen and salivary gland infection (190) demonstrating that, events downstream of salivary glands could restrict salivary gland colonisation. To test this hypothesis, WT and $M78^-$ was given i.p to immunocompetent ($IA^{+/-}$) and immunodeficient MHC II^- ($IA^{-/-}$) mice that lack classic $CD4^+$ T cells (Fig. 4.16a). $M78^-$ salivary gland defect in $IA^{+/-}$ mice was significantly rescued in $IA^{-/-}$ but not to WT levels (Fig. 4.16b). Interestingly, WT salivary gland titers in $IA^{-/-}$ was significantly greater than in $IA^{+/-}$ mice (Fig. 4.16b). This suggests that $CD4^+$ T cells restrict salivary gland infection in an organ upstream of the salivary glands. Surprisingly, both WT and $M78^-$ were undetectable in the liver and spleen of $IA^{+/-}$ and $^{-/-}$ mice by plaque assay (data not shown), suggesting infection was cleared.

4.2.5 M78 C-terminus is critical for virus dissemination

M78 C-terminus was previously shown to be necessary for MCMV dissemination in immunocompetent C57BL/6 mice (162). To determine whether the C-terminal mutant of M78 would be rescued by $CD4^+$ T cell loss, $IA^{+/-}$ and $IA^{-/-}$ mice were infected via the i.n route with WT, $M78^-$ and the C-terminal mutant (M78 Δ c155). M78 Δc155 was undetectable in the lungs or salivary glands of $IA^{+/-}$ and $IA^{-/-}$ mice compared to WT (Fig. 4.16c). Again, $M78^-$ salivary defect in $IA^{+/-}$ was significantly rescued in $IA^{-/-}$ (Fig. 4.16c). WT salivary gland titer was no different between $IA^{+/-}$ and $IA^{-/-}$ mice, again confirming that M78 was necessary for this effect. In the lung, $M78^-$ titers were slightly higher in $IA^{-/-}$ than $IA^{+/-}$ mice but not to significant levels compared to WT (Fig. 4.16c). This result confirms that, M78 is not only required for infection and virus dissemination to the salivary gland as previously described (162) but also for evading $CD4^+$ T cells.

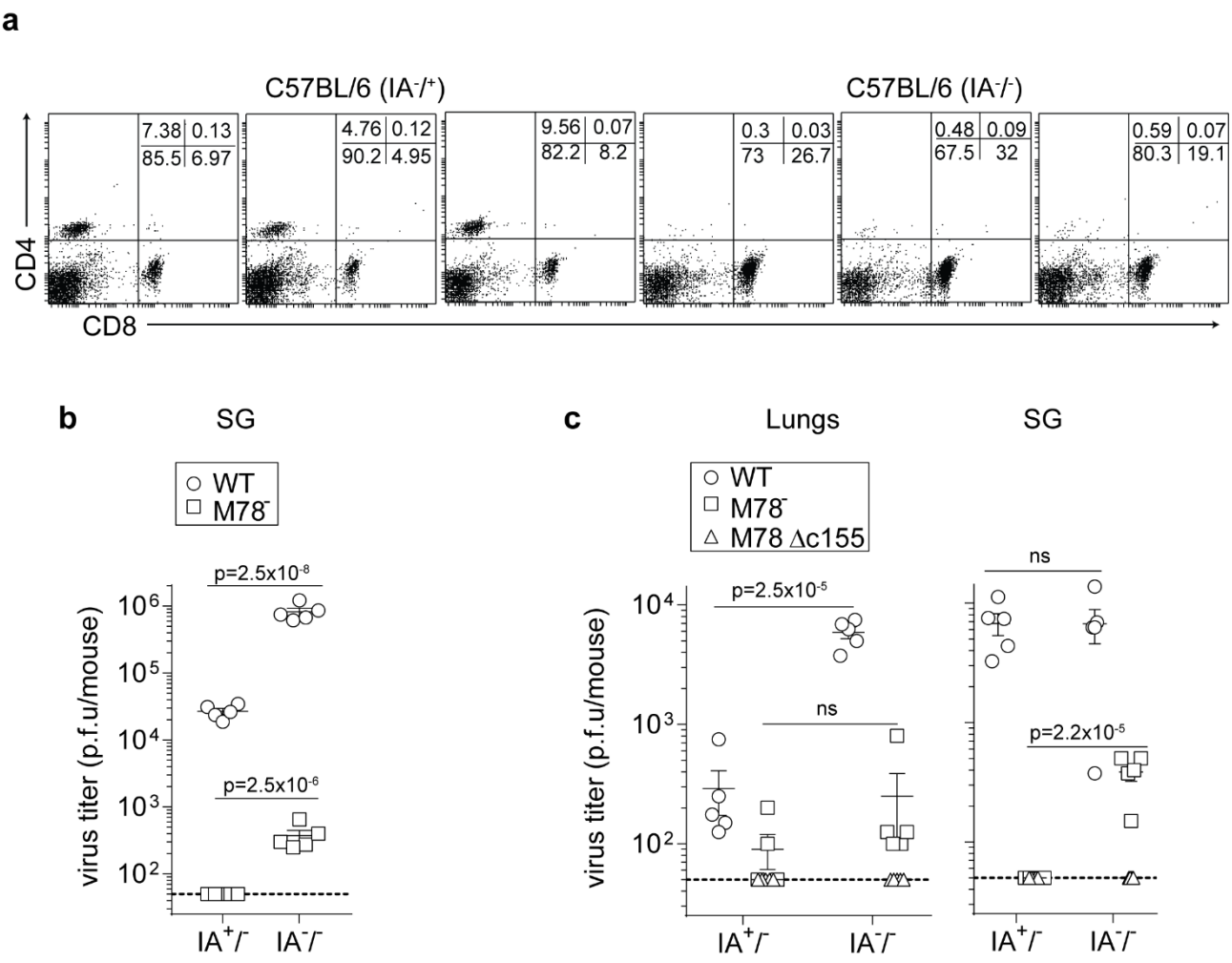

Fig. 4. 16. M78 C-terminus is critical for virus dissemination.

a) C57BL/6 ($IA^{+/-}$) and MHC II^- ($IA^{-/-}$) mice were tail bled and lymphocytes were directly stained for CD4 using FITC rat anti-mouse CD4 clone GK1.5 and PE rat anti-mouse CD8β in the presence of mouse Fc receptor block rat anti-mouse CD16/CD32 clone 2.4G2 (4ºC,1 hr). The cells were washed and analysed on BD Accurri C6 flow cytometer. **b)** C57BL/6 ($IA^{+/-}$) and MHC II^- ($IA^{-/-}$) mice infected i.p with $3x10^4$ p.f.u/100µL WT or $M78^-$ **b** or i.n **c** with $3x10^4$ p.f.u/30µL WT, $M78^-$ or M78 cΔ155 under anaesthesia. After 10 days, infectious virus in the lungs and salivary glands was determined. Symbols show individual titers per mice and error bars show difference in mean values (n=5 per group). Data were analysed using unpaired 2-tailed student t-test. $M78^-$ salivary gland defect in $IA^{+/-}$ was significantly rescued in $IA^{-/-}$ mice. M78 C-terminal mutant M78 cΔ155 failed to replicate in the lungs and spread to the salivary glands in $IA^{+/-}$ or $IA^{-/-}$ mice.

4.3 Discussion

In vitro, M78^{-} replicated slightly less than WT at low MOI in MHC II$^{+/+}$ and MHC II$^{-/-}$ RAW 264.7 macrophage cells. This was restored at high MOI, suggesting M78 is required for efficient infection of macrophage cells upon entry. This was shown in a single step replication kinetics, when centrifugation improved virion attachment to the cell membrane and enhanced M78^{-} virus infection. It would be interesting to determine whether centrifugation makes a significant difference to initial infection, as it is somewhat artificial. As previously shown, M78^{-} virus had no replication defect in fibroblasts cells but replicated slightly less than WT in epithelial cells (162). This suggests M78 could have an epithelial infection defect. *In vivo*, the first target cells in the lungs are resident macrophage, infiltrating dendritic cells (166) which are less lytic and type II alveolar epithelial cells that support lytic virus replication (191). M78^{-} virus readily infected these cells as WT at day 1, 3 and 5 by IE1 staining. The virus also replicated to WT levels by plaque assay and by QPCR at day 3, 5 and 7. This suggests epithelial infection, as macrophages are less lytic and not productive. Thus, M78^{-} replication defect in epithelial cells *in vitro* should be interpreted with caution as both WT and M78^{-} infected less SPC cells in the lung and replicated to similar levels.

MCMV degradation of MHC II was not strain specific and the C-terminus of M78 was dispensable. M78 expressed alone in MHC II expressing cell lines relocalised MHC II to endosomes but was not sufficient for its degradation, implying a co-factor or another viral gene. *In vitro*, direct antigen presentation using ovalbumin as model antigen restricted but did not impair CD4^{+} T cell response. A lack of recombinant M78^{-} virus to directly quantity how MHC II degradation impairs CD4^{+} T cell response in the context of endogenous presentation limits the scope of interpretation.

Anti-IFN-γ partially rescued M78^{-} salivary gland defect. This suggests that anti-IFN-γ function could be independent of M78 CD4^{+} T cell function and may restrict M78^{-} virus trafficking or spread. Where and how IFN-γ restricts M78^{-} infected cells to spread is unknown. Nevertheless, M78 appears to be a multi-functional protein that targets different aspects of the host immune response to evade surveillance and disseminate virus. Unlocking the M78 regions contributing to these different functions could be key to developing an anti-viral therapy.

CHAPTER 5: USING ORF73-DEFICIENT, OVALBUMIN+ MHV-68, TO TRACK ANTIGEN-SPECIFIC CD4^{+} T CELLS IN AN ESTABLISHED PROTECTION MODEL

5.1 Introduction

Gamma-herpesviruses establish latency, predominately in B cells (150, 192-194). However, epithelial, dendritic and macrophage cells can also harbour the virus (118, 119, 195, 196). During latency when no preformed infectious virus is detected, gamma-herpesviruses maintain their genome as circularised, extrachromosomal episomes/plasmids (197-200). This unresponsive or dormant state is critical for immune evasion, as gene expression is regulated during replication, persistence and reactivation from latency (149, 153). EBV, encodes two proteins crucial to maintaining latency; latent origin of replication *ori*P, a cis acting protein and EBV nuclear antigen 1 (EBNA-1) a trans-acting gene. The dyad domains of oirP bind and interact with the host cell mitotic chromosomes and chromatin (201, 202). This allows EBV DNA to replicate as an extrachromosomal plasmid and segregate in infected cells during cell division (203, 204). A similar mechanism was shown for bovine papilloma virus proteins E1 and E2 (205). Kaposi's sarcoma herpesvirus virus (KSHV), herpesvirus saimiri (HVS) and MHV-68, members of the gamma-2-hepesvirus subfamily encode a conserved ORF73, a latency associated nuclear antigen (LANA) with similar function but limited sequence similarity to EBNA-1 (206-208).

KSHV LANA, is a 1162 amino acid protein that has been extensively studied. Like EBNA-1, it interacts with virus origin of replication (209) and terminal repeats in the viral genome via its C-terminal domain (210, 211). The N-terminal domain is thought to facilitate docking onto mitotic chromosomes by binding nucleosomes through histones H2A and H2B (212). This is hypothesised to enable KSHV replication and episome maintenance by tethering the KHSV DNA to host chromosomes (213). Thus, during cell division the viral genome is equally partitioned to each daughter cell in dividing latently infected cells (213). MHV-68 ORF73, a 368 amino acid protein also functions similarly to LANA (213), a common strategy utilised by all gamma-herpesviruses to persist in infected mammalian cells (214). How the latency associated viral proteins encoded by gamma-herpesviruses affect $CD4^+$ T cell responses is not clear.

In KSHV, LANA interferes with $CD4^+$ T cell responses by hindering MHC II expression in infected cells, via multiple mechanisms, to restrict antigen presentation. MHC II expression is controlled by the key regulator of MHC II transcription, the class II transactivator (C2TA)

(215). C2TA interacts with cell type specific promoters to drive MHC II expression in a cell type specific manner. Promoters I (PI) is active in macrophage and dendritic cells, PIII acts on B cells and PIV is inducible by IFN-γ (215, 216). *In vitro* assays demonstrate that LANA can interact with IRF-4 to suppress MHC II in primary effusion lymphoma (PEL) cells by binding to PIII and PIV C2TA promoters (217, 218). LANA can also bind to the MHC II enhanceosome that consists of cyclic AMP response element-binding protein (CREB) and nuclear factor Y (NF-Y) complex and regulatory factor X (RFX) complex proteins to restrict C2TA recruitment to the MHC II promoters (219, 220). As a result, infected cells are unable to present viral antigens to $CD4^+$ T cells, making them invisible to target. This is hypothesised to allow virus escape from immune surveillance and colonise the host. Whether this happens *in vivo* is unknown.

Unlike KSHV, MHV-68 does not interfere with MHC II expression in antigen presenting cells. Instead, ORF73 mediates the transcription of genes associated with the lytic and latent cycles during infection. ORF73 is transcribed as an immediate early transcript (221) and also during latency (151). This suggests ORF73 can regulate viral gene expression early to evade immune response, or prevent expression of certain latent proteins or host cell stress response elements (148). *In vitro*, ORF73 mutants show replication defects in fibroblasts (NHI 3T3 and MEFs), albeit at later times during replication (148, 222). *In vivo*, ORF73 mutants show lytic replication defect in the lung following intranasal infection and severe attenuation in the spleen (149, 152). How ORF73 modulates $CD4^+$ T cell response during infection is not well characterised. Adoptive transfer of gp150 specific $CD4^+$ T cells showed expansion and contraction of $CD4^+$ T cells as infection progressed from lytic to latent. This occurred independent of lytic (ORF73 mutants) or persistent (wild type) infection (223). However, the assay was limited by measuring cell numbers and frequency of proliferation rather than virus load to determine whether absence of ORF73 affected $CD4^+$ T cell response.

In a study by *Smith et al., 2006*, cytoplasmic ovalbumin expressed in tandem with ORF73 failed to stimulate $CD4^+$ T cells specific for $OVA_{323-339}$ peptide in BALB/c mice (160). Improving presentation of the $OVA_{323-339}$ had no effect on latency either in BALB/c or C57BL/6 mice. The authors found that secreted cytoplasmic OVA expressed under the control of ORF73 stimulated $CD8^+$ T cells in C57BL/6 mice but not $CD4^+$ T cells in BALB/c mice (160). The authors reasoned that latent antigen specific $CD4^+$ T cells in BALB/c mice were either unable to recognise infected cells or lacked the effector functions required for

control, despite killing of MHC II^{+} cells pulsed with OVA$_{323-339}$ peptide *in vitro*. It is possible that OVA$_{323-339}$ peptide expression driven by ORF73 during infection is below the threshold of detection by CD4^{+} T cells. Thus, the small subset of primed CD4^{+} T cells have no cytolytic activity against latently infected B cells or myeloid cells.

To study how a latency defect affects CD4^{+} T cell response, a trackable animal model using MHV-68 that lacks functional ORF73 expressing soluble cytoplasmic ovalbumin was constructed. Ovalbumin expression was driven by the lytic M3 promoter. The rational was to track CD4^{+} T cell responses to MHV-68 during lytic infection and analyse the activation and proliferation profile of OVA$_{323-339}$-specific CD4^{+} T cells. It was hypothesised that, in the absence of ORF73, CD4^{+} T cells will be sensitised to recognise lytically infected cells and control lytic and latent infection.

Aim

The aim of this thesis chapter is to describe the process of making an ORF73 deletion mutant expressing cytoplasmic ovalbumin. The overall aim is to use this ORF73-deficient, ovalbumin+ MHV-68, to track antigen-specific CD4+ T cells in an established protection model.

5.2 Results

5.2.1 Diagnosing the presence of ovalbumin in the psk pA sOVA M3 shuttle vector

To determine the presence of ovalbumin in the psk pA sOVA M3 shuttle vector previously used to generate MHV-68 recombinant OVA^+ viruses (160, 173), competent DH5α *E.coli* cells were transformed with the shuttle vector and cultured in agar and LB broth containing Kan and Cam. To check for sucrose sensitivity, transformed bacteria were plated on sucrose agar. No colonies were observed on either Cam or sucrose agar plates (data not shown) confirming the absence of Cam gene and the presence of SacB, a marker for negative selection in the shuttle vector. Plasmid DNA extracted from the 6 clones grown on Kan enriched LB broth was digested with EcoRI and a 1.6Kb band was detected on a 1% agarose gel (Fig. 5.1a), consistent with previous observations.

5.2.2 Transformation of BAC^+ Δ73 mutant DH10B *E.coli*

Competent BAC^+ Δ73 mutant DH10B *E.coli* (149) was transformed with plasmid DNA (clone 5) and cultured in CamR and KanR agar at 30^{o}C to allow homologous recombination. Positive clones were plated onto Kan or Cam and Kan agar plates and incubated at 42^{o}C to select for BAC co-integrate. The colonies were then replated on Cam agar and incubated at 37^{o}C to allow for the segregation of co-integrate colonies into either wild type (no ovalbumin) or recombinant. To select for co-integrates, the bacteria were plated onto sucrose supplemented with Cam and incubated at 30^{o}C. 24 single colonies were then plated onto Cam and Kan agar and Cam LB broth. DNA was extracted from 12 randomly selected individual colonies and screened for the presence of ovalbumin and ORF73 deletion mutation by restriction digest.

5.2.3 Confirmation of BAC^+ Δ73 sOVA by restriction digest

EcoRI digest showed a 7.4Kb band (Fig. 5.1b-white arrow) present in all clones. This is a BAC cassette that encodes the eGFP marker (positive selection) and the two loxP sites (Fig. 5.1b- white arrow) as previously described (155). Incorporation of psk pA sOVA M3 into the BAC during homologous recombination introduced a new EcoRI site which led to a loss of 15.7kb band (Fig. 5.1b-yellow arrow) and a gain of 12.9kb band (Fig. 5.1b-red arrow) in BAC^+ Δ73 mutants' clones 6, 13 and 24 and in WT clones 2, 11, 21 or 23 (Fig. 5.1b). The 18kb band observed in clones 7 and 20 is the result of fusion of the terminal repeats during replication in the BAC^+ Δ73 DH10B *E.coli* (Fig. 5.1b). An end repair during

BAC$^+$ Δ73 generation led to a loss of a BstEII site at position 11101. This led to a loss of 4.3kb bands (Fig. 5.1c-red arrow) and a gain of 10.2kb (Fig. 5.1c-yellow arrow) in Δ73 mutants' clones 6, 6.4, 6.5, 13, 14 and 24 compared to pHA3 plasmid, which contains MHV-68 genome as a BAC. Homologous recombination in the BAC Δ73 DH10B *E.coli* also generated BAC MHV-68 WT clones 2 and 21 that lost the 10.2kb band as pHA3 (Fig. 5.1c, yellow arrow). Insertion of the 1.6kb psk pA sOVA M3 into the BAC derived Δ73 mutant led to a gain of 13.8kb (Fig. 5.1c- purple arrow) in clones 6, 6.4, 6.5, and 13, 14 and 24 except clones 2 and 21. Based on restriction digest analyses clones 6, 6.4 and 6.5, 13 and 24 were identified as BAC$^+$ Δ73 sOVA mutants. BAC$^+$ Δ73 sOVA clones 6, 13, 14, 21 and 24 and WT clones 2 and 21 were used for further manipulation.

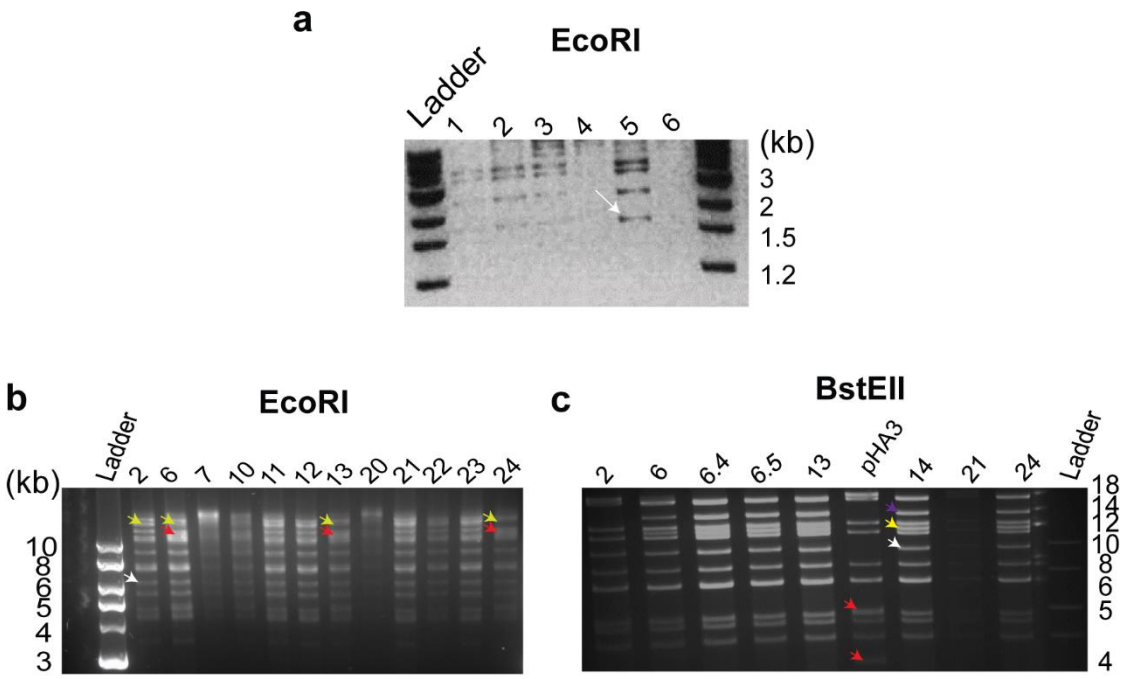

Fig. 5. 1. Analysis of shuttle vector and diagnosis of BAC$^+$ Δ73 sOVA plasmid DNA.

a) Plasmid DNA extracted from cultured colonies of psk pA sOVA M3 shuttle vector digested with EcoRI. **b, c**) Plasmid DNA extracted from cultured colonies of BAC$^+$ Δ73 sOVA were digested with restriction enzymes EcoRI and BstEII and resolved on 1% agarose gel. Arrows represent bands in **a** 1.6kb band represented by white arrow, **b**) EcoRI bands; 7.4kb shown as white arrow represents the BAC cassette, red- 12.9kb band in mutants' clone 6, 13 and 24 and yellow- 15.7kb in wild type clones' 2, 11, 12, 20, 21, 22 and 23 due to introduction of new EcoRI site. **c)** BstEII bands; purple- 13.8kb insertion of OVA in clones 6.4, 6.5, 13, 14 and 24; yellow- 12.7kb band in BAC$^+$ Δ73 mutants with

OVA insertion, white; 10.2kb in BAC^+ Δ73 mutants, red; 5kb and 7.4kb bands internal repeat regions.

5.2.4 Reconstitution of BHK-21 cells

To reconstitute the BAC, BHK-21 cells were transfected with BAC^+ Δ73 sOVA DNA extracted from wild type like clones 2 and 21 and mutant clones 6, 13, 14, 21 and 24. The cells were then monitored for GFP expression. GFP was found to be expressed in cells transfected with clones' 13, 14 and 24 (data not shown). Virus stocks were prepared from reconstituted BAC^+ Δ73 sOVA clones 13 and 14. The presence of the BAC cassette has been shown to interfere with virus replication *in vivo* (157). To remove the BAC cassette, NIH-3T3 cells expressing Cre were infected with BAC^+ Δ73 sOVA clone 13 and 14. The cells were monitored for loss of GFP expression and virus stocks prepared. To validate the absence of the BAC, MEFs were infected with BAC^+ and BAC^- WT and the recombinant BAC^+ and BAC^- Δ73 sOVA clone 13. BAC^+ Δ73 sOVA clone 13 infected MEFs expressed GFP as wild type while BAC^- Δ73 sOVA infected cells did not express GFP similar to BAC^- WT (Fig. 5.2 a, b). To confirm infection, the BAC^+ and BAC^- Δ73 sOVA and WT infected cells were stained for lytic antigens and visualised by fluorescence. BAC^+ viruses were GFP as expected and lytic antigen positive while BAC^- viruses were GFP negative and lytic antigen positive (Fig. 5.2a, b). This confirmed Cre recombinase cleaved one of the flanking loxP sites that encodes the eGFP cassette.

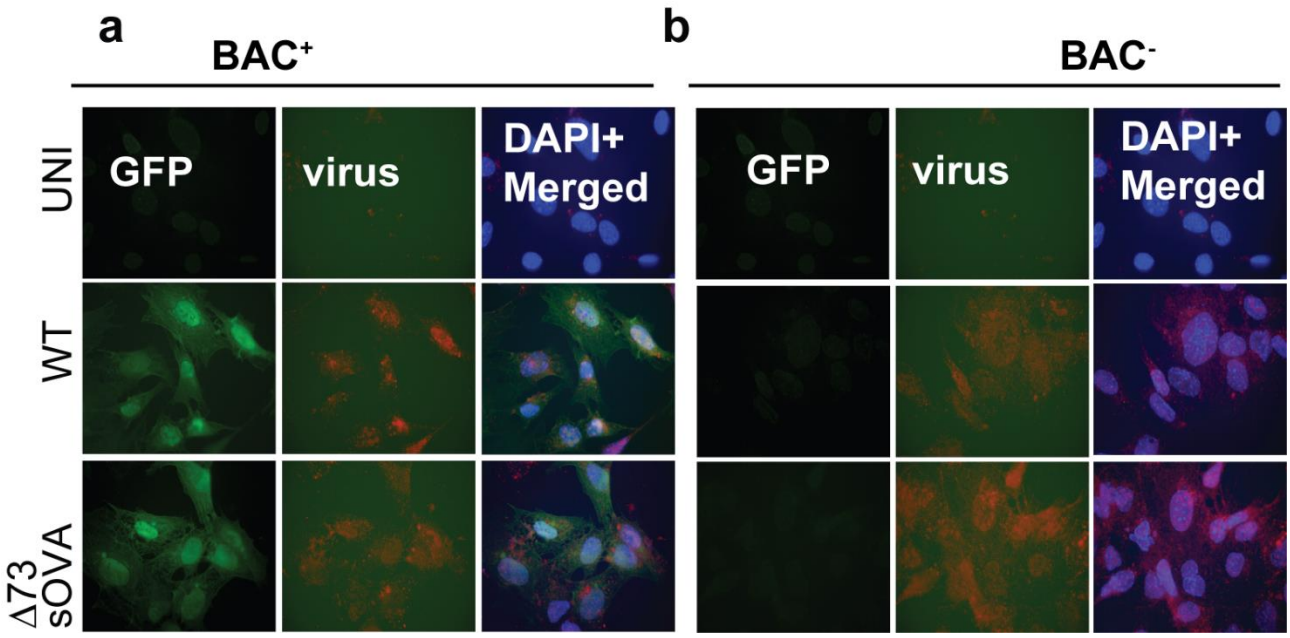

Fig. 5. 2. Confirmation of BAC cassette cleavage by Cre recombinase.

a, b) MEFs were infected (MOI 1, 18 hrs) with BAC^+ or BAC^- WT and Δ73 sOVA mutant. The cells were then fixed, permeablised and blocked in 2%NDS/PBS. Lytic antigens were stained with rabbit anti-MHV-68 in 2%NDS/PBS and detected with Alexa Fluor 594 donkey anti-rabbit IgG (H+L). DAPI was used to stain cell nuclei. Images were acquired using Nikon immunofluorescence microscope at 100X objective. Images are representative of 2 independent experiments.

5.2.5 Expression of ovalbumin in MHV-68 Δ73 sOVA constructs.

To confirm OVA expression, MEFs were infected with either BAC^+ or BAC^- WT or Δ73 sOVA and other MHV-68 recombinant OVA viruses that lack the BAC cassette as controls. Indirect detection for lytic antigens showed positive for lytic antigens in BAC^+ and BAC^- viruses (Fig. 5.3 a, b). Ovalbumin expression was detected in BAC^+ and BAC^- Δ73 sOVA, MHV-68 m3 mOVA and MHV-68 m3 sOVA but not in WT or MHV-68 IiOVA infected cells. To validate the IF results, NIH-3T3 cells were infected with BAC^- MHV-68 recombinant viruses and Δ73 sOVA and analysed for OVA expression using western blot. Ovalbumin was detected in both culture medium and cell lysate of cells infected with MHV-68 sOVA and Δ73 sOVA but only in the latter in all infected cells except for IiOVA (Fig. 5.3c). This suggests that OVA is expressed and retained in the cytoplasm of MHV-68 mOVA infected cells and only secreted into the medium in MHV-68 sOVA viruses that retain their signal

peptide. The absence of IiOVA OVA detection suggest the antibody is not effective at detecting $OV_{A323-339}$ peptide.

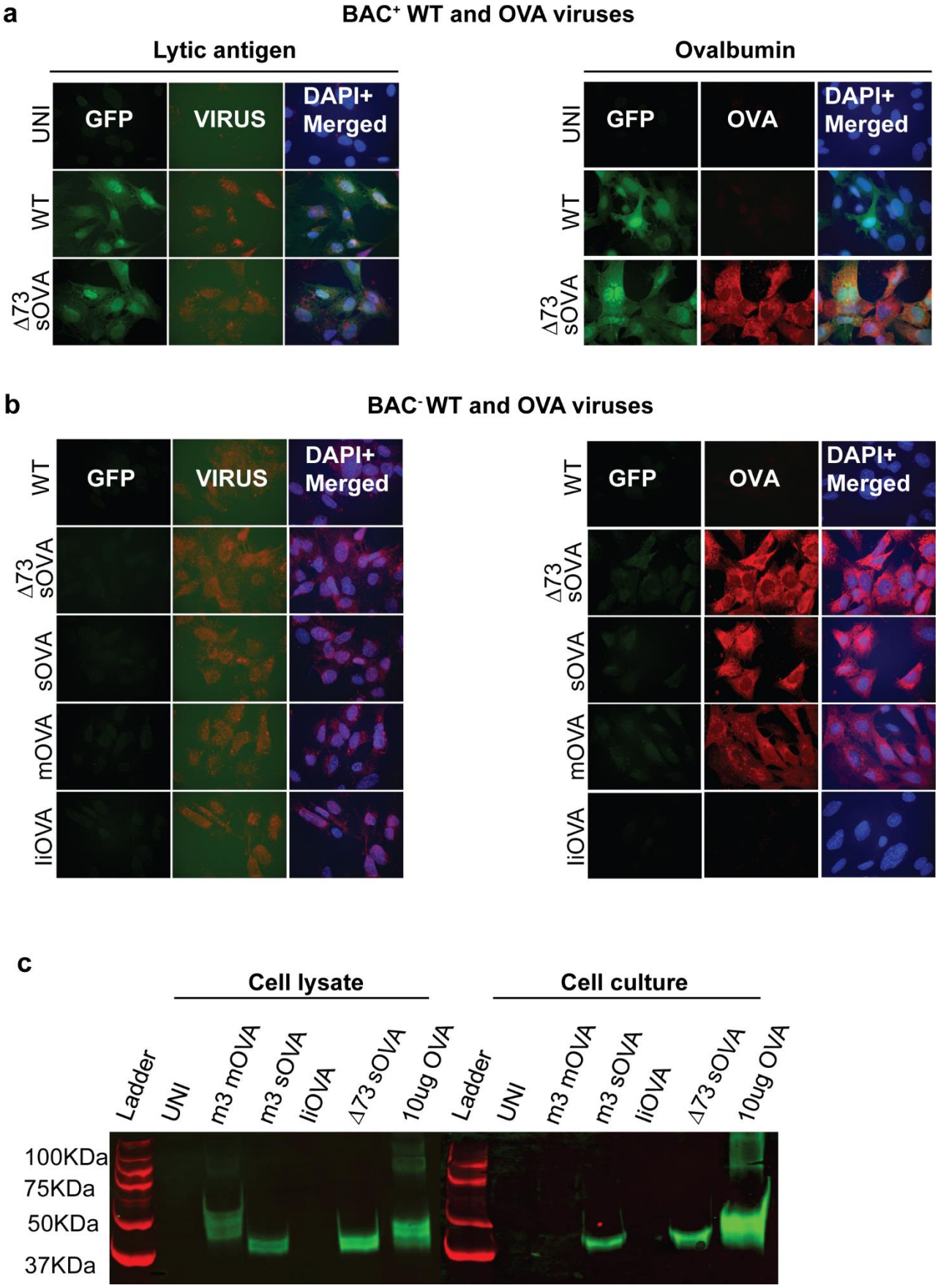
a
BAC+ WT and OVA viruses
Lytic antigen
Ovalbumin
UNI
WT
Δ73 sOVA
GFP
VIRUS
OVA
DAPI+ Merged
b
BAC- WT and OVA viruses
sOVA
mOVA
liOVA
c
Cell lysate
Cell culture
Ladder
UNI
m3 mOVA
m3 sOVA
liOVA
Δ73 sOVA
10ug OVA
100KDa
75KDa
50KDa
37KDa

Fig. 5. 3. Detection of ovalbumin in Δ73 sOVA.

a, b) MEFs were infected (MOI 1, 18 hrs) with BAC^+ or BAC^- WT, MHV-68 OVA recombinants and Δ73 sOVA. The cells were fixed, permeablised and blocked in 2%NDS/PBS and stained with rabbit anti-OVA or rabbit anti-MHV-68. Lytic antigens and ovalbumin was detected using Alexa Fluor 594 donkey anti-rabbit and DAPI to stain cell nuclei. Images were acquired using Nikon immunofluorescence microscope at 100X objective. Images are representative of 3 independent experiments. **c)** $1x10^6$ 3T3 cells were left uninfected or infected (MOI 1, 18 hrs) with MHV-68 OVA expressing viruses in 24 well plates. Cell lysate and culture media were diluted in 3X Laemmli buffer (1:1 ratio), boiled for 5 minutes at 95^{o}C and resolved on 10-12% SDS-PAGE gel. The proteins were transferred onto methanol activated PDVF membrane, blocked in 10% skim milk/PBST (1 hr, RT) and blotted using polyclonal rabbit anti-OVA in 5% skim milk/PBST (4^{o}C,18 hrs), then washed in 0.1%PBST and detected with IRDye 800CW goat anti-rabbit IgG (H+L) in 5% skim milk/PBST. A band of 43 KDa was detected. Data are representative of 3 independent experiments.

5.2.6 Characterising OVA expression and presentation using a defined CD4+ T cell assay.

I-A^d-restricted, $OVA_{323–339}$-specific DO11.10 hybridoma cells respond to ovalbumin by expressing the $OVA_{323-339}$-specific T cell receptor (Tcr). This receptor binds $OVA_{323-339}$ peptide complex presented on MHC class II (1-A^d/1-A^b) by professional antigen presenting cells (pAPCs) (167). To test $CD4^+$ T cell stimulation in the presence of infection and confirm presentation of $OVA_{323-339}$, BALB/c-3T3-C2TA and RAW-C2TA cells were either infected with WT or OVA-recombinant MHV-68 or left uninfected in the presence of $OVA_{323–339}$-specific DO11.10 hybridoma cells. Uninfected cells were incubated with ten-fold serial dilution of $OVA_{323-339}$ peptide.

In BALB/c-3T3-C2TA cells, MHV-68 mOVA provided sub-optimal stimulation to $CD4^+$ T cells that was significantly lower than 1 µM peptide control (Fig. 5.4a, $p<0.05$). MHV-68 sOVA, IiOVA and Δ73 sOVA provided no IL-2 stimulation (Fig. 5.4a). This suggests that in fibroblasts, sOVA and IiOVA infected cells are not efficient at processing and presenting $OVA_{323-339}$ to $CD4^+$ T cells to secrete IL-2.

The same experiment was repeated in RAW-C2TA. MHV-68 mOVA infected cells, provided comparable stimulation to $CD4^+$ T cells as 1 µM peptide control (Fig. 5.4b, $p>0.05$). IiOVA and Δ73 sOVA infected cells provided better stimulation to $CD4^+$ T cells than MHV-68 sOVA but were still significantly lower than 1 µM $OVA_{323-339}$ (Fig. 5.4b, $p<0.0001$). The assay however demonstrated the ability of BALB/c-3T3-C2TA and RAW-C2TA to present $OVA_{323-339}$ peptide to $I\text{-}A^d$-restricted, $OVA_{323–339}$-specific DO11.10 $CD4^+$ T cell hybridoma cells. In the context of priming, MHV-68 mOVA and IiOVA viruses provided the best stimulation than sOVA viruses in RAW-C2TA. This provides an excellent diagnostic tool in combination with immunoblotting or immunofluorescence to confirm expression of ovalbumin.

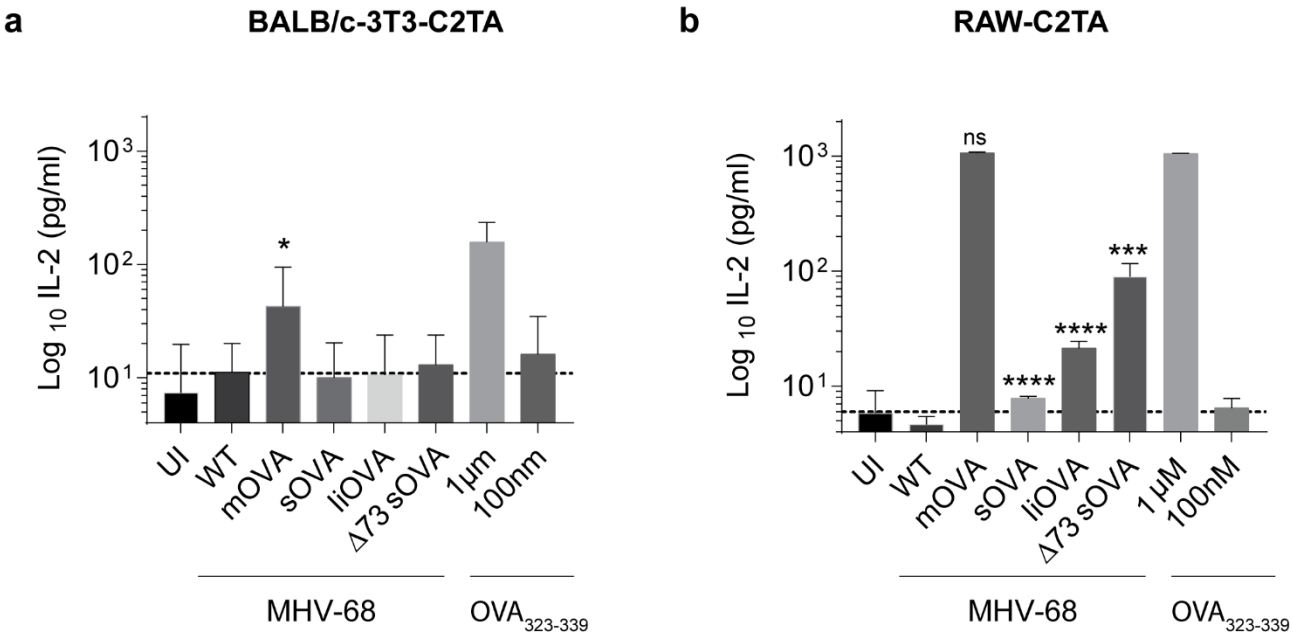

Fig. 5. 4. MHV-68 OVA viruses induce IL-2 secretion.

a) $3x10^4$ BALB/c-3T3-C2TA cells were either left uninfected or infected (MOI 0.3, 18 hrs) with WT or MHV-68 OVA in the presence of $3x10^4$ $OVA_{323-339}$ peptide $CD4^+$ T cell hybridomas. 18 hrs later, supernatants were assayed for IL-2 secretion using ELISA. **b)** $3x10^4$ RAW-C2TA cells were either left uninfected or infected (MOI 2, 72 hrs) with WT or MHV-68 OVA. $3x10^4$ $OVA_{323-339}$ peptide $CD4^+$ T cell hybridomas were then added. Uninfected cells were incubated in the presence of 10-fold serially diluted $OVA_{323-339}$. 18 hrs later, supernatants were assayed for IL-2 secretion using ELISA. Error bars show ± SEM from the mean of duplicate cultures from 3 independent experiments. Data was analysed using unpaired student 2 tailed t-test (ns, $p>0.05$; * $p<0.05$; *** $p<0.001$, **** $p<0.0001$).

5.2.7 Δ73 sOVA is dispensable for replication *in vitro*

To determine the growth kinetics of Δ73 sOVA virus, BHK-21 and RAW-C2TA cells were infected in suspension with WT or Δ73 sOVA at low MOI 0.01. The production of infectious virus was monitored over a course of seven days. At different times post infection, cells and supernatants were harvested and stored at -80ºC. Virus titer was determined by plaque assay on BHK-21 cells. Δ73 sOVA replicated to wild type levels in both cell lines (Fig. 5.5a, b).

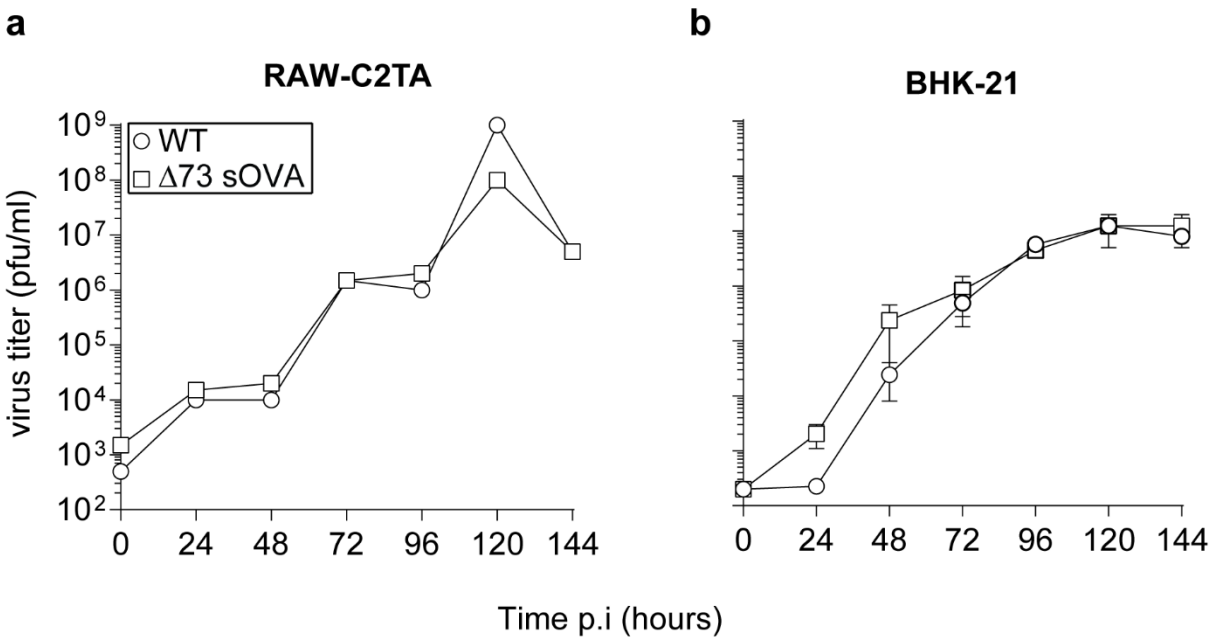

Fig. 5. 5. *In vitro* characterization of BAC⁻ Δ73 sOVA.

a, b) RAW-C2TA and BHK-21 cells were infected with BAC⁻ WT and BAC⁻ Δ73 sOVA at MOI 0.01. Cells and supernatants were harvested at different times p.i and virus titer determined by plaque assay on BHK-21 cells. Titers at 0 h represent input virus. Results are presented as log titer/ml, error bars show difference in mean between duplicate infections. Symbols represent virus per time point. Data are representative of 2 independent experiments.

5.2.8 Δ73 sOVA is severely attenuated in lymphoid organs

To determine whether there was any defect *in vivo*, 6-8 weeks old BALB/c mice were infected via the i.n route with WT or Δ73 sOVA under anaesthesia to determine virus replication in the lower respiratory tract. Infectious virus in the lungs was determined by plaque assay at seven days post infection. Δ73 sOVA replicated significantly less than wild type with a mean titer of 2.22 compared to 4.04 which was statistically significant (Fig. 5.6a, $p<0.001$). To determine whether this was consistent across different mice strains, adult C57BL/6 mice were then infected via the i.n route with or without anaesthesia with the aim of determining replication in the upper and lower respiratory tract respectively.

In the lower respiratory tract (lungs), Δ73 sOVA also replicated less than wild type with a mean titer of 2.38 compared to 4.15 of wild type which was significantly different (Fig. 5.6b, $p<0.001$). This was similar to BALB/c mice. In mediastinal lymph nodes, which drain the lungs, no preformed infectious virus was recovered from Δ73 sOVA infected mice 6 days p.i compared to WT. This was also observed at day 14 in not only the mediastinal lymph node but also the spleen of Δ73 sOVA infected mice (Fig. 5.6b).

In the upper respiratory tract (nose), Δ73 sOVA also replicated a log less than WT with a mean titer of 1.94 to 2.92 (Fig. 5.6c, $p<0.05$). In superficial cervical lymph nodes, which drain the nose, no preformed infectious virus was recovered from Δ73 sOVA infected mice 7 days p.i compared to WT (Fig. 5.6c, $p<0.001$). This was also observed at day 18, a period of lymphoproliferation in not only the superficial cervical lymph nodes but also the spleen of Δ73 sOVA infected mice (Fig. 5.6c, $p<0.001$). The observed lytic and latency replication defect of Δ73 sOVA in the lung and nose of C57BL/6 mice is consistent with published results for ORF73 mutation (149, 152). However an OFR73 null virus was found to cause latency in the spleen following i.p injection (153). This was in sharp contrast to Fowler's result that showed ORF73 frameshift and ORF73 deletion mutants were both impaired in inducing latency in the spleen 14 days post i.p injection.

a

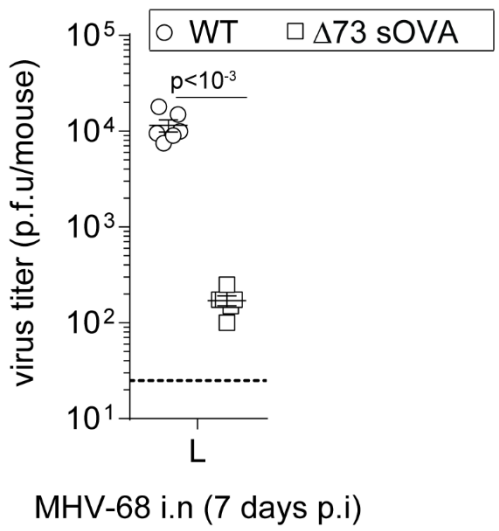

MHV-68 i.n (7 days p.i)

b

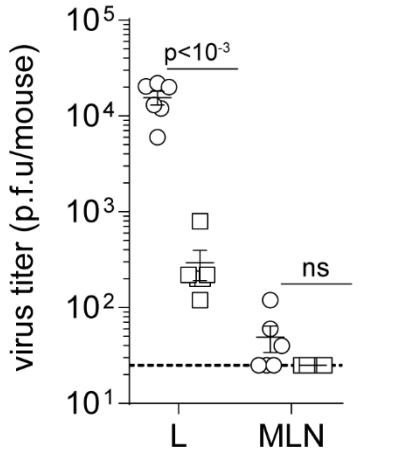

MHV-68 i.n (6 days p.i)

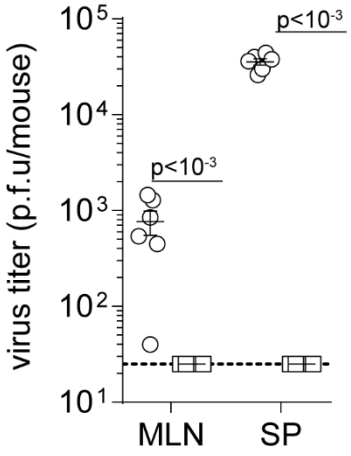

MHV-68 i.n (14 days p.i)

c

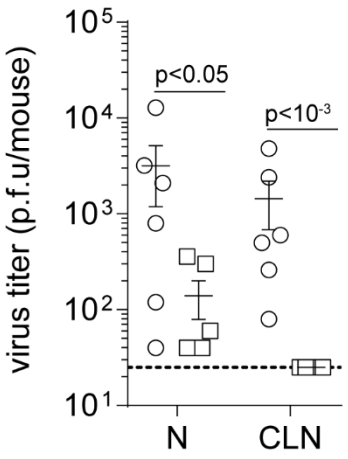

MHV-68 i.n (7 days p.i)

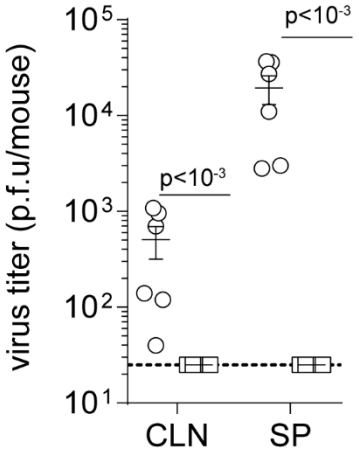

MHV-68 i.n (18 days p.i)

Fig. 5. 6. *In vivo* characterisation of Δ73 sOVA.

BALB/c in **a** and C57BL/6 in **b** and **c** mice were infected i.n with $3x10^4$ p.f.u/30µL PBS. At different times post infection, infectious virus in the nose and lung was determined by plaque assay on BHK-21 cells following a freeze and thaw cycle. Virus in MLN, SCLN and SP were detected by infectious centre assay. Each data point represents the mean of six animals and error bars show difference in titer between mice. Data was analysed using multiple student 2 tail test using Bonferroni-Dunn post-test for multiple comparisons. Horizontal dashed line denotes limit of detection. Data are representative of 2 independent experiments.

5.2.9 Δ73 sOVA virus stimulates B and $CD4^+$ T cells in BALB/c mice

5.2.9.1 Antibody responses

To determine immune responses to Δ73 sOVA, adult BALB/c mice were infected via the i.n route and sera analysed 13 days later by ELISA for MHV-68 and OVA-specific antibodies. Mice infected with Δ73 sOVA had predominately IgG responses to MHV-68, although it was significantly lower compared to IiOVA, MHV-68 mOVA and sOVA infected mice (Fig. 5.7a, $p<0.001$). IgM was still present at low levels in all infected mice except in Δ73 sOVA but not to significant levels (Fig. 5.7a, $p>0.05$). OVA-specific responses were also predominately IgG except in Δ73 sOVA where IgG levels were significantly lower compared to sera from mOVA and sOVA infected mice (Fig. 5.7b, $p<0.001$). IgM to OVA was only detected in MHV-68 mOVA infected mice but not to significant levels (Fig. 5.7b, $p>0.05$). Interestingly, no IgM or IgG to OVA was detected in IiOVA infected mice (Fig. 5.7b). This suggest that, $OVA_{323-339}$ does not provide a robust antibody response.

5.2.9.2 $CD4^+$ T IFN-γ responses

$CD4^+$ T cells isolated from the lungs, cervical lymph nodes and the spleen of MHV-68 mOVA and IiOVA, mounted robust $OVA_{323-339}$-specific $CD4^+$ T cell IFN-γ response 13 days post infection (Fig. 5.7c). However, $CD4^+$ T cells in sOVA and Δ73 sOVA infected mice were unable to secrete IFN-γ upon re-stimulation. This suggests that MHV-68 mOVA and IiOVA stimulate strong endogenous $OVA_{323-339}$ $CD4^+$ T cell responses while the sOVA constructs are less effective consistent with published results (160).

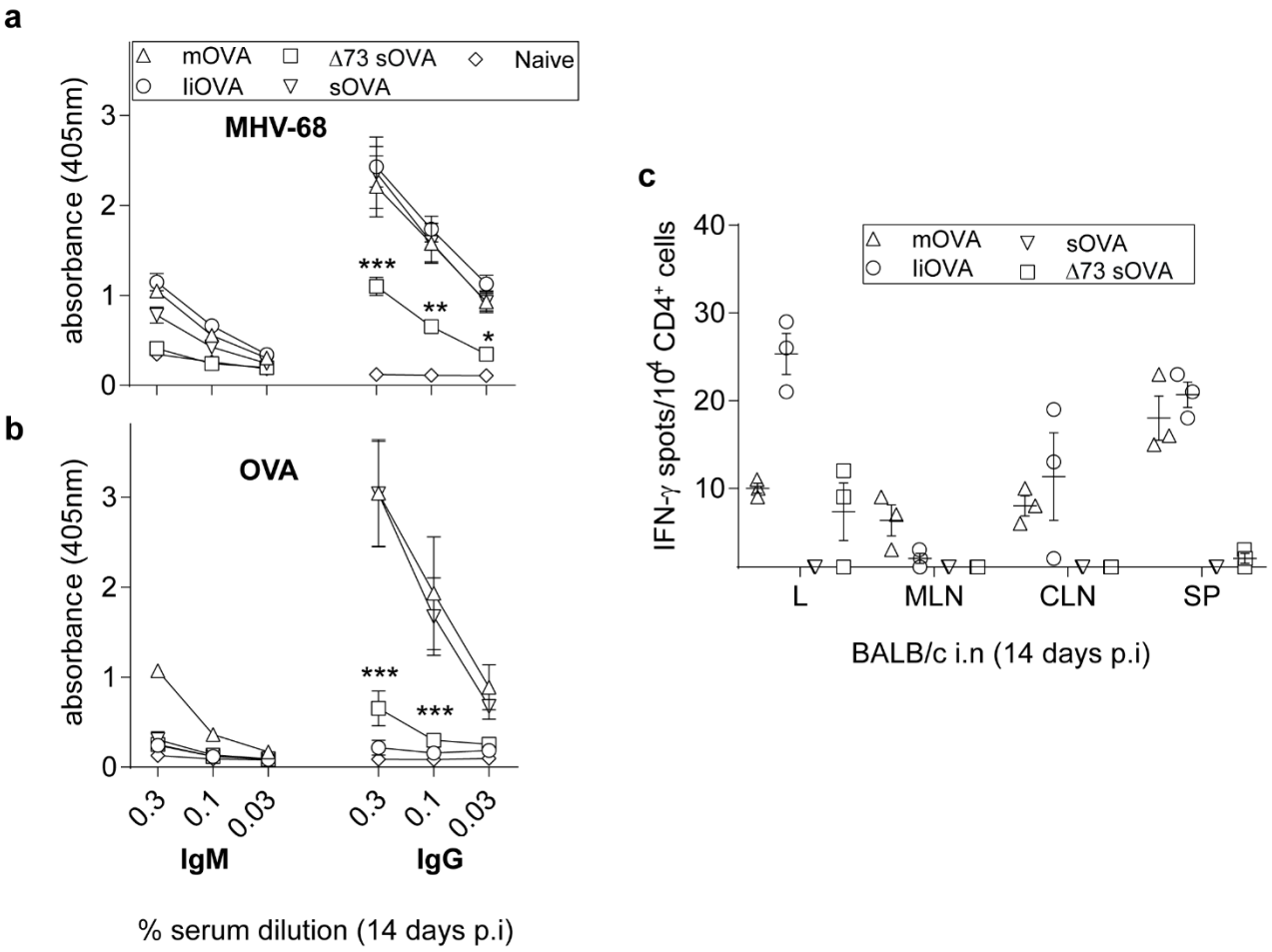

Fig. 5. 7. Δ73 sOVA induces antibody and IFN-γ in BALB/c mice.

BALB/c mice were infected i.n with MHV-68 recombinant viruses' mOVA, sOVA, Δ73 sOVA and IiOVA at $3x10^4$ p.f.u/30µL PBS. 14 days post infection sera, were analysed for virus **a** and OVA **b** specific IgM and IgG responses by ELISA. Error bars show difference in mean (n=3 per group). Data was analysed using unpaired student 2 tailed t-test (ns, $p>0.05$; * $p<0.05$; *** $p<0.001$, **** $p<0.0001$). **c)** The frequency of IFN-γ-producing $CD4^+$ T cells from pooled L, MLN, SCLN and SP upon stimulation with uninfected splenocytes in the presence of 5 µM $OVA_{323-339}$ was determined by ELISPOT. Each symbol represents the number of spots per $3x10^4$ effector cells (n=3 per group). Data are representative of 2 independent experiments.

5.3 Discussion

In this thesis chapter, the construction of Δ73 sOVA is described with the aim of addressing the role of ORF73 in modulating $CD4^+$ T cell responses. The results presented show no observed replication defect in either BHK-21 or RAW-C2TA cells *in vitro* consistent with published data, particularly on BHK-21 (148, 149, 152). ORF73 disruption has however been shown to cause a replication defect in primary and in immortalised murine embryonic fibroblasts and NIH-3T3 cells (148, 222). Whether Δ73 sOVA shows this replication defect remains to be determined. Nevertheless, this suggests a cell type replication defect, which could be attributed to a difference in cell cycle (148). *In vivo*, there was a 1 to 2 log replication defect in the lungs of BALB/c and in C57BL/6 mice as previously reported (152). In the upper respiratory tract (nose) of C57BL/6 mice, an ORF73 replication defect was also observed. This suggests that, i) ORF73 could be dispensable for replication in certain cell types *in vitro* and *in vivo* particularly in mucosal sites during lytic replication, ii) modulates innate immune responses during lytic infection for example neutrophil recruitment, tumour necrosis factor alpha and interferon signalling or iii) restricts $CD4^+$ T cell responses via unknown mechanism during latency (148, 152).

In the lymph nodes and spleen, Δ73 sOVA was severely attenuated in reactivating from latency at early (day 6 or 7) and late (day 14 or 18) times during infection. Whether Δ73 sOVA infected cells in these organs remains to be determined. ORF73 deletion mutant was however found to cause an early splenic infection that was undetectable by day 14 following i.p infection. The virus was able to infect cells in the spleen but failed to establish latency and colonise germinal centre B cells (149). Thus, the observed Δ73 sOVA defect is consistent with the predicted role of ORF73 in plasmid episome maintenance (153) and in induction of latency and host colonisation (149, 152, 153). In a study by *Paden et al., 2010*, ORF73 deficient virus was found to establish latency but failed to reactivate in the spleen of C57BL/6 mice following i.p infection. The difference in establishment of latency could be limited by either how the ORF73 deficient viruses were generated or the assays used to determine latency from reactivation. What is undisputable is the failure of ORF73 deficient viruses to reactivate and persist regardless of the route of infection or mouse strain used. This implies that, viral genome in actively dividing infected cells is lost in ORF73 deficient infected cells.

Preliminary MHV-68 specific antibody response to sOVA, MHV-68 mOVA and IiOVA, which all have intact ORF73, showed elevated levels of IgG to MHV-68. This was more evident when OVA-specific IgG response was measured. The low level IgG response could be a reflection of viral load. Another possible reason could be limited number of persistently infected antigen presenting dendritic or B cells in the lymph nodes or the spleen even if $CD4^+$ T cells in the lungs are primed (224). This was illustrated in a study by *Fowler et al., 2003* who found no viral genome positive cells in the spleen of ORF73 deficient infected mice (149, 152). The failure to establish germinal center B cell infection and expansion suggests affinity maturation and plasma cell differentiation is impaired. In C57BL/6 mice however, there was no difference in germinal centre formation between wild type and ORF73 deficient virus (153) which argues against ORF73 involvement in germinal center formation in establishment of latency . Nevertheless, how ORF73 affects antibody response is still not clear.

Another interesting feature of Δ73 sOVA virus was the ineffective stimulation of $OVA_{323-339}$-specific $CD4^+$ T cells in BALB/c mice. MHV-68 mOVA and IiOVA provided robust $OVA_{323-339}$ specific $CD4^+$ T cell IFN-γ response compared to the sOVA viruses as expected. *In vitro*, MHV-68 mOVA virus was more effective at stimulating $CD4^+$ T cell hybridomas specific for the $OVA_{323-339}$ peptide to secrete IL-2 than the IiOVA and the sOVA constructs. Thus, it is plausible that, the form of antigen limits stimulation of $CD4^+$ T.

To understand in detail how ORF73 would affect $CD4^+$ T cell response, a virus specific $CD4^+$ T IFN-γ response would be appropriate. Another effective control would be to generate Δ73 expressing membrane bound ovalbumin (Δ73 mOVA) as a direct comparison to MHV-68 mOVA. This would provide a powerful tool to study $CD4^+$ T cell response during lytic infection.

Δ73 sOVA was made to take advantage of the ovalbumin system and track $OVA_{323-339}$-specific KJ1-26 $CD4^+$ T cells adoptively transferred in BALB/c mice. However, $CD4^+$ T cells in DO11.10 transgenic mice were found to be heterogeneous to the clonotypic marker KJ1-26 for $OVA_{323-339}$-specific $CD4^+$ T cells (reviewed in chapter 3). This made tracking $OVA_{323-339}$-specific $CD4^+$ T cells *in vivo* difficult. The data presented in this thesis chapter nevertheless is consistent with the predicted role of ORF73 in induction of latency and host colonisation particularly in lymphoid sites. It provides a model in which OVA-

specific $CD4^+$ T cells can be studied to understand why $CD4^+$ T cells are not effective at controlling lytic infection. It could also provide further insight into innate immunity and how adaptive immune response is shaped in the face of immune evasion. With the unexpected antibody profile to MHV-68 and OVA in Δ73 sOVA infected mice, dissecting how ORF73 expression alters antibody response and whether this is $CD4^+$ T cell dependent could provide valuable insight into vaccination.

CHAPTER 6: GENERAL DISCUSSION AND FUTURE DIRECTIONS

6.1 MHV-68 vaccination restricts lytic infection

In this thesis, $CD4^+$ T cell directed vaccine against MHV-68 was trialled using recombinant MCMV mOVA virus as a live attenuated vaccine. The results showed, lytically primed OVA-specific $CD4^+$ T cells reduced lytic infection via IFN-γ and significantly reduced splenomegaly when $OVA_{323-339}$ peptide was expressed in tandem with the ORF73 promotor. This implied that, during latency, $CD4^+$ T cells can engage infected cells. Why then, don't these $OVA_{323-339}$-specific $CD4^+$ T cells restrict latency when ovalbumin is expressed under the lytic promoter M3? It is possible that M3 driven ovalbumin is below the threshold of detection when virus replication is shut off. Consequently, infected cells become undetectable by circulating memory $CD4^+$ T cells. Alternatively, the small subset of primed circulating memory $CD4^+$ T cells may not have cytolytic activity against predominately latently infected cells that are probably not presenting the $OVA_{323-339}$ epitope (160).

An attempt to track $OVA_{323-339}$-specific $CD4^+$ T cells using DO11.10 transgenic mice was unsuccessful. This would have provided an excellent opportunity to understand why during latency $OVA_{323-339}$ specific $CD4^+$ T cells become ineffective. Another setback experienced in tracking and mapping out the migration patterns of $OVA_{323-339}$-specific $CD4^+$ T cells was MHC II tetramers. None of the MHC II tetramers worked against different peptide registrars derived from $OVA_{323-339}$ on $CD4^+$ T cells isolated from DO11.10 transgenic mice or in MCMV mOVA vaccinated mice (data not shown). MHC II tetramers have inherent problems associated with low T-cell receptor (TCR)–MHC avidity and or low frequency of $CD4^+$ T cells specific to the peptide (225-227). The latter seems unlikely in a transgenic or OVA primed mouse than in a naïve mice. As MHC II tetramer reagents improve, or new technologies such as recombinant artificial antigen presenting cells (226) or dextramers (228) emerge, identifying what subset of primed $OVA_{323-339}$-specific $CD4^+$ T cells drive or restrict B cell lymphoproliferation and splenomegaly, and when this occurs would be key to understanding how MHV-68 exploits $CD4^+$ T cells.

The vaccination results also demonstrated that $OVA_{254-267}$ primed $CD8^+$ T cells can effectively control MHV-68 lytic infection (7 days) and acute latent infection (13 to18 days) but failed during persistent infection (21 to 100 days). This effect was strain dependent. BALB/c and F1 mice failed to control lytic and acute latent infection. Other model systems, using MHV-68 lytic epitopes p65 (139) and latent epitopes M2 (140), targeting $CD8^+$ T cells, have all yielded similar results, that is early reduction in virus load but no change in

persistent infection as infection progresses to day 21 or 30. Antibody induced protection was also strain dependent. BALB/c mice given recombinant vaccinia virus expressing gH/gL effectively controlled lytic and acute latent infection while C75BL/6 mice failed. This perhaps shows that, gH/gL $CD4^+$ T cell specific epitopes are present in BALB/c and not in C57BL/6 mice.

Human vaccine trials using gp350 has shown that, targeting cell surface glycoprotein gp350 to prevent B cell infection and limit EBV disease is not an effective strategy at controlling infection. MHV-68 gp150, a positional homologue of EBV gp350 showed similar outcome in mice (138). The reduction in infectious mononucleosis observed with the gp350 vaccine has however provided an opportunity to model a vaccine that can restrict the severity of IM in infected young adults. This is progress. However, the challenge still remains to developing an effective EBV vaccine that can control infection. Identifying other viral genes or combinations of viral epitopes to vaccinate with requires further research.

The use of cytomegaloviruses as potential vaccine vectors against persistent viruses like HIV is a recent development. In the macaque model for AIDS, Rhesus CMV provided robust SIV gag-specific $CD8^+$ T cell response against a gag expressing RhCMV in CMV^+ macaques. The ability to re-infect CMV^+ animals and induce potent SIV-specific $CD4^+$ and $CD8^+$ T cell responses with complete protection in 50% of vaccinated rhesus macaques for over 12 months despite continual virus challenge (145, 146). This showed that CMV as vaccine vectors have potential. Subsequently, it was shown that RhCMV induced unconventional $CD8^+$ T cell epitope targeting via MHC-E that was not replicated by any other conventional vaccine vector or SIV infection itself (146, 147). Re-infection of CMV^+ macaques however raises potential questions about immunosuppression. Similarly, in this thesis, MCMV degraded MHC II in antigen presenting cells to protect infected cells from $CD4^+$ T cell engagement. This restricted $CD4^+$ T cell stimulation *in vitro*. How this affects vaccination is rather difficult to decipher. However, it is tempting to speculate that $CD4^+$ T cell priming would be impaired particularly if infected antigen presenting cells endogenously present peptide.

CHAPTER 7: REFERENCES

1. **Young LS, Rickinson AB.** 2004. Epstein-Barr virus: 40 years on. Nat Rev Cancer **4:**757-768.
2. **Cohen JI.** 2000. Epstein–Barr Virus Infection. New England Journal of Medicine **343:**481-492.
3. **Young LS, Dawson CW.** 2014. Epstein-Barr virus and nasopharyngeal carcinoma. Chinese Journal of Cancer **33:**581-590.
4. **Cohen JI.** 2015. Epstein-barr virus vaccines. Clin Trans Immunol **4:**e32.
5. **Henle G, Henle W, Diehl V.** 1968. Relation of Burkitt's tumor-associated herpes-ytpe virus to infectious mononucleosis. Proceedings of the National Academy of Sciences of the United States of America **59:**94-101.
6. **Thompson MP, Kurzrock R.** 2004. Epstein-Barr Virus and Cancer. Clinical Cancer Research **10:**803.
7. **Epstein MA, Achong BG.** 1973. The EB virus. Annual review of microbiology **27:**413-436.
8. **Epstein MA, Probert M.** 1973. The possible significance of morphological transformation of human fibroblasts by EB virus in vitro. Bibliotheca haematologica **39:**444-447.
9. **Kanegane H, Nomura K, Miyawaki T, Tosato G.** 2002. Biological aspects of Epstein–Barr virus (EBV)-infected lymphocytes in chronic active EBV infection and associated malignancies. Critical Reviews in Oncology/Hematology **44:**239-249.
10. **Odumade OA, Hogquist KA, Balfour HH, Jr.** 2011. Progress and problems in understanding and managing primary Epstein-Barr virus infections. Clin Microbiol Rev **24:**193-209.
11. **Okano M, Thiele GM, Davis JR, Grierson HL, Purtilo DT.** 1988. Epstein-Barr virus and human diseases: recent advances in diagnosis. Clin Microbiol Rev **1:**300-312.
12. **Balfour HH, Jr.** 2007. Epstein-Barr virus vaccine for the prevention of infectious mononucleosis--and what else? J Infect Dis **196:**1724-1726.
13. **Balfour HH, Odumade OA, Schmeling DO, Mullan BD, Ed JA, Knight JA, Vezina HE, Thomas W, Hogquist KA.** 2013. Behavioral, Virologic, and Immunologic Factors Associated With Acquisition and Severity of Primary Epstein–Barr Virus Infection in University Students. Journal of Infectious Diseases **207:**80-88.
14. **Penn I, Hammond W, Brettschneider L, Starzl TE.** 1969. Malignant Lymphomas in Transplantation Patients. Transplantation proceedings **1:**106-112.

15. **Taylor AL, Marcus R, Bradley JA.** 2005. Post-transplant lymphoproliferative disorders (PTLD) after solid organ transplantation. Critical Reviews in Oncology/Hematology **56:**155-167.
16. **Taylor AL, Watson CJE, Bradley JA.** 2005. Immunosuppressive agents in solid organ transplantation: Mechanisms of action and therapeutic efficacy. Critical Reviews in Oncology/Hematology **56:**23-46.
17. **Hoshida Y, Li T, Dong Z, Tomita Y, Yamauchi A, Hanai J, Aozasa K.** 2001. Lymphoproliferative disorders in renal transplant patients in Japan. International journal of cancer **91:**869-875.
18. **Kuppers R.** 2003. B cells under influence: transformation of B cells by Epstein-Barr virus. Nature reviews. Immunology **3:**801-812.
19. **Capello D, Cerri M, Muti G, Berra E, Oreste P, Deambrogi C, Rossi D, Dotti G, Conconi A, Viganò M, Magrini U, Ippoliti G, Morra E, Gloghini A, Rambaldi A, Paulli M, Carbone A, Gaidano G.** 2003. Molecular histogenesis of posttransplantation lymphoproliferative disorders. Blood **102:**3775-3785.
20. **Preiksaitis JK.** 2004. New Developments in the Diagnosis and Management of Posttransplantation Lymphoproliferative Disorders in Solid Organ Transplant Recipients. Clinical Infectious Diseases **39:**1016-1023.
21. **Nalesnik MA.** 2001. The diverse pathology of post-transplant lymphoproliferative disorders: the importance of a standardized approach. Transplant Infectious Disease **3:**88-96.
22. **Landais E, Saulquin X, Houssaint E.** 2005. The human T cell immune response to Epstein-Barr virus. The International journal of developmental biology **49:**285-292.
23. **Elstrom RL, Andreadis C, Aqui NA, Ahya VN, Bloom RD, Brozena SC, Olthoff KM, Schuster SJ, Nasta SD, Stadtmauer EA, Tsai DE.** 2006. Treatment of PTLD with rituximab or chemotherapy. American journal of transplantation : official journal of the American Society of Transplantation and the American Society of Transplant Surgeons **6:**569-576.
24. **Niedobitek G, Hamiltondutoit S, Herbst H, Finn T, Vetner M, Pallesen G, Stein H.** 1989. Identification of Epstein-Barr Virus-Infected Cells in Tonsils of Acute Infectious-Mononucleosis by Insitu Hybridization. Human Pathology **20:**796-799.
25. **Klein E, Ernberg I, Masucci MG, Szigeti R, Wu YT, Masucci G, Svedmyr E.** 1981. T-Cell Response to B-Cells and Epstein-Barr Virus Antigens in Infectious Mononucleosis. Cancer Research **41:**4210.

26. **Fishman JA.** 2013. Overview: cytomegalovirus and the herpesviruses in transplantation. American journal of transplantation : official journal of the American Society of Transplantation and the American Society of Transplant Surgeons **13 Suppl 3:**1-8; quiz 8.
27. **Epstein MA, Achong BG, Barr YM.** VIRUS PARTICLES IN CULTURED LYMPHOBLASTS FROM BURKITT'S LYMPHOMA. The Lancet **283:**702-703.
28. **Burkitt D.** 1958. A sarcoma involving the jaws in african children. British Journal of Surgery **46:**218-223.
29. **Brady G, MacArthur GJ, Farrell PJ.** 2007. Epstein–Barr virus and Burkitt lymphoma. Journal of Clinical Pathology **60:**1397-1402.
30. **Zajac-Kaye M, Gelmann EP, Levens D.** 1988. A point mutation in the c-myc locus of a Burkitt lymphoma abolishes binding of a nuclear protein. Science **240:**1776.
31. **Blum KA, Lozanski G, Byrd JC.** 2004. Adult Burkitt leukemia and lymphoma. Blood **104:**3009.
32. **van den Bosch CA.** 2004. Is endemic Burkitt's lymphoma an alliance between three infections and a tumour promoter? The Lancet Oncology **5:**738-746.
33. **Jaffe ES.** 2001. World Health Organization classification of Tumors. Pathology and genetics of Tumours of hematopoietic and lymphoid tissues.
34. **Carbone A.** 2003. Emerging pathways in the development of AIDS-related lymphomas. The Lancet Oncology **4:**22-29.
35. **Lazzi S, Ferrari F, Nyongo A, Palummo N, De Milito A, Zazzi M, Leoncini L, Luzi P, Tosi P.** 1998. HIV-associated malignant lymphomas in Kenya (Equatorial Africa). Human Pathology **29:**1285-1289.
36. **Old LJ, Boyse EA, Oettgen HF, Harven ED, Geering G, Williamson B, Clifford P.** 1966. PRECIPITATING ANTIBODY IN HUMAN SERUM TO AN ANTIGEN PRESENT IN CULTURED BURKITT'S LYMPHOMA CELLS. Proceedings of the National Academy of Sciences of the United States of America **56:**1699-1704.
37. **de Schryver A, Friberg S, Klein G, Henle W, Henle G, de-Thé G, Clifford P, Ho HC.** 1969. Epstein–Barr virus-associated antibody patterns in carcinoma of the post-nasal space. Clinical and Experimental Immunology **5:**443-459.
38. **Pathmanathan R, Prasad U, Chandrika G, Sadler R, Flynn K, Raab-Traub N.** 1995. Undifferentiated, nonkeratinizing, and squamous cell carcinoma of the nasopharynx. Variants of Epstein-Barr virus-infected neoplasia. The American Journal of Pathology **146:**1355-1367.

39. **Wenig BM.** 1999. Nasopharyngeal carcinoma. Annals of Diagnostic Pathology **3:**374-385.
40. **Wildeman MA, Fles R, Herdini C, Indrasari RS, Vincent AD, Tjokronagoro M, Stoker S, Kurnianda J, Karakullukcu B, Taroeno-Hariadi KW, Hamming-Vrieze O, Middeldorp JM, Hariwiyanto B, Haryana SM, Tan IB.** 2013. Primary Treatment Results of Nasopharyngeal Carcinoma (NPC) in Yogyakarta, Indonesia. PLOS ONE **8:**e63706.
41. **Jeyakumar A, Brickman TM, Jeyakumar A, Doerr T.** 2006. Review of nasopharyngeal carcinoma. Ear, nose, & throat journal **85:**168-170, 172-163, 184.
42. **Parkin DM, Muir CS.** 1992. Cancer Incidence in Five Continents. Comparability and quality of data. IARC scientific publications**:**45-173.
43. **Shanmugaratnam K, Sobin LH.** 1993. The World Health Organization histological classification of tumours of the upper respiratory tract and ear. A commentary on the second edition. Cancer **71:**2689-2697.
44. **Henle G, Henle W.** 1976. Epstein-barr virus-specific IgA serum antibodies as an outstanding feature of nasopharyngeal carcinoma. International journal of cancer **17:**1-7.
45. **Zhang L, Chen Q-Y, Liu H, Tang L-Q, Mai H-Q.** 2013. Emerging treatment options for nasopharyngeal carcinoma. Drug Design, Development and Therapy **7:**37-52.
46. **Lee AWM, Lin JC, Ng WT.** 2012. Current Management of Nasopharyngeal Cancer. Seminars in Radiation Oncology **22:**233-244.
47. **Burke AP, Yen TS, Shekitka KM, Sobin LH.** 1990. Lymphoepithelial carcinoma of the stomach with Epstein-Barr virus demonstrated by polymerase chain reaction. Modern pathology : an official journal of the United States and Canadian Academy of Pathology, Inc **3:**377-380.
48. **Min KW, Holmquist S, Peiper SC, O'Leary TJ.** 1991. Poorly differentiated adenocarcinoma with lymphoid stroma (lymphoepithelioma-like carcinomas) of the stomach. Report of three cases with Epstein-Barr virus genome demonstrated by the polymerase chain reaction. American journal of clinical pathology **96:**219-227.
49. **Akiba S, Koriyama C, Herrera-Goepfert R, Eizuru Y.** 2008. Epstein-Barr virus associated gastric carcinoma: Epidemiological and clinicopathological features. Cancer Science **99:**195-201.
50. **Murphy G, Pfeiffer R, Camargo MC, Rabkin CS.** 2009. Meta-analysis Shows That Prevalence of Epstein-Barr Virus-Positive Gastric Cancer Differs Based on Sex and Anatomic Location. Gastroenterology **137:**824-833.

51. **Fukayama M, Ushiku T.** 2011. Epstein-Barr virus-associated gastric carcinoma. Pathology - Research and Practice **207:**529-537.
52. **Marshall BJ, Warren JR.** 1984. Unidentified curved bacilli in the stomach of patients with gastritis and peptic ulceration. Lancet **1:**1311-1315.
53. **Parsonnet J, Friedman GD, Vandersteen DP, Chang Y, Vogelman JH, Orentreich N, Sibley RK.** 1991. Helicobacter pylori Infection and the Risk of Gastric Carcinoma. New England Journal of Medicine **325:**1127-1131.
54. **Operskalski EA, Visscher BR, Malmgren RM, Detels R.** 1989. A case-control study of multiple sclerosis. Neurology **39:**825-829.
55. **Bray P, W Culp K, McFarlin D, S Panitch H, D Torkelson R, P Schlight J.** 1992. Demyelinating disease after neurologically complicated Epstein-Barr virus infection, vol. 42.
56. **Ascherio A, Munch M.** 2000. Epstein-Barr virus and multiple sclerosis. Epidemiology **11:**220-224.
57. **Ascherio A, Munger KL, Lennette ET, et al.** 2001. Epstein-barr virus antibodies and risk of multiple sclerosis: A prospective study. JAMA **286:**3083-3088.
58. **Levin LI, Munger KL, Rubertone MV, et al.** 2005. Temporal relationship between elevation of epstein-barr virus antibody titers and initial onset of neurological symptoms in multiple sclerosis. JAMA **293:**2496-2500.
59. **Thacker EL, Mirzaei F, Ascherio A.** 2006. Infectious mononucleosis and risk for multiple sclerosis: a meta-analysis. Annals of neurology **59:**499-503.
60. **Tselis A.** 2012. Epstein-Barr virus cause of multiple sclerosis. Current opinion in rheumatology **24:**424-428.
61. **Fingeroth JD, Weis JJ, Tedder TF, Strominger JL, Biro PA, Fearon DT.** 1984. Epstein-Barr virus receptor of human B lymphocytes is the C3d receptor CR2. Proceedings of the National Academy of Sciences **81:**4510-4514.
62. **Gerber P, Lucas S, Nonoyama M, Perlin E, Goldstein L.** 1972. ORAL EXCRETION OF EPSTEIN-BARR VIRUS BY HEALTHY SUBJECTS AND PATIENTS WITH INFECTIOUS MONONUCLEOSIS. The Lancet **300:**988-989.
63. **Sixbey J, Lemon S, Pagano J.** 1986. A SECOND SITE FOR EPSTEIN-BARR VIRUS SHEDDING: THE UTERINE CERVIX. The Lancet **328:**1122-1124.
64. **Israele V, Shirley P, Sixbey JW.** 1991. Excretion of the Epstein-Barr virus from the genital tract of men. Journal of Infectious diseases **163:**1341-1343.

65. **Crawford DH, Swerdlow AJ, Higgins C, McAulay K, Harrison N, Williams H, Britton K, Macsween KF.** 2002. Sexual History and Epstein-Barr Virus Infection. The Journal of Infectious Diseases **186:**731-736.

66. **Crawford DH, Macsween KF, Higgins CD, Thomas R, McAulay K, Williams H, Harrison N, Reid S, Conacher M, Douglas J, Swerdlow AJ.** 2006. A Cohort Study among University Students: Identification of Risk Factors for Epstein-Barr Virus Seroconversion and Infectious Mononucleosis. Clinical Infectious Diseases **43:**276-282.

67. **Rickinson AB, Long HM, Palendira U, Münz C, Hislop AD.** Cellular immune controls over Epstein–Barr virus infection: new lessons from the clinic and the laboratory. Trends in Immunology **35:**159-169.

68. **Babcock GJ, Decker LL, Freeman RB, Thorley-Lawson DA.** 1999. Epstein-Barr Virus–Infected Resting Memory B Cells, Not Proliferating Lymphoblasts, Accumulate in the Peripheral Blood of Immunosuppressed Patients. The Journal of experimental medicine **190:**567-576.

69. **H Wolf HzH, V Becker.** 1973. EB Viral Genomes in Epithelial Nasopharyngeal Carcinoma Cells. nature new biology **244:**245-247.

70. **Tan LC, Mowat AG, Fazou C, Rostron T, Roskell H, Dunbar PR, Tournay C, Romagné F, Peyrat M-A, Houssaint E, Bonneville M, Rickinson AB, McMichael AJ, Callan MFC.** 2000. Specificity of T cells in synovial fluid: high frequencies of CD8(+) T cells that are specific for certain viral epitopes. Arthritis Research **2:**154-164.

71. **Callan MFC, Tan L, Annels N, Ogg GS, Wilson JDK, O'Callaghan CA, Steven N, McMichael AJ, Rickinson AB.** 1998. Direct Visualization of Antigen-specific CD8(+)T Cells during the Primary Immune Response to Epstein-Barr Virus In Vivo. The Journal of experimental medicine **187:**1395-1402.

72. **Steven NM, Annels NE, Kumar A, Leese AM, Kurilla MG, Rickinson AB.** 1997. Immediate Early and Early Lytic Cycle Proteins Are Frequent Targets of the Epstein-Barr Virus–induced Cytotoxic T Cell Response. The Journal of experimental medicine **185:**1605-1618.

73. **Hislop AD, Annels NE, Gudgeon NH, Leese AM, Rickinson AB.** 2002. Epitope-specific Evolution of Human CD8⁺ T Cell Responses from Primary to Persistent Phases of Epstein-Barr Virus Infection. The Journal of experimental medicine **195:**893-905.

74. **Hislop AD, Ressing ME, van Leeuwen D, Pudney VA, Horst D, Koppers-Lalic D, Croft NP, Neefjes JJ, Rickinson AB, Wiertz EJHJ.** 2007. A CD8(+) T cell immune evasion protein specific to Epstein-Barr virus and its close relatives in Old World primates. The Journal of experimental medicine **204:**1863-1873.

75. **Rowe M, Glaunsinger B, van Leeuwen D, Zuo J, Sweetman D, Ganem D, Middeldorp J, Wiertz EJHJ, Ressing ME.** 2007. Host shutoff during productive Epstein–Barr virus infection is mediated by BGLF5 and may contribute to immune evasion. Proceedings of the National Academy of Sciences of the United States of America **104:**3366-3371.

76. **Zuo J, Currin A, Griffin BD, Shannon-Lowe C, Thomas WA, Ressing ME, Wiertz EJHJ, Rowe M.** 2009. The Epstein-Barr Virus G-Protein-Coupled Receptor Contributes to Immune Evasion by Targeting MHC Class I Molecules for Degradation. PLoS Pathogens **5:**e1000255.

77. **Rocha B, Tanchot C.** 2004. Towards a cellular definition of CD8+ T-cell memory: the role of CD4+ T-cell help in CD8+ T-cell responses. Current Opinion in Immunology **16:**259-263.

78. **Khanolkar A, Yagita H, Cannon MJ.** 2001. Preferential Utilization of the Perforin/Granzyme Pathway for Lysis of Epstein–Barr Virus-Transformed Lymphoblastoid Cells by Virus-Specific CD4+ T Cells. Virology **287:**79-88.

79. **Haigh TA, Lin X, Jia H, Hui EP, Chan ATC, Rickinson AB, Taylor GS.** 2008. EBV Latent Membrane Proteins (LMPs) 1 and 2 as Immunotherapeutic Targets: LMP-Specific CD4⁺ Cytotoxic T Cell Recognition of EBV-Transformed B Cell Lines. The Journal of Immunology **180:**1643-1654.

80. **Khanna R, Burrows SR, Steigerwald-Mullen PM, Thomson SA, Kurilla MG, Moss DJ.** 1995. Isolation of Cytotoxic T Lymphocytes from Healthy Seropositive Individuals Specific for Peptide Epitopes from Epstein–Barr Virus Nuclear Antigen 1: Implications for Viral Persistence and Tumor Surveillance1. Virology **214:**633-637.

81. **Amyes E, Hatton C, Montamat-Sicotte D, Gudgeon N, Rickinson AB, McMichael AJ, Callan MFC.** 2003. Characterization of the CD4(+) T Cell Response to Epstein-Barr Virus during Primary and Persistent Infection. The Journal of experimental medicine **198:**903-911.

82. **Precopio ML, Sullivan JL, Willard C, Somasundaran M, Luzuriaga K.** 2003. Differential Kinetics and Specificity of EBV-Specific CD4⁺

and CD8⁺ T Cells During Primary Infection. The Journal of Immunology **170:**2590.

83. **Gu SY, Huang TM, Ruan L, Miao YH, Lu H, Chu CM, Motz M, Wolf H.** 1995. First EBV vaccine trial in humans using recombinant vaccinia virus expressing the major membrane antigen. Developments in biological standardization **84:**171-177.
84. **Sokal EM, Hoppenbrouwers K, Vandermeulen C, Moutschen M, Leonard P, Moreels A, Haumont M, Bollen A, Smets F, Denis M.** 2007. Recombinant gp350 vaccine for infectious mononucleosis: a phase 2, randomized, double-blind, placebo-controlled trial to evaluate the safety, immunogenicity, and efficacy of an Epstein-Barr virus vaccine in healthy young adults. J Infect Dis **196:**1749-1753.
85. **Moutschen M, Leonard P, Sokal EM, Smets F, Haumont M, Mazzu P, Bollen A, Denamur F, Peeters P, Dubin G, Denis M.** 2007. Phase I/II studies to evaluate safety and immunogenicity of a recombinant gp350 Epstein-Barr virus vaccine in healthy adults. Vaccine **25:**4697-4705.
86. **Rees L, Tizard EJ, Morgan AJ, Cubitt WD, Finerty S, Oyewole-Eletu TA, Owen K, Royed C, Stevens SJ, Shroff RC, Tanday MK, Wilson AD, Middeldorp JM, Amlot PL, Steven NM.** 2009. A phase I trial of epstein-barr virus gp350 vaccine for children with chronic kidney disease awaiting transplantation. Transplantation **88:**1025-1029.
87. **Elliott SL, Suhrbier A, Miles JJ, Lawrence G, Pye SJ, Le TT, Rosenstengel A, Nguyen T, Allworth A, Burrows SR, Cox J, Pye D, Moss DJ, Bharadwaj M.** 2008. Phase I trial of a CD8+ T-cell peptide epitope-based vaccine for infectious mononucleosis. Journal of virology **82:**1448-1457.
88. **Kirschner AN, Lowrey AS, Longnecker R, Jardetzky TS.** 2007. Binding-Site Interactions between Epstein-Barr Virus Fusion Proteins gp42 and gH/gL Reveal a Peptide That Inhibits both Epithelial and B-Cell Membrane Fusion. Journal of virology **81:**9216-9229.
89. **Chesnokova LS, Hutt-Fletcher LM.** 2011. Fusion of Epstein-Barr Virus with Epithelial Cells Can Be Triggered by αvβ5 in Addition to αvβ6 and αvβ8, and Integrin Binding Triggers a Conformational Change in Glycoproteins gHgL. Journal of virology **85:**13214-13223.
90. **Li Q, Turk SM, Hutt-Fletcher LM.** 1995. The Epstein-Barr virus (EBV) BZLF2 gene product associates with the gH and gL homologs of EBV and carries an epitope critical to infection of B cells but not of epithelial cells. Journal of virology **69:**3987-3994.

91. **Cohen J.** 2017. 42nd International Herpesvirus Workshop, Ghent, Belgium.
92. **Ablashi DV, Gerber P, Easton J.** 1979. Oncogenic herpesviruses of nonhuman primates. Comparative immunology, microbiology and infectious diseases **2:**229-241.
93. **Frank A, Andiman WA, Miller G.** 1976. Epstein-Barr Virus and Nonhuman Primates: Natural and Experimental Infection11Supported by Grants from the American Cancer Society VC107, Damon Runyon Memorial Funds DRG-1147, and from the National Institutes of Health CA-12055, CA-16038, AI-11611, HD-00177, p. 171-201. *In* Kleln G, Weinhouse S, Haddow A (ed.), Advances in Cancer Research, vol. 23. Academic Press.
94. **Cho Y-G, Ramer J, Rivailler P, Quink C, Garber RL, Beier DR, Wang F.** 2001. An Epstein–Barr-related herpesvirus from marmoset lymphomas. Proceedings of the National Academy of Sciences **98:**1224-1229.
95. **Moghaddam A, Rosenzweig M, Lee-Parritz D, Annis B, Johnson RP, Wang F.** 1997. An Animal Model for Acute and Persistent Epstein-Barr Virus Infection. Science **276:**2030-2033.
96. **Sashihara J, Hoshino Y, Bowman JJ, Krogmann T, Burbelo PD, Coffield VM, Kamrud K, Cohen JI.** 2011. Soluble Rhesus Lymphocryptovirus gp350 Protects against Infection and Reduces Viral Loads in Animals that Become Infected with Virus after Challenge. PLoS Pathogens **7:**e1002308.
97. **Minor PD.** 2015. Live attenuated vaccines: Historical successes and current challenges. Virology **479:**379-392.
98. **Hambleton S, Gershon AA.** 2005. Preventing Varicella-Zoster Disease. Clinical Microbiology Reviews **18:**70-80.
99. **Takahashi M, Otsuka T, Okuno Y, Asano Y, Yazaki T, Isomura S.** LIVE VACCINE USED TO PREVENT THE SPREAD OF VARICELLA IN CHILDREN IN HOSPITAL. The Lancet **304:**1288-1290.
100. **Hata A, Asanuma H, Rinki M, Sharp M, Wong RM, Blume K, Arvin AM.** 2002. Use of an inactivated varicella vaccine in recipients of hematopoietic-cell transplants. N Engl J Med **347:**26-34.
101. **Galea SA, Sweet A, Beninger P, Steinberg SP, LaRussa PS, Gershon AA, Sharrar RG.** 2008. The Safety Profile of Varicella Vaccine: A 10-Year Review. The Journal of Infectious Diseases **197:**S165-S169.

102. **Blaskovic D, Stancekova M, Svobodova J, Mistrikova J.** 1980. Isolation of five strains of herpesviruses from two species of free living small rodents. Acta virologica **24:**468.
103. **Nash AA, Dutia BM, Stewart JP, Davison AJ.** 2001. Natural history of murine gamma-herpesvirus infection. Philosophical transactions of the Royal Society of London. Series B, Biological sciences **356:**569-579.
104. **Mistrikova J, Raslova H, Mrmusova M, Kudelova M.** 2000. A murine gammaherpesvirus. Acta virologica **44:**211-226.
105. **Simas JP, Efstathiou S.** 1998. Murine gammaherpesvirus 68: a model for the study of gammaherpesvirus pathogenesis. Trends Microbiol **6:**276-282.
106. **Virgin HWt, Latreille P, Wamsley P, Hallsworth K, Weck KE, Dal Canto AJ, Speck SH.** 1997. Complete sequence and genomic analysis of murine gammaherpesvirus 68. Journal of virology **71:**5894-5904.
107. **Tan CS, Frederico B, Stevenson PG.** 2014. Herpesvirus delivery to the murine respiratory tract. J Virol Methods **206:**105-114.
108. **Milho R, Frederico B, Efstathiou S, Stevenson PG.** 2012. A heparan-dependent herpesvirus targets the olfactory neuroepithelium for host entry. PLoS Pathog **8:**e1002986.
109. **Milho R, Smith CM, Marques S, Alenquer M, May JS, Gillet L, Gaspar M, Efstathiou S, Simas JP, Stevenson PG.** 2009. In vivo imaging of murid herpesvirus-4 infection. The Journal of general virology **90:**21-32.
110. **Shivkumar M, Milho R, May JS, Nicoll MP, Efstathiou S, Stevenson PG.** 2013. Herpes simplex virus 1 targets the murine olfactory neuroepithelium for host entry. Journal of virology **87:**10477-10488.
111. **Farrell HE, Lawler C, Tan CSE, MacDonald K, Bruce K, Mach M, Davis-Poynter N, Stevenson PG.** 2016. Murine Cytomegalovirus Exploits Olfaction To Enter New Hosts. mBio **7**.
112. **Ehtisham S, Sunil-Chandra NP, Nash AA.** 1993. Pathogenesis of murine gammaherpesvirus infection in mice deficient in CD4 and CD8 T cells. Journal of virology **67:**5247-5252.
113. **François S, Vidick S, Sarlet M, Desmecht D, Drion P, Stevenson PG, Vanderplasschen A, Gillet L.** 2013. Illumination of Murine Gammaherpesvirus-68 Cycle Reveals a Sexual Transmission Route from Females to Males in Laboratory Mice. PLOS Pathogens **9:**e1003292.

114. **Frederico B, Milho R, May JS, Gillet L, Stevenson PG.** 2012. Myeloid infection links epithelial and B cell tropisms of Murid Herpesvirus-4. PLoS Pathog **8:**e1002935.
115. **Gaspar M, May JS, Sukla S, Frederico B, Gill MB, Smith CM, Belz GT, Stevenson PG.** 2011. Murid Herpesvirus-4 Exploits Dendritic Cells to Infect B Cells. PLoS Pathog **7:**e1002346.
116. **Cardin RD, Brooks JW, Sarawar SR, Doherty PC.** 1996. Progressive loss of CD8+ T cell-mediated control of a gamma-herpesvirus in the absence of CD4+ T cells. The Journal of experimental medicine **184:**863-871.
117. **Frederico B, Chao B, May JS, Belz GT, Stevenson PG.** 2014. A murid gamma-herpesviruses exploits normal splenic immune communication routes for systemic spread. Cell Host Microbe **15:**457-470.
118. **Weck KE, Kim SS, Virgin HW, Speck SH.** 1999. Macrophages Are the Major Reservoir of Latent Murine Gammaherpesvirus 68 in Peritoneal Cells. Journal of virology **73:**3273-3283.
119. **Flaño E, Husain SM, Sample JT, Woodland DL, Blackman MA.** 2000. Latent Murine γ-Herpesvirus Infection Is Established in Activated B Cells, Dendritic Cells, and Macrophages. The Journal of Immunology **165:**1074-1081.
120. **Coleman CB, Nealy MS, Tibbetts SA.** 2010. Immature and Transitional B Cells Are Latency Reservoirs for a Gammaherpesvirus. Journal of virology **84:**13045-13052.
121. **Christensen JP, Cardin RD, Branum KC, Doherty PC.** 1999. CD4+ T cell-mediated control of a γ-herpesvirus in B cell-deficient mice is mediated by IFN-γ. Proceedings of the National Academy of Sciences **96:**5135-5140.
122. **Stevenson PG, Belz GT, Altman JD, Doherty PC.** 1998. Virus-specific CD8+ T cell numbers are maintained during γ-herpesvirus reactivation in CD4-deficient mice. Proceedings of the National Academy of Sciences **95:**15565-15570.
123. **Stevenson PG, Efstathiou S, Doherty PC, Lehner PJ.** 2000. Inhibition of MHC class I-restricted antigen presentation by gamma 2-herpesviruses. Proceedings of the National Academy of Sciences of the United States of America **97:**8455-8460.
124. **Bridgeman A, Stevenson PG, Simas JP, Efstathiou S.** 2001. A Secreted Chemokine Binding Protein Encoded by Murine Gammaherpesvirus-68 Is Necessary for the Establishment of a Normal Latent Load. The Journal of experimental medicine **194:**301-312.

125. **Tarakanova VL, Suarez F, Tibbetts SA, Jacoby MA, Weck KE, Hess JL, Speck SH, Virgin HW.** 2005. Murine Gammaherpesvirus 68 Infection Is Associated with Lymphoproliferative Disease and Lymphoma in BALB β2 Microglobulin-Deficient Mice. Journal of virology **79:**14668-14679.
126. **Gangappa S, Kapadia SB, Speck SH, Virgin Iv* HW.** 2002. Antibody to a Lytic Cycle Viral Protein Decreases Gammaherpesvirus Latency in B-Cell-Deficient Mice. Journal of virology **76:**11460-11468.
127. **Sparks-Thissen RL, Braaten DC, Hildner K, Murphy TL, Murphy KM, Virgin Iv HW.** 2005. CD4 T cell control of acute and latent murine gammaherpesvirus infection requires IFNγ. Virology **338:**201-208.
128. **Sangster MY, Topham DJ, D'Costa S, Cardin RD, Marion TN, Myers LK, Doherty PC.** 2000. Analysis of the Virus-Specific and Nonspecific B Cell Response to a Persistent B-Lymphotropic Gammaherpesvirus. The Journal of Immunology **164:**1820-1828.
129. **Usherwood EJ, Ross AJ, Allen DJ, Nash AA.** 1996. Murine gammaherpesvirus-induced splenomegaly: a critical role for CD4 T cells. Journal of General Virology **77:**627-630.
130. **Dutia BM, Clarke CJ, Allen DJ, Nash AA.** 1997. Pathological changes in the spleens of gamma interferon receptor-deficient mice infected with murine gammaherpesvirus: a role for CD8 T cells. Journal of virology **71:**4278-4283.
131. **Sarawar SR, Cardin RD, Brooks JW, Mehrpooya M, Hamilton-Easton AM, Mo XY, Doherty PC.** 1997. Gamma interferon is not essential for recovery from acute infection with murine gammaherpesvirus 68. Journal of virology **71:**3916-3921.
132. **Stevenson PG, Simas JP, Efstathiou S.** 2009. Immune control of mammalian gamma-herpesviruses: lessons from murid herpesvirus-4. The Journal of general virology **90:**2317-2330.
133. **Wright DE, Colaco S, Colaco C, Stevenson PG.** 2009. Antibody limits in vivo murid herpesvirus-4 replication by IgG Fc receptor-dependent functions. The Journal of general virology **90:**2592-2603.
134. **Stewart JP, Janjua NJ, Pepper SD, Bennion G, Mackett M, Allen T, Nash AA, Arrand JR.** 1996. Identification and characterization of murine gammaherpesvirus 68 gp150: a virion membrane glycoprotein. Journal of virology **70:**3528-3535.
135. **Liu L, Flaño E, Usherwood EJ, Surman S, Blackman MA, Woodland DL.** 1999. Lytic Cycle T Cell Epitopes Are Expressed in Two Distinct Phases During MHV-68 Infection. The Journal of Immunology **163:**868-874.

136. **Stewart JP, Micali N, Usherwood EJ, Bonina L, Nash AA.** 1999. Murine gamma-herpesvirus 68 glycoprotein 150 protects against virus-induced mononucleosis: a model system for gamma-herpesvirus vaccination. Vaccine **17:**152-157.
137. **Liu L, Usherwood EJ, Blackman MA, Woodland DL.** 1999. T-cell vaccination alters the course of murine herpesvirus 68 infection and the establishment of viral latency in mice. Journal of virology **73:**9849-9857.
138. **Ruiss R, Ohno S, Steer B, Zeidler R, Adler H.** 2012. Murine gammaherpesvirus 68 glycoprotein 150 does not contribute to latency amplification in vivo. Virology Journal **9:**107-107.
139. **Stevenson PG, Belz GT, Castrucci MR, Altman JD, Doherty PC.** 1999. A gamma-herpesvirus sneaks through a CD8(+) T cell response primed to a lytic-phase epitope. Proceedings of the National Academy of Sciences of the United States of America **96:**9281-9286.
140. **Usherwood EJ, Ward KA, Blackman MA, Stewart JP, Woodland DL.** 2001. Latent antigen vaccination in a model gammaherpesvirus infection. Journal of virology **75:**8283-8288.
141. **Rickabaugh TM, Brown HJ, Martinez-Guzman D, Wu TT, Tong L, Yu F, Cole S, Sun R.** 2004. Generation of a latency-deficient gammaherpesvirus that is protective against secondary infection. Journal of virology **78:**9215-9223.
142. **Tibbetts SA, McClellan JS, Gangappa S, Speck SH, Virgin HWt.** 2003. Effective vaccination against long-term gammaherpesvirus latency. Journal of virology **77:**2522-2529.
143. **Fowler P, Efstathiou S.** 2004. Vaccine potential of a murine gammaherpesvirus-68 mutant deficient for ORF73. The Journal of general virology **85:**609-613.
144. **Hansen SG, Vieville C, Whizin N, Coyne-Johnson L, Siess DC, Drummond DD, Legasse AW, Axthelm MK, Oswald K, Trubey CM, Piatak M, Lifson JD, Nelson JA, Jarvis MA, Picker LJ.** 2009. Effector-memory T cell responses are associated with protection of rhesus monkeys from mucosal SIV challenge. Nature medicine **15:**293-299.
145. **Hansen SG, Ford JC, Lewis MS, Ventura AB, Hughes CM, Coyne-Johnson L, Whizin N, Oswald K, Shoemaker R, Swanson T, Legasse AW, Chiuchiolo MJ, Parks CL, Axthelm MK, Nelson JA, Jarvis MA, Piatak M, Lifson JD, Picker LJ.** 2011. Profound early control of highly pathogenic SIV by an effector memory T-cell vaccine. **473:**523.

146. **Hansen SG, Sacha JB, Hughes CM, Ford JC, Burwitz BJ, Scholz I, Gilbride RM, Lewis MS, Gilliam AN, Ventura AB, Malouli D, Xu G, Richards R, Whizin N, Reed JS, Hammond KB, Fischer M, Turner JM, Legasse AW, Axthelm MK, Edlefsen PT, Nelson JA, Lifson JD, Fruh K, Picker LJ.** 2013. Cytomegalovirus vectors violate CD8+ T cell epitope recognition paradigms. Science **340:**1237874.

147. **Hansen SG, Wu HL, Burwitz BJ, Hughes CM, Hammond KB, Ventura AB, Reed JS, Gilbride RM, Ainslie E, Morrow DW, Ford JC, Selseth AN, Pathak R, Malouli D, Legasse AW, Axthelm MK, Nelson JA, Gillespie GM, Walters LC, Brackenridge S, Sharpe HR, López CA, Früh K, Korber BT, McMichael AJ, Gnanakaran S, Sacha JB, Picker LJ.** 2016. Broadly targeted CD8+ T cell responses restricted by major histocompatibility complex-E. Science (New York, N.Y.) **351:**714-720.

148. **Forrest JC, Paden CR, Allen RD, Collins J, Speck SH.** 2007. ORF73-Null Murine Gammaherpesvirus 68 Reveals Roles for mLANA and p53 in Virus Replication. Journal of virology **81:**11957-11971.

149. **Fowler P, Marques S, Simas JP, Efstathiou S.** 2003. ORF73 of murine herpesvirus-68 is critical for the establishment and maintenance of latency. The Journal of general virology **84:**3405-3416.

150. **Marques S, Efstathiou S, Smith KG, Haury M, Simas JP.** 2003. Selective Gene Expression of Latent Murine Gammaherpesvirus 68 in B Lymphocytes. Journal of virology **77:**7308-7318.

151. **Martinez-Guzman D, Rickabaugh T, Wu T-T, Brown H, Cole S, Song MJ, Tong L, Sun R.** 2003. Transcription Program of Murine Gammaherpesvirus 68. Journal of virology **77:**10488-10503.

152. **Moorman NJ, Willer DO, Speck SH.** 2003. The gammaherpesvirus 68 latency-associated nuclear antigen homolog is critical for the establishment of splenic latency. Journal of virology **77:**10295-10303.

153. **Paden CR, Forrest JC, Moorman NJ, Speck SH.** 2010. Murine Gammaherpesvirus 68 LANA Is Essential for Virus Reactivation from Splenocytes but Not Long-Term Carriage of Viral Genome. Journal of virology **84:**7214-7224.

154. **Stoker M, Macpherson IAN.** 1964. Syrian Hamster Fibroblast Cell Line BHK21 and its Derivatives. Nature **203:**1355.

155. **Adler H, Messerle M, Wagner M, Koszinowski UH.** 2000. Cloning and Mutagenesis of the Murine Gammaherpesvirus 68 Genome as an Infectious Bacterial Artificial Chromosome. Journal of virology **74:**6964-6974.

156. **Shimonkevitz R, Colon S, Kappler JW, Marrack P, Grey HM.** 1984. Antigen recognition by H-2-restricted T cells. II. A tryptic ovalbumin peptide that substitutes for processed antigen. The Journal of Immunology **133:**2067.
157. **Adler H, Messerle M, Koszinowski UH.** 2001. Virus reconstituted from infectious bacterial artificial chromosome (BAC)-cloned murine gammaherpesvirus 68 acquires wild-type properties in vivo only after excision of BAC vector sequences. Journal of virology **75:**5692-5696.
158. **May JS, Colaco S, Stevenson PG.** 2005. Glycoprotein M Is an Essential Lytic Replication Protein of the Murine Gammaherpesvirus 68. Journal of virology **79:**3459-3467.
159. **Sparks-Thissen RL, Braaten DC, Kreher S, Speck SH, Virgin HW.** 2004. An Optimized CD4 T-Cell Response Can Control Productive and Latent Gammaherpesvirus Infection. Journal of virology **78:**6827-6835.
160. **Smith CM, Rosa GT, May JS, Bennett NJ, Mount AM, Belz GT, Stevenson PG.** 2006. CD4+ T cells specific for a model latency-associated antigen fail to control a gammaherpesvirus in vivo. European journal of immunology **36:**3186-3197.
161. **May JS, Stevenson PG.** 2010. Vaccination with murid herpesvirus-4 glycoprotein B reduces viral lytic replication but does not induce detectable virion neutralization. Journal of General Virology **91:**2542-2552.
162. **Davis-Poynter N, Yunis J, Farrell HE.** 2016. The Cytoplasmic C-Tail of the Mouse Cytomegalovirus 7 Transmembrane Receptor Homologue, M78, Regulates Endocytosis of the Receptor and Modulates Virus Replication in Different Cell Types. PLOS ONE **11:**e0165066.
163. **Davis-Poynter NJ, Lynch DM, Vally H, Shellam GR, Rawlinson WD, Barrell BG, Farrell HE.** 1997. Identification and characterization of a G protein-coupled receptor homolog encoded by murine cytomegalovirus. Journal of virology **71:**1521-1529.
164. **Snyder CM, Allan JE, Bonnett EL, Doom CM, Hill AB.** 2010. Cross-Presentation of a Spread-Defective MCMV Is Sufficient to Prime the Majority of Virus-Specific CD8+ T Cells. PLOS ONE **5:**e9681.
165. **Fleming P, Davis-Poynter N, Degli-Esposti M, Densley E, Papadimitriou J, Shellam G, Farrell H.** 1999. The Murine Cytomegalovirus Chemokine Homolog, m131/129, Is a Determinant of Viral Pathogenicity. Journal of virology **73:**6800-6809.

166. **Farrell HE, Bruce K, Lawler C, Oliveira M, Cardin R, Davis-Poynter N, Stevenson PG.** 2017. Murine Cytomegalovirus Spreads by Dendritic Cell Recirculation. mBio **8:**e01264-01217.
167. **Robertson JM, Jensen PE, Evavold BD.** 2000. DO11.10 and OT-II T Cells Recognize a C-Terminal Ovalbumin 323–339 Epitope. The Journal of Immunology **164:**4706-4712.
168. **Doherty PC, Christensen JP, Belz GT, Stevenson PG, Sangster MY.** 2001. Dissecting the host response to a gamma-herpesvirus. Philosophical transactions of the Royal Society of London. Series B, Biological sciences **356:**581-593.
169. **Collins CM, Speck SH.** 2014. Expansion of Murine Gammaherpesvirus Latently Infected B Cells Requires T Follicular Help. PLOS Pathogens **10:**e1004106.
170. **Braaten DC, Sparks-Thissen RL, Kreher S, Speck SH, Virgin HW.** 2005. An Optimized CD8(+) T-Cell Response Controls Productive and Latent Gammaherpesvirus Infection. Journal of virology **79:**2573-2583.
171. **Smith CM, Gill MB, May JS, Stevenson PG.** 2007. Murine Gammaherpesvirus-68 Inhibits Antigen Presentation by Dendritic Cells. PLoS ONE **2:**e1048.
172. **Lybarger L, Wang X, Harris MR, Virgin HW, Hansen TH.** 2003. Virus Subversion of the MHC Class I Peptide-Loading Complex. Immunity **18:**121-130.
173. **Bennett NJ, May JS, Stevenson PG.** 2005. Gamma-herpesvirus latency requires T cell evasion during episome maintenance. PLoS Biol **3:**e120.
174. **Tan CSE, Lawler C, Stevenson PG.** 2017. CD8(+) T cell evasion mandates CD4(+) T cell control of chronic gamma-herpesvirus infection. PLoS Pathogens **13:**e1006311.
175. **Stevenson PG, Cardin RD, Christensen JP, Doherty PC.** 1999. Immunological control of a murine gammaherpesvirus independent of CD8+ T cells. The Journal of general virology **80 (Pt 2):**477-483.
176. **McClellan JS, Tibbetts SA, Gangappa S, Brett KA, Virgin HW.** 2004. Critical Role of CD4 T Cells in an Antibody-Independent Mechanism of Vaccination against Gammaherpesvirus Latency. Journal of virology **78:**6836-6845.
177. **Dutia BM, Reid SJ, Drummond DD, Ligertwood Y, Bennet I, Rietberg W, Silvia O, Jarvis MA, Nash AA.** 2009. A Novel Cre Recombinase Imaging System for Tracking Lymphotropic Virus Infection In Vivo. PLOS ONE **4:**e6492.
178. **Chen T, Hudnall SD.** 2006. Anatomical mapping of human herpesvirus reservoirs of infection. Modern Pathology **19:**726.

179. **Luppi M, Barozzi P, Schulz TF, Setti G, Staskus K, Trovato R, Narni F, Donelli A, Maiorana A, Marasca R, Sandrini S, Torelli G, Sheldon J.** 2000. Bone Marrow Failure Associated with Human Herpesvirus 8 Infection after Transplantation. New England Journal of Medicine **343:**1378-1385.
180. **Rosa GT, Gillet L, Smith CM, de Lima BD, Stevenson PG.** 2007. IgG Fc Receptors Provide an Alternative Infection Route for Murine Gamma-Herpesvirus-68. PLoS ONE **2:**e560.
181. **Gillet L, May JS, Stevenson PG.** 2007. Post-Exposure Vaccination Improves Gammaherpesvirus Neutralization. PLoS ONE **2:**e899.
182. **Gill MB, Gillet L, Colaco S, May JS, de Lima BD, Stevenson PG.** 2006. Murine gammaherpesvirus-68 glycoprotein H–glycoprotein L complex is a major target for neutralizing monoclonal antibodies. Journal of General Virology **87:**1465-1475.
183. **Gillet L, Colaco S, Stevenson PG.** 2008. The Murid Herpesvirus-4 gH/gL Binds to Glycosaminoglycans. PLoS ONE **3:**e1669.
184. **Glauser DL, Gillet L, Stevenson PG.** 2012. Virion endocytosis is a major target for murid herpesvirus-4 neutralization. The Journal of general virology **93:**1316-1327.
185. **Adler H, Steer B, Juskewitz E, Kammerer R.** 2014. To the editor: Murine gammaherpesvirus 68 (MHV-68) escapes from NK-cell-mediated immune surveillance by a CEACAM1-mediated immune evasion mechanism. European journal of immunology **44:**2521-2522.
186. **Sharp EL, Davis-Poynter NJ, Farrell HE.** 2009. Analysis of the subcellular trafficking properties of murine cytomegalovirus M78, a 7 transmembrane receptor homologue. Journal of General Virology **90:**59-68.
187. **Lo B, Hansen S, Evans K, Heath JK, Wright JR.** 2008. Alveolar Epithelial Type II Cells Induce T Cell Tolerance to Specific Antigen. The Journal of Immunology **180:**881.
188. **Debbabi H, Ghosh S, Kamath AB, Alt J, deMello DE, Dunsmore S, Behar SM.** 2005. Primary type II alveolar epithelial cells present microbial antigens to antigen-specific CD4+ T cells. American Journal of Physiology-Lung Cellular and Molecular Physiology **289:**L274-L279.
189. **Gereke M, Jung S, Buer J, Bruder D.** 2009. Alveolar Type II Epithelial Cells Present Antigen to CD4+ T Cells and Induce Foxp3+ Regulatory T Cells. American Journal of Respiratory and Critical Care Medicine **179:**344-355.
190. **Oliveira SA, Shenk TE.** 2001. Murine cytomegalovirus M78 protein, a G protein-coupled receptor homologue, is a constituent of the virion and facilitates

accumulation of immediate-early viral mRNA. Proceedings of the National Academy of Sciences of the United States of America **98:**3237-3242.

191. **Farrell HE, Lawler C, Oliveira MT, Davis-Poynter N, Stevenson PG.** 2016. Alveolar Macrophages Are a Prominent but Nonessential Target for Murine Cytomegalovirus Infecting the Lungs. Journal of virology **90:**2756-2766.
192. **Babcock GJ, Decker LL, Volk M, Thorley-Lawson DA.** 1998. EBV Persistence in Memory B Cells In Vivo. Immunity **9:**395-404.
193. **Miyashita EM, Yang B, Babcock GJ, Thorley-Lawson DA.** 1997. Identification of the site of Epstein-Barr virus persistence in vivo as a resting B cell. Journal of virology **71:**4882-4891.
194. **Babcock GJ, Hochberg D, Thorley-Lawson DA.** 2000. The Expression Pattern of Epstein-Barr Virus Latent Genes In Vivo Is Dependent upon the Differentiation Stage of the Infected B Cell. Immunity **13:**497-506.
195. **Li H, Ikuta K, Sixbey JW, Tibbetts SA.** 2008. A Replication-Defective Gammaherpesvirus Efficiently Establishes Long-Term Latency in Macrophages but Not in B Cells In Vivo. Journal of virology **82:**8500-8508.
196. **Stewart JP, Usherwood EJ, Ross A, Dyson H, Nash T.** 1998. Lung Epithelial Cells Are a Major Site of Murine Gammaherpesvirus Persistence. The Journal of experimental medicine **187:**1941-1951.
197. **Usherwood EJ, Stewart JP, Nash AA.** 1996. Characterization of tumor cell lines derived from murine gammaherpesvirus-68-infected mice. Journal of virology **70:**6516-6518.
198. 1996. The Kaposi sarcoma-associated herpesvirus (KSHV) is present as an intact latent genome in KS tissue but replicates in the peripheral blood mononuclear cells of KS patients. The Journal of experimental medicine **184:**283-288.
199. **Delecluse HJ, Bartnizke S, Hammerschmidt W, Bullerdiek J, Bornkamm GW.** 1993. Episomal and integrated copies of Epstein-Barr virus coexist in Burkitt lymphoma cell lines. Journal of virology **67:**1292-1299.
200. **Cesarman E, Moore P, Rao P, Inghirami G, Knowles D, Chang Y.** 1995. In vitro establishment and characterization of two acquired immunodeficiency syndrome-related lymphoma cell lines (BC-1 and BC-2) containing Kaposi's sarcoma-associated herpesvirus-like (KSHV) DNA sequences. Blood **86:**2708-2714.
201. **Marechal V, Dehee A, Chikhi-Brachet R, Piolot T, Coppey-Moisan M, Nicolas J-C.** 1999. Mapping EBNA-1 Domains Involved in Binding to Metaphase Chromosomes. Journal of virology **73:**4385-4392.

202. **Kanda T, Otter M, Wahl GM.** 2001. Coupling of Mitotic Chromosome Tethering and Replication Competence in Epstein-Barr Virus-Based Plasmids. Molecular and Cellular Biology **21:**3576-3588.
203. **Yates J, Warren N, Reisman D, Sugden B.** 1984. A cis-acting element from the Epstein-Barr viral genome that permits stable replication of recombinant plasmids in latently infected cells. Proceedings of the National Academy of Sciences of the United States of America **81:**3806-3810.
204. **Yates JL, Warren N, Sugden B.** 1985. Stable replication of plasmids derived from Epstein-Barr virus in various mammalian cells. Nature **313:**812-815.
205. **Lehman CW, Botchan MR.** 1998. Segregation of viral plasmids depends on tethering to chromosomes and is regulated by phosphorylation. Proceedings of the National Academy of Sciences of the United States of America **95:**4338-4343.
206. **Virgin HW, Latreille P, Wamsley P, Hallsworth K, Weck KE, Dal Canto AJ, Speck SH.** 1997. Complete sequence and genomic analysis of murine gammaherpesvirus 68. Journal of virology **71:**5894-5904.
207. **Russo JJ, Bohenzky RA, Chien M-C, Chen J, Yan M, Maddalena D, Parry JP, Peruzzi D, Edelman IS, Chang Y, Moore PS.** 1996. Nucleotide sequence of the Kaposi sarcoma-associated herpesvirus (HHV8). Proceedings of the National Academy of Sciences of the United States of America **93:**14862-14867.
208. **Hall KT, Giles MS, Calderwood MA, Goodwin DJ, Matthews DA, Whitehouse A.** 2002. The Herpesvirus Saimiri Open Reading Frame 73 Gene Product Interacts with the Cellular Protein p32. Journal of virology **76:**11612-11622.
209. **Purushothaman P, Dabral P, Gupta N, Sarkar R, Verma SC.** 2016. KSHV Genome Replication and Maintenance. Frontiers in Microbiology **7:**54.
210. **Ballestas ME, Kaye KM.** 2001. Kaposi's sarcoma-associated herpesvirus latency-associated nuclear antigen 1 mediates episome persistence through cis-acting terminal repeat (TR) sequence and specifically binds TR DNA. Journal of virology **75:**3250-3258.
211. **Fejér G, Medveczky MM, Horvath E, Lane B, Chang Y, Medveczky PG.** 2003. The latency-associated nuclear antigen of Kaposi's sarcoma-associated herpesvirus interacts preferentially with the terminal repeats of the genome in vivo and this complex is sufficient for episomal DNA replication. Journal of General Virology **84:**1451-1462.

212. **Barbera AJ, Chodaparambil JV, Kelley-Clarke B, Joukov V, Walter JC, Luger K, Kaye KM.** 2006. The Nucleosomal Surface as a Docking Station for Kaposi's Sarcoma Herpesvirus LANA. Science **311:**856-861.
213. **Habison AC, Beauchemin C, Simas JP, Usherwood EJ, Kaye KM.** 2012. Murine Gammaherpesvirus 68 LANA Acts on Terminal Repeat DNA To Mediate Episome Persistence. Journal of virology **86:**11863-11876.
214. **Blake N.** 2010. Immune evasion by gammaherpesvirus genome maintenance proteins. Journal of General Virology **91:**829-846.
215. **Reith W, LeibundGut-Landmann S, Waldburger J-M.** 2005. Regulation of MHC class II gene expression by the class II transactivator. Nature reviews. Immunology **5:**793-806.
216. **Muhlethaler-Mottet A, Otten LA, Steimle V, Mach B.** 1997. Expression of MHC class II molecules in different cellular and functional compartments is controlled by differential usage of multiple promoters of the transactivator CIITA. The EMBO Journal **16:**2851-2860.
217. **Cai Q, Banerjee S, Cervini A, Lu J, Hislop AD, Dzeng R, Robertson ES.** 2013. IRF-4-Mediated CIITA Transcription Is Blocked by KSHV Encoded LANA to Inhibit MHC II Presentation. PLoS Pathogens **9:**e1003751.
218. **Schmidt K, Wies E, Neipel F.** 2011. Kaposi's Sarcoma-Associated Herpesvirus Viral Interferon Regulatory Factor 3 Inhibits Gamma Interferon and Major Histocompatibility Complex Class II Expression. Journal of virology **85:**4530-4537.
219. **Thakker S, Purushothaman P, Gupta N, Challa S, Cai Q, Verma SC.** 2015. Kaposi's Sarcoma-Associated Herpesvirus Latency-Associated Nuclear Antigen Inhibits Major Histocompatibility Complex Class II Expression by Disrupting Enhanceosome Assembly through Binding with the Regulatory Factor X Complex. Journal of virology **89:**5536-5556.
220. **Lim C, Sohn H, Gwack Y, Choe J.** 2000. Latency-associated nuclear antigen of Kaposi’s sarcoma-associated herpesvirus (human herpesvirus-8) binds ATF4/CREB2 and inhibits its transcriptional activation activity. Journal of General Virology **81:**2645-2652.
221. **Ahn JW, Powell KL, Kellam P, Alber DG.** 2002. Gammaherpesvirus Lytic Gene Expression as Characterized by DNA Array. Journal of virology **76:**6244-6256.
222. **Song MJ, Hwang S, Wong WH, Wu T-T, Lee S, Liao H-I, Sun R.** 2005. Identification of viral genes essential for replication of murine γ-herpesvirus 68 using

signature-tagged mutagenesis. Proceedings of the National Academy of Sciences of the United States of America **102:**3805-3810.

223. **Hu Z, Blackman MA, Kaye KM, Usherwood EJ.** 2015. Functional Heterogeneity in the CD4(+) T Cell Response to Murine γ-Herpesvirus 68. Journal of immunology (Baltimore, Md. : 1950) **194:**2746-2756.
224. **Usherwood EJ, Stewart JP, Robertson K, Allen DJ, Nash AA.** 1996. Absence of splenic latency in murine gammaherpesvirus 68-infected B cell-deficient mice. Journal of General Virology **77:**2819-2825.
225. **Vollers SS, Stern LJ.** 2008. Class II major histocompatibility complex tetramer staining: progress, problems, and prospects. Immunology **123:**305-313.
226. **Mallet-Designe VI, Stratmann T, Homann D, Carbone F, Oldstone MBA, Teyton L.** 2003. Detection of Low-Avidity CD4⁺ T Cells Using Recombinant Artificial APC: Following the Antiovalbumin Immune Response. The Journal of Immunology **170:**123.
227. **Crawford F, Kozono H, White J, Marrack P, Kappler J.** 1998. Detection of Antigen-Specific T Cells with Multivalent Soluble Class II MHC Covalent Peptide Complexes. Immunity **8:**675-682.
228. **Massilamany C, Krishnan B, Reddy J.** 2015. Major Histocompatibility Complex Class II Dextramers: New Tools for the Detection of antigen-Specific, CD4 T Cells in Basic and Clinical Research. Scandinavian Journal of Immunology **82:**399-408.

APPENDIX

6.2 Ethics approval certificates

Animal Ethics certificate letter 1

THE UNIVERSITY OF QUEENSLAND
AUSTRALIA

UQ Research and Innovation
Director, Research Management Office
Nicole Thompson

Animal Ethics Approval Certificate

12-Jan-2016

Please check all details below and inform the Animal Welfare Unit within 10 working days if anything is incorrect.

Activity Details

Chief Investigator:	Associate Professor Philip Stevenson, Clinical Medical Virology Centre
Title:	Herpesvirus pathogenesis in mice
AEC Approval Number:	SASVRC/301/13/ARC/NHMRC/BELGIUM
Previous AEC Number:	
Approval Duration:	18-Oct-2013 to 18-Oct-2016
Funding Body:	ARC, NHMRC
Group:	Health Sciences
Other Staff/Students:	Nicholas Davis-Poynter, Katy Madden, Joseph Yunis, Cindy Tan, Helen Farrell, Pedro Monterio E LouroMachadoDeSimas, Clara Lawler
Location(s):	Herston Medical Research Centre St Lucia Bldg 75 - AIBN St Lucia Bldg 76 - Chemistry (SCMB) St Lucia Bldg 57 - Centre of Advanced Imaging

Summary

Subspecies	Strain	Class	Gender	Source	Approved	Remaining
Mice - genetically modified	B6.class II-/-	Adults	Mix	Institutional Breeding Colony	270	217
Mice - genetically modified	CD11c Cre	Adults	Mix	Institutional Breeding Colony	1296	936
Mice - genetically modified	Mx Cre	Adults	Mix	Institutional Breeding Colony	1296	1110
Mice - genetically modified	CD169-DTR	Adults	Mix	Institutional Breeding Colony	432	179
Mice - genetically modified	NK-p46-Cre	Adults	Mix	Institutional Breeding Colony	0	0
Mice - genetically modified	NES-Cre	Adults	Mix	Institutional Breeding Colony	0	0
Mice - genetically modified	iNOS-/-	Adults	Mix	Institutional Breeding Colony	324	324
Mice - genetically modified	DO.11.10T	Adults	Mix	Institutional Breeding Colony	216	168
Mice - genetically modified	MacBlue	Adults	Mix	Institutional Breeding Colony	216	216
Mice - non genetically modified	C57BL/6	Adults	Mix	Commercial breeding colony	798	490
Mice - non genetically modified	BALB/c	Adults	Mix	Commercial breeding colony	1755	1152

Animal Ethics certificate letter 2

THE UNIVERSITY OF QUEENSLAND
AUSTRALIA

UQ Research and Innovation
Director, Research Management Office
Nicole Thompson

Animal Ethics Approval Certificate

23-Aug-2016

Please check all details below and inform the Animal Welfare Unit within 10 working days if anything is incorrect.

Activity Details

Chief Investigator:	Dr Philip Stevenson, Child Health Research Centre
Title:	Host defence against herpesviruses
AEC Approval Number:	SCMB/341/16
Previous AEC Number:	SASVRC/301/13/ARC/NHMRC/BELGIUM
Approval Duration:	23-Aug-2016 to 23-Aug-2019
Funding Body:	ARC, NHMRC
Group:	Molecular Biosciences
Other Staff/Students:	Helen Farrell, Joseph Yunis, Clara Lawler, Kym French, Kimberley Bruce
Location(s):	St Lucia Bldg 76 - Chemistry (SCMB)

Summary

Subspecies	Strain	Class	Gender	Source	Approved	Remaining
Mice - genetically modified	DO11.10	Adults	Mix		459	459
Mice - genetically modified	rosa26-tdtomato	Adults	Mix		243	243
Mice - genetically modified	B6.MHC Class II -/-	Adults	Mix		486	486
Mice - genetically modified	cr2-/-	Adults	Mix		432	432
Mice - genetically modified	csf-1r-cre	Adults	Mix		324	324
Mice - non genetically modified	C57BL/6	Adults	Mix		1404	1404
Mice - non genetically modified	BALB/c	Adults	Mix		1404	1404
Mice - non genetically modified	C57BL/6 x BALB/c F1	Adults	Mix		675	675

Permits

Provisos

Approval Details

Description	Amount	Balance
Mice - genetically modified (B6.MHC Class II -/-, Mix, Adults,)		
23 Aug 2016 Initial approval	486	486

Animal Welfare Unit
UQ Research and Innovation
The University of Queensland

Cumbrae-Stewart Building
Research Road
Brisbane Qld 4072 Australia

+61 7 336 52925 (Enquiries)
+61 7 334 68710 (Enquiries)
+61 7 336 52713 (Coordinator)

animalwelfare@research.uq.edu.au
uq.edu.au/research

Animal Ethics certificate letter 3

THE UNIVERSITY OF QUEENSLAND
AUSTRALIA

UQ Research and Innovation
Director, Research Management Office
Nicole Thompson

Animal Ethics Approval Certificate

20-Jan-2016

Please check all details below and inform the Animal Welfare Unit within 10 working days if anything is incorrect.

Activity Details

Chief Investigator:	Dr Philip Stevenson, Child Health Research Centre
Title:	Using cre lox recombination to define how herpesviruses spread and how they are controlled
AEC Approval Number:	SCMB/479/15/NHMRC
Previous AEC Number:	SCMB/365/15/NHMRC
Approval Duration:	21-Jan-2016 to 21-Jan-2019
Funding Body:	
Group:	Health Sciences
Other Staff/Students:	Helen Farrell, Joseph Yunis, Clara Lawler, Cindy Tan, Orry Wyer, Kimberley Bruce, Katrina Geary, Sean O'Laughlin, Kevin Wathen-Dunn
Location(s):	St Lucia Bldg 76 - Chemistry (SCMB)

Summary

Subspecies	Strain	Class	Gender	Source	Approved	Remaining
Mice - genetically modified	CD11c+/ Cre x I-A flox/flox	Adults	Mix	Institutional Breeding Colony	390	390
Mice - genetically modified	LysM+/Cre x I-A flox.flox	Adults	Mix	Institutional Breeding Colony	390	390
Mice - genetically modified	CD19+/Cre x I-A flox/flox	Adults	Mix	Institutional Breeding Colony	390	390
Mice - genetically modified	CD11c-Cre	Adults	Mix	Institutional Breeding Colony	280	280
Mice - genetically modified	LysMCre	Adults	Mix	Institutional Breeding Colony	300	300
Mice - genetically modified	CD19.Cre	Adults	Mix	Institutional Breeding Colony	340	340
Mice - genetically modified	CD11c+/ Cre x IFN ab R flox/flox	Adults	Mix	Institutional Breeding Colony	390	390
Mice - genetically modified	CD19+/Cre x IFN ab R flox/flox	Adults	Mix	Institutional Breeding Colony	390	390
Mice - genetically modified	LysM+/Cre x IFN ab R flox/flox	Adults	Mix	Institutional Breeding Colony	390	390
Mice - genetically modified	MX1-Cre	Adults	Mix	Institutional Breeding Colony	300	300
Mice - genetically modified	CD11c+/ Cre x ROSA26-tdTomato	Adults	Mix	Institutional Breeding Colony	30	30
Mice - genetically modified	LysM+/Cre x ROSA26-tdTomato	Adults	Mix	Institutional Breeding Colony	30	30

Animal Welfare Unit
UQ Research and Innovation
The University of Queensland

Cumbrae-Stewart Building
Research Road
Brisbane Qld 4072 Australia

+61 7 336 52925 (Enquiries)
+61 7 334 68710 (Enquiries)
+61 7 336 52713 (Coordinator)

animalwelfare@research.uq.edu.au
uq.edu.au/research